

**Development of sustainable bioprocess for biodiesel production from novel
freshwater microalga *Chlorella sorokiniana* FC6 IITG**

A Thesis

Submitted for the Degree of
DOCTOR OF PHILOSOPHY

by

**VIKRAM KUMAR
(11615102)**

Under supervision of
Dr. Debasish Das



March 2017

**Centre for Energy
Indian Institute of Technology Guwahati
Guwahati 781 039, Assam, India**



INDIAN INSTITUTE OF TECHNOLOGY GUWAHATI

CENTRE FOR ENERGY

STATEMENT

I do hereby declare that the content embodied in this thesis is the result of investigations carried out by me in the Centre for Energy, Indian Institute of Technology Guwahati, Guwahati, Assam, India under the supervision of Dr. Debasish Das.

In keeping with the general practice of reporting scientific observations, due acknowledgements have been made wherever the work described is based on the findings of other investigators.

Date: March, 2017

Vikram Kumar



INDIAN INSTITUTE OF TECHNOLOGY GUWAHATI

CENTRE FOR ENERGY

CERTIFICATE

It is certified that the work described in this thesis entitled “**Development of sustainable bioprocess for biodiesel production from novel freshwater microalga *Chlorella sorokiniana* FC6 IITG**” by Mr. Vikram Kumar for the award of degree of Doctor of Philosophy is an authentic record of the results obtained from the research work carried out under my supervision in the Centre for Energy, Indian Institute of Technology Guwahati, Guwahati, India. The work embodied in this thesis has not been submitted elsewhere for a degree.

Dr. Debasish Das

Associate Professor

(Thesis Supervisor)

Department of Biosciences & Bioengineering

Indian Institute of Technology Guwahati

Guwahati 781 039, India

Acknowledgements

I wish to express my sincere gratitude to my research supervisor, *Dr. Debasish Das*, Department of Biosciences and Bioengineering and Centre for Energy, for giving me an opportunity to pursue this research work, and for his continuous care, precious advice, guidance, encouragement, and supervision of the research. I must acknowledge the unconditional freedom to think, plan, execute and express, that I was given in every step of my research work, while keeping faith and confidence on my capabilities.

My gratitude goes to my doctoral committee members, *Dr. Pranab Goswami*, *Dr. Kaustubha Mohanty* and *Dr. Vaibhab V. Goud* for their constructive criticism and suggestions, which helped me to improve my work pertaining to Ph.D. thesis.

My sincere gratitude to *Dr. Alope Kumar Ghoshal* and *Dr. L. Sahoo* for their timely advice and encouragement during my research work at IIT Guwahati.

I owe my thanks to the *Department of Biosciences and Bioengineering*, *Centre for Energy*, and *Central Instrumentation Facility*, IIT Guwahati for providing me the necessary facilities to fulfill my Ph.D. thesis objectives.

My heartfelt thanks are due to *lab in charges* Dr. Lepakshi Barbora, Mr. Debarshi Baruah, Mr. Dhiren HuZuri, Mrs. Anita, Mrs. Prarthana, Mr. Nurul, Mr. Dipankar, Mr. Chandan and Mr. Niranajan during the course of my research.

I would also like to thank *IIT Guwahati* for providing financial assistance, *MHRD* and *DST* for funding my Ph.D. project, which made this study possible.

It was pleasure to work with *Dr. Muthusivaramapandian, Basavaraj, Baskar, Kumaran, Saumya, Mehak, Meenakshi, Mayur, Bidhu, Barsha, Reeshav, Bikas, Suraj and Shamik*. Thanks to them for their suggestions, time, help in practical things and kindness throughout my Ph.D., this is an unforgettable experience.

I thank to my *friends* for being supportive and providing a welcome diversion from the critical situations during my Ph.D., whenever I needed. I must acknowledge all my friends for their love, encouragement and support.

My special thanks and appreciation goes to *my parents, my wife Swati, my son Ahan* as well as my *family members* for their blessings, love, patience, support and understanding throughout my studies and most of all to the *Almighty God* who made everything possible.

Date: March, 2017

Vikram Kumar

Abstract

Exhaustive fuel reserves worldwide has renewed and invigorated interest towards alternate sources of fuel which would serve dual function of being renewable and sustainable to the environment. In purview of modern trends, microalgal cultivation has gained significant interest as a pioneer for the sustainable production of biodiesel attributed to its innate ability to accumulate substantially large amounts of neutral lipids as compared to oil plants. Current state of art makes it economically infeasible for commercialization which can be accounted to the several bottlenecks that persist during the upstream and downstream processes. Rationale for strain improvement as well as process strategy modification are being essential for development towards a more sustainable process as far as biodiesel production is concerned.

In the present study, indigenous microalgal strains were isolated and screened for maximum neutral lipid accumulation. The best strain with inherent ability to accumulate neutral lipid was further taken for detailed characterization and evaluation under different cultivation conditions such as photoautotrophic, heterotrophic and mixotrophic mode. Oil quality in terms of fatty acid compositions of the biomass obtained from different cultivation conditions were also evaluated by gas chromatography (GC). In order to achieve enhanced biomass and lipid productivity two process engineering strategies were developed: (i) one stage two phase high cell density mixotrophic fed-batch cultivation and (ii) synchronized growth and neutral lipid accumulation under mixotrophic growth in fed-batch and chemostat mode achieved via manipulation of substrates feeding mode and supplementation of lipid

elicitors in the growth medium. Finally, electrochemical harvesting method was employed to pre-concentrate the microalgal culture broth as a sustainable alternatives to the existing methods and the biomass was converted to biodiesel via *in situ* transesterification.

The key findings were: A novel indigenous microalgal strain *Chlorella sorokiniana* FC6 IITG was isolated and identified (GENEBANK Accession no.: JX453208) to accumulate total lipid up to 16% (w/w, DCW) under un-optimized growth conditions in shake flask condition. Characterization of the strain under different pH and temperature revealed the inherent robustness of the strain in terms of its growth in wide range of pH from 4 to 10 and at temperatures of range 20-44°C. The strain was also found to be capable of utilizing organic carbon sources under heterotrophic and mixotrophic growth conditions. Media optimization resulted in 19% improvement of biomass titer (0.69 g L⁻¹) for the strain as compared with the un-optimized photoautotrophic growth conditions. Further evaluation of the strain in automated bioreactor under different trophic (photoautotrophic, heterotrophic and mixotrophic) modes showed significant variation in the biomass productivity (142.06 to 455.50 mg L⁻¹ day⁻¹) and total lipid productivity (47.20 to 111.85 mg L⁻¹ day⁻¹). Mixotrophic batch cultivation was found to be superior to photoautotrophic & heterotrophic mode in terms of biomass and lipid productivity of 455.5 mg L⁻¹ day⁻¹ and 111.85 mg L⁻¹ day⁻¹ respectively. A single-stage two phase fed-batch mixotrophic cultivation strategy resulted in higher biomass titer of 15.81 g L⁻¹ with a lipid content of 54.95%, w/w DCW and significant improvement in biomass and lipid productivity (1.93 g L⁻¹ day⁻¹ and 550 mg L⁻¹ day⁻¹ respectively) from batch cultivation. Further, improvement in biomass and lipid productivity was achieved by process engineering strategy to achieve simultaneous growth and lipid accumulation by using lipid inducers (a combination of sodium chloride and sodium acetate). Synchronized growth and lipid accumulation under fed-batch & chemostat operation mode resulted in lipid productivity of 0.97 g L⁻¹ day⁻¹ and 1.27 g L⁻¹ day⁻¹

respectively. Maximum lipid productivity of $1.27 \text{ g L}^{-1} \text{ day}^{-1}$ which is comparable to the existing cultures reported in various literatures. Electrochemical harvesting showed 72% microalgae recovery efficiency at optimum operational parameter which could be a viable option for pre-concentration of microalgae. Fatty acid methyl ester (FAME) composition analysis reveals the majority of fatty acid was C16:0, C16:1, C18:0, C18:1 and C18:2 which depicts its suitability as biodiesel. Therefore, biodiesel obtained from *Chlorella sorokiniana* FC6 IITG grown under mixotrophic fed-batch or chemostat condition under the influence of inducer molecule can be used for commercial applications as it satisfies overall ASTM D6751-15a and EN 14,214 standards. The abovementioned qualitative and quantitative analysis further strengthens the claim of this novel indigenous strain as a potent cell factory for biodiesel production.

CONTENTS

	Page no.
Abstract	i
Contents	iv
List of Figures	xi
List of Tables	xx
1. Introduction	1
1.1 Background and motivation	1
1.2 Objectives of the study	3
1.3 Approach	3
1.4 Organization of the thesis	5
1.5 References	6
2. Review of literature	7
2.1 Global energy scenarios and alternate renewable energy resources	7
2.2 Biofuels	10
2.3 Microalgae are emerging renewable feedstock for biodiesel production	14
2.4 Classification and biology of microalgae	17
2.5 Biosynthesis of fatty acids and triacylglycerols	18
2.6 Microalgae cultivation: mode of nutrition and reactor types	20
2.7 Process engineering strategies for improved biomass and lipid productivity	28
2.8 Dewatering technologies for harvesting of microalgae	29
2.9 Processing of microalgal biomass for biodiesel generation	34

2.10	References	37
3.	Sampling, isolation and identification of the suitable microalgal strain for biodiesel production	48
3.1	Background and motivation	49
3.2	Materials and methods	50
3.2.1	Sampling and isolation of indigenous microalgal strains	50
3.2.2	Screening of neutral lipid accumulating microalgal strain	50
3.2.3	Identification of the microalgal strain	52
3.2.4	Analytical techniques	53
3.2.4.1	<i>Analysis of growth</i>	53
3.2.4.2	<i>Quantitative estimation of intracellular neutral lipid accumulation by Nile-red method</i>	53
3.2.4.3	<i>Qualitative detection of intracellular neutral lipid accumulation by confocal microscope</i>	54
3.2.4.4	<i>Analysis of fatty acids methyl esters (FAME) derived from microalgae</i>	55
3.3	Results and discussion	56
3.3.1	Sampling and isolation of indigenous microalgal strains	56
3.3.2	Screening and selection of neutral lipid accumulating microalgal strains	57
3.3.3	Selection of the growth medium for selected indigenous microalgal strain	58
3.3.4	Morphometric and molecular identification of the organism	59
3.3.5	Fatty acid profile of the stored lipid obtained from <i>Chlorella sorokiniana</i> FC6 IITG	60
3.4	Conclusions	61
3.5	References	63

4. Development of direct transesterification (DT) method for accurate quantification of microalgal lipid content	65
4.1 Background and motivation	66
4.2 Materials and methods	68
4.2.1 Algal culture and biomass preparation	68
4.2.2 Selection of best combination of transesterification method and biomass type	69
4.2.3 Optimization of process parameters for transesterification by statistical design	71
4.2.4 Field emission scanning electron microscopic analysis	73
4.2.5 FAME analysis using GC	73
4.2.6 Fourier transform infrared spectrophotometer (FTIR) Analysis	74
4.2.7 Statistical analysis	74
4.3 Results and discussion	74
4.3.1 Selection of best combination of biomass type and transesterification method	74
4.3.2 Optimization of process parameters for transesterification	77
4.3.3 Effect of transesterification methods on hydrolysis and transesterification efficiency	82
4.3.4 Fourier transform infrared (FTIR) spectroscopy	85
4.4 Conclusions	86
4.5 References	88
5. Physicochemical characterization of the strain and media optimization for maximization of growth	91
5.1 Background and motivation	92
5.2 Materials and methods	93
5.2.1 Microalgal strain, media composition and inoculum preparation	93

5.2.2	Characterization of the strain under different physicochemical conditions	94
5.2.3	Media optimization for biomass maximization using statistical tools	95
5.2.3.1	<i>Optimization of glucose and acetate concentration for growth of FC6</i>	96
5.2.4	Analytical methods	96
5.2.4.1	<i>Analysis of growth and fatty acids methyl esters (FAME) derived from microalgae</i>	96
5.2.5	Quality of biodiesel generated from <i>Chlorella sorokiniana</i> FC6 IITG	97
5.3	Results and discussion	98
5.3.1	Effect of pH and temperature on biomass titer and intracellular lipid content	98
5.3.2	Effect of nitrogen sources on biomass titer and intracellular lipid content	99
5.3.3	Effect of carbon sources on biomass titer and intracellular lipid content of FC6	101
5.3.4	Media optimization for growth of FC6 under different cultivation conditions	103
5.3.4.1	<i>Optimization of BG11 media for photoautotrophic growth</i>	103
5.3.4.2	<i>Optimization of carbon sources under heterotrophic and mixotrophic conditions</i>	108
5.3.5	Effect of physicochemical parameters on FAME composition and quality of biodiesel	108
5.4	Conclusions	114
5.5	References	116
6	Biochemical characterization of the strain under different cultivation conditions	119
6.1	Background and motivation	120
6.2	Materials and methods	121

6.2.1	Microalgal strain, media composition and inoculum preparation	121
6.2.2	Evaluation of the strain under different trophic modes	122
6.2.3	Analysis of growth, substrates utilization and biomass composition	123
6.2.3.1	<i>Analysis of growth</i>	123
6.2.3.2	<i>Analysis of nitrate utilization</i>	124
6.2.3.3	<i>Analysis of sodium acetate utilization</i>	125
6.2.3.4	<i>Analysis of phosphate utilization</i>	125
6.2.3.5	<i>Analysis of glucose utilization</i>	126
6.2.3.6	<i>Analysis of intracellular carbohydrate formation</i>	126
6.2.3.7	<i>Analysis of intracellular protein formation</i>	127
6.2.3.8	<i>Analysis of intracellular chlorophyll formation</i>	128
6.2.3.9	<i>Analysis of fatty acids methyl esters (FAME) derived from microalgae</i>	128
6.2.4	Quality assessment of biodiesel generated from FC6 under different cultivation conditions	129
6.3	Results and discussion	129
6.3.1	Characterization of <i>Chlorella sorokiniana</i> FC6 IITG under different trophic mode in an automated bioreactor	129
6.3.2	Composition of FAME obtained from <i>Chlorella sorokiniana</i> FC6 IITG grown under different cultivation conditions	135
6.3.3	Evaluation of biodiesel quality obtained from <i>Chlorella sorokiniana</i> FC6 IITG grown under different cultivation conditions	137
6.4	Conclusions	138
6.5	References	140
7	Process development for high cell density lipid rich microalgae cultivation and enhanced lipid productivity via synchronized growth and lipid accumulation under fed-batch & chemostat mode	144

7.1	Background and motivation	145
7.2	Materials and methods	147
7.2.1	Generation of high cell density lipid rich biomass using single-stage two phase fed-batch mode	147
7.2.2	Screening and optimization of elicitor molecules for lipid induction	148
7.2.3	Process development for synchronized growth and neutral lipid accumulation automated photobioreactor under fed-batch & chemostat operation mode	150
7.2.4	Analysis of growth, substrate utilization and FAME composition	151
7.3	Results and discussion	153
7.3.1	Generation of high cell density lipid rich biomass using single-stage two phase fed-batch mode	153
7.3.2	Screening of elicitor molecules for improved lipid productivity of <i>Chlorella sorokiniana</i> FC6 IITG	157
7.3.2.1	<i>Evaluation and optimization of combined effect of sodium acetate and sodium chloride on neutral lipid productivity</i>	161
7.3.3	Process development for synchronized biomass and neutral lipid accumulation in an automated photobioreactor	165
7.3.3.1	<i>Fed-batch cultivation with intermittent feeding of limiting nutrients and elicitors</i>	166
7.3.3.2	<i>Continuous mode of cultivation of FC6</i>	167
7.3.4	FAME composition and biodiesel property	170
7.4	Conclusions	173
7.5	References	174
8	Development of electrochemical dewatering process for efficient harvesting of microalgae	178
8.1	Background and Motivation	179
8.2	Materials and Methods	182

8.2.1	Microalgal strain, media composition and microalgae cultivation	182
8.2.2	Pre-concentration of algal biomass via electrochemical harvesting using carbon electrode	182
8.2.3	Analytical methods	184
8.3	Results and Discussions	184
8.3.1	Pre-concentration of algal biomass via electrochemical harvesting using carbon electrode	184
8.3.1.1	<i>Effect of applied voltage on microalgal recovery efficiency</i>	185
8.3.1.2	<i>Effect of broth pH on microalgal recovery efficiency</i>	186
8.3.1.3	<i>Effect of electrolyte on microalgal recovery efficiency</i>	187
8.3.1.4	<i>Effect of electrochemical harvesting process on lipid yield and fatty acid composition</i>	188
8.4	Conclusions	193
8.5	References	194
9	Conclusions	198
	Future Prospects	201
	APPENDIX	202
	List of Publications	
	Vitae	

List of Figures

Figure	Description	Page No.
1.1	Process engineering approaches employed to generation of lipid rich algal biomass and direct transesterification for biodiesel production from a novel indigenous microalgal strain	4
2.1	Statistical distribution of the world's primary energy consumption. Oil consumption is expressed in percentage	8
2.2	Global Carbon dioxide emissions from fossil fuels and trend of carbon dioxide in atmosphere	8
2.3	Transesterification of triacylglycerols for the production of fatty acid methyl esters (biodiesel) with glycerol as byproduct using sodium hydroxide as catalyst and methanol as an acyl acceptor	12
2.4	Diagrammatic representation of generalized structural of an eukaryotic green algae	18
2.5	Overview of metabolic pathways of microalgal lipid and starch biosynthesis. 3PG, 3 phosphoglyceric acid; ACCase, acetyl-CoA carboxylase; ACP, acyl carrier protein; AGPase, ADP-glucose pyrophosphorylase; G3P, glyceraldehyde-3-phosphate; KSIII, 3-ketoacyl-acyl-carrier protein synthetase III; Rubisco, ribulose-1,5-bisphosphate carboxylase/oxygenase; RuBP, ribulose-1,5-bisphosphate; TE, thioesterase; TAG, Triacyl glycerol	19
2.6	Schematic representation of the open raceway ponds used for cultivation of microalgal strains	22
2.7	A schematic view of a tubular photobioreactor used for cultivation of microalgae at "Las Palmerillas" experimental station, Almería, Spain	25
2.8	A schematic diagram of bubble column photobioreactor with illustration of flow regimes used for cultivation of microalgae	25
2.9	Schematic view of a closed flat panel photobioreactor for cultivation of microalgae	26

Figure	Description	Page No.
3.1	Standard correlation graph for the estimation of neutral lipid (triolein) by Nile-red based assay method in fluorescent spectrophotometer. F.I. (a.u.) represents fluorescence intensity. All the experiments were conducted in triplicate and the data were represented as mean \pm standard error.	54
3.2	Standard correlation graph for the estimation of total lipid as fatty acid methyl esters assayed in gas chromatograph with standard FAME mix C14-C22	56
3.3	Screening and selection of high lipid accumulating indigenous microalgal strains. The neutral lipid content was measured using Nile-red method.	57
3.4	Confocal imaging of strain FC6 under higher magnification (A) superimposed image of bright field cells, auto-fluorescence of cells stained with Nile Red and fluorescence from Nile red-neutral lipid complex; (B) Cells showing auto-fluorescence in red color and Nile red-neutral lipid complex fluorescence as golden yellow color. The images were obtained using confocal microscope with Olympus software.	58
3.5	Selection of best growth media for the growth of indigenous microalgal strain FC6. Six different media compositions were used as detailed in section 3.2.2 (Table 3.1)	59
3.6	Morphometric identification of FC6 Strain: (A) Cells under phase contrast microscope and (B) Field effect scanning electron microscopic image of the cell obtained at 2.0KV EHT and 5 KX magnification	60
3.7	Molecular analysis of FC6. Phylogenetic tree based on 18S rDNA sequences of the strain and genus within the order <i>Chlorellales</i> . The tree was constructed using neighbor-joining method with Jukes-cantor model. Bootstrap test (1000 replicates in %) is shown next to the branches and taxon name starts with the gene accession number. The isolated strain reported in this study is marked with (●)	61
4.1	Schematic representation of eight different transesterification methods (M1-M8) conducted with three different types of biomass used in the present study. A total of 24 experiments were carried out to select best combination of transesterification and biomass type with FAME yield as process response. M1 represent conventional method of extraction-transesterification. M2, M3 & M4 represent one step DT methods with NaOH, HCl and H ₂ SO ₄ as the catalyst respectively. M5-M8 represents two stage DT with different combination of acid-base catalyst. All the transesterification experiments were performed with	70

Figure	Description	Page No.
	methanol as the solvent at a temperature of 90 °C and a constant shaking of 150 rpm in a shaking water bath	
4.2	FAME yield (% , w/w DCW) of the <i>Chlorella</i> sp. FC2 IITG obtained from eight different transesterification methods (M1-M8) and three different types of biomass. The significant difference among the biomass types is represented as ‘*’ and the significant difference among the methods M1-M8 for each type of biomass are represented as ‘a’ obtained from one way analysis of variance (corresponding p-values for * = 0; ** = 0.022; a = 0)	75
4.3	Response surface plots representing the effect of various parameters and their interaction on FAME yield. (A) methanol to biomass ratio and NaOH to biomass ratio (B) reaction time and NaOH to biomass ratio (C) reaction time and methanol to biomass ratio (D) methanol to biomass ratio and H ₂ SO ₄ to biomass ratio (E) reaction time and H ₂ SO ₄ to biomass ratio (F) reaction time and methanol to biomass ratio	80
4.4	Comparison of FAME yield (% , w/w DCW) obtained by Bligh Dyer method (BD) and optimized DT method (ODT). FC2-BD and FC2-ODT represents conventional Bligh Dyer method and optimized DT method respectively for <i>Chlorella</i> sp. FC2 IITG. FC6-BD and FC6-ODT represents conventional Bligh Dyer method and optimized DT method respectively for <i>Chlorella sorokiniana</i> FC6 IITG.	82
4.5	Field emission scanning electron microscopic images for the (A) control (untreated) algal cells and the residual materials obtained after DT methods (B) M4, (C) M8 and (D) optimized M7. The images were in uniform scale of 10 µm. For details on the sample preparation method refer to the material and method section 4.2.4.	83
4.6	Comparison of transesterification efficiency for eight different transesterification methods (M1-M8) and optimized M7 method with glyceryl-triheptadecanoate as internal standard. For experimental details refer Fig. 4.1	85
4.7	(A) Microalgal biodiesel produced from <i>Chlorella</i> sp. FC2 IITG biomass via optimized two stage DT method (B) FTIR spectra of algal biodiesel, mustard biodiesel and petro-diesel	86
5.1	Effect of (A) temperature and (B) initial medium pH on biomass titer in terms of dry cell weight (double crossed bars) and total lipid content in terms of fatty acid methyl esters (black shaded bars) of the strain FC6 under photoautotrophic growth condition	99
5.2	Effect of various nitrogen sources on biomass titer in terms of dry cell weight (double crossed bars) and total lipid content in terms of fatty acid methyl esters (black shaded bars) of the strain FC6. Different	100

Figure	Description	Page No.
	nitrogen sources with equimolar concentration of nitrogen (0.018 M) was used under photoautotrophic condition: Sn sodium nitrate; Pn potassium nitrate; Sni sodium nitrite; Ac ammonium chloride; Ur urea; Me meat extract; G glycine; Ye yeast extract; P peptone	
5.3	Effect of various carbon sources under (A) heterotrophic cultivation and (B) mixotrophic cultivation, on biomass titer in terms of dry cell weight (double crossed bars) and total lipid content in terms of fatty acid methyl esters (black shaded bars) of the strain FC6. Different carbon sources with equimolar concentration (6M) of carbon was used for heterotrophic & mixotrophic conditions: GL glucose; Fr fructose; Su sucrose; Lac lactose; Mal maltose; Sa sodium acetate	102
5.4	Response surface plot representing the effect of various parameters and their interaction on biomass titer (g L^{-1}) by FC6: (A) trace element and sodium nitrate, (B) phosphate and sodium nitrate, (C) trace element and phosphate, (D) microelement and sodium nitrate, (E) microelement and phosphate, (F) microelement and trace element	106
5.5	Comparison of biomass titer (g L^{-1}) from un-optimized BG11 media and optimized BG11 media under shake flask photoautotrophic growth condition	107
5.6	(A) Effect of different concentrations of sodium acetate on growth of the strain under heterotrophic condition, (B) Effect of different concentrations of glucose on growth under mixotrophic cultivation	108
6.1	Correlation between dry cell weight of the biomass and absorbance measured at 690 nm in a spectrophotometer under (A) photoautotrophic, (B) heterotrophic and (C) mixotrophic growth conditions	124
6.2	Correlation graph between concentration of the substrates and their respective area in HPLC for the estimation of (A) sodium nitrate, C_{NO_3} represents concentration of sodium nitrate and (B) sodium acetate, C_{SA} represents concentration of sodium acetate	125
6.3	Correlation graph between concentration of the substrates and their respective absorbance in UV-Visible spectrophotometer for estimation of (A) phosphate, C_{PO_4} represents concentration of phosphate and (B) glucose, C_{Glu} represents concentration of glucose	126
6.4	Correlation graph between concentration of the substrates and their respective absorbance in UV-Visible spectrophotometer for the estimation of (A) carbohydrate, C_{carb} represents carbohydrate concentration; and (B) protein, C_{Prot} represents protein concentration	127

Figure	Description	Page No.
6.5	Dynamic profiles of growth and changes in intracellular lipid accumulation of the strain FC6 under photoautotrophic (●), heterotrophic (○) and mixotrophic (▼) conditions: (A) growth, (B) lipid percentage in the biomass. The strain was grown under different growth condition at 28 °C and 400 rpm in a 3 L automated bioreactor. Light intensity of 150 $\mu\text{E m}^{-2} \text{s}^{-1}$ for 16:8 h light: dark cycle and aeration with CO ₂ of 1% (v/v) was provided under photoautotrophic condition. The conditions for mixotrophic cultivation was same as photoautotrophic growth with additional supplementation of glucose in the BG11 medium. The heterotrophic growth was conducted under complete dark with supplementation of sodium acetate in the BG11 medium	130
6.6	Substrate utilization profile of the strain <i>Chlorella sorokiniana</i> FC6 IITG grown under photoautotrophic (●), heterotrophic (○) and mixotrophic (▼) conditions: (A) nitrate utilization profile, (B) phosphate utilization profile, (C) glucose utilization profile under mixotrophic growth (▼) and sodium acetate utilization profile under heterotrophic cultivation condition (○). The strain was grown under different growth condition at 28 °C and 400 rpm in a 3 L automated bioreactor. Light intensity of 150 $\mu\text{E m}^{-2} \text{s}^{-1}$ for 16:8 h light: dark cycle and aeration with CO ₂ of 1% (v/v) was provided under photoautotrophic condition. The conditions for mixotrophic cultivation was same as photoautotrophic growth with additional supplementation of glucose in the BG11 medium. The heterotrophic growth was conducted under complete dark with supplementation of sodium acetate in the BG11 medium	132
6.7	Intracellular composition of macromolecules in the strain <i>Chlorella sorokiniana</i> FC6 IITG grown under different trophic modes: (A) Carbohydrate content; (B) protein content; and (C) total chlorophyll content. The strain was grown grown under photoautotrophic (●), heterotrophic (○) and mixotrophic (▼) conditions on modified BG11 medium at 28°C and 400 rpm in a 3 L automated bioreactor	134
7.1	Dynamic profiles of growth, lipid and step-wise increase in light intensity under single stage fed-batch mixotrophic cultivation: (a) biomass (●) and lipid content (▲) and (b) step-wise increase in light intensity. The strain was grown in a 3 L automated bioreactor at 28°C, 400 rpm with 150 to 350 $\mu\text{E m}^{-2} \text{s}^{-1}$ light intensity for 16:8 h light: dark cycle and aerated with CO ₂ of 1% (v/v). The white and black bars on X-axis shows the 16 h light and 8 h dark cycle. The process involves two phases: first phase represents the production of high cell density biomass with intermittent feeding of nitrate, phosphate and glucose along with dynamic change in light intensity and second phase represents lipid induction phase with sodium acetate as elicitor for lipid enrichment	155

Figure	Description	Page No.
7.2	Dynamic profiles of substrate utilization and intermittent feeding of substrates for single stage fed-batch mixotrophic cultivation of FC6 (a) phosphate profile (b) nitrate profile (c) glucose profile (▼) and sodium acetate profile (●). For experimental details, refer to the legend of figure 7.2	156
7.3	Effect of inducer molecules with their various levels of concentration on lipid content and lipid productivity of the FC6 grown under mixotrophic cultivation in shake flask. Different symbols indicate significant difference in biomass titer and lipid productivity obtained from the use of various lipid inducers analyzed using one way analysis of variance (*-represents $P = 0$; **-represents $0 < P < 0.05$; ***-represents $0.05 < P < 0.5$ and #-represents > 0.5). For statistical analysis the lowest concentration of the respective lipid inducer was kept as control group	158
7.4	Effect of inducer molecules with their various levels of concentration on lipid content and lipid productivity of the FC6 grown under mixotrophic cultivation in shake flask. Different symbols indicate significant difference in biomass titer and lipid productivity obtained from the use of various lipid inducers analyzed using one way analysis of variance (*-represents $P = 0$; **-represents $0 < P < 0.05$; ***-represents $0.05 < P < 0.5$ and #-represents > 0.5). For statistical analysis the lowest concentration of the respective lipid inducer was kept as control group	159
7.5	Effect of various elicitors on growth and lipid productivity of <i>Chlorella sorokiniana</i> FC6 IITG. The organism was grown on optimized BG11 medium supplemented with individual elicitor molecule and 15 g L^{-1} glucose as the primary carbon source for growth under mixotrophic condition in shake flask at 28°C , 150 rpm, and continuous light intensity of $30 \mu\text{E m}^{-2} \text{ s}^{-1}$. The values mentioned on top of bars represents the concentration of respective elicitor at which it supports maximum lipid productivity. Different symbols indicate significant difference in biomass titer and lipid productivity obtained from the use of various lipid inducers analyzed using one way analysis of variance (*-represents $P = 0$; **-represents $0 < P < 0.05$ and ***-represents $0.05 < P < 0.5$). The condition with glucose and no additional lipid inducer was taken as the control for statistical analysis	160
7.6	Combined effect of different concentrations of sodium chloride and sodium acetate in the ratio of 1:1 (w/w) on lipid content and lipid productivity of the strain grown under mixotrophic condition in shake flask	162
7.7	Response surface plot representing the interaction effect of sodium chloride and sodium acetate on lipid productivity ($\text{mg L}^{-1}\text{day}^{-1}$) of FC6 grown under mixotrophic condition in shake flask	164

Figure	Description	Page No.
7.8	Dynamic profiles for growth, intracellular lipid content, biomass & lipid productivity and substrate utilization pattern for the strain FC6 grown under mixotrophic fed-batch mode of operation in automated bioreactor of 7.5 L at 28°C, 250 rpm with 350 $\mu\text{E m}^{-2} \text{s}^{-1}$ continuous light intensity. The profiles represents: (A) biomass formation (—●—) & neutral lipid content (—□—); (B) biomass productivity (—●—) & neutral lipid productivity (—□—); (C) Nitrate (—▼—) & phosphate (—▽—) concentration, and (D) Glucose (—◆—) & sodium acetate (—◇—) concentrations. Solid arrow mark (↑) shows the feeding of respective substrate	166
7.9	Dynamic profiles for growth, intracellular lipid content, biomass and lipid productivity for the strain FC6 grown under mixotrophic continuous mode of operation in an automated bioreactor of 7.5 L at 28°C, 250 rpm with 350 $\mu\text{E m}^{-2} \text{s}^{-1}$ continuous light intensity. The profiles represents: (A) biomass formation (—●—) & neutral lipid content (—□—) and (B) biomass productivity (—●—) and neutral lipid productivity (—□—). The values of <i>D</i> depicts the dilution rate maintained in continuous cultivation	168
7.10	Dynamic profiles for substrate utilization and concentration of lipid inducer for the strain FC6 grown under mixotrophic continuous mode of operation in an automated bioreactor of 7.5 L at 28°C, 250 rpm with 350 $\mu\text{E m}^{-2} \text{s}^{-1}$ continuous light intensity. The profiles represents: (A) phosphate (—▼—) & nitrate (—▽—) concentration and (B) glucose (—◆—) & sodium acetate (—◇—) concentration. The values of <i>D</i> depicts the dilution rate maintained in continuous cultivation	169
8.1	Schematic diagram of electrochemical harvesting unit	183
8.2	Effect of applied voltage on microalgal recovery efficiency during electrochemical harvesting treatment. Data expressed as mean \pm standard error (n= 3)	185
8.3	Effect of initial culture pH on microalgal recovery efficiency in electrochemical harvesting treatment. Data expressed as mean \pm standard error (n= 3)	187
8.4	Effect of electrolyte (NaCl) concentration on microalgal recovery efficiency of <i>Chlorella sorokiniana</i> FC6 IITG in electrochemical harvesting treatment. Data expressed as mean \pm standard error (n= 3)	188
8.5	Effect of applied current and initial culture pH on lipid yields of biomass harvested by electrochemical harvesting process. Data expressed as mean \pm standard error (n= 3).	190

List of Tables

Table	Description	Page No.
2.1	Comparison of various biodiesel producing feedstock	12
2.2	Comparison of first, second and third generation biofuel with petro-diesel	13
2.3	Oil content obtained from various microalgal strains measured in weight percentage of the dry cell weight	16
2.4	Benefits and limitations of open ponds and various type of photobioreactor for algal cultivation	23
2.5	Comparison of various dewatering techniques on the basis of microalgae recovery efficiencies and energy consumption	30
3.1	Common growth media used for isolation of microalgal strains from freshwater habitats	51
4.1	Actual and coded levels of the selected three transesterification parameters used in both the stages of CCD-RSM experimental design	72
4.2	CCD matrix of independent transcription parameters used in RSM with corresponding experimental and predicted measurements of FAME yield (% , w/w DCW) in first and second stages	72
4.3	ANOVA for the quadratic regression model obtained from CCD-RSM employed in optimization of parameters involved in two stage sequential direct transesterification of lipid from <i>Chlorella</i> sp. FC2 IITG	79
5.1	Actual levels of the BG11 media components used in CCD-RSM experimental design for optimization of FC6 growth under photoautotrophic condition	95
5.2	CCD matrix of independent media components used in RSM with corresponding experimental and predicted measurements of biomass titer (g L^{-1})	103

Table	Description	Page No.
5.3	ANOVA for the quadratic regression model obtained from CCD-RSM employed in optimization of media components for the growth of FC6	104
5.4	BG11 Media components, their corresponding concentrations and the biomass titer (g L^{-1}) predicted by optimization tools	105
5.5	Fatty acid profile of autotrophically cultured algae <i>Chlorella sorokiniana</i> FC6 IITG at different temperature and pH	110
5.6	Effect of nitrogen sources on FAME composition under photoautotrophic cultivation	110
5.7	Effect of carbon sources on FAME composition under heterotrophic and mixotrophic cultivation	112
5.8	Effect of physicochemical parameters on the quality of biodiesel obtained from the microalga <i>Chlorella sorokiniana</i> FC6 IITG	113
6.1	Kinetic parameters for growth and lipid formation of FC6 cultivated under photoautotrophic, heterotrophic and mixotrophic cultivation conditions	131
6.2	Fatty acid methyl esters (FAME) profile of strain FC6 grown under different cultivation conditions	136
6.3	Quality analysis of the biodiesel obtained under different cultivation conditions from the microalga <i>Chlorella sorokiniana</i> FC6 IITG and comparison with European/ASTM standards	138
7.1	Screening of elicitor molecules for lipid induction and also supports synchronized growth and lipid accumulation in <i>Chlorella sorokiniana</i> FC6 IITG	149
7.2	Actual levels of the inducer concentration used in CCD-RSM experimental design for optimization of inducer concentration for maximum lipid productivity under mixotrophic condition	162
7.3	CCD matrix of independent inducer components used in RSM with corresponding experimental and predicted measurements of lipid productivity ($\text{mg L}^{-1} \text{ day}^{-1}$)	163
7.4	ANOVA for the quadratic regression model obtained from CCD-RSM employed in optimization of inducer concentration for the maximization of lipid productivity	164
7.5	Fatty acid methyl esters (FAME) profile of strain FC6 grown under different cultivation mode	171

Table	Description	Page No.
7.6	Estimated properties of algal biodiesel obtained from strain FC6 grown under different operational modes	172
8.1	Fatty acid composition (%) of microalgae <i>Chlorella sorokiniana</i> FC6 IITG harvested by electrochemical harvesting coupled with centrifugation and compared with control	191
8.2	Estimated properties of the algal biodiesel obtained from <i>Chlorella sorokiniana</i> FC6 IITG biomass harvested by electrochemical harvesting followed by centrifugation	192



CHAPTER 1

Introduction

1.1 Background and motivation

About 90% of the world's total energy demand is met from the fossil fuel resources which has led to its depletion and according to the present statistics these resources cannot last more than 50-60 years from now (Yen et al., 2013; BP statistical review 2015). This extensive utilization has also led to increased greenhouse gas emissions resulting in global warming which remains a major issue to be addressed. To that end, several researchers are attending to identify sustainable, renewable, alternate clean energy resources that can fulfill the current energy demands by replacing conventional fossil fuels with less environmental issues (Lam and Lee, 2012). Among the various potential sources of renewable energy, biofuels are of most interest and are expected to play a crucial role in the global energy infrastructure of the future. Biodiesel is one of the most commonly used biofuels which has been recognized as an ideal recyclable energy carrier, and thus also as a possible primary energy source (Chisti, 2007). Production of biodiesel has evolved through several generations based on the type of feedstocks utilized while, oleaginous microalgae have been considered as one of the most promising 3rd generation feedstock for renewable and sustainable production of biodiesel (Chisti, 2007). This increasing importance of microalgae are attributed to its key inherent properties such as higher photosynthetic efficiency, higher biomass and lipid productivity in comparison to other plant resources and their ability to grow under wide range of cultivation conditions (Hu et al., 2008; Ho et al., 2014).

Microalgae are known to have twenty times more productivity (in terms of oil) than oil seed crops thus providing chances for the complete replacement of fossil fuel utilization (Subhadra, 2010). However, the current state of art technologies has several bottlenecks in different stages of upstream and downstream processes which hinders the commercialization of biodiesel production processes. For example strain selection, growth of microalgal strains under outdoor conditions, contamination, light penetration through dense culture, harvesting, drying, extraction and transesterification are the major rate limiting steps that hinders commercialization of microalgal biodiesel (Lam and Lee, 2012). Thus, sustainability and techno-economic feasibility of algae based biodiesel calls for a significant improvement at both the strain level and the process level.

Strain selection is an important step in developing a feasible bioprocess (Mutanda et al., 2011). In spite of several oleaginous microalgae with high lipid content are being identified, novel indigenous strains with robustness (capable of growing under fluctuating environmental conditions) and high net lipid productivity need to be isolated. Indigenous microalgal strains will be of good choice as these organism can adapt to the changes in environmental conditions in that particular native habitats. It is also important to note that microalgal growth and lipid production are two mutually exclusive phenomena and therefore, the optimized condition required for growth may not be suitable for oil production (Muthuraj et al., 2014). Thus, the techno-economic feasibility of the process is governed by three key parameters: (i) biomass titer (ii) neutral lipid content and (iii) lipid productivity (Muthuraj et al., 2014). Thus to achieve process sustainability all these parameter has to be simultaneously enhanced. To that end, a process engineering approach needs to be employed which involves novel engineering strategies to achieve lipid rich high cell density cultivation or synchronized enhancement of growth and lipid accumulation. Further, sustainability can be achieved by designing an effective harvesting method. Ho et al. (2014) concluded that

more critical engineering innovation in both upstream and downstream processes are required to harness the full potential of microalgae based biodiesel production.

1.2 Objectives of the study

- ✓ *Sampling, isolation and identification of the suitable microalgal strain for biodiesel production.*
- ✓ *Development of direct transesterification (DT) method for accurate quantification of microalgal lipid content.*
- ✓ *Physicochemical characterization of the strain and media optimization for maximization of growth.*
- ✓ *Biochemical characterization of the strain under different cultivation conditions.*
- ✓ *Process development for high cell density lipid rich cultivation and enhanced lipid productivity via synchronized growth and lipid accumulation under fed-batch & chemostat mode.*
- ✓ *Development of electrochemical dewatering process for efficient harvesting of microalgae.*

1.3 Approach

The present study targeted to isolate and screen novel indigenous microalgal strains from the North-East part of India with high neutral lipid content and process engineering approaches for generation of lipid rich algal biomass (Fig. 1.1). The best strain with inherent ability to accumulate neutral lipid was further taken for identification using a polyphasic approach involving both morphological and molecular analyses. As multiple microalgal strains are involved, there was a need to develop a universal in situ transesterification method for accurate quantification of total lipids in terms of fatty acid methyl esters (FAME). The selected strain was characterized and evaluated under different

nutritional/environmental parameters to understand its robustness. Further evaluation of the production potentials of the strain was carried out in an optimized growth media under different cultivation modes such as photoautotrophic, heterotrophic and mixotrophic conditions. Oil quality in terms of fatty acid compositions of the biomass obtained from different cultivation conditions was evaluated by gas chromatography (GC).

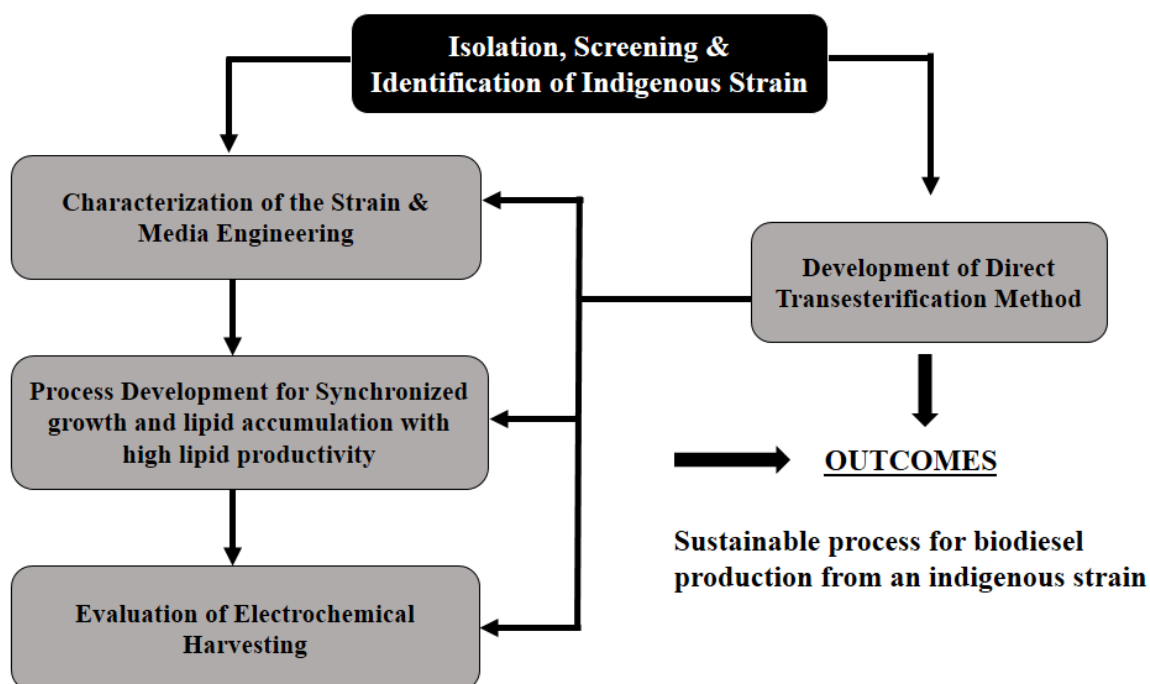


Fig. 1.1 Process engineering approaches employed to generation of lipid rich algal biomass and direct transesterification for biodiesel production from a novel indigenous microalgal strain

As an alternate to growth limited lipid accumulation and two stage nutrient starvation strategy which impose commercial scale operational difficulties, lipid elicitors were screened that support synchronized growth and neutral lipid accumulation in the strain was adapted in the present study. In the next step, high density of lipid rich biomass with maximum lipid productivity was achieved by dynamic increase in light intensity with growth and intermittent feeding of limiting nutrients (fed-batch operation). Fed-batch employing single stage two phase strategies which involves biomass generation in first phase and enhancement of lipid accumulation in second phase by using lipid elicitors was

demonstrated. Further improvement in the net lipid productivity of the strain was achieved by designing process engineering strategies to achieve synchronized growth and neutral lipid accumulation under fed-batch and chemostat in nutrient sufficient condition. Finally, an effective harvesting strategy and processing technology was designed for sustainable biodiesel production. Thus, the final outcome of the present study is to come up with a sustainable bioprocess for biodiesel production from microalgae (Fig. 1.1). The thesis comprises of nine chapters as outlined in the following section.

1.4 Organization of the thesis

The thesis comprises of 9 chapters. Chapter 1 outlines general introduction, objective and scope of the present work along with the approaches required to resolve the current issues. Chapter 2 provides a detailed review on the present processes and advancements made in the field of algal biodiesel and highlights the major bottlenecks with the current technologies. Chapter 3 deals with sampling, isolation, and identification of the suitable microalgal strain for biodiesel production. Chapter 4 involves the development of direct transesterification (DT) method for accurate quantification of microalgal lipid content. Chapter 5 describes the physicochemical characterization of the strain and media optimization. Chapter 6 details the biochemical characterization of the strain under different growth conditions. Chapter 7 deals with the process development for enhanced lipid productivity and generation of lipid rich microalgae biomass via (i) intermittent feeding of limiting nutrients (fed-batch mode) for high cell density cultivation followed by addition of lipid inducer for lipid enrichment and (ii) process engineering for simultaneous growth and lipid accumulation in fed-batch & chemostat culture. Chapter 8 explains the evaluation of electrochemical dewatering processes for efficient harvesting of microalgae. Finally, chapter 9 summarizes the present study with the conclusions made and future prospects of the work.

1.5 References

1. BP Statistical Review of World Energy 2015.
<http://www.bp.com/en/global/corporate/about-bp/energy-economics/statistical-review-of-world-energy.html>
2. Chisti, Y., 2007. Biodiesel from microalgae. *Biotechnol. Adv.* 25, 294-306.
3. Ho, S.H., Ye., X., Hasunuma, T., Chang, J.S., Kondo, A., 2014. Perspectives on engineering strategies for improving biofuel production from microalgae-A critical review. *Biotechnol. Adv.* 32, 1448-1459.
4. Hu, Q., Sommerfeld, M., Jarvis, E., Ghirardi, M., Posewitz, M., Seibert, M., Darzins, A., 2008. Microalgal triacylglycerols as feedstocks for biofuel production: perspectives and advances. *Plant J.* 54, 621-639.
5. Lam, M.K., Lee, K.T., 2012. Microalgae biofuels: a critical review of issues, problems and the way forward. *Biotechnol. Adv.* 30, 673-90.
6. Mutanda, T., Ramesh, D., Karthikeyan, S., Kumari, S., Anandraj, A., Bux, F. 2011. Bioprospecting for hyper lipid producing microalgal strains for sustainable biofuel production. *Bioresour. Technol.* 102, 57-70.
7. Muthuraj, M., Kumar, V., Palabhanvi, B., Das, D., 2014. Evaluation of indigenous microalgal isolate *Chlorella* sp. FC2 IITG as a cell factory for biodiesel production and scale up in outdoor conditions. *J. Ind. Microbiol. Biotechnol.* 41, 499-511.
8. Subhadra, B.G., 2010. Sustainability of algal biofuel production using integrated renewable energy park (IREP) and algal biorefinery approach. *Energy policy.* 38, 5892-5901.
9. Yen, H.W., Hu, I.C., Chen, C.Y., Ho, S.H., Lee, D.J., Chang, J.S., 2013. Microalgae based biorefinery from biofuels to natural products. *Bioresour. Technol.* 135, 166-174.

CHAPTER 2

Review of literature

2.1 Global energy scenarios and alternate renewable energy resources

Global population explosion associated with simultaneous increase in industrialization and rapid increase in use of fossil fuel reserves has led to the scarcity of natural oil on the surface of ever changing Earth. According to British Petroleum (BP) Statistical Review of World Energy June 2015, available global reserves of oil, natural gas and coal were estimated to be 1.70 trillion barrels, 187.1 trillion cubic meters and 0.89 trillion tons respectively. The consumption pattern of the 86% of primary energy worldwide has been majorly supported by oil which accounts to a total of 33% followed closely by coal which shares around 30% and 24% of the consumption by natural gas while rest of the energy demands are met by hydroelectricity, nuclear energy and renewable energy (Fig. 2.1). World consumption of oil when considered on a per day basis comes to 91.33 million barrels of which India alone consumes around 4.2%. This demand for energy on a worldwide scale is expected to rise by 37% from 2013 to 2035, or at a staggering rate of 1.4% per year. With this exponential consumption pattern, it is predicted that the fossil fuel reserves across the world will be exhausted in the next 50 years. (BP statistical review 2015). Current norms have widely accepted and blamed this unchecked use of fossil fuels for the alarming increase in the levels of greenhouse gases in the environment with an accumulation of 403.94 ppm of CO₂ (Fig. 2.2) which is way beyond its threshold value (<http://cdiac.ornl.gov>).

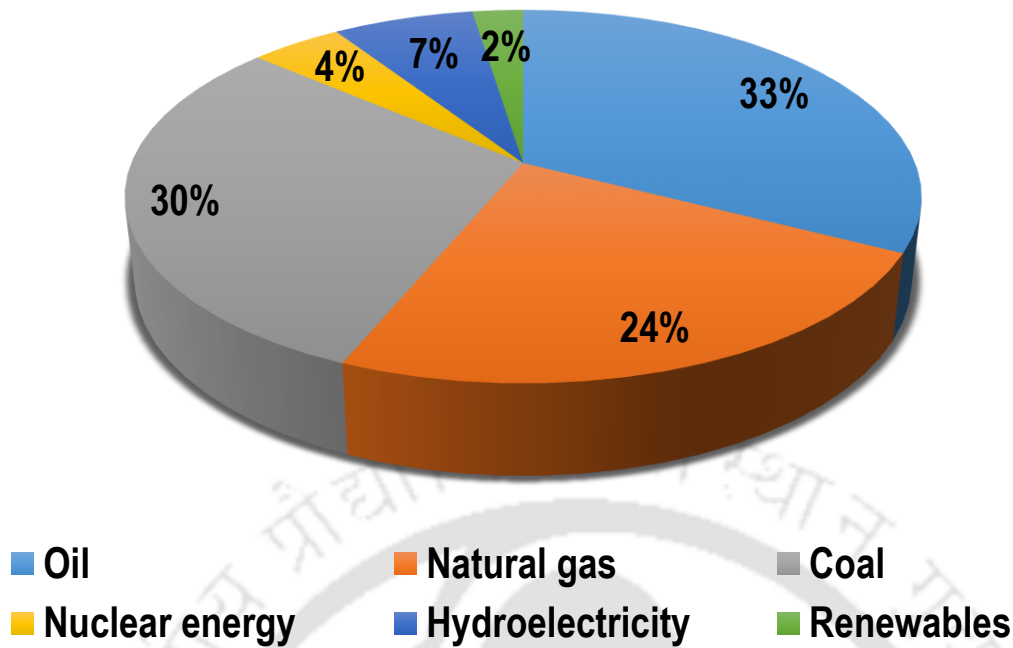


Fig. 2.1 Statistical distribution of the world’s primary energy consumption. Oil consumption is expressed in percentage (source: BP Statistical review 2015)

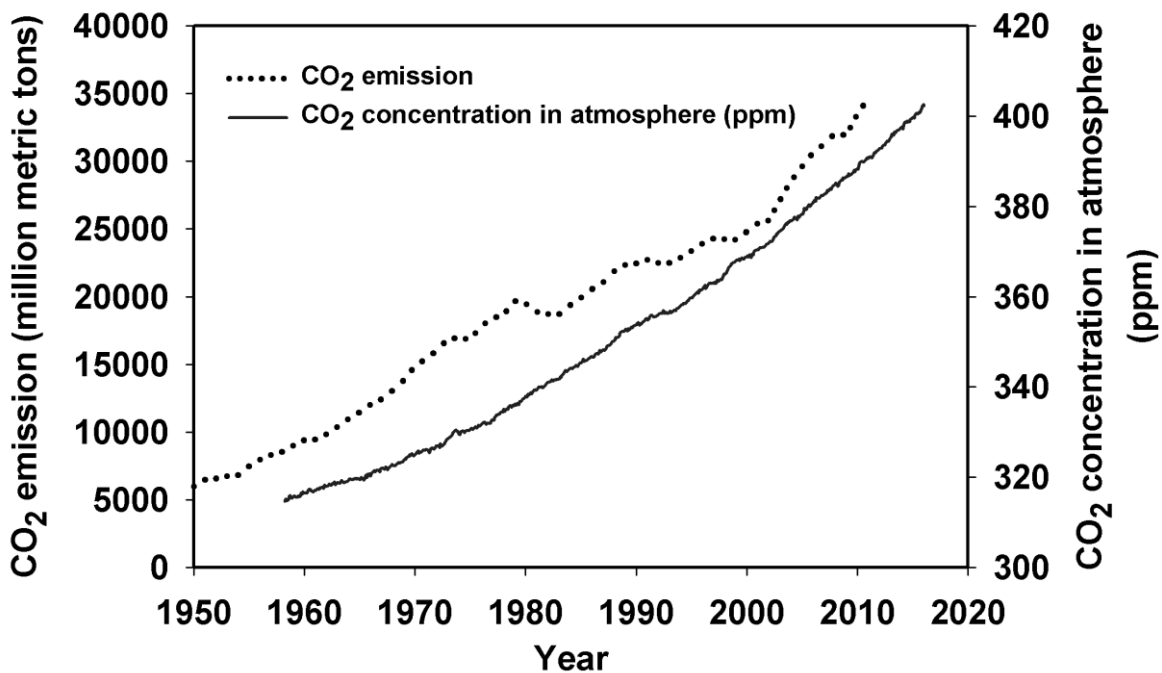


Fig. 2.2 Global Carbon dioxide emissions from fossil fuels and trend of carbon dioxide concentration in the atmosphere (source: <http://cdiac.ornl.gov>; <ftp://ftp.cmdl.noaa.gov>)

The world’s CO₂ emissions in to the atmosphere is increasing day by day and a rise of ~ 43% was reported in the year 2015 from 2000 with an average growth of 2 ppm year⁻¹ in the last ten years (Fig. 2.2). Global carbon dioxide (CO₂) emissions from fossil fuel

combustion and from industrial processes (cement and metal production) increased in 2013 to the new record of 35.3 billion tons CO₂, which is 0.7 billion tons higher than 2012. The International Energy Agency (IEA) has claimed that CO₂ emission levels in 2030 will be 63% and 90% higher than in 2014 and 1990 respectively (Ganesh, 2014). Increased level of CO₂ emission resulted in elevation of global temperature by 0.85°C from 1880 to 2012, and is projected to raise further by 1.4-5.8°C in 2100 (De Silva et al., 2015). This provides a motivation for a look out for alternate fuel sources. To combat this mercurial rise in the levels of CO₂, effective reduction in fossil fuel consumption and enhanced use of alternate renewable sources should be followed. Transportation sector which attributes to be the major consumer of fossil fuels globally (Singh et al., 2011) is not supported by solar, wind, wave, geothermal, hydropower and nuclear reactions which are currently the major alternative renewable energy resources available for electricity generation. (Parmar et al., 2011). There is a dearth in efforts to create renewable fuels which can provide an option to eliminate or limit the use of petro-diesel, otherwise considered to be the backbone of the transportation sector. Energy generation with the utilization of biomass has gained significant interest over the years, as one of the potential alternatives due to the following facts (i) can be utilized for generation of various forms of biofuels: liquid (ethanol, methanol, butanol, biodiesel, Fischer-Tropsch diesel), gaseous (hydrogen and methane), and solid state fuels; (ii) it is renewable in nature and can be made sustainable in future; (iii) high energy yielding efficiencies; (iv) reduced greenhouse gas emissions as compared to other fuels; (v) sustainability in terms of net zero carbon emissions making the whole process carbon neutral and (vi) significant economic potential as it may cost low (Demirbas, 2008; Singh and Gu, 2010). Therefore, biofuels were believed to be one of the viable option that can fulfil the current fuel demands (Demirbas, 2010). However, there exists several bottlenecks in achieving sustainability that requires immense attention of the researchers.

2.2 Biofuels

Biofuels are non-fossil fuels which can be defined as the fuels produced directly or indirectly from organic material such as biomass which involves both plant and animal waste. Biofuel is widely regarded as renewable, cleaner, safer and more eco-friendly energy resources, and importantly many of the biofuels can be used directly in existing internal combustion engine without modification (Hepbasli, 2008; Parmar et al., 2011). Rapid growth in the generation of liquid biofuels globally over the past few years have made them as a potential answer to the crisis arising due to the consumption of non-renewable resources (Brennan and Owende, 2010). Global biofuel production has increased from the equivalent of 16,445 thousand tons of oil in 2004 to the equivalent of 70,792 thousand tons of oil in 2014, an increase of nearly 330% (BP Statistical review 2015). There seems to be a global consent that biofuel has advantages such as renewability, cleanliness which not only can resolve conventional fossil energy supply problems, optimize energy structure and ensure national energy security but also can lower greenhouse gas emissions, reduce ecological degradation, promote regional economic growth, and increase farmers' income (Ji and Long, 2016). Biofuels are generally divided into three categories: first-generation, second-generation and third-generation biofuels.

First-generation biofuels i.e. biodiesel and bio-ethanol is primarily produced from cereals, grains, sugar crops and edible oil seeds. Bio-ethanol is generally produced from the fermentation of C6 sugars (mostly glucose) using classical or genetically modified yeast strains such as *Saccharomyces cerevisiae* (Lee and Lavoie, 2013). Although very advantageous process but increases in the sugar price are a problem for the bioethanol business. The first generation biofuels have garnered commercial level success and already established in USA, Brazil, and the European Union. These biofuels are mainly derived from food and oil crops including sugarcane, sugar beet, vegetable oils and animal fats.

However, impact of these biofuels in transportation sector is still limited due to their direct competition with food for crops use and agricultural land (Brennan and Owende, 2010; Adenle et al., 2013). The second generation biofuels mostly derived from wide array of feedstock, ranging from lignocellulosic agricultural residue, forest residue, residue from wood processing industries and non-edible components from food crops along with biomass of non-food crops such as jatropha, mahua to municipal organic solid wastes (Alam et al., 2012; Kocar and Civas; 2013). Therefore they are not directly competing with arable land with food & feed crop and have a relatively lower environment impact than first generation, reduces greenhouse emission. However, second generation biofuels have low conversion rates and the conversion processes are not economically feasible at this moment (Alam et al., 2012; Adenle et al., 2013).

Biofuel derived from microalgae are classified as third generation biofuels and have potential for large-scale production. Many algal species have been found to grow rapidly and produce substantial amounts of triacylglycerols or oil (oleaginous algae). Therefore, it is fore-casted that algae could be employed as cell factories to produce biofuels (Chisti, 2007; Hu et al., 2008; Service, 2009). Normally, microalgae are cultivated in open raceway ponds and photo-bioreactors (PBR) to produce biomass and subsequently harvested and converted to biodiesel. Biodiesel are made up of fatty acid methyl esters (FAMES) derived from the transesterification of neutral lipids (biological oils or triacylglycerols) in the presence of alcohol as shown in Fig. 2.3 (Chisti, 2007). Table 2.1 shows various feedstock for biodiesel production. From the tabulated data, microalgae seem to be very promising as renewal feedstock to produce biodiesel as an alternate of fossils fuel (Milano et al., 2016). Algae offer many advantages in the search for sustainable, renewable bioenergy feed-stocks and have the potential to provide orders of magnitude more oil per acre of land than

traditional oil seed crops (Dismukes et al., 2008). The comparison of first, second and third generation biofuel with petro-diesel is summarized in table 2.2.

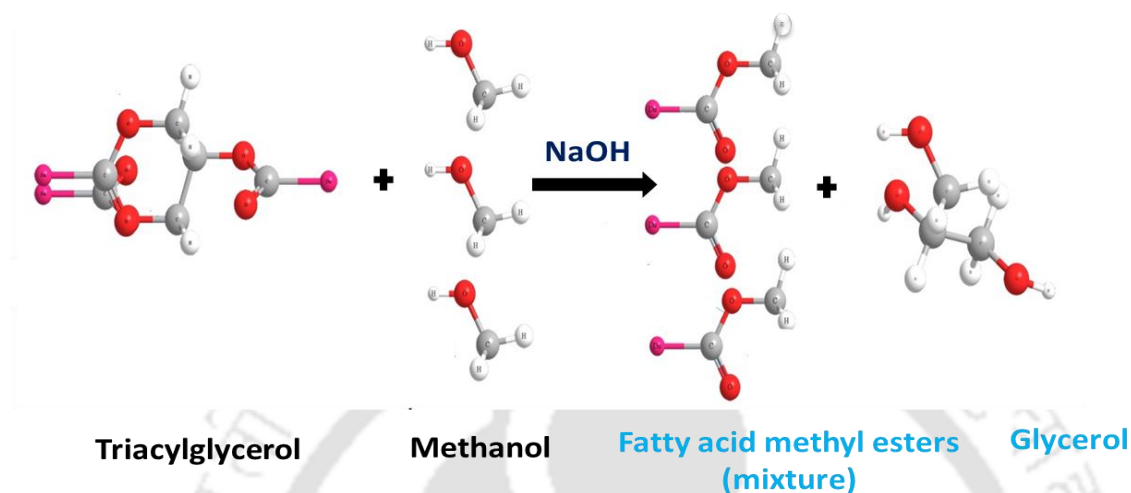


Fig. 2.3 Transesterification of triacylglycerols for the production of fatty acid methyl esters (biodiesel) with glycerol as byproduct using sodium hydroxide as catalyst and methanol as an acyl acceptor

Table 2.1 Comparison of various biodiesel producing feedstock (table obtained from Milano et al., 2016)

Generation	Crop	Oil (% oil by wt)	Oil yield (L oil ha ⁻¹ year ⁻¹)
First	Corn	44	172
	Hemp	33	363
	Soybean	18	446-636
	Safflower	20.1	779
	Chinese Tallow	12-45	907
	Camelina	42	915
	Sunflower	40	952-1070
	Peanut	70	1059
	Canola	41	974-1190
Second	Castor	48	1307-1413
	Jatropha	20-60	1892
	Polanga	65-75	2000
	Karanj	25-40	2590
	Coconut	65-75	2689
	Oil palm	36	5366-5950
Third	Microalgae	30-70	58.7-136.9k

Table 2.2 Comparison of first, second and third generation biofuel with petro-diesel (Suganya et al., 2016)

	Petro-diesel	First generation	Second generation	Third generation
Technology	Petroleum refinery	Microbial fermentation; enzymatic and chemical method	Pretreatment; hydrolysis and followed by fermentation, transesterification	Fractionation of algal biomass; metabolic engineering of microalgae for direct synthesis for biofuel, transesterification
Feedstocks	Crude petroleum	Vegetable oils and corn sugar feedstocks	Lignocellulosic biomass; agricultural and forest residue; non-food crop; plant and animal waste biomass	Microalgae
Products	Diesel; petrol; LPG kerosene and CNG	Biodiesel; bio-ethanol	Biooil; biodiesel; bioethanol; FT oil; butanol; mixed alcohol	Biodiesel; bioethanol; biohydrogen; biomethane; biobutanol; other fuels
Advantages	High energy density: highly compact portable source of energy used for most forms of mechanical transportation	Demonstrated technology; reduced GHG emissions in comparison to fossil fuels; environmental friendly; economic and social security	Less water and nutrition requirement; Can grow in waste lands with poor soil quality and also in dry climate; Improves soil properties and yields feed for animals; Not competing with food; Reduced GHG emissions and promotes carbon neutral process	Oil productivity is very high when compared with other biomass; can grow in non-arable lands; not competing with agricultural land; can grow in marine, brackish, and waste waters; multiproduct paradigm; algal biofuel contains no sulfur, is non-toxic and biodegradable; algae thrive on carbon dioxide from gas- and coal-fired power plant; increased scope for carbon negative
Disadvantages	Depletion of fossils fuel reserve; environmental pollution; economical and ecological problems	Limited feedstocks; food vs fuel competition; blended partially with conventional fuel	May compete for arable land, To achieve maximum productivity it may take 2-3 years, seasonal outputs, still needs technological outbreaks to reduce the cost	Technological development is required to achieve sustainable production of biodiesel

2.3 Microalgae are emerging renewable feedstock for biodiesel production

Algae are a very diverse group of photosynthetic organism responsible for photosynthetic activity account for almost 50% of the photosynthesis that takes place on the Earth and they produce approximately half of the atmospheric oxygen by using greenhouse gas carbon dioxide to grow photo autotrophically. Microalgae can be utilized as cell factories for a wide range of potentially useful products, but are rarely used for commercial purposes (Wijffels, 2007; Chisti, 2007). Wide range of feedstock was suggested by the researcher to produce biofuel, in order to eliminate the vulnerability of energy sector. Biodiesel and bioethanol produced from terrestrial plants have attracted the attention of the world as potential renewable feedstock for biofuel generation. The availability of crops that serve as feedstock for biofuel production is limited (Chisti, 2008). However, due to “food versus fuel” debate as well as competition with arable land for first and second generation biofuels, they have brought much controversy and debate on their sustainability (Goh and Lee, 2010). Therefore, it is necessary to find alternate feedstock, suitable for biofuel production, which does not drain the edible feedstock supply. One alternative and promising feedstock to the conventional crop is microalgae.

US Department of energy (DOE) funded an Aquatic Species Program (ASP) for the period 1978 to 1996, which basically was formed with the objective of drawing up a process inculcating sustainable generation of biodiesel from microalgae. The program evaluated various aspects of algal biodiesel generation which includes strain isolation, screening of suitable strain, characterization of strain, understanding the biology and production biochemistry followed by process development and cost analysis. The major roadblock as obtained from the aforesaid program was that the cost of biodiesel production was twice of the cost for petroleum diesel (Sheehan et al., 1998). The program was terminated in the latter

stages of 1996 resulting due to increased biodiesel prices which shunned government aid and lowering of petroleum cost. However, it was just a matter of time before microalgal biodiesel was again rejuvenated with interest being showered by the researchers and investors alike due to a rise in petro-diesel prices and crippling reserves of conventional energy sources (Brennan and Owende, 2010). Several countries including India have initiated prominent research in the area of algal biotechnology for sustainable biofuel production.

Microalgae have the inherent ability to harvest and convert solar energy into chemical energy through photosynthesis and have many desirable attributes as energy sources. They also exhibit higher growth rate than plants (Brennan and Owende, 2010; Ndimba et al., 2013). The advantages of microalgae over higher plants as a source of transportation biofuels are numerous such as: (i) microalgae synthesize and accumulate large quantities of neutral lipids in the form of triacylglycerol (20–80% dry cell weight), (ii) rapid reproduction rate and high growth rates (e.g. doublings time, 1-3 day⁻¹), (iii) oil yield per area of microalgae cultures could greatly surpass the yield of best oilseed crops, (iv) 15–300 times more lipid productivity than the traditional crops, (v) microalgae can be cultured in saline/brackish water/coastal seawater on non-arable land, and do not compete for resources with conventional agriculture, (vi) microalgae can grow in marginal lands (e.g. desert, arid and semi-arid lands) that are not suitable for conventional agriculture, (vii) microalgae can utilize nitrogen and phosphorus from a variety of wastewater sources (e.g. agricultural runoff, concentrated animal feed operations, and industrial and municipal waste-waters), providing the additional benefit of wastewater bioremediation, (viii) microalgae sequester CO₂ from flue gases emitted from thermal power plants and other sources, thereby reducing emissions of a major greenhouse gas. 1.8 kg of CO₂ is required to produce 1 kg of algal biomass, (ix) multiproduct paradigm ranging from simple to complex bio-organics, value-

added co-products or by-products (e.g. biopolymers, proteins, polysaccharides, pigments, animal feed and fertilizer) and does not need herbicide and pesticide, and (x) algae biodiesel contains no sulfur, is non-toxic and highly biodegradable (Khan et al., 2009; Suganya et al., 2016). Table 2.3 shows the lipid content of various microalgae strain with maximum lipid accumulation abilities. Algae as group of organism can be highly diverse as they are found in different aquatic environments and they range in sizes from being a single cell to long seaweeds. Microalgae typically grow photosynthetically in nature but some species also possesses the ability to grow heterotrophically and mixotrophically.

Table 2.3 Oil content obtained from various microalgal strains measured in weight percentage of the dry cell weight (source: Chisti, 2007; Mata et al., 2010; Suganya et al., 2016)

Algal strain	Lipid content (%, w/w dry weight biomass)
<i>Botryococcus braunii</i>	25–75
<i>Chlamydomonas reinhardtii</i>	21
<i>Chlorella emersonii</i>	25–63
<i>Chlorella minutissima</i>	57
<i>Chlorella protothecoides</i>	14–57
<i>Chlorella sorokiniana</i>	19–22
<i>Chlorella</i> sp.	10–48
<i>Chlorella vulgaris</i>	5–58
<i>Cryptocodinium cohnii</i>	20–51
<i>Dunaliella salina</i>	6–25
<i>Dunaliella</i> sp.	17–67
<i>Dunaliella tertiolecta</i>	16–71
<i>Ellipsoidion</i> sp.	27
<i>Nannochloris</i> sp.	20–56
<i>Nannochloropsis oculata</i> .	22–29
<i>Nannochloropsis</i> sp.	12–53
<i>Neochloris oleoabundans</i>	29–65
<i>Pavlova lutheri</i>	35
<i>Pavlova salina</i>	30
<i>Phaeodactylum tricorutum</i>	18–57
<i>Prostanthera incisa</i>	62
<i>Prymnesium parvum</i>	22–39
<i>Pyrrosia laevis</i>	69.1
<i>Scenedesmus dimorphus</i>	16–40
<i>Scenedesmus obliquus</i>	11–55
<i>Schizochytrium</i> sp.	50–77

Microalgae can be considered as model cell factories as their storage and accumulation capacity can be gauged on the basis of different mode of cultivation and conditions presented, thus making them easy to manipulate as per the requirement and direction of research (Muthuraj et al., 2014a). Microalgal lipids represent an opportunity to fulfill the global energy demand for transportation fuels. Phospholipids are the major type of lipid found in microalgae which act as the structural lipids for the cell, being a major component in the cell wall and these are found in great abundance during the cellular exponential growth phase. During the stationary phase of growth their ability to store energy as neutral lipids (TAG) depend on the species and culture conditions, although diacylglycerols (DAG), and monoacylglycerols (MAG) are also identified (Riekhof et al., 2005; Barsanti and Gualtieri, 2006).

2.4 Classification and biology of microalgae

The term “algae” refers to a polyphyletic (follows diverse evolutionary lineages), artificial assemblage of organisms. Algae include microscopic single cell forms (microalgae) and macroscopic multicellular loose or filmy conglomerations, giant kelp forms termed as macroalgae. More than 40,000 species already identified and with many more yet to be identified, algae are classified in to multiple major groupings as follows: cyanobacteria (Cyanophyceae), green algae (Chlorophyceae), diatoms (Bacillariophyceae), yellow-green algae (Xanthophyceae), golden algae (Chrysophyceae), red algae (Rhodophyceae), brown algae (Phaeophyceae), dinoflagellates (Dinophyceae) and ‘picoplankton’ (Prasinophyceae and Eustigmatophyceae). Fig. 2.4 shows the generalized structure of a eukaryotic green algal cell. Algal cells comprise complex intracellular organelles such as endoplasmic reticulum, golgibodies, mitochondria, nucleus and chloroplast for their effective functioning. The starch granules are observed in the chloroplasts while the lipid bodies are observed all over the cytoplasm. Thylakoid

membranes are stacked in a network resembling the plant thylakoids along with a short chloroplast DNA in it. The cell wall of eukaryotic cells may or may not have mucilage layers in their extracellular matrix and it varies with species to species.

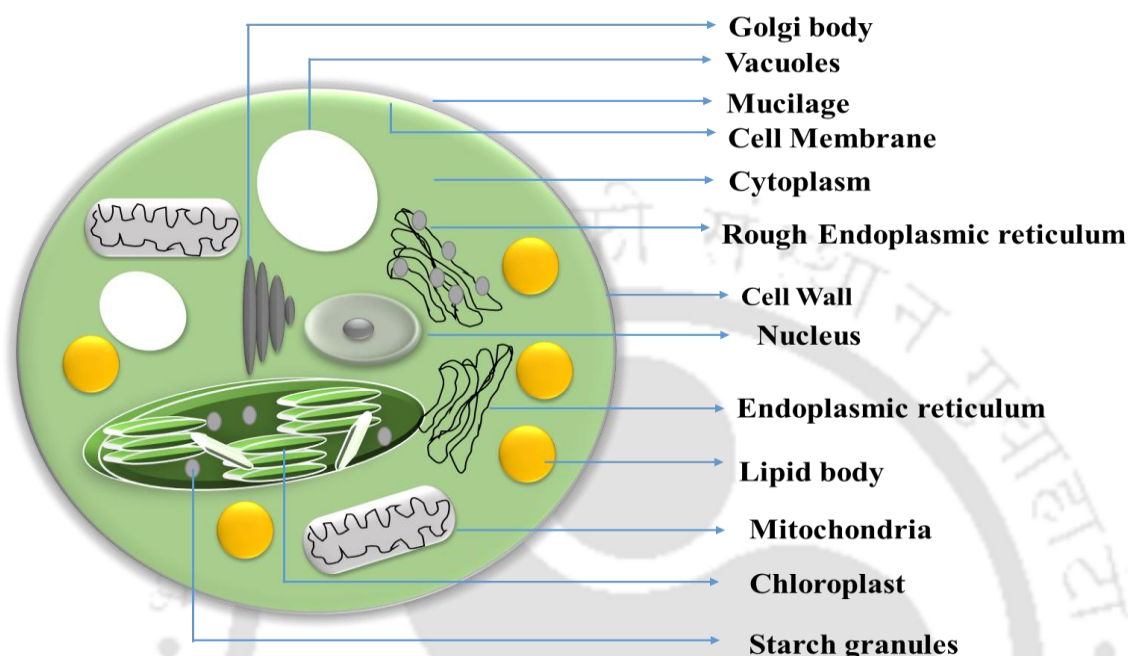


Fig. 2.4 Diagrammatic representation of generalized structural of an eukaryotic green algae (Adopted and modified from Barsanti and Gualtieri, 2006)

Different strains of algae have different combinations of chlorophyll (Chl) and carotenoids molecules. Some strains have only Chl-*a*, some have both Chl-*a* and Chl-*b*, while some strains have all Chl-*a*, Chl-*c* and Chl-*d*. (Barsanti and Gualtieri, 2006; Suganya et al., 2016).

2.5 Biosynthesis of fatty acids and triacylglycerols

Information on lipid metabolism for microalgae, particularly the biosynthetic pathways of fatty acids and TAG, is scarce as it has been poorly studied relative to higher plants. In algae, the *de novo* synthesis of fatty acid occurs primarily in the chloroplast. The global synthesis pathway of TAG in cells is comprised of three major steps: (i) carboxylation of acetyl-CoA to form malonyl-CoA, the committing step of fatty acid biosynthesis, (ii) acyl

chain elongation and (iii) TAG formation (Fig. 2.5). Acetyl-CoA carboxylase (ACC) initiates lipid biosynthesis, which catalyzes the important committal step of the fatty acid synthetic pathway, the biotin-dependent carboxylation of acetyl-CoA to form malonyl-CoA. On the contrary, fatty acid synthesis in plants occurs solely in plastids of developing seeds, and ACC uses the acetyl-CoA that is found in this organelle (Dyer and Mullen, 2005). Once malonyl-CoA is synthesized, it is transferred by malonyl-CoA: ACP transacylase to the acyl-carrier protein (ACP) of the fatty acid synthase (FAS) multi-enzymatic complex (Dyer and Mullen, 2005).

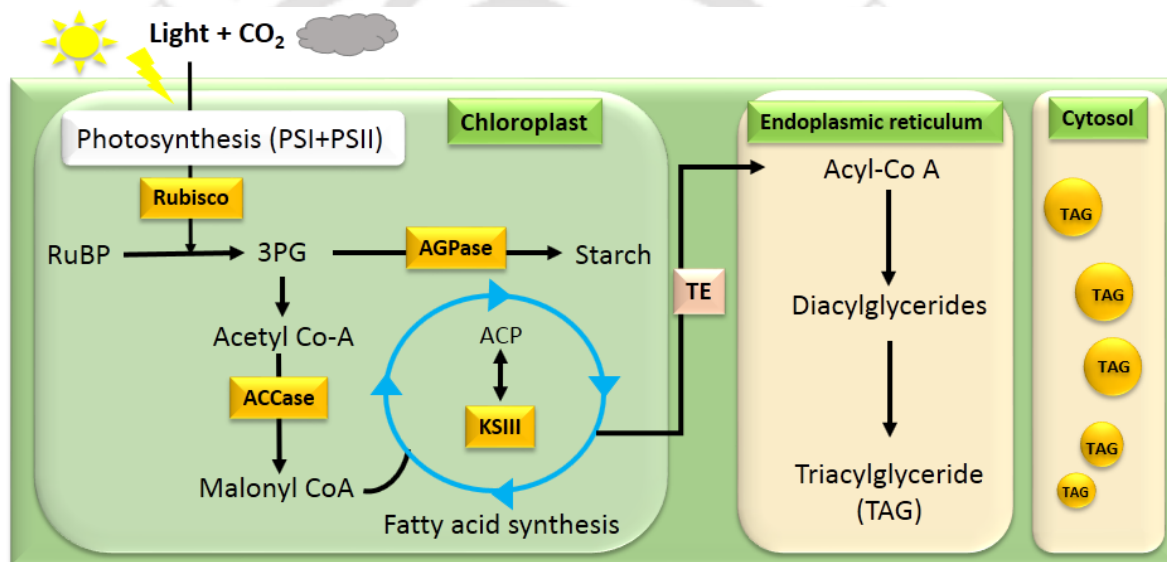


Fig. 2.5 Overview of metabolic pathways of microalgal lipid and starch biosynthesis. 3PG, 3 phosphoglyceric acid; ACCase, acetyl-CoA carboxylase; ACP, acyl carrier protein; AGPase, ADP-glucose pyrophosphorylase; G3P, glyceraldehyde-3-phosphate; KSIII, 3-ketoacyl-acyl-carrier protein synthetase III; Rubisco, ribulose-1,5-bisphosphate carboxylase/oxygenase; RuBP, ribulose-1,5-bisphosphate; TE, thioesterase; TAG, Triacyl glycerol (adopted and modified from Ho et al., 2014)

Synthesis of the phospholipids and neutral lipids takes place at the surface of endoplasmic reticulum in cytoplasm. The fatty acid chains generated in the chloroplasts are transferred from CoA to position 1 and 2 of the glycerol-3-phosphate which results in the formation of lysophosphatidic acid and phosphatidic acid respectively. The phosphatidic acid is dephosphorylated to form diacyl glycerol which further gets converted to triacyl glycerol in

the final step by the addition of 3rd acyl chain in the glycerol backbone. The polar lipids like phosphatidylcholine, galactolipids are formed from the precursor phosphatidic acid and diacyl glycerol which further gets integrated in to the membranes. Microalgae typically accumulate wide range of TAGs with varying chain lengths among which C16 and C18 (saturated and mono-unsaturated) are the major fractions that comprises about 70% of the total fatty acids (Riekhof et al., 2005).

2.6 Microalgae cultivation: mode of nutrition and reactor types

Microalgae, a promising aquatic biomass source of sustainable biofuels production can be cultivated under different nutritional modes such as photoautotrophic, heterotrophic and mixotrophic conditions. Selection of suitable nutritional mode for microalgae cultivation is a crucial step for successful applications in the biofuel industry. The most important and the preferably used mode of cultivation is the photoautotrophic mode which uses sunlight as the energy source and CO₂ as the carbon source for growth (Huang et al., 2010). Lipid productivity of the algal strains varies significantly from species to species (4 to 61 mg L⁻¹ day⁻¹) under photoautotrophic cultivation (Rodolfi et al., 2009; Lim et al., 2012).

The major advantage with photoautotrophic cultivation mode is the utilization of inorganic CO₂ for growth of microalgae which is usually fulfilled with the flue gas from industries in large scale operations, which contributes to global CO₂ reduction (Mata et al., 2010). As the medium is not rich in organic nutrients very less contamination is expected under photoautotrophic cultivation mode which enables use of open race way ponds and outdoor cultivation for algal growth (Mata et al., 2010). However, the photoautotrophic cultivation presents severely limiting biomass production due to cellular self-shading resulting in low light availability per cell. The low biomass concentration obtained in the photoautotrophic

culture increases the biomass harvesting cost. A feasible alternative for photoautotrophic culture is to use a heterotrophic and mixotrophic culture in which organic carbons such as sugars and organic acids are used as carbon sources.

Under heterotrophic cultivation mode, the organism is grown under dark condition in the presence of organic carbon as the source of energy and carbon (Wang et al., 2012) which bypasses the requirement of a light source and associated light penetration problems. The lipid productivity varies from 0.7 to 1.8 g L⁻¹ day⁻¹ which is significantly higher than obtained in photoautotrophic conditions (Chen et al., 2011). The major disadvantage of such cultivation mode is the cost of complex organic carbon source used for the growth of microalgae. Many alternative cheaper carbon sources are being tested for maximizing the growth under heterotrophic cultivation condition, however much attention is still required in the field to have a sustainable bioprocess for biodiesel production.

Mixotrophic growth mode is another alternative that uses both the organic and inorganic carbon compounds as a source of carbon for growth along with light as the energy source. Thus providing the opportunity for the strain to follow both heterotrophic and photoautotrophic route of cultivation in which the growth is not strictly limited either by light or carbon availability. The lipid productivity under mixotrophic condition varies from 0.01 to 0.27 g L⁻¹ day⁻¹ in different microalgal strains (Wang et al., 2014). Mixotrophic cultivation of *C. sorokiniana* showed the best growth performance in terms of the growth rate & lipid productivity as compared to photoautotrophic and heterotrophic mode (Li et al., 2014). Maximum net lipid productivity were also reported for mixotrophic followed by heterotrophic and photoautotrophic cultivation conditions (Chen et al., 2011; Cheirsilp and Torpee, 2012). Recent technologies have addressed these feasibility issues by using waste waters rich in organic compounds thereby coupling mixotrophic biodiesel production with waste water treatment (Wang et al., 2014).

Different kinds of photobioreactors mainly open pond and closed systems, have been proposed and utilized for microalgae cultivation. Lagoons, natural lakes and ponds which are large and shallow in nature are considered as open pond systems. Open raceway ponds as shown in Fig. 2.6 are the commonly used artificial open system which comprises an oval or rectangle shaped pond with a depth of ~0.2 to 0.5 m arranged along with paddles for proper mixing and sparger for air/CO₂ circulation (Fig. 2.6).

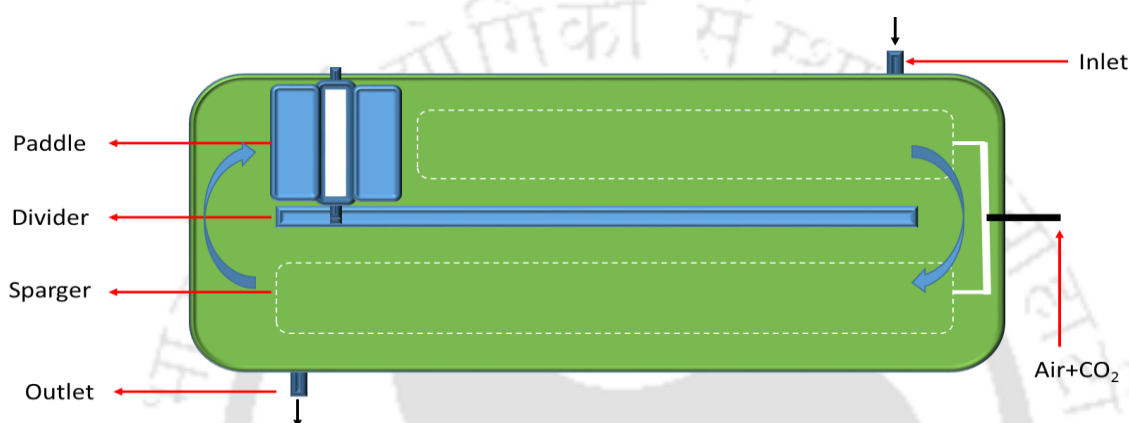


Fig. 2.6 Schematic representation of the open raceway ponds used for cultivation of microalgal strains

In a raceway pond system the microalgae culture, water and nutrition are circulated around a racetrack using paddle wheels. This will keep the microalgal cell suspended in water and allow utilization of CO₂ from atmosphere. The major advantage of using open raceway pond is its low installation and operational cost with compared to photobioreactors. Therefore, the large scale algal production systems are installed as open raceway ponds. The largest commercial open pond system spreads for 200 ha each and grows *Dunaliella salina* for β -carotene synthesis located in Australia (Borowitzka and Hallegraeff, 2007). However, there are certain flip sides to this strategy which limits the success of commercialization with the major limiting factors being poor light penetration due to cell shading effect and non-efficient dissolution of CO₂ in the medium. The other important issue with open ponds is the risk of contamination due to protozoans and other microbes (algae, bacterial and fungal

species) which can be avoided by using a larger inoculum size. Maintenance of extreme environmental conditions in the pond also avoids the growth of unwanted species while maintaining the species of interest with inherent properties to sustain in the extremities. For instance, organisms like *Spirulina* (able to grow in high alkaline pH), *Dunaliella salina* (able to grow in high salinity), *Chlorella* sp. (able to grow in waste waters with high nutrient conditions) and *Scenedesmus* sp. (able to grow at high CO₂ concentrations) are identified that can grow in extreme conditions. The major benefits and limitations are detailed in the table 2.4.

Table 2.4 Benefits and limitations of open ponds and various type of closed photobioreactor for algal cultivation (modified from Brennan and Owende, 2010)

Reactor system	Benefits	Limitations
Open pond	<ul style="list-style-type: none"> • Low installation cost and operational cost • Easy operation • Less energy inputs • Utilize non-agricultural land • Best for open outdoor conditions • Easy scalability 	<ul style="list-style-type: none"> • Large land requirement • Less biomass productivity compared to other reactor types • Poor light penetration • Reduced mass transfer and CO₂ mixing • Risk of contamination
Flat-panel photobioreactor	<ul style="list-style-type: none"> • Large illumination area • High biomass productivity • High mass transfer • Easy operation and sterilization • Suitable for outdoor conditions 	<ul style="list-style-type: none"> • Scale up difficulty • Difficulty in controlling temperature • Wall growth possibility • Increased hydrodynamic stress • High installation cost
Tubular photobioreactor	<ul style="list-style-type: none"> • Large illumination area • Cheap installation and operational cost • Suitable for outdoor conditions • High biomass productivities 	<ul style="list-style-type: none"> • Reduced mass transfer • Difficulty in controlling temperature • Wall growth possibility • Large land requirement • High installation cost
Column photobioreactor	<ul style="list-style-type: none"> • Proper CO₂ mixing and less shear • Low energy consumption • Easy sterilization 	<ul style="list-style-type: none"> • Small illumination area • High installation cost • Poor light penetration

In order to overcome the major problems associated with open pond systems, closed photobioreactor technologies were developed. The use of closed photobioreactor systems

ensures a contamination free cultivation of microalga as it is inherently exclusive to the outside environmental conditions and micro-organism culture environment can be properly maintained at all-time points, enabling their use in enhancing value added products like pharmaceutical and nutraceuticals. Various type of closed photobioreactor system has been developed such as tubular, flat panel and column photobioreactors (Table 2.4).

Tubular photobioreactor are arranged as an array of tubes assembled horizontally, vertically or inclined at an axial angle with a top-fitted airlift system ensuring proper mixing of air and CO₂ (Fig. 2.7). Characteristically the tubes are made of transparent glass sheet or acrylic or plastic material which diametrically measures about 0.1 m or less thereby enhancing and maximizing light penetration. The largest commercial scale tubular reactor facilities constructed for growth of photoautotrophic cells, with a capacity of 25 m³ and 700 m³ are functional at Mera Pharmaceuticals, Hawaii (Olaizola, 2003) and Klotze, Germany (Pulz, 2001; Janssen et al., 2003; Spolaore et al., 2006) respectively. Though tubular PBRs find extensive usage in large scale cultivation for microalgae but are often restricted due to O₂ accumulation, CO₂ depletion, and pH variations in the system. To that end, industries deploy the use of multiple units of these reactors to avoid any such bottleneck (de Andrade et al., 2016). Similarly bubble column photobioreactors also has received immense attention due to their high mass transfer capabilities, mixing options and best controllable growth conditions like pH and CO₂ purging. Such a reactor can be constructed by just hanging a polyethylene bag vertically on a skeletal framework or necessary support (Fig. 2.8). Structurally these reactors maintain an inner diameter within the range of 0.3 to 0.5 m with their heights ranging from 1 to 2.5 m.

Flat panel PBRs were designed with the sole objective of supporting enhanced high cell density cultivations with an effective facilitative mass transfer capabilities, avoiding oxygen

build up. Fig. 2.9 depicts schematic view of the flat panel closed photobioreactor that can be operated under photoautotrophic, heterotrophic and mixotrophic conditions.

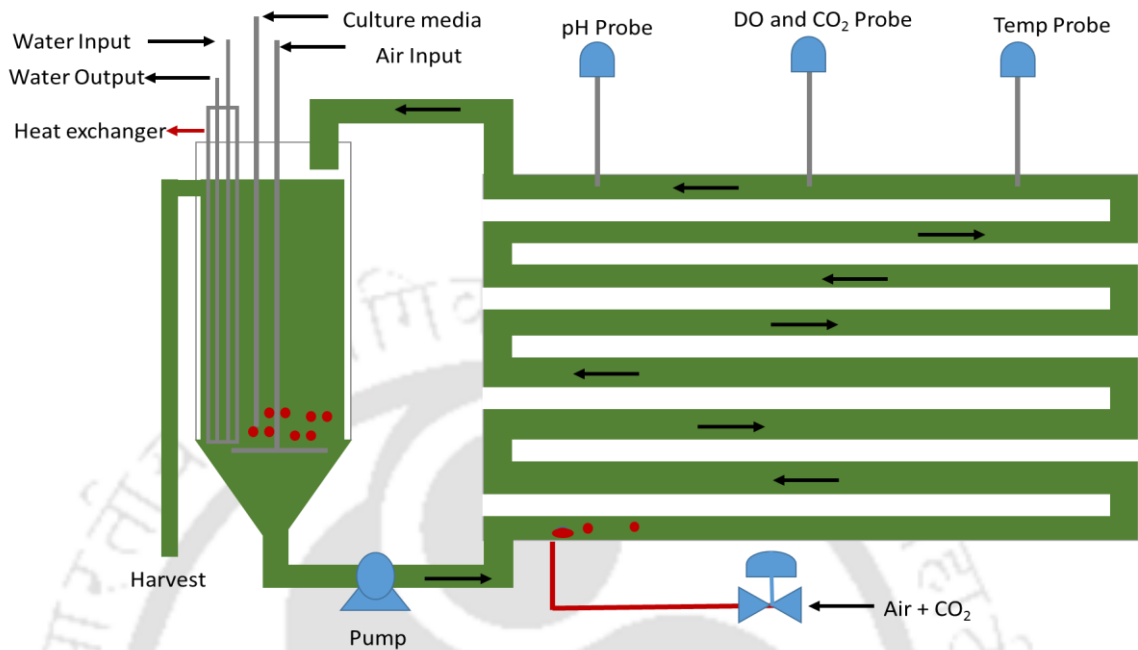


Fig. 2.7 A schematic view of a tubular photobioreactor used for cultivation of microalgae at “Las Palmerillas” experimental station, Almería, Spain (adopted and modified from de Andrade et al., 2016)

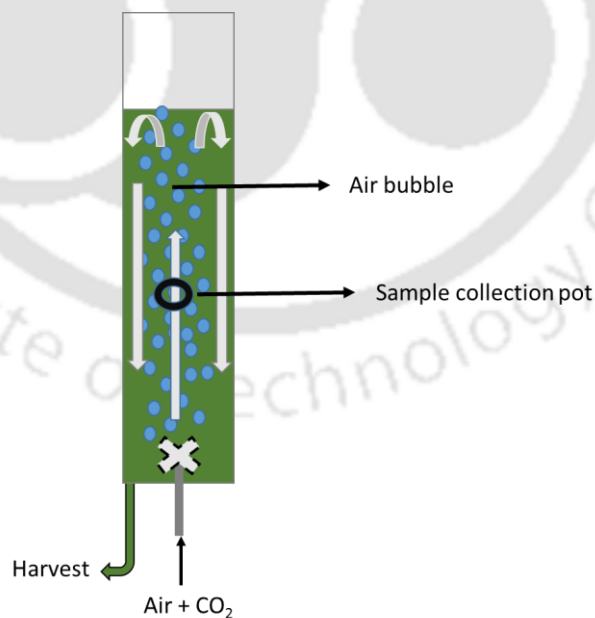


Fig. 2.8 A schematic diagram of bubble column photobioreactor with illustration of flow regimes used for cultivation of microalgae (adopted from Khoo et al., 2016)

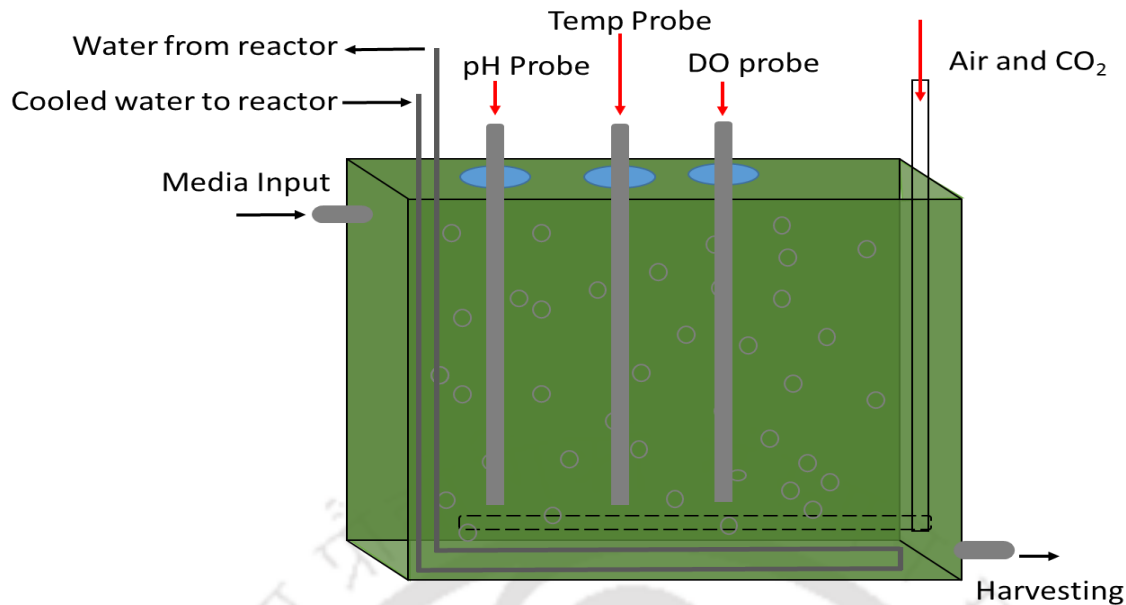


Fig. 2.9 Schematic view of a closed flat panel photobioreactor for cultivation of microalgae

With an inner width of 10-20 mm made up of thin transparent glass or polyacrylic sheet, the reactor resembles a thin cuboid. High density culture are mixed with a countercurrent flow which enables proper light distribution throughout the body of reactor (Hu et al., 1998; Degen et al., 2001; Richmond et al., 2003). Several advantages of these closed PBRs over open ponds such as (i) high photosynthetic efficiency; (ii) light availability; (iii) efficient CO₂ mixing ability; (iv) ability to control the process parameters like temperature, pH etc.; and (v) less chances of contamination makes them a robust culture systems available for the growth of algae (Maity et al., 2014). These reactors do have various advantages and disadvantages as depicted in table 2.4.

For a photosynthetic organism, light embodies the most essential and critical parameter that influences the choice of species and is often the rate limiting step in mostly all of culture systems except heterotrophic mode (Kaewpintong et al., 2007; Walker, 2009). The light intensity decreases exponentially as per the equation 2.1 with distance from a reactor surface as the biomass concentration increases.

$$I_d/I_0 = e^{(-\gamma d)} \quad (2.1)$$

Where I_d represents the light intensity at depth d , I_0 is the original incident intensity, γ is the turbidity (Chen et al., 2011). In accordance with the above equation it can be deduced that a short light path will favor the optimized light transmission per cell enabling them to attain higher photosynthetic efficiencies. In order to overcome these problems associated with light penetration, various illumination strategies are being incorporated in the design parameters directed towards enhanced biodiesel production (Ma and Hanna, 1999). The large natural light source available is the sunlight in which the light intensity varies from 0 lux to 1×10^5 lux in the night and day times respectively. Moreover, with this dynamic changes in light intensity the oil yield may vary between 100 and 130 $\text{m}^{-3} \text{ha}^{-1}$ while, under controlled artificial illumination the yield may rise up to 170 $\text{m}^{-3} \text{ha}^{-1}$ in laboratory conditions (Chisti, 2007). In general, the laboratory scale PBRs utilize fluorescent lamps, light emitting diodes (LEDs), optical fibers etc., as the light source. A more efficient system was suggested based on the combinatorial usage of LEDs and solar based optical fibres as a possible artificial illumination system with lowered electricity Chen et al. (2011) for large scale outdoor cultivation. Substantial improvement is still impending in this possible field of study. In hybrid systems, both open ponds as well as closed photobioreactor operating at different modes or at different growth phases are used in combination to get better results. In general, the first stage of growth is performed in a PBR for increasing the biomass concentration to the maximum with very less contamination, while the second stage of growth was conducted in an open pond under stress conditions for lipid accumulation. Such two stage strategies are also followed in many microalgal systems like *Chlorella*, *Scenedesmus* and *Nannochloropsis* sp. etc. (Rodolfi et al., 2009) for enhancing the net lipid productivity.

2.7 Process engineering strategies for improved biomass and lipid productivity

In general, nutrient starvation or limiting condition strategy is extensively employed to enhance the neutral lipid content of the cells but at the cost of reduced growth rate and biomass titer (Yeh and Chang, 2011; Menon et al., 2013; Muthuraj et al., 2014a). Increase in calorific values of *Chlorella* strains was observed when the culture grown in low nitrogen medium (Illman et al., 2000). Thus, success of microalgae based biodiesel production largely depends on two mutually exclusive parameters: biomass titer and lipid content which governs the techno economic feasibility of the whole process (Seth and Wangikar, 2015). Two stage cultivation strategies are being developed in which first stage targets high cell density cultivation followed by the second stage involving the enhancement of neutral lipid content by exposing the cells to nutrient starvation condition or by addition of certain lipid elicitors molecules (Muthuraj et al., 2014b). Fed-batch operation mode is one the most promising strategies for enhanced biomass productivity due to flexibility of intermittent feeding of rate limiting nutrients during cultivation (Abdollahi and Dubljevic, 2012). Biomass and lipid productivity of *Nannochloris* sp. and *Chlorella* sp. are increased by intermittent feeding of nitrogen, but their lipid content is not increased due to nitrogen sufficient condition (Hsieh and Wu, 2009; Takagi et al., 2000). However, fed-batch operation mode may not always be suitable for microalgae growth, especially when the microalgae are grown under phototrophic or mixotrophic conditions due to poor light penetration. Light limitation in turn leads a low biomass productivity. To overcome this problem, a fed-batch operation involving a stepwise increase in light intensity was proposed, and this strategy was shown to dramatically enhance the growth and lipid productivity of microalgae under mixotrophic conditions (Cerón-García et al., 2013; Cheirsilp and Torpee, 2012). However, although fed-batch operations coupled with stepwise increases in light intensity may be

effective, they are very difficult to control, especially when microalgae are being cultured outdoors with a naturally fluctuating light intensity over time. Under phototrophic or mixotrophic conditions, the increasing turbidity associated with microalgal growth usually becomes a significant growth-limiting factor due to the self-shading effect. Chemostat cultivation may therefore be an attractive alternative because continuous feeding of fresh medium effectively dilutes the cell density inside the photobioreactor. Relatively improved biomass productivity was observed in chemostat due to the continuous feeding of medium to support growth. In addition, continuous cultivation systems are generally low cost and easy to operate. Hence, continuous processes are suitable for large-scale cultivation of microalgae for industrial applications (Marchetti et al., 2012; Sforza et al., 2013). However, the most effective strategy to obtain maximum lipid productivity will be through synchronized growth and neutral lipid accumulation (Tevetia et al., 2014; Klok et al., 2013). Therefore, net lipid productivity which considers both the lipid content and biomass productivity is used as the performance index for the selection of the best productive strains and the process development for biodiesel production (Chen et al., 2011). Various hybrid systems involving these cultivation conditions were also designed for optimal commercial scale biodiesel production processes. However, a complete realization of these technologies at commercial scale still remains unachieved.

2.8 Dewatering technologies for harvesting of microalgae

From industry accounts harvesting of microalgae is usually costly and accounted about 20–30% of total biofuels production cost (Christenson and Sims, 2011; Pragya et al., 2013). The miniscule size of the algal cells, low density difference between algae and growth medium and diluted cultures of algae make the process of harvesting challenging on an industrial scale. Therefore, the harvesting strategy has to be based on a low energy method which will in turn bring down the cost of production and make the entire algal

biodiesel production economically feasible and viable. Microalgae harvesting can generally be divided into a two-step process: (i) bulk harvesting or preconcentration of biomass and (ii) thickening. The purpose of bulk harvesting is to separate microalgal biomass from the bulk suspension. By this method, the total solid matter can reach 2–7% using flocculation, flotation, or gravity sedimentation (Brennan and Owende, 2010). The purpose of thickening is to concentrate the algal slurry obtained from bulk harvesting, with filtration and centrifugation. This process is more energy intensive as compared with the bulk harvesting (Brennan and Owende, 2010). Several combinatorial strategies have been proposed with the selection criteria depending on species, final product etc., (Brennan and Owende, 2010). The major techniques available for harvesting and to concentrate the algal cells include gravity settling, centrifugation, flocculation, filtration, flotation, electrocoagulation, electrolysis and electrophoresis (Pragya et al., 2013). The choice of methodology related to harvesting should be applicable to a wide range of algal species with an objective of less consumption of energy and chemicals. Table 2.5 compares various dewatering techniques available based on their energy consumption and recovery efficiencies.

Table 2.5 Comparison of various dewatering techniques on the basis of microalgae recovery efficiencies and energy consumption (table obtained and modified from Misra et al., 2014)

Method	Microalgae recovery efficiency (%)	Energy consumption (kWh kg ⁻¹)
Centrifugation	99	16
Pressure filtration	99	0.18
Vacuum filtration	99	1.23
Tangential flow filtration	89	3.58
Polymer flocculation	80	36.81
Electrocoagulation-flocculation (Al and Fe electrodes)	92	2
Electrochemical harvesting (non-sacrificial electrodes)	94.52	1.6

The most common and conventional harvesting method is gravity sedimentation, which employs the method of settling out suspended cells using gravitational force which forms concentrated slurry at the bottom and clear liquid at the top (Uduman et al., 2010). In general, all the algal cells may have tendency to settle down at the bottom through gravitational force however, the rate of settling depends upon the species characteristics. Therefore, the efficiency is enhanced by using lamellar separators and sedimentation tanks for oleaginous algal systems. Commercially viable as of now is the addition of flocculants which has greatly increased the rate of sedimentation (Pragya et al., 2013).

Flocculation is one possible route to pre-concentrate the microalgae cell. Flocculation is a process that aggregates the algal cells to form flocs which is applicable to many species and large broth volumes (Uduman et al., 2010). External addition of flocculants neutralize the electronegative charge of 2.5 – 11.5 which microalgal cells carry on their surface and help in accentuated particle bridging, resulting in cell aggregation (Pragya et al., 2013). Different flocculating agents are available that have differential influence on flocculation process which include inorganic (alum, ferric sulfate and lime) and polymeric forms (Purifloc, Zetag 51, Dow 21M, Dow C-31, Chitosan) (Uduman et al., 2010). Polymeric form of flocculants include both ionic and non-ionic molecules which works by forming electrostatic or chemical bonding forces and the efficiency depends up on their charge density and chain length of the polymer. Addition of iron or aluminium based coagulants causes the charge neutralization in the algal cells based upon their charge density.

Adding to the interest garnered is autoflocculation which results in the spontaneous sediments of the cells (Park et al., 2011). Changing the environmental pH or low temperature conditions alters the cell wall composition of the algae thereby inducing aggregation of the cells. NaOH increases the pH to alkali side which induces many algal cells to aggregate themselves (Chen et al., 2011; Vandamme et al., 2012). Recent studies on

bioflocculation induced by the co-culturing of *Nannochloropsis* cells with bacterium is an energy efficient strategy for algal harvesting (Wang et al., 2012). Immobilization of microalgae on exogenous fungal mycelium of *Aspergillus nomius* CCK-PDA7#6 could be promising separation method to harvest both marine and freshwater microalgae (Talukder et al., 2014).

Alternate phenomenon in which air bubbles carry solid particles & algal cells to the upper surface and gets skimmed off is called floatation (Uduman et al., 2010). This is a more efficient method for sedimenting algal solutions (Pragya et al., 2013). Depending upon the bubble size, the floatation can be divided in to dissolved air floatation, dispersed floatation and electrolytic floatation (Chen et al., 2011). Dissolved air floatation is the commonly used along with chemical flocculation as the effectiveness of this method depends on the particulate size i.e. with larger particle size, higher efficiency is achieved. Electronegatively charged algal cells interact with bubbles of size 700-1500 formed in dispersed air floatation method. Dispersed air floatation method forms the bubbles of size 700-1500 μm which interacts with the negatively charged algal cells. Increment in the bubble cationic charge enhances the interaction and efficiency of algal cell removal (Rawat et al., 2011). Ozone is used in the dispersed air floatation and harvesting *Chlorella vulgaris* using ozone floatation method resulted in an increase in lipid content also. However, use of ozone for floatation is not economically feasible for biodiesel production (Rawat et al., 2011). H_2 ion discharge from a cathode employed by electrolytic floatation ensures attraction of negatively charged algal cells and moves them to the surface.

In centrifugation, gravity sedimentation is replaced as the force driving separation by a much greater force. Centrifugation ensures removal of all types of microalgae reliably and efficiently (Rawat et al., 2011). Separation time can be greatly reduced by applying a force of 4,000 to 14,000 times gravitational force (Perry and Chilton 1973), in case of

centrifugation. The use of centrifugation for harvesting the relatively low concentration (0.04%–0.07%) of total suspended solids in the pond water is restricted by the high cost of power required in handling large quantities of water (Park et al., 2011).

Harvesting using electrophoresis, does not require any chemical addition. An electric field makes charged algae to go out of the solution. Hydrogen, generated by electrolysis of water, sticks to the microalgal flocs and takes them to the surface. Environmental compatibility, safety, versatility, selectivity and energy efficiency are a few benefits of using this method. Major disadvantages towards commercialization of this process is the fouling of the cathodes and systems due to high temperatures arising out of high power requirements (Chen et al., 2011). It is well known fact that microalgal cell wall has negative charge (Crist et al., 1994; Safi et al., 2014). The negative charge imparted to the microalgal cell wall is due to the presence of acidic polysaccharide (pectin) in its composition (Crist et al., 1994). Due to this fact it can form clump when neutralized by oppositely charged particle. The coagulation phenomenon of microalgal cells after charge neutralization can be exploited for biomass harvesting. Different chemical or natural coagulants and flocculants are investigated for microalgal harvesting based on the abovementioned concept (Safi et al., 2014). However high doses of flocculants required for harvesting may affect the quality of byproducts as well as pose challenges to downstream processing biodiesel production (Anthony et al., 2013). Electrochemical microalgal harvesting is novel approach, which also uses the charge neutralization and coagulation principal. Electrochemical technologies are already proven technologies for the environmental and process applications (Neti and Misra, 2012). Electrochemical techniques such as electroflotation and electrocoagulation offer the possibility of an innovative, cheap, and effective method of algae harvesting that requires minimum addition of chemicals (Alfajara et al., 2002; Gao et al., 2010a; Gao et al., 2010b). Electrocoagulation (EC) is an electrochemical technique designed to disperse coagulating

metal ions from oxidizing metal electrodes. This process involves oxidation of anode which causes the electrode depletion and thus replacement is needed. Anode depletion is the main disadvantage of the EC process in terms of cost and metallic contamination in the harvested microalgae (Perreault et al., 2010; Kim et al., 2012a; Kim et al., 2012b). The use of a nonsacrificial electrode in the electrochemical harvesting (ECH) process would alleviate the disadvantage. Thus it becomes critical to investigate the performance and feasibility of ECH process applying nonsacrificial electrodes. This technology can be implemented for harvesting of microalgal biomass, which can be used not only for biodiesel production but for number of other purposes like biomethane, nutraceuticals and animal feed generation (Misra et al., 2014).

2.9 Processing of microalgal biomass for biodiesel generation

For biodiesel production, lipids or fatty acids need to be extracted from the harvested biomass followed by transesterification. Lipid extraction is energy exhaustive step and require proper pretreatment and disruption methods for higher extraction efficiency (Hidalgo et al., 2013). High water content in the algal cultivation creates severe limitation in extraction, transesterification and shelf-life. Therefore, energy consuming drying step is required to dry the biomass before extraction and transesterification. Usually spray drying, drum drying and sun drying are used to remove the water content in the algal biomass (Pragya et al., 2013). However, these methods are highly energy consuming and time consuming which makes the whole process uneconomical (Pragya et al., 2013).

Several physical methods used for cell disruption includes grinding, homogenization, microwave processing, sonication, bead beating, osmolysis and freeze drying. On the other hand, the chemical methods include solvent lysis, supercritical fluids, ionic liquids and direct transesterification methods (Parmar et al., 2011). Bligh and Dyer method guided solvent extraction is used efficiently in large scale processing where the extraction

efficiency is dependent on species and water retained in biomass. Supercritical fluids, microwave radiations and sonication assisted extraction methods amongst the other modes of harvesting are highly efficient with very high processing costs that affect the economy at a large scale process (Hidalgo et al., 2013).

Second stage involve transesterification of algal lipid with the use of acid or alkali or other heterogeneous catalysts along with alcohol. Strong bases like NaOH and KOH are commonly used as alkali catalysts in large scale transesterification processes attributed to higher yields in short time period. The major disadvantages with these alkali catalysts is the soap formation which has to be removed in the end product before use. Presence of catalysts in the biodiesel may affect the engine functions and may be corrosive to engines (Hidalgo et al., 2013). The soap formation with NaOH restricts the use of such catalysts in the free fatty acid rich biomass for transesterification. In such cases, the acid catalysts which include HCl or H₂SO₄ are used as catalysts for efficient transesterification without soap formation. However, use of acid catalysts requires large reaction times even at higher temperatures (Hidalgo et al., 2013). On the contrary, researchers using heterogeneous catalysts has gained impetus due to their non-corrosive, eco-friendly nature, higher efficiency even at lower concentration and easy separation from the end product (Hidalgo et al., 2013).

Heterogenous alkali catalysts such as magnesium oxide, calcium oxide, strontium oxide, barium oxide, aluminium oxide and their combinations are commonly used for the transesterification process (Liu et al., 2007). Solid heterogeneous acid catalysts are also used for lipid transesterification which includes zirconium oxide, titanium oxide, zeolites, ion exchange resins and heteropolyacids. In Mcgyan ® process, porous metallic oxides of ZrO, TiO and Al₂O₃ was used for effective transesterification is one of the demonstrated examples that signifies the use of heterogeneous catalysts in large scale transesterification

processes (Krohn et al., 2011). Making the commercialization of the process questionable is the daunting cost and elevated energy consumption at a industrial level.

Effective alternate to the existing conventional processes is the *in-situ* transesterification method where the lipid extraction and transesterification are carried out in a single stage process (Johnson and Wen, 2009; Hidalgo et al., 2013). The aforementioned process involves the use of a solvent which can acts as both the extracting solvent and acyl acceptor in the transesterification process along with a catalyst that can also act as a hydrolyzing agent. A single stage direct transesterification method was developed which uses sulfuric acid as catalyst, methanol as an acyl acceptor with conventional heating at 90°C for 40 minutes (Johnson and Wen, 2009) which bypasses the requirement of a separate extraction process. Single stage conversion heavily relies on the effective drying of wet algal biomass (Johnson and Wen, 2009). Therefore, there is a need to develop an efficient and reliable method for large scale production of biodiesel while eliminating separate extraction step. To that end, a supercritical transesterification processes are being developed with increased concentration of methanol to achieve maximum transesterification efficiency with wet algal biomass (Patil et al., 2011a). Processes such as microwave radiations, sonication etc., are also being reported to show higher conversion efficiencies (Patil et al., 2011b). But use of these strategies in commercial scale process will be economically infeasible. The need of the hour is to develop a transesterification step which would seriously lower the costs involved rendering the process to be implemented on industrial scale.

2.10 References

1. Abdollahi, J, Dubljevic, S., 2012. Lipid production optimization and optimal control of heterotrophic microalgae fed-batch bioreactor. *Chem. Eng. Sci.* 84, 619-27.
2. Adenle, A.A., Haslam, G.E., Lee, L., 2013. Global assessment of research and development for algae biofuel production and its potential role for sustainable development in developing countries. *Energy Policy.* 61, 182-95
3. Alam, F., Date, A., Rasjidin, R., Mobin, S., Moria, H., Baqui, A., 2012. Biofuel from algae-is it a viable alternative? *Procedia Eng.* 49, 221-227
4. Alfafara, C.G., Nakano, K., Nomura, N., Igarashi, T., Matsumura, M., 2002. Operating and scale-up factors for the electrolytic removal of algae from eutrophied lake water. *J. Chem. Technol. Biotechnol.* 77, 871-876
5. Anthony, R.J., Ellis, J.T., Sathish, A., Rahman, A., Miller, C.D., Sims, R.C., 2013. Effect of coagulant/flocculants on bioproducts from microalgae. *Bioresour. Technol.* 149, 65-70
6. Barsanti, L., Gualtieri, P., 2006. *Algae anatomy biochemistry and biotechnology.* Taylor & Francis Group, London UK.
7. Borowitzka, M.A., Hallegraeff, G., 2007. Economic importance of algae. In: *Algae of Australia: introduction* (McCarthy PM, Orchard AE, eds). ABRS, Canberra.
8. BP Statistical Review of World Energy 2015. <http://www.bp.com/en/global/corporate/about-bp/energy-economics/statistical-review-of-world-energy.html>
9. Brennan, L., Owende, P., 2010. Biofuels from microalgae—a review of technologies for production, processing, and extractions of biofuels and co-products. *Renew. Sustain. Energy Rev.* 14, 557-577.

10. Cerón-García, M., Fernández-Sevilla, J., Sánchez-Mirón, A., García-Camacho, F., Contreras-Gómez, A., Molina-Grima, E., 2013. Mixotrophic growth of *Phaeodactylum tricorutum* on fructose and glycerol in fed-batch and semi-continuous modes. *Bioresour. Technol.* 147, 569-576.
11. Cheirsilp, B., Torpee, S., 2012. Enhanced growth and lipid production of microalgae under mixotrophic culture condition: effect of light intensity, glucose concentration and fed-batch cultivation. *Bioresour. Technol.* 110, 510-516.
12. Chen, C.Y., Yeh, K.L., Aisyah, R., Lee, D.J., Chang, J.S., 2011. Cultivation, photobioreactor design and harvesting of microalgae for biodiesel production: A critical review. *Bioresour. Technol.* 102, 1649-1655.
13. Chisti, Y., 2007. Biodiesel from microalgae. *Biotechnol Adv.* 25, 294-306.
14. Chisti, Y., 2008. Biodiesel from microalgae beats bioethanol. *Trends Biotechnol.* 26, 126-131.
15. Christenson, L., Sims, R., 2011. Production and harvesting of microalgae for wastewater treatment, biofuels, and bioproducts. *Biotechnol. Adv.* 29, 686-702.
16. Crist, D.R., Grist, R.H., Martin, J.R., Watson, J.R., 1994. Ion exchange systems in proton-metal reactions with algal cell walls. *FEMS Microbiol. Rev.* 14, 309-313.
17. de Andrade, G.A., Berenguel, M., Guzmán, J.L., Pagano, D.J. and Ación, F.G., 2016. Optimization of biomass production in outdoor tubular photobioreactors. *J. Process Control*, 37, 58-69.
18. De Silva, G., Ranjith, P., Perera, M. 2015. Geochemical aspects of CO₂ sequestration in deep saline aquifers: A review. *Fuel.* 155, 128-143.
19. Degen, J., Uebele, A., Retze, A., Schmid-Staiger, U., Trosch, W., 2001. A novel photobioreactor with baffles for improved light utilization through the flashing light effect. *J. Biotechnol.* 92, 89-94.

20. Demirbas, A., 2008. Biofuels sources, biofuel policy, biofuel economy and global biofuel projections. *Energ. Convers. Manage.* 49, 2106-2116.
21. Demirbas, A., 2010. Use of algae as biofuel sources. *Energ. Convers. Manage.* 51, 2738-2749.
22. Dismukes, G.C., Carrieri, D., Bennette, N., Ananyev, G.M., Posewitz, M.C., 2008. Aquatic phototrophs: efficient alternatives to land-based crops for biofuels. *Curr. Opin. Biotechnol.* 19, 235-240.
23. Dyer, J.M., Mullen, R.T., 2005. Development and potential of genetically engineered oilseeds. *Seed Sci. Res.* 15, 255-267.
24. <ftp://ftp.cmdl.noaa.gov>
25. Ganesh, I. 2014. Conversion of carbon dioxide into methanol—a potential liquid fuel: Fundamental challenges and opportunities (a review). *Renew. Sustain. Energy Rev.* 31, 221-257.
26. Gao, S., Du, M., Tian, J., Yang, J., Yang, J., Ma, F., Nan, J., 2010a. Effects of chloride ions on electro-coagulation–flotation process with aluminum electrodes for algae removal. *J. Hazard. Mater.* 182, 827-834.
27. Gao, S., Yang, J., Tian, J., Ma, F., Tu, G., Du, M., 2010b. Electro-coagulation–flotation process for algae removal. *J. Hazard. Mater.* 177, 336-343.
28. Goh, C.S., Lee, K.T., 2010. A visionary and conceptual macroalgae based third generation bioethanol (TGB) biorefinery in Sabah, Malaysia as an underlay for renewable and sustainable development. *Renew. Sustain. Energy Rev.* 14, 842-848.
29. Hepbasli, A., 2008. A key review on exergetic analysis and assessment of renewable energy resources for a sustainable future. *Sustain Energy Rev.* 12, 593-661.

30. Hidalgo, P., Toro, C., Cuidad, G., Navia, R., 2013. Advances in direct transesterification of microalgal biomass for biodiesel production. *Rev. Environ. Sci. Biotechnol.* 12, 179-199.
31. Ho, S.H., Ye, X., Hasunuma, T., Chang, J.S., Kondo, A., 2014. Perspectives on engineering strategies for improving biofuel production from microalgae – a critical review. *Biotechnol. Adv.* 32, 1448-1459.
32. Hsieh, C.H., Wu, W.T., 2009. Cultivation of microalgae for oil production with a cultivation strategy of urea limitation. *Bioresour. Technol.* 100, 3921-3926.
33. <http://cdiac.ornl.gov>
34. Hu, Q., Kurano, N., Kawachi, M., Iwasaki, I., Miyachi, A., 1998. Ultrahigh-cell-density culture of a marine alga *Chlorococcum littoralein* a flat-plate photobioreactor. *Appl. Microbiol. Biotechnol.* 46, 655-662.
35. Hu, Q., Sommerfeld, M., Jarvis, E., Ghirardi, M., Posewitz, M., Seibert, M., Darzins, A., 2008 Microalgal triacylglycerols as feedstocks for biofuel production: perspectives and advances. *Plant J.* 54, 621-639.
36. Huang, G.H., Chen, F., Wei, D., Zhang, X.W., Chen, G., 2010. Biodiesel production by microalgal biotechnology. *Applied Energy.* 87, 38-46.
37. Illman, A.M., Scragg, A.H., Shales, S.W., 2000. Increase in *Chlorella* strains calorific values when grown in low nitrogen medium. *Enzyme Microb. Technol.* 27, 631-635.
38. Janssen, M., Tramper, J., Mur, L.R., Wijffels, R.H., 2003. Enclosed outdoor photobioreactors: light regime, photosynthetic efficiency, scale-up, and future prospects. *Biotechnol. Bioeng.* 81(2), 193-210.
39. Ji, X., Long, X., 2016. A review of the ecological and socioeconomic effects of biofuel and energy policy recommendations. *Renew. Sustain. Energy Rev.* 61, 41-52.

40. Johnson, M., Wen, Z., 2009. Production of biodiesel fuel from the microalga *Schizochytrium limacinum* by direct transesterification of algal biomass. *Energy Fuels* 23, 5179-5183.
41. Kaewpintong, K., Shotipruk, A., Powtongsook, S., Pavasant, P., 2007. Photoautotrophic high-density cultivation of vegetative cells of *Haematococcus pluvialis* in airlift bioreactor. *Bioresour. Technol.* 98, 288-295.
42. Khan, S.A., Rashmi, Hussain, M.Z., Prasad, S., Banerjee, U.C., 2009. Prospects of biodiesel production from microalgae in India. *Renew. Sustain. Energy Rev.* 13, 2361-2372.
43. Khoo, C.G., Lam, M.K. and Lee, K.T., 2016. Pilot-scale semi-continuous cultivation of microalgae *Chlorella vulgaris* in bubble column photobioreactor (BC-PBR): Hydrodynamics and gas-liquid mass transfer study. *Algal Research*, 15, 65-76.
44. Kim, J., Ryu, B.G., Kim, B.K., Han, J.I., Yang, J.W., 2012a. Continuous microalgae recovery using electrolysis with polarity exchange. *Bioresour. Technol.* 111, 268-275.
45. Kim, J., Ryu, B.G., Kim, K., Kim, B.K., Han, J.I., Yang, J.W., 2012b. Continuous microalgae recovery using electrolysis: effect of different electrode pairs and timing of polarity exchange. *Bioresour. Technol.* 123, 164-170.
46. Klok, A.J., Martens, D.E., Wijffels, R.H., Lamers, P.P., 2013. Simultaneous growth and neutral lipid accumulation in microalgae. *Bioresour. Technol.* 134, 233-243.
47. Kocar, G., Civas N., 2013. An overview of biofuels from energy crops: Current status and future prospects. *Renew. Sustain. Energy Rev.* 28, 900-916.
48. Krohn, B.J., McNeff, C.V., Yan, B., Nowlan, D., 2011. Production of algae-based biodiesel using the continuous catalytic Mcgyan® process. *Bioresour. Technol.* 102, 94-100.

49. Lee, R.A., Lavoie, J.M., 2013. From first to third generation biofuels: Challenges of producing a commodity from a biomass of increasing complexity. *Animal Frontiers*. 3, 6-11.
50. Li, T., Zheng, Y., Yu, L., Chen, S., 2014. Mixotrophic cultivation of a *Chlorella sorokiniana* strain for enhanced biomass and lipid production. *Biomass Bioenergy*. 66, 204-213.
51. Lim., D.K.Y., Garg, S., Timmins, M., Zhang, E.S.B., Thomas-Hall, S.R., Schuhmann, H., Li, Y., Schenk, P.M., 2012. Isolation and Evaluation of Oil-Producing Microalgae from Subtropical Coastal and Brackish Waters. *PLoS ONE* 7, 1-13.
52. Liu, X., He, H., Wang, Y., Zhu, S., 2007. Transesterification of soybean oil to biodiesel using SrO as a solid base catalyst. *Catalysis Communications* 8, 1107-1111.
53. Ma, F.R., Hanna, M.A., 1999. Biodiesel production: a review. *Bioresource Technology* 70, 1-15.
54. Maity, J.P., Bundschuh, J., Chen, C.Y., Bhattacharya, P., 2014. Microalgae for third generation biofuel production, mitigation of greenhouse gas emissions and wastewater treatment: present and future perspectives – A mini review. *Energy* DOI: 10.1016/j.energy.2014.04.003
55. Marchetti, J., Bougaran, G., Le, Dean, L., Megrier, C., Lukomska, E., Kaas, R., Olivo, E., Baron, R., Robert, R., Cadoret, J.P., 2012. Optimizing conditions for the continuous culture of *Isochrysis affinis galbana* relevant to commercial hatcheries. *Aquaculture*. 326, 106-115.
56. Mata, T.M., Martins, A.A., Caetano, N.S., 2010. Microalgae for biodiesel production and other applications: a review. *Renew. Sustain. Energy. Rev.* 14, 217-32.

57. Menon, K.R., Balan, R., Suraishkumar, G.K., 2013. Stress induced lipid production in *Chlorella vulgaris*: relationship with specific intracellular reactive species levels. *Biotechnol. Bioeng.* 110, 1627-1636.
58. Milano, J., Ong, H.C., Masjjuki, H.H., Chong, W.T., Lam, M.K., Loh, P.K., Vellayan, V., 2016. Microalgae biofuels as an alternative to fossil fuel for power generation. *Renew. Sust. Energ.* 58, 180-197.
59. Misra, R., Guldhe, A., Singh, P., Rawat, I., Bux, F., 2014. Electrochemical harvesting process for microalgae by using nonsacrificial carbon electrode: a sustainable approach for biodiesel production. *Chem. Eng. J.* 255, 327-333.
60. Muthuraj, M., Chandra, N., Palabhanvi, B., Kumar, V., Das, D., 2014b. Process Engineering for High-Cell-Density Cultivation of Lipid Rich Microalgal Biomass of *Chlorella* sp. FC2 IITG. *Bioenerg. Res.* 8, 726-739.
61. Muthuraj, M., Kumar, V., Palabhanvi, B., Das, D., 2014a. Evaluation of indigenous microalgal isolate *Chlorella* sp. FC2 IITG as a cell factory for biodiesel production and scale up in outdoor conditions. *J. Ind. Microb. Biotechnol.* 41, 499-511.
62. Ndimba, B.K., Ndimba, R.J., Johnson, T.S., Waditee-Sirisattha, R., Baba, M., Sirisattha, S., Shiraiwa, Y., Agrawal, G.K., Rakwal, R., 2013. Biofuels as a sustainable energy source: an update of the applications of proteomics in bioenergy crops and algae. *J. Proteom.* 93, 234-244.
63. Neti, N.R., Misra, R., 2012. Efficient degradation of reactive blue 4 in carbon bed electrochemical reactor. *Chem. Eng. J.* 184, 23-32.
64. Olaizola, M. 2003. Commercial development of microalgal biotechnology: from the test tube to the marketplace. *Biomol. Eng.* 20, 459-466.
65. Park, J.B.K., Craggs, R.J., Shilton, A.N., 2011. Recycling algae to improve species control and harvest efficiency from a high rate algal pond. *Water Res.* 45, 6637-6649.

- Vandamme, D., Foubert, I., Fraeye, I., Meeschaert, B., Muylaert, K., 2012. Flocculation of *Chlorella vulgaris* induced by high pH: role of magnesium and calcium and practical implications. *Bioresour. Technol.* 105, 114-119.
66. Parmar, A., Singh, N.K., Pandey, A., Gnansounou, E., Madamwar, D., 2011. Cyanobacteria and microalgae: a positive prospect for biofuels. *Bioresour. Technol.* 102, 10163-10172.
67. Patil, P., Gude, V., Mannarswamy, A., Cooke, P., Munson-McGee, S., Nirmalakhandan, N., Lammers, P., Deng, S., 2011b. Optimization of microwave-assisted transesterification of dry algal biomass using response surface methodology. *Bioresour. Technol.* 102, 1399-1405.
68. Patil, P., Gude, V., Mannarswamy, A., Deng, S., Cooke, P., Munson-McGee, S., Rhodes, I., Lammers, P., Nirmalakhandan, N., 2011a. Optimization of direct conversion of wet algae to biodiesel under supercritical methanol conditions. *Bioresour. Technol.* 102, 118-122.
69. Perreault, F., Dewez, D., Fortin, C., Juneau, P., Diallo, A., Popovic, R., 2010. Effect of aluminum on cellular division and photosynthetic electron transport in *Euglena gracilis* and *Chlamydomonas acidophila*. *Environ. Toxicol. Chem.* 29, 887-892.
70. Perry, R.H., Chilton, C.H., 1973. *Chemical engineers' handbook*, 5th edn. McGraw Hill, Tokyo.
71. Pragya, N., Pandey, K.K., Sahoo, P.K., 2013. A review on harvesting, oil extraction and biofuels production technologies from microalgae. *Renew. Sust. Energ. Rev.* 24, 159-171
72. Pulz, O., 2001. Photobioreactors: production systems for phototrophic microorganisms. *Appl. Microbiol. Biotechnol.* 57, 287-293.

73. Rawat, I., Kumar, R.R., Mutanda, T., Bux, F., 2011. Dual role of microalgae: phycoremediation of domestic wastewater and biomass production for sustainable biofuels production. *Appl. Energy* 88, 3411-3424.
74. Richmond, A., Cheng-Wu, Z., Zarmi, Y., 2003. Efficient use of strong light for high photosynthetic productivity: interrelationships between the optical path, the optimal population density and cell-growth inhibition. *Biomol. Eng.* 20, 229-239.
75. Riekhof, W.R., Sears, B.B., Benning, C. 2005. Annotation of genes involved in glycerolipid biosynthesis in *Chlamydomonas reinhardtii*: discovery of the betaine lipid synthase BTA1Cr. *Eukaryot. Cell.* 4, 242-252.
76. Rodolfi, L., Zittelli, G.C., Bassi, N., Padovani, G., Biondi, N., Bonini, G., Tredici, M.R., 2009. Microalgae for oil: strain selection, induction of lipid synthesis and outdoor mass cultivation in a low-cost photobioreactor. *Biotechnol. Bioeng.* 102, 100-112.
77. Safi, C., Zebib, B., Merah, O., Pontalier, P.Y., Vaca-Garcia, C., 2014. Morphology, composition, production, processing and applications of *Chlorella vulgaris*: a review. *Renew. Sustain. Energy Rev.* 35, 65-278.
78. Service, R.F., 2009. ExxonMobil fuels venter's efforts to run vehicles on algae-based oil. *Science.* 325(5939), 379-379.
79. Seth, J. R., Wangikar, P. P., 2015. Challenges and opportunities for microalgae-mediated CO₂ capture and biorefinery. *Biotechnol. Bioeng.* 112, 1281-1296.
80. Sforza, E., Enzo, M., Bertucco, A., 2013. Design of microalgal biomass production in a continuous photobioreactor: an integrated experimental and modeling approach. *Chem. Eng. Res. Des.* 92, 1153-1162.
81. Sheehan, J., Dunahay, T., Benemann, J., Roessler, P.G., 1998. US Department of Energy's Office of Fuels Development, A Look Back at the US Department of Energy's

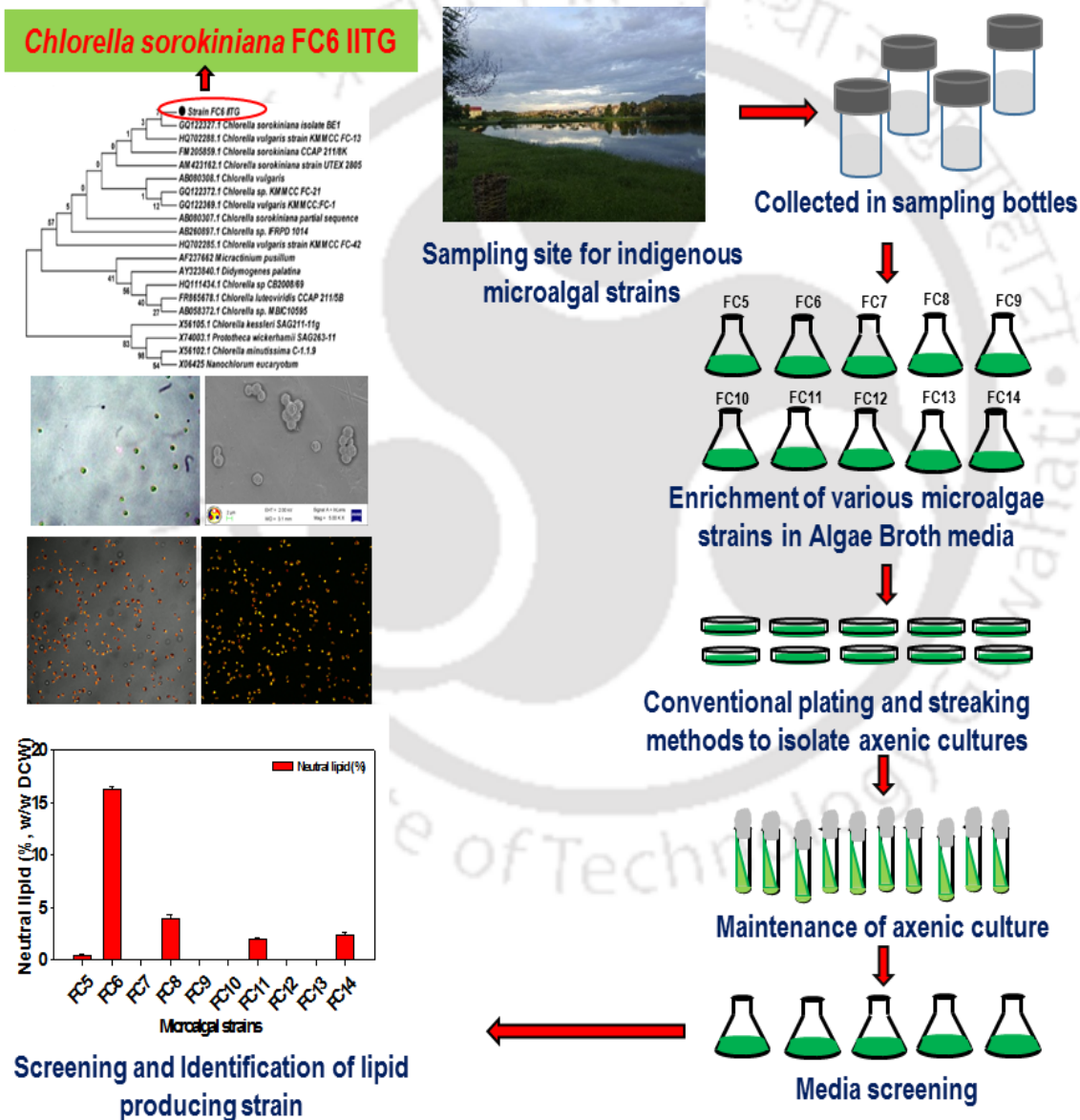
Aquatic Species Program – Biodiesel from Algae, Close Out Report TP-580-24190.
Golden, CO: National Renewable Energy Laboratory.

82. Singh, A., Nigam, P.S., Murphy, J.D., 2011. Renewable fuels from algae: an answer to debatable land based fuels. *Bioresour. Technol.* 102, 10-16.
83. Singh, J., Gu, S., 2010. Commercialisation potential of microalgae for biofuels production. *Renew. Sustain. Energy Rev.* 14, 2596-2610.
84. Spolaore, P., Joannis-Cassan, C., Duran, E., Isambert, A., 2006. Commercial applications of microalgae. *J. Biosci. Bioeng.* 101, 87-96.
85. Suganya, T., Varman, M., Masjuki, H., Renganathan, S. 2016. Macroalgae and microalgae as a potential source for commercial applications along with biofuels production: A biorefinery approach. *Renew. Sustain. Energy Rev.* 55, 909-941.
86. Takagi, M., Watanabe, K., Yamaberi, K., Yoshida, T., 2000. Limited feeding of potassium nitrate for intracellular lipid and triglyceride accumulation of *Nannochloris* sp. UTEX LB1999. *Appl. Microbiol. Biotechnol.* 54, 112-117.
87. Talukder, M.M.R., Das, P., Wu, J.C., 2014. Immobilization of microalgae on exogenous fungal mycelium: A promising separation method to harvest both marine and freshwater microalgae. *Biochem. Eng. J.* 91, 53-57.
88. Tevatia, R., Allen, J., Blum, P., Demirel, Y., Black, P., 2014. Modeling of rhythmic behavior in neutral lipid production due to continuous supply of limited nitrogen: Mutual growth and lipid accumulation in microalgae. *Bioresour. Technol.* 170, 152-159.
89. Uduman, N., Qi, Y., Danquah, M.K., Forde, G.M., Hoadley, A., 2010. Dewatering of microalgal cultures: a major bottleneck to algae-based biofuels. *J. Renew. Sustain. Energy.* 2, 1-15.

90. Vandamme, D., Foubert, I., Fraeye, I., Meeschaert, B., Muylaert, K., 2012. Flocculation of *Chlorella vulgaris* induced by high pH: role of magnesium and calcium and practical implications. *Bioresour. Technol.* 105, 114-119.
91. Walker, D.A., 2009. Biofuels, facts, fantasy and feasibility. *J. Appl. Phycol.* 21, 509-517.
92. Wang, H., Laughinghouse, H.D., Anderson, M.A., Chen, F., Williams, E., Place, A.R., Zmora, O., Zohar, Y., Zheng, T., Hill, R., 2012. Novel bacterial isolate from Permian groundwater, capable of aggregating potential biofuel-producing microalga *Nannochloropsis oceanica* IMET1. *Appl. Environ. Microbiol.* 78, 1445-1453.
93. Wang, J., Yang, H., Wang, F., 2014. Mixotrophic cultivation of microalgae for biodiesel production: status and prospects. *Appl. Microbiol. Biotechnol.* 172, 3307-3329.
94. Wijffels, R.H., 2007. Potential of sponges and microalgae for marine biotechnology. *Trends Biotechnol.* 26, 26-31.
95. Yeh, K., Chang, J., 2011. Nitrogen starvation strategies and photobioreactor design for enhancing lipid production of a newly isolated microalga *Chlorella vulgaris* ESP-31: implications for biofuels. *Biotechnol. J.* 6, 1358-1366.

CHAPTER 3

Sampling, isolation and identification of the suitable microalgal strain for biodiesel production



Sampling, isolation screening and identification of neutral lipid accumulating indigenous microalgal strain for biodiesel production.

3.1 Background and motivation

Oleaginous microalgae are considered as one of the most promising feedstock for renewable and sustainable production of biodiesel. However, microalgae based biodiesel production technology suffer from several limitations at different stages of the upstream and downstream processes e.g. strain selection, growth of microalgal strains under outdoor conditions, contamination, light penetration through dense culture, harvesting, drying, extraction and transesterification (Lam and Lee, 2012). Therefore, there is a need to design a sustainable process using hyper producing strains with improved biomass and lipid productivity. Recently, efforts have been aimed to identify robust microalgal strains with enhanced biomass productivity, and high net lipid productivity along with suitable fatty acid methyl ester (FAME) content for biodiesel production (Lam and Lee, 2012). To that end, high oil-accumulating indigenous robust strains with resistance towards changing climatic conditions and undesired contaminations is a prerequisite for sustainable process development (Mutanda et al., 2011). This can be achieved by identifying indigenous producer strains that are well adapted with the fluctuating natural habitats of that particular region. On the other hand, success of algae based biodiesel production depends on three key parameters (a) biomass productivity, (b) lipid yield and (c) lipid productivity which governs the techno economic feasibility of the whole process. To that end, it is indispensable to develop an efficient process with a suitable producer strain aiming at both optimal growth and lipid productivity (Hu et al., 2008).

In the present study, different microalgal strains from different habitats in and around Guwahati, Assam, India were collected, isolated and screened for neutral lipid accumulation. The strain with maximum lipid content was selected and the fatty acid composition were further evaluated to check their suitability for biodiesel production.

3.2 Materials and methods

3.2.1 Sampling and isolation of indigenous microalgal strains

The fresh water samples from fresh water bodies in and around Guwahati, North East region of India were collected in 250 mL sample bottles. 10 mL of the samples were transferred to 90 mL of the commercially available algal growth media (medium composition detailed in table 3.1) in 250 mL Erlenmeyer flasks and incubated in orbital shaker (Multitron-Pro, Infors HT, Switzerland) at 150 rpm, 28°C under light intensity of 30 $\mu\text{E m}^{-2} \text{s}^{-1}$ for 16:8 h light dark cycles. After incubation for two weeks, algal strains enriched in the algal broth media were plated in their respective algal agar media for further isolation. Individual algal cultures were isolated using conventional serial dilution and plating methods. The axenicity was confirmed through optical examination under light microscope (Eclipse E200, Nikon, Japan) and by spreading the culture on soya bean casein digest agar plates or broth for 3 days at 37°C to check the bacterial contaminants and for 5 days at 28°C to check the presence of fungal contaminants. The isolated axenic algal strains were stored as glycerol stock at -80°C and as slants at 28°C under light illumination in algae culture room.

3.2.2 Screening of neutral lipid accumulating microalgal strain

All the ten isolated microalgal strain (named as FC5 to FC14) were screened for neutral lipid accumulation using Nile-red based staining method (detailed in section 3.2.4.2) and also observed under confocal laser scan microscope for qualitative confirmation (detailed in section 3.2.4.3). The seed culture was prepared by inoculating two loops full of slant culture ($\sim 1.0 \times 10^6$ no. of cells) into 250 mL Erlenmeyer flask containing 100 mL of respective media composition (Table 3.1) and incubated aerobically in an orbital shaker and condition were kept same as mentioned in previous section 3.2.1.

Table 3.1 Common growth media used for isolation of microalgal strains from freshwater habitats (Barsanti and Gualtieri, 2006)

Freshwater medium	Suitable for algal family	Compositions (g L ⁻¹)*
Watanabe (AF6)	Euglenophyceae, Volvocalean algae, Xanthophytes, many Cryptophytes, Dinoflagellate and green ciliates; specific for algae requiring slightly acidic medium	NaNO ₃ 0.14, NH ₄ NO ₃ 0.022, MgSO ₄ 0.03, KH ₂ PO ₄ 0.01, K ₂ HPO ₄ 0.005, CaCl ₂ ·4H ₂ O 0.01, ammonium ferric citrate 0.002, citric acid 0.002, biotin 0.002, thiamine 10 µg, vitamin B6 1 µg, vitamin B12 1 µg, Na ₂ -EDTA 0.005, FeCl ₃ 0.098, MnCl ₂ ·4H ₂ O 0.18, ZnCl ₂ ·4H ₂ O 57 µg, Na ₂ MoO ₄ ·2H ₂ O 12.5 µg
Beijerinck (BJA)	Chlorophyceae	NH ₄ NO ₃ 0.15, K ₂ HPO ₄ 0.02, MgSO ₄ ·7H ₂ O 0.02, CaCl ₂ ·2H ₂ O 0.01, KH ₂ PO ₄ 0.363, K ₂ HPO ₄ 0.69, H ₃ BO ₃ 0.01, MnCl ₂ ·4H ₂ O 0.005, EDTA 0.05, CuSO ₄ ·5H ₂ O 0.0015, ZnSO ₄ ·H ₂ O 0.022, CoCl ₂ ·6H ₂ O 0.0015, FeSO ₄ ·7H ₂ O 0.005, (NH ₄) ₆ Mo ₇ O ₂₄ ·4H ₂ O 0.001
BG-11	Cyanophyceae	NaNO ₃ 1.5, K ₂ HPO ₄ ·3H ₂ O 0.004, MgSO ₄ ·7H ₂ O 0.075, CaCl ₂ ·2H ₂ O 0.036, Na ₂ CO ₃ 0.02, citric acid 0.006, ferric ammonium citrate 0.006, EDTA 0.001, and A5 + Co solution (1 mL L ⁻¹) that consists of H ₃ BO ₃ 2.86, MnCl ₂ ·H ₂ O 1.81, ZnSO ₄ ·7H ₂ O 0.222, CuSO ₄ ·5H ₂ O 0.079, Na ₂ MoO ₄ ·2H ₂ O 0.39, and Co(NO ₃) ₂ ·6H ₂ O 0.049
Bold Basal (BBM)	Broad spectrum medium for Chlorophyceae, Xanthophyceae, Chrysophyceae and Cyanophyceae unsuitable for algae with vitamin requirements	KH ₂ PO ₄ 0.175, CaCl ₂ ·2H ₂ O 0.025, MgSO ₄ ·7H ₂ O 0.075, NaNO ₃ 0.25, K ₂ HPO ₄ 0.075, NaCl 0.025, H ₃ BO ₃ 0.011, ZnSO ₄ ·7H ₂ O 0.00882, MnCl ₂ ·4H ₂ O 0.00144, MoO ₃ 0.00071, CuSO ₄ ·5H ₂ O 0.00157, Co(NO ₃) ₂ ·6H ₂ O 0.00049, Na ₂ EDTA 0.05, KOH 0.0031, FeSO ₄ 0.005, H ₂ SO ₄ 1 µL
Algae Broth (AB)	Commercial medium obtained from Himedia Pvt. Ltd., India	NaNO ₃ 1, MgSO ₄ ·7H ₂ O 0.513, K ₂ HPO ₄ 0.25, NH ₄ Cl 0.050, CaCl ₂ ·2H ₂ O 0.058, FeCl ₃ 0.003
Diatom	Bacillariophyceae	Ca(NO ₃) ₂ ·4H ₂ O 0.02, KH ₂ PO ₄ 0.0124, MgSO ₄ ·7H ₂ O 0.025, NaHCO ₃ 0.016, EDTA FeNa 0.0023, EDTA Na ₂ 0.0023, H ₃ BO ₃ 0.0025, MnCl ₂ ·4H ₂ O 0.00139, (NH ₄) ₆ Mo ₇ O ₂₄ ·4H ₂ O 0.001, Biotin 0.04 mg, Thiamine HCl 0.04 mg, Cyanocobalamine 0.04 mg, Na ₂ SiO ₃ ·9H ₂ O 57 mg

*-represents that the concentration of certain trace elements and vitamins are expressed in µg L⁻¹ or mg L⁻¹ as mentioned

An inoculation volume of 1% (v/v) was used to inoculate the flasks containing 100 mL algae broth media. Samples were taken at regular time intervals and used for the analysis of growth (details in section 3.2.4.1). Growth supporting medium for the selected strain was obtained by growing the strain in six different medium compositions as listed in Table 3.1 (Barsanti and Gualtieri, 2006). Seed culture (1%, v/v) was inoculated in 100 mL of six different media in 250 mL conical flasks and growth condition were kept same as mentioned in previous section 3.2.1. Sampling was done for every 24 hours for determination of dry cell weight and neutral lipid content. The media supporting the maximum growth of the strain was selected as the growth and maintenance medium for this particular strain. The strain with maximum neutral lipid accumulation was selected for further characterization and process development.

3.2.3 Identification of the microalgal strain

The FC6 strain with the ability to accumulate maximum amount of neutral lipid was considered for identification and further characterizations. Identification of the strain was carried out via morphometric analysis using Field-Effect scanning electron microscope (FESEM, Carl Zeiss SIGMA VP, Germany) and molecular analysis by 18S rDNA sequencing. For FESEM analysis, the grown FC6 cells were pelleted through centrifugation at $8,000 \times g$ for 5 minutes at 4°C and fixed with 2% (v/v) glutaraldehyde in 0.2 M phosphate buffer of pH 7.4. The fixed cells were then washed with buffer to remove media components and sequentially dehydrated with a range of 50 to 100% ethanol followed by overnight incubation in acetone. The sample obtained was coated with gold using a sputter coater (SC7620 “Mini” Polaron, Quorum Technologies, UK) and used for examination under FESEM. Genomic DNA of the strain was extracted using DNeasy Plant Mini Kit (Qiagen,

Valencia, CA) and the sequences were amplified for 18S rDNA using the universal forward primers 5'-GGTGATCCTGCCAGTAGTCATATGCTTG-3' (ss5) and reverse primer 5'-GATCCTTCCGCAGGTTACCTACGGAAACC-3' (ss3) in a thermal cycler (Matsumoto et al., 2010). Amplified fragments were sequenced in an ABIPRISM 3700 DNA sequencer (Applied Biosystems, USA). Homology to the partial 18S rDNA gene sequence of FC6 strain obtained was analyzed using BLAST. Based on similarities of 18S rDNA sequences between strain FC6 and related species, a phylogenetic tree was constructed using the software ClustalX 2.1 and MEGA 5.0.

3.2.4 Analytical techniques

3.2.4.1 Analysis of growth

Algal growth was estimated by measuring the absorbance of cells at 690 nm (Muthuraj et al., 2014) with a UV-visible spectrophotometer (Cary 50, Varian, Australia) and the dry cell weight (DCW) were obtained using the correlation equation. A known volume of algal biomass from the broth was collected and centrifuged at $8000 \times g$, 4°C for 10 minutes followed by washing with normal saline (0.8 % w/v sodium chloride) to make the biomass free from media components. The obtained cell pellet was further subjected to drying at a temperature of 60°C till a constant weight was reached and the dry cell weight was obtained gravimetrically. The absorbance values were converted in to dry cell weight (DCW) through appropriate calibration equations. For photoautotrophic condition: one cell density = $0.1896 \text{ g dry cells L}^{-1}$ ($R^2 = 0.99$).

3.2.4.2 Quantitative estimation of intracellular neutral lipid accumulation by Nile-red method

For Nile-red based neutral lipid analysis, cell pellet with absorbance of 0.7 was re-suspended in 1.0 mL of 25% (v/v) dimethyl sulfoxide. Nile red was added to the re-

suspended pellets at the concentration of $4 \mu\text{g mL}^{-1}$ and incubated at 50°C in a water bath for one minute. The fluorescence spectra was obtained in a spectrophotometer (Fluoromax 3, Horiba, USA) with excitation at 480 nm and emission in the region 550 to 650 nm. The auto-fluorescence of algal cells and the intrinsic fluorescence of Nile red were subtracted from the fluorescence of Nile red neutral lipid complex obtained at 580 nm. Triolein (Supelco, USA) was used as standard for Nile-red based neutral lipid estimation and the correlation graph is as shown in Fig. 3.1 and correlation equation is as follows:

$$\text{Fluorescence Intensity (a.u.)} = 3961.85 * \text{Triolein conc. (mg mL}^{-1}\text{)}, \quad R^2 = 0.99$$

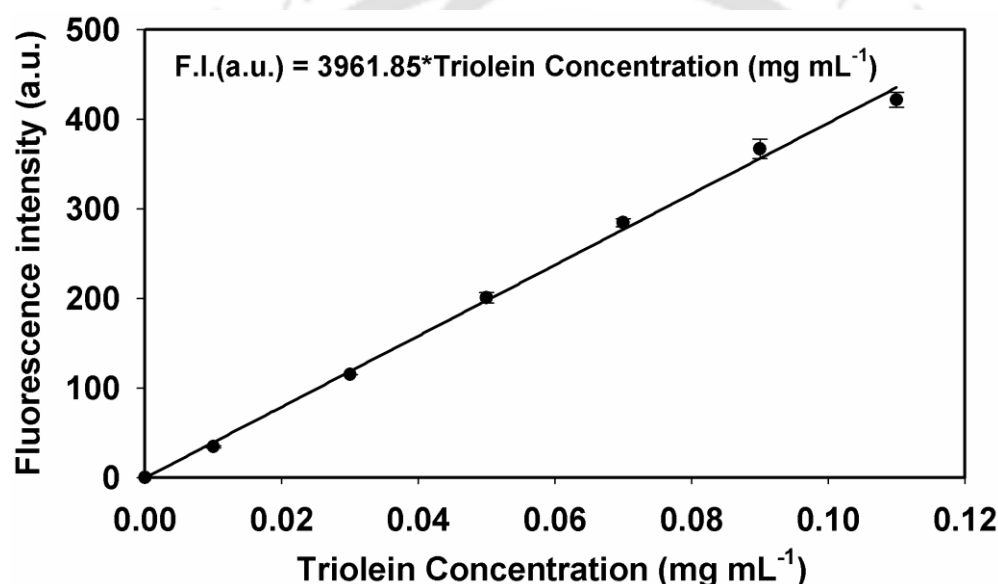


Fig. 3.1 Standard correlation graph for the estimation of neutral lipid (triolein) by Nile-red based assay method in fluorescent spectrophotometer. F.I. (a.u.) represents fluorescence intensity. All the experiments were conducted in triplicate and the data were represented as mean \pm standard error

3.2.4.3 *Qualitative detection of intracellular neutral lipid accumulation by confocal microscope*

Qualitative detection of neutral lipid accumulation in microalgal strain was performed under confocal microscope using Nile-red based staining method. The cell pellet with an absorbance 0.7 was concentrated and re-suspended in 1.0 mL of 25% (v/v) dimethyl sulfoxide (DMSO). Nile red was added to the re-suspended pellets at a concentration of 4

$\mu\text{g mL}^{-1}$ and incubated at 50°C in a water bath for 1 min. The methodology for Nile-red staining was developed in our laboratory by modifying the method suggested by Chen et al. (2009). The stained algal cells were loaded on the slide and viewed under confocal microscope (LSM Meta 510, Zeiss, Germany) at 10 X and 63 X oil immersion. The excitation light at a wavelength of 480 nm was generated using argon laser and the emissions were obtained at a bandwidth of 530-600 nm for Nile-red lipid complex. The auto-fluorescence of chlorophyll containing cells were obtained at wavelength greater than 630 nm.

3.2.4.4 Analysis of fatty acids methyl esters (FAME) derived from microalgae

Nascimento et al. (2012) reported that lipid productivity and fatty acid profile of the oleaginous microalgae is the key criteria for the suitability of microalgal strain for biodiesel production. Fatty acid profile greatly affect the quality of biodiesel. Fatty acid profile was evaluated in terms of fatty acid methyl ester obtained by transesterification of extracted microalgal lipid using alkali catalyst. Lipid was extracted from wet algal biomass by Bligh Dyer method. In case of Bligh and Dyer method 3.75 mL of 1:2 chloroform: methanol was added to 100 mg wet biomass, and sonicated at 30% amplitude for 30 s. Additional chloroform of 1.25 mL was added and sonicated once again followed by addition of 1.25 mL distilled water. The two phase systems were separated through centrifugation. Extracted algal oil was treated with 1 mL of 0.5N NaOH in methanol for 40 min for transesterification. After transesterification, FAME was extracted in hexane layer and analyzed for fatty acid profile using gas chromatography (GC). FAME were injected in GC equipped with flame ionization detector (GC-FID, Varian 450) and CP-Sil 8CB column (30 m x 0.25 mm i.d., 0.25 μm film thickness) with nitrogen as the carrier gas at a flow rate of 1.2 mL min^{-1} . The injector temperature was kept at 250°C with a split ratio of 1:20 and the oven temperature was kept at 100°C (5 min) followed by ramping at a rate of 5°C per min till 250°C followed

by 15 min hold. The detector temperature was kept at 280°C and the injection volume of 1 μL was used for analysis. FAME mix C14-C22 (Supelco, USA) was used as the standard for the fatty acid composition analysis using GC-FID and the total lipid was quantified in terms of FAME using calibration curve shown in Fig. 3.2.

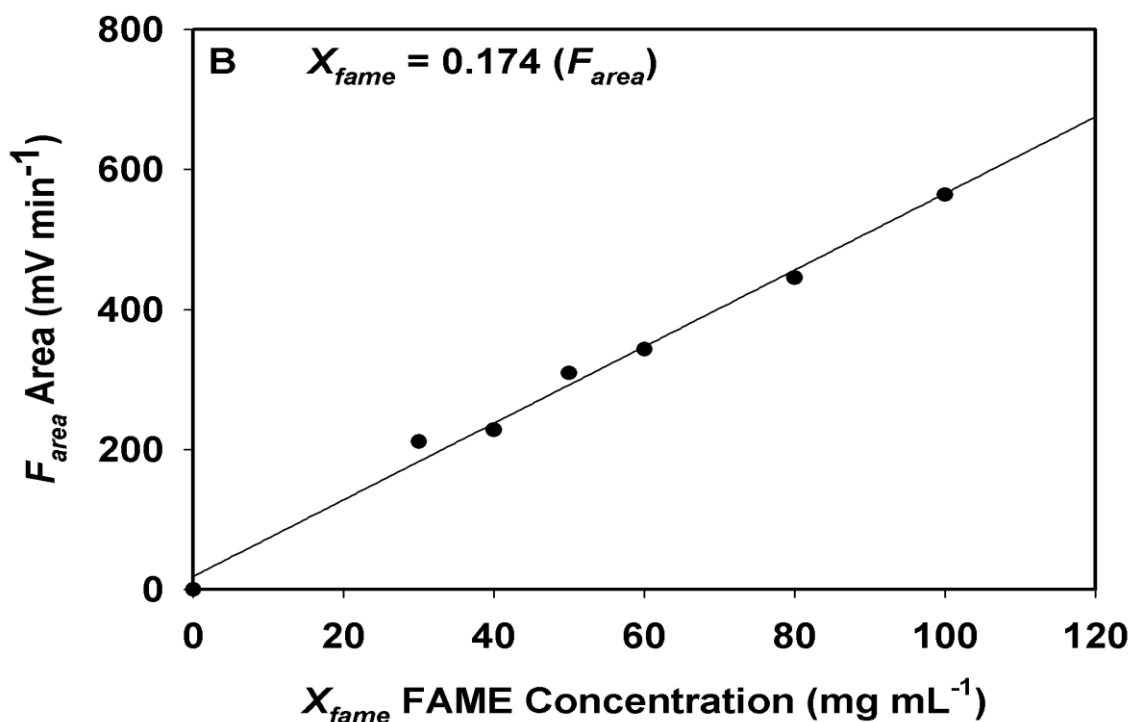


Fig. 3.2 Standard correlation graph for the estimation of total lipid as fatty acid methyl esters assayed in gas chromatograph with standard FAME mix C14-C22

3.3 Results and discussion

3.3.1 Sampling and isolation of indigenous microalgal strains

The rationale behind microalgal bio-prospecting is to identify high neutral lipid accumulating strains. Even though many microalgal strains were isolated and characterized for biodiesel production, indigenous species of microalgae with high lipid yields are especially valuable in the biofuel industry as they can flourish well in their native environment. To that end, the present study targeted the isolation and screening of indigenous microalgal strains from areas in and around Guwahati, India. Ten different microalgal strains were isolated and named as FC5, FC6, FC7, FC8, FC9, FC10, FC11,

FC12, FC13 and FC14. To obtain a pure culture conventional serial dilution, plating and streaking method was used. The collected strains were stored as slants and as glycerol stocks (20% w/v, glycerol) at -80°C . Further axenic culture was screened for high lipid accumulation under photoautotrophic condition.

3.3.2 Screening and selection of neutral lipid accumulating microalgal strains

The main aim of screening is to identify the “Oleaginous” algal strain which can accumulate substantial amount of neutral lipids. The neutral lipid content of the organism was quantified by Nile-red method detailed in section 3.2.5.2. Among the ten microalgal strains screened, five strains showed neutral lipid accumulation as shown in Fig. 3.3 only in BG11 growth media. Other five strains did not show any neutral lipid accumulation even after incubation for a period of over 30 days under photoautotrophic conditions. As observed from the fluorescence intensity of neutral lipid Nile-red complex FC6 was found to be the best neutral lipid accumulating organism (Fig. 3.3). The neutral lipid content in FC6 culture was found to be 16.30% (w/w, DCW) at the end of 30 days of cultivation followed by FC8 with 4.0% (w/w, DCW) as shown in Fig. 3.3.

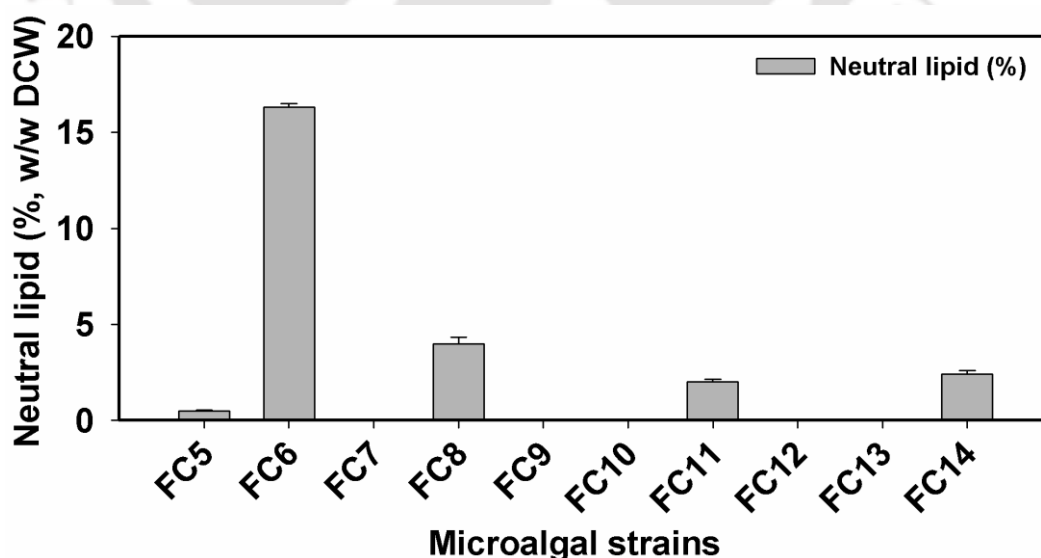


Fig. 3.3 Screening and selection of high lipid accumulating indigenous microalgal strains in BG11 media. The neutral lipid content was measured using Nile-red method.

Further, neutral lipid accumulation was confirmed by Nile-red neutral lipid complex under confocal microscope analysis of microalgal cell (Fig. 3.4). With the maximum total lipid content, FC6 was identified as the best neutral lipid accumulating strain among the screened indigenous strains. Thus, the strain was chosen for further detailed identification and media screening experiments.

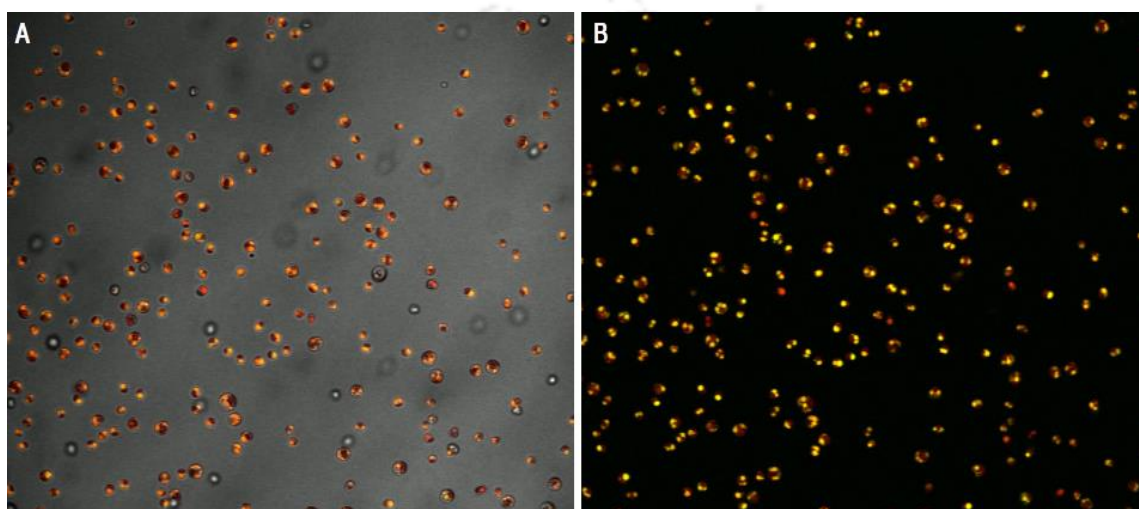


Fig. 3.4 Confocal imaging of strain FC6 under higher magnification (A) superimposed image of bright field cells, auto-fluorescence of cells stained with Nile red and fluorescence from Nile red-neutral lipid complex; (B) Cells showing auto-fluorescence in red color and Nile red-neutral lipid complex fluorescence as golden yellow color. The images were obtained using confocal microscope with Olympus software.

3.3.3 Selection of the suitable growth medium for selected indigenous microalgal strain

The growth medium for selected FC6 strain was screened by growing it in six different medium compositions. The best media for the growth were screened on the basis of dynamic profile of its growth for 16 days (Fig. 3.5). Amongst all medium composition used, BG11 medium supported the maximum growth with a biomass concentration of 0.69 g L⁻¹ (Fig. 3.5). This may be attributed to the availability of high concentration of sodium nitrate in the BG11 medium supporting maximum growth of the strain.

Less growth was observed in case of Watanabe media followed by Beijerinck media, Bold Basal media, Algae broth media and Diatom medium (0.47 g L⁻¹, 0.37 g L⁻¹, 0.31 g L⁻¹, 0.16 g L⁻¹ and 0.12 g L⁻¹ and respectively). The reduced growth in Bold Basal Media, Beijerinck media and Diatom media may be attributed to the lower concentration of nitrate source 0.25 g L⁻¹, 0.15 g L⁻¹ and 0.02g L⁻¹ respectively. Thus, BG11 media was chosen as the best growth supporting medium for the selected strain and further medium optimization was performed to enhance the biomass titer.

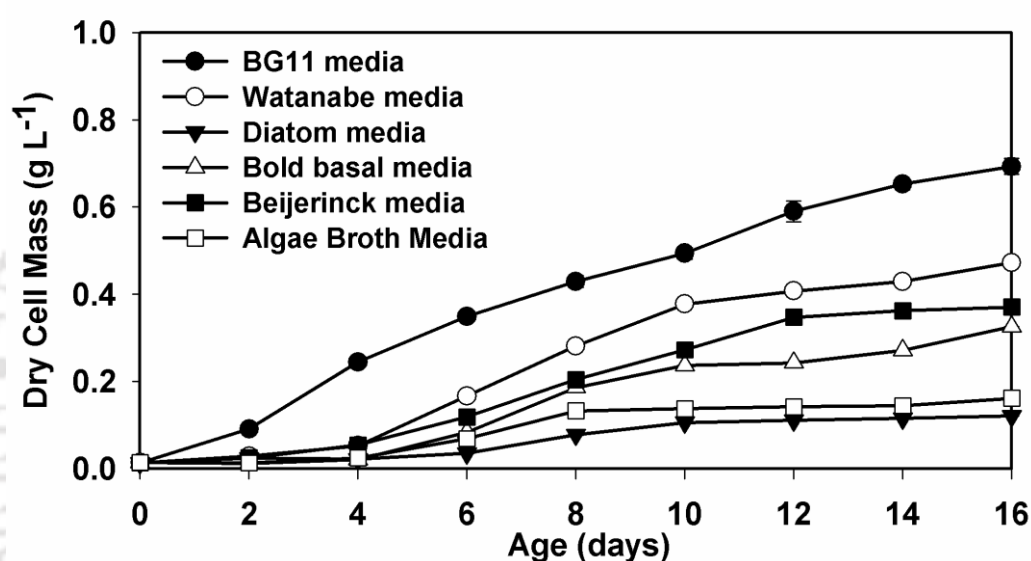


Fig. 3.5 Selection of best growth media for the growth of indigenous microalgal strain FC6. Six different media compositions were used as detailed in section 3.2.2 (Table 3.1)

3.3.4 Morphometric and molecular identification of the organism

The colonies on BG11 agar plate were green in color, spherical convex in shape and shiny with regular edges. Observation under light microscope showed that the cells are spherical in shape, green in color, non-motile and measured about 4-6 μm in diameter (Fig. 3.6 A). FESEM analysis of the cells showed the absence of flagella and spikes over their surface (Fig. 3.6 B). The partial 18S rDNA sequence of length 1074 base pairs was obtained through sequencing and submitted to the Genbank (Accession No.: JX453208). BLAST analysis showed that the isolate is novel in terms of its 18S rDNA sequence and belongs to

the genus *Chlorella* sp. with a maximum similarity of 97%. Phylogenetic analysis of the strain and 19 other organisms under the order *Chlorellales* with 97% similarity showed that the strain belongs to *Chlorella sorokiniana*.

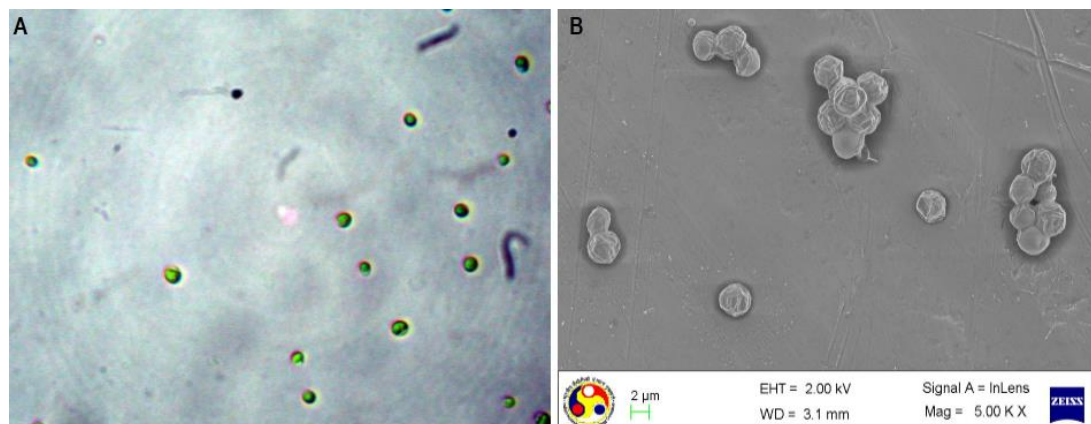


Fig. 3.6 Morphometric identification of the strain FC6: (A) Cells under phase contrast microscope and (B) Field effect scanning electron microscopic image of the cell obtained at 2.0KV EHT and 5 KX magnification

Thus based on the morphometric analysis and molecular analysis, the isolated strain was designated as *Chlorella sorokiniana* FC6 IITG (Fig. 3.7). The strain *Chlorella sorokiniana* FC6 IITG is referred as FC6 in this thesis.

3.3.5 Fatty acid profile of the stored lipid obtained from *Chlorella sorokiniana* FC6 IITG

In order to evaluate the suitability of selected microalgal strain for biodiesel production, fatty acid composition of stored lipid was analyzed. The FAME composition of FC6 was analyzed using gas chromatography. Palmitic acid (C16:0), oleic acid (C18:1), and linoleic acid (C18:2) were the three major fractions that constitute the majority of total fatty acid compositions. These fatty acids were also found to be abundant in other *Chlorella* sp. reported in the literature. In the present study, the selected strain was able to produce fatty acids with 85% contributions from saturated (C16:0) and unsaturated (C18:2, C18:2) fatty acids, which are considered to be the key elements for suitable quality biodiesel (Liu et al.,

2011). Hence, *Chlorella sorokiniana* FC6 IITG can be a potential candidate for good-quality biodiesel production.

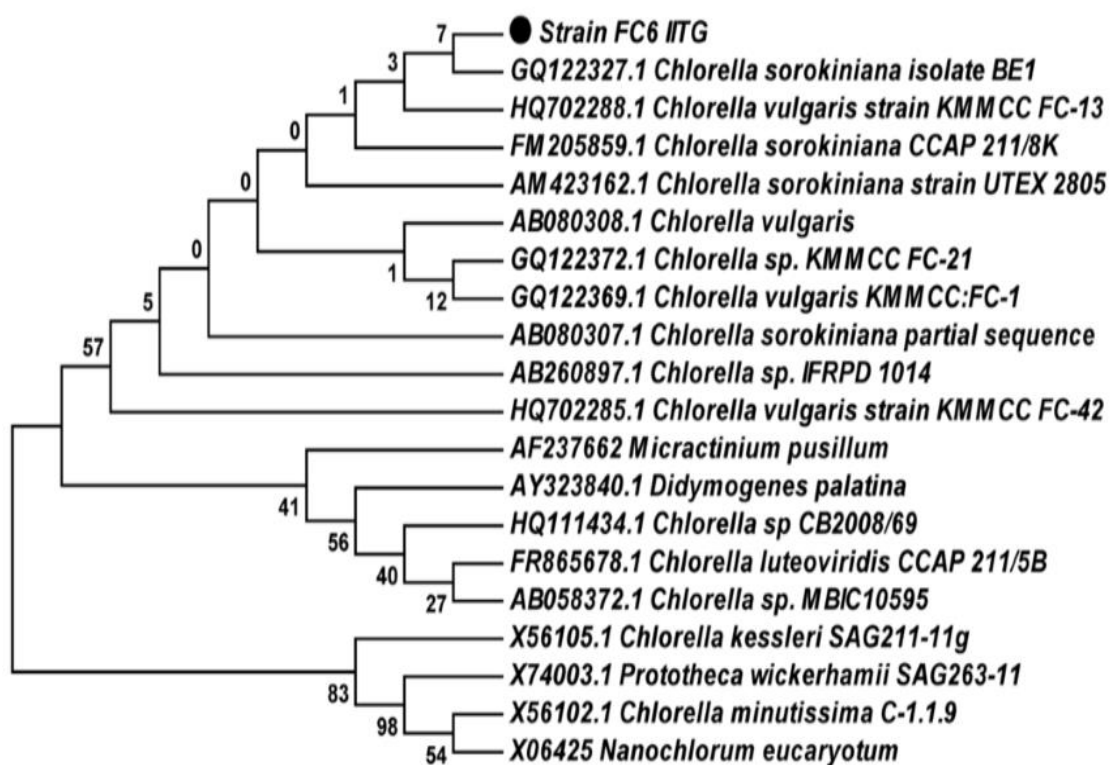


Fig. 3.7 Molecular identification of FC6. Phylogenetic tree based on 18S rDNA sequences of the strain and genus within the order *Chlorellales*. The tree was constructed using neighbor-joining method with Jukes-cantor model. Bootstrap test (1000 replicates in %) is shown next to the branches and taxon name starts with the gene accession number. The isolated strain reported in this study is marked with (●).

3.4 Conclusions

Ten different microalgal strains were isolated and screened for neutral lipid accumulation. Five different strains were found to accumulate neutral lipid with FC6 showing maximum total lipid content of 16% (w/w, DCW). Thus, FC6 was chosen for further identification and media screening to support maximum growth to the selected organism. Among the various media tested BG11 media was found most suitable for FC6 strain. The strain was identified as *Chlorella sorokiniana* and therefore designated as *Chlorella sorokiniana* FC6 IITG. FAME analysis of the strain *Chlorella sorokiniana* FC6

IITG showed palmitic acid (C16:0), oleic acid (C18:1), and linoleic acid (C18:2) as the major constitute of total fatty acid compositions which are considered to be the key elements for suitable quality biodiesel.



3.5 References

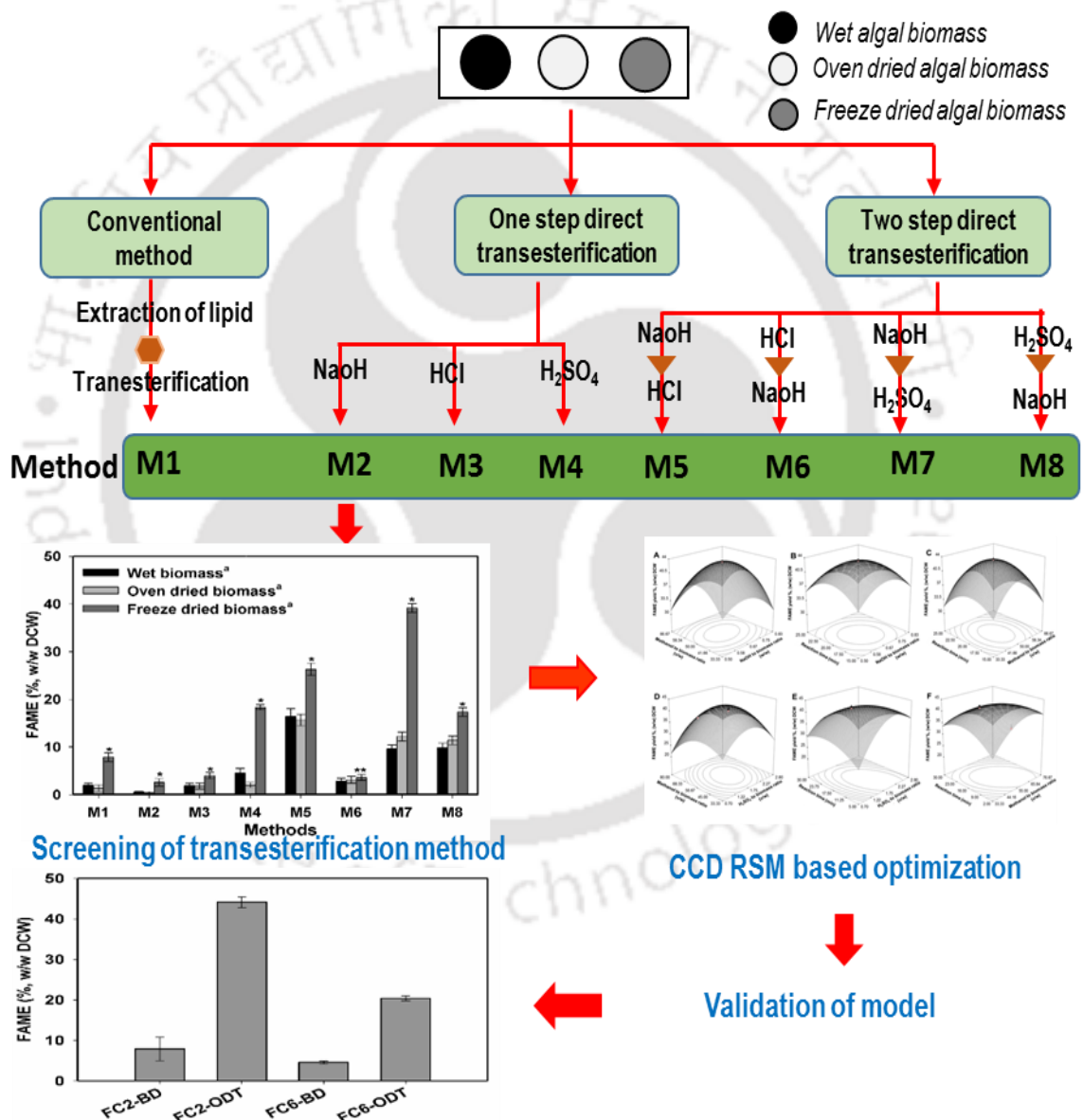
1. Barsanti, L., Gualtieri, P., 2006. *Algae: Anatomy, Biochemistry, and Biotechnology*, CRC Press, Taylor & Francis, London.
2. Chen, W., Zhang, C.W., Song, L.R., Sommerfeld, M., Hu, Q., 2009. A high throughput Nile-red method for quantitative measurement of neutral lipids in microalgae. *J. Microbiol. Methods.* 77, 41-47.
3. Cooksey, K.E., Guckert, J.B., Williams, S.A., Callis, P.R., 1987. Fluorometric determination of the neutral lipid-content of microalgal cells using Nile red. *J. Microbiol. Methods.* 6, 333-345.
4. Elsey, D., Jameson, D., Raleigh, B., Cooney, M.J., 2007. Fluorescent measurement of microalgal neutral lipids. *J. Microbiol. Methods.* 68: 639-642.
5. Hu, Q., Sommerfeld, M., Jarvis, E., Ghirardi, M., Posewitz, M., Seibert, M., Darzins, A., 2008. Microalgal triacylglycerols as feedstocks for biofuel production: perspectives and advances. *Plant J.* 54, 621-639.
6. Lam, M.K., Lee, K.T., 2012. Microalgae biofuels: a critical review of issues, problems and the way forward. *Biotechnol. Adv.* 30, 673-90.
7. Liu, J., Huang, J., Sun, Z., Zhong, Y., Jiang, Y., Chen, F., 2011. Differential lipid and fatty acid profiles of photoautotrophic and heterotrophic *Chlorella zofingiensis*: Assessment of algal oils for biodiesel production. *Bioresour. Technol.* 102, 106-110.
8. Mutanda, T., Ramesh, D., Karthikeyan, S., Kumari, S., Anandraj, A., Bux, F. 2011. Bioprospecting for hyper lipid producing microalgal strains for sustainable biofuel production. *Bioresour. Technol.* 102, 57-70.
9. Muthuraj, M., Kumar, V., Palabhanvi, B., Das, D., 2014. Evaluation of indigenous microalgal isolate *Chlorella* sp. FC2 IITG as a cell factory for biodiesel production and scale up in outdoor conditions. *J. Ind. Microbiol. Biotechnol.* 41, 499-511.

10. Nascimento, I.A., Marques, S.S.I., Cabanelas, I.T.D., Pereira, S.A., Druzian, J.I., de Souza, C.O., Vich, D.V., de Carvalho, G.C., Nascimento, M.A., 2013. Screening Microalgae Strains for Biodiesel Production: Lipid Productivity and Estimation of Fuel Quality Based on Fatty Acids Profiles as Selective Criteria. *Bioenerg. Res.* 6, 1-13.



CHAPTER 4

Development of direct transesterification (DT) method for accurate quantification of microalgal lipid content



Development of direct transesterification (DT) method for accurate quantification of microalgal lipid content.

4.1 Background and motivation

Microalgae based biodiesel production has gained significant interest as a potential alternative source that can effectively fulfill the energy requirements due to its competitive combustion efficiency with less sulfur emission and carbon negative properties (Singh and Cu, 2010). Oleaginous microalgae has ability to accumulate lipid up to 40-70% (w/w) of dry biomass, lipid contents depends on cultivation condition and individual microalgae. Total lipid content of microalgae reflects energy yield from the biomass and hence, has largest impact on overall process economy for biodiesel production (Devis et al., 2011). Conventional lipid quantification method underestimated the FAME yield of total lipid due to inadequate extraction and loss of some lipid due to more unit operation step. Therefore, accurate and reliable quantification of microalgal lipid content is the key towards selection of suitable algal strains, optimizing growth condition and process monitoring. The traditional method of lipid estimation proposed by Bligh and Dyer (Bligh and Dyer, 1959) relies on extraction of intracellular lipid from algal biomass using chloroform and methanol. However, this method of lipid estimation may suffer from various limitations: (i) incomplete extraction of lipid from algal biomass, (ii) extraction is dependent on the polarity of the solvent as well as composition of the algal lipids (Palmquist and Jenkins, 2003; Pruvost et al., 2009) and (iii) possibility of simultaneous extraction of non-saponifiable compounds such as pigments (Pruvost et al., 2009). It has been demonstrated that fine tuning of process parameters of Bligh and Dyer method resulted in increased lipid yield, pointing towards incomplete extraction of the original method (Iverson et al., 2001; Folch et al., 1957). Further extraction of the oil from algal biomass remains the major challenge in the overall process due to the rigid cell wall structure and smaller size of the algal cells (Johnson and Wen, 2009). Due to lower efficiency of conventional extraction method, various physical and chemical pretreatment methods were incorporated in the extraction procedure, which

augmented further expenses without considerable increase in extraction efficiency. These methods involve large amount of solvents such as hexane, chloroform, and methanol causing adverse effects on health and environment (Cheng et al., 2011). Therefore, there is a need to develop an efficient and reliable method for laboratory scale quantification of algal lipid eliminating separate extraction step.

Use of *in situ* transesterification or direct transesterification (DT) of the algal biomass for converting lipids into biodiesel may be a viable option which can bypass expenses of extraction and the harmful effects of the solvents used in conventional methods over the environment (Wahlen et al., 2011). Johnson and Wen (2009) demonstrated that one step DT of *Schizochytrium limacinum* yielded higher amounts of FAME than conventional extraction based methods. A sequential two stage DT method with higher FAME yield was reported for three different algal strains (Griffiths et al., 2010). However, development of efficient and rapid DT method is still evolving in the literature. Moreover, the DT methods reported in the literature need to be further optimized to increase transesterification efficiency. To that end, a reliable DT method with increased hydrolysis and FAME conversion efficiencies need to be designed, which is a prerequisite for selection of strains with high lipid content.

The present research reports the quantification of algal lipid via DT of whole biomass (a) to eliminate separate step for lipid extraction; (b) to be applicable to various microalgal strains and; (c) to improve transesterification efficiency. Initially, array of 24 experiments were conducted to select the best combination of transesterification and the type of biomass (wet, oven dried and lyophilized biomass). Each biomass type was tested against eight different transesterification methods to screen the best combination in terms of FAME yield. The combination with maximum FAME yield was further optimized using statistically designed

RSM experiments. The process parameters: catalyst to biomass ratio, methanol to biomass ratio and reaction time were optimized for maximizing the transesterification efficiency.

4.2 Materials and methods

4.2.1 Algal culture and biomass preparation

It is to note that the efficient DT method was first developed for a previously well characterized strain *Chlorella* sp. FC2 IITG isolated in our laboratory (Muthuraj et al., 2014). The method was further validated for the present strain *Chlorella sorokiniana* FC6 IITG. Seed culture of *Chlorella* sp. FC2 IITG and *Chlorella sorokiniana* FC6 IITG was grown in a 250 mL flask containing 100 mL BG11 medium (medium composition detailed in table 3.1 of chapter 3). The flasks were incubated in an orbital shaker with continuous shaking at 150 rpm, temperature 28°C and illumination of 20 $\mu\text{mol photons m}^{-2} \text{s}^{-1}$ with a light: dark cycle of 16:8 h. Mid log phase grown seed culture was used as inoculum (1%, v/v) to obtain lipid rich biomass via heterotrophic cultivation of *Chlorella* sp. FC2 IITG and photoautotrophic cultivation of *Chlorella sorokiniana* FC6 IITG in a 5.0 L automated bioreactor (Biostat B Plus, Sartorius Stedim Biotech, Germany) containing 3.0 L BG11 medium and grown at temperature 28°C, agitation 400 rpm and aeration 1vvm. Under heterotrophic cultivation BG11 medium was supplemented with 15 g L⁻¹ of glucose as the sole source of energy and carbon (Muthuraj et al., 2013). The pH was maintained at 7.4 through addition of 0.25 M NaOH/HCl. Under photoautotrophic condition 1% (v/v) CO₂ mixed with air was used as carbon source and illumination of 20 $\mu\text{mol photons m}^{-2} \text{s}^{-1}$ with a light: dark cycle of 16:8 h was used as energy source. Once the culture reached the stationary phase, cells were harvested by centrifugation at 8000 x g at 4°C for 10 min. The pellets were washed twice in saline (0.85%, w/v NaCl) and frozen immediately at -80°C. The frozen cells were directly used as wet algal biomass (water content 80%, w/w) whereas

the cells dried in a hot air oven at 80°C for 24 hours were used as oven dried algal biomass (water content 0%, w/w). The cells were lyophilized for 12 hours at 0.08 mtorr vacuum to obtain the freeze dried algal biomass (water content 33%, w/w). Depending upon the experimental designs, different biomass type in the form of lyophilized or oven dried or wet biomass was used for transesterification. All the screening experiments and DT optimization were performed in the heterotrophic biomass of *Chlorella* sp. FC2 IITG and the evaluation of the optimized method was carried out in photoautotrophic biomass of *Chlorella sorokiniana* FC6 IITG.

4.2.2 Selection of best combination of transesterification method and biomass type

Eight different transesterification methods were carried out to screen the best combination of transesterification method and type of biomass for FAME production (Fig. 4.1). While M1 represents conventional method of lipid extraction proposed by Bligh and Dyer (1959) followed by transesterification, the remaining seven methods (M2-M8) represent *in situ* transesterification and their combinations in one or two stage process. All methods were carried out with three different types of algal biomass which includes wet, oven dried and lyophilized biomass to evaluate the effect of biomass on transesterification. Wet biomass of 100 mg and its equivalent lyophilized biomass of 30 mg and oven dried biomass of 20 mg were used in each method. In case of Bligh and Dyer method (M1), 3.75 mL of 1:2 chloroform: methanol was added to 100 mg wet biomass, and sonicated at 30% amplitude for 30 s. Additional chloroform of 1.25 mL was added and sonicated once again followed by addition of 1.25 mL distilled water. The two phase systems were separated through centrifugation. However, extraction of lipid from lyophilized and oven dried biomass was carried out with extra addition of 0.8 mL and 0.7 mL of distilled water respectively, to make the final volume equal in all three types of biomass for the method M1.

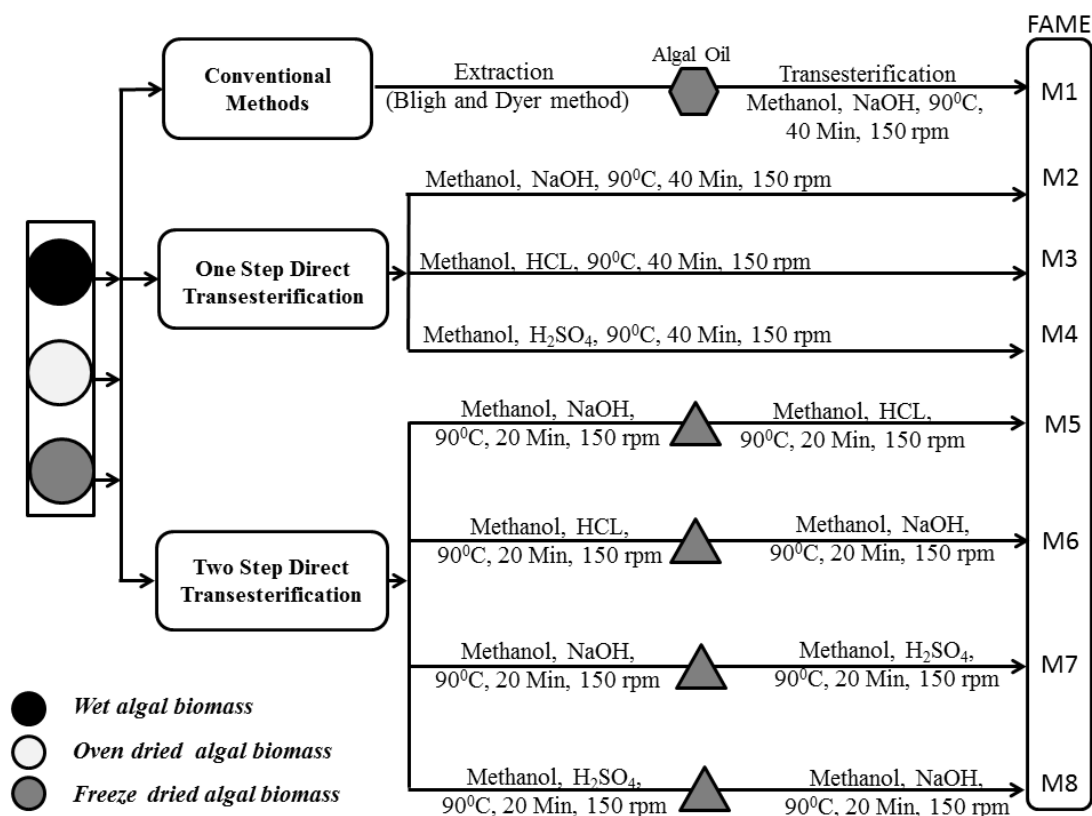


Fig. 4.1 Schematic representation of eight different transesterification methods (M1-M8) conducted with three different types of biomass used in the present study. A total of 24 experiments were carried out to select best combination of transesterification and biomass type with FAME yield as process response. M1 represent conventional method of extraction-transesterification. M2, M3 & M4 represent one step DT methods with NaOH, HCl and H₂SO₄ as the catalyst respectively. M5-M8 represents two stage DT with different combination of acid-base catalyst. All the transesterification experiments were performed with methanol as the solvent at a temperature of 90 °C and a constant shaking of 150 rpm in a shaking water bath

All the transesterification experiments were performed with methanol as the solvent and acid (H₂SO₄ or HCl) and/or base (NaOH) as catalysts, at a temperature of 90°C and a constant shaking of 150 rpm in a water bath. Glyceryl-triheptadecanoate (C17 from Sigma Aldrich, USA) was used as the internal standard to assess the transesterification efficiency of each method. The transesterification efficiency was calculated as follows:

$$\begin{aligned} & \text{transesterification efficiency (\%)} \\ &= \frac{\text{amount of C17:1 methyl ester obtained}}{\text{amount of fatty acid C17:1 added}} \times 100 \end{aligned}$$

In the conventional method (M1) the extracted algal oil was treated with 1 mL of 0.5N NaOH in methanol for 40 min, whereas in one step DT method, algal biomass was directly treated with 1 mL of 0.5N NaOH in methanol (M2), 1 mL of 5% HCL (v/v) in methanol (M3) and 1 mL 5% (v/v) H₂SO₄ in methanol (M4) for 40 min (Fig. 4.1). In the two step DT methods, the sequential treatment of algal biomass with 1 mL of alkali catalyst (0.5 N NaOH in methanol) followed by acid catalyst (5%, v/v HCl in methanol or 5%, v/v H₂SO₄ in methanol) (M5, M7) and vice versa (M6, M8) were carried out for 20 min for each step of transesterification (Fig. 4.1). After transesterification, FAME was extracted in upper hexane layer by centrifugation at 8000 x g for 5 min and used for GC analysis. The selection of best transesterification method was carried out by comparing the FAME yield (% , w/w DCW). In case of two stage DT methods the FAME yield was obtained after both the stages of transesterification.

4.2.3 Optimization of process parameters for transesterification by statistical design

Preliminary screening experiments resulted in sequential two stage DT method M7 with lyophilized biomass as the best combination for FAME production (Fig. 4.1). In the next step, RSM combined with central composite design (CCD) was applied to optimize the process parameters for this combination (Patil et al., 2011; Jeong et al., 2009). The method M7 involved two stages with NaOH treatment in the first stage followed by H₂SO₄ treatment in the second stage. Catalyst to biomass ratio (CBR), methanol to biomass ratio (MBR) and reaction time (RT) were the three factors selected for FAME optimization and their levels are shown in Table 4.1. The actual level of parameters used were determined using separate experiments conducted to study the individual effect of the parameters on FAME yield. The reaction temperature was kept constant for both the stages of transesterification at 90 °C. The CCD was formulated using the software Design Expert 8.0.0 (Stat-Ease Inc, Minneapolis, USA) with three factors and five levels (Table 4.2).

Table 4.1 Actual and coded levels of the selected three transesterification parameters used in both the stages of CCD-RSM experimental design

Parameters and their levels used in first stage (alkali catalyst) optimization					
Trans-esterification parameters	Parameter levels with coded and un-coded values				
	-1.68	-1	0	1	1.68
X ₁ NaOH to Biomass ratio (W/W)	0.39	0.5	0.67	0.83	0.95
X ₂ Methanol to Biomass ratio (V/W)	21.96	33.33	50	66.67	78.04
X ₃ Reaction Time (min)	11.59	15	20	25	28.41

Parameters and their levels used in second stage (acid catalyst) optimization					
Trans-esterification parameters	Parameter levels with coded and un-coded values				
	-1.68	-1	0	1	1.68
X ₁ H ₂ SO ₄ to Biomass ratio (V/W)	0.04	0.70	1.67	2.65	3.31
X ₂ Methanol to Biomass ratio (V/W)	21.96	33.33	50	66.67	78.04
X ₃ Reaction Time (min)	3.18	10	20	30	36.82

Table 4.2 CCD matrix of independent transcription parameters used in RSM with corresponding experimental and predicted measurements of FAME yield (% , w/w DCW) in first and second stages

Std. Order	CCD design for first stage (alkali catalyst) optimization					CCD design for second stage (acid catalyst) optimization				
	X1	X2	X3	FAME yield (%)		X1	X2	X3	FAME yield (%)	
				Exp.	Pred.				Exp.	Pred.
1	0.50	33.33	15.00	30.34	30.91	0.70	33.33	10.00	25.16	23.33
2	0.83	33.33	15.00	29.35	29.50	2.65	33.33	10.00	30.00	30.85
3	0.50	66.67	15.00	27.55	27.19	0.70	66.67	10.00	29.94	28.13
4	0.83	66.67	15.00	29.95	30.77	2.65	66.67	10.00	41.68	41.43
5	0.50	33.33	25.00	30.55	30.19	0.70	33.33	30.00	28.60	28.73
6	0.83	33.33	25.00	24.70	25.58	2.65	33.33	30.00	21.93	23.62
7	0.50	66.67	25.00	26.81	27.16	0.70	66.67	30.00	25.13	24.16
8	0.83	66.67	25.00	27.62	27.53	2.65	66.67	30.00	23.14	24.84
9	0.39	50.00	20.00	32.83	33.14	0.04	50.00	20.00	14.34	17.05
10	0.95	50.00	20.00	32.30	31.47	3.31	50.00	20.00	26.27	23.92
11	0.67	21.96	20.00	24.38	23.94	1.67	21.96	20.00	30.20	29.63
12	0.67	78.04	20.00	22.69	22.58	1.67	78.04	20.00	34.00	34.66
13	0.67	50.00	11.59	34.62	34.25	1.67	50.00	3.18	37.17	38.86
14	0.67	50.00	28.41	31.00	30.84	1.67	50.00	36.82	31.10	29.50
15	0.67	50.00	20.00	43.45	43.40	1.67	50.00	20.00	42.00	41.61
16	0.67	50.00	20.00	43.29	43.40	1.67	50.00	20.00	41.29	41.61

The CCD required 16 experiments which included eight factorial points, six axial points and two replicates of center point to search linear, quadratic and interaction effect of

transesterification parameters with FAME yield. The model response Y , FAME yield was expressed as second order polynomial equation is as shown in equation 4.1.

$$Y = \beta_0 + \sum_{i=1}^k \beta_i X_i + \sum_{i=1}^k \beta_{ii} X_i^2 + \sum_{i=1, i < j}^{k-1} \sum_{j=2}^k \beta_{ij} X_i X_j \quad (4.1)$$

Where, X_i is the i^{th} parameter, k is the total number of parameters and β_0 , β_i , β_{ii} and β_{ij} are the regression coefficients. Optimization for each stage was carried out separately and during one stage of optimization, the other stage transesterification parameters were kept constant. During first stage of optimization, the second stage parameters H_2SO_4 to biomass ratio, MBR and RT were kept at constant value of 2 (v/w), 60 (v/w) and 15 (min) respectively. Whereas, the optimum parameters obtained from first stage of RSM were kept as constant during the second stage optimization.

4.2.4 Field emission scanning electron microscopic analysis

Scanning electron microscopy (SEM) experiments were performed using a field emission gun scanning electron microscope (FESEM-Carl Zeiss, SIGMA VP instrument) in order to visualize the degree of hydrolysis of the algal samples during DT. The residual algal biomass after transesterification and the control algal biomass samples were dehydrated rapidly through an alcohol series (70-90% ethanol) after repeated washing in phosphate buffer of pH 7.0, followed by re-suspension in 100% ethanol and left overnight. The microalgal samples were deposited on a specimen stub with the adhesive carbon strip and coated with gold sputtering to allow a better conduction of the sample.

4.2.5 FAME analysis using GC

FAMEs were quantified directly in GC equipped with flame ionization detector (GC-FID, Varian 450) and CP-Sil 8CB column (30 m x 0.25 mm i.d., 0.25 μm film thickness) with nitrogen as the carrier gas at a flow rate of 1.2 mL min^{-1} . The injector

temperature was kept at 250°C with a split ratio of 1:20 and the oven temperature was kept at 100°C (5 min) followed by ramping at a rate of 5°C per min till 250°C followed by 15 min hold. The detector temperature was kept at 280°C and the injection volume of 1 µL was used for analysis. FAME mix C14-C22 (Supelco, USA) was used as the standard for GC-FID.

4.2.6 Fourier transform infrared spectrophotometer (FTIR) Analysis

The infrared spectra were analyzed by Fourier transform infrared spectrophotometer (IR Affinity-1 Shimadzu) from 500 to 4000 cm^{-1} to analyze the functional group of the diesel and biodiesel using KBr pellets.

4.2.7 Statistical analysis

Statistical analyses of the results obtained were performed using the software Minitab version 16.1.1 (Lead Technologies Inc.). All the experiments were conducted in triplicate and the data were expressed as mean \pm standard error. The significant difference in the various biomass types used and significant difference among the methods M1-M8 for each type of biomass were analyzed through one-way analysis of variance by evaluating their p-values.

4.3 Results and discussion

4.3.1 Selection of best combination of biomass type and transesterification method

Eight different transesterification methods were screened for three types of biomass to quantify the total intracellular fatty acid content in heterotrophically grown *Chlorella* sp. FC2 IITG. Among the various feed stocks used, lyophilized biomass exhibited the highest FAME yield with all the combinations of transesterification methods (Fig. 4.2). Freeze drying of the algal biomass prevents the oxidation of fatty acids and reduces the water content in them to less than approximately 35% which might have resulted in higher FAME

yield. In case of oven dried biomass the reduction in FAME yield may be due to the oxidation of fatty acids (Oehrl et al., 2001). For instance, reduction in total lipid content was reported when algal biomass was dried at temperature greater than 60°C in an atmosphere with oxygen/air (Widjaja et al., 2009). Oxidation of fatty acids results in formation of ketone bodies or aldehydes resulting in overall reduction of fatty acid content (Widjaja et al., 2009). Oehrl et al. (2001) demonstrated that unsaturated fatty acids are prone to oxidation than saturated fatty acids. In the present study, GC-FID profiling of the total fatty acids in *Chlorella* sp. FC2 IITG revealed the abundance of unsaturated fatty acids (>75% w/w, of total FAME) which might have undergone oxidation in the course of oven drying.

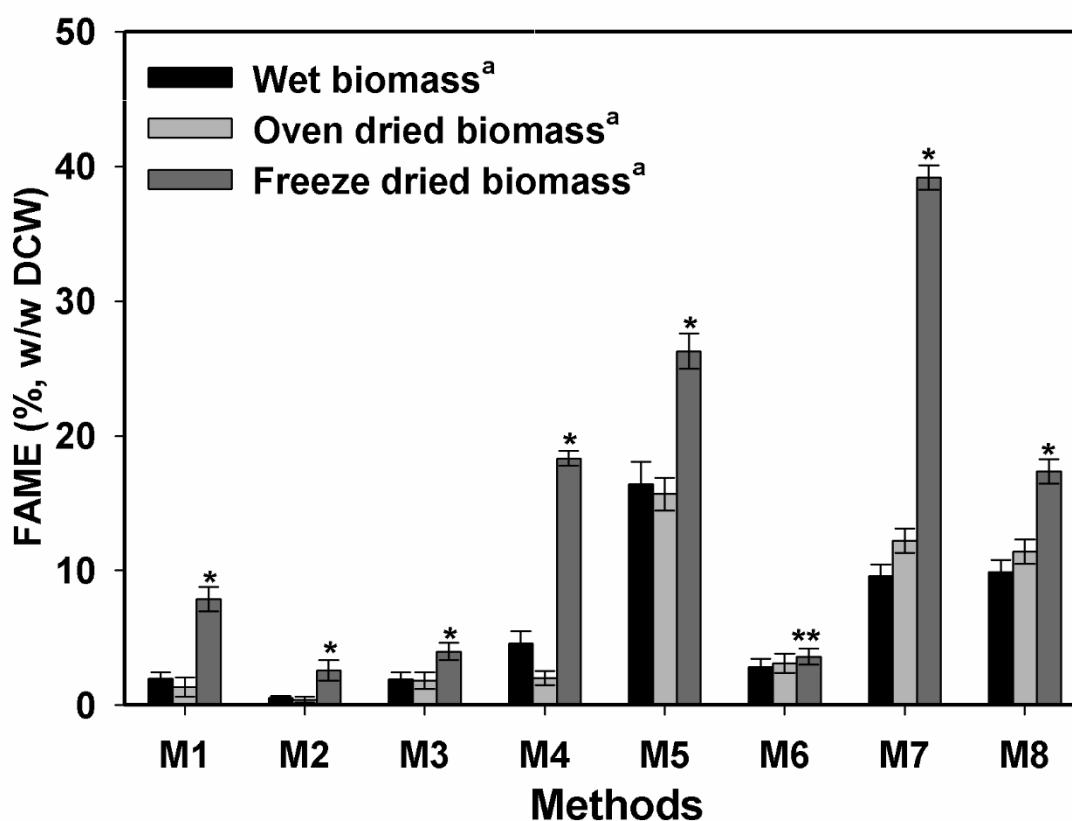


Fig. 4.2 FAME yield (% w/w DCW) of the *Chlorella* sp. FC2 IITG obtained from eight different transesterification methods (M1-M8) and three different types of biomass. The significant difference among the biomass types is represented as “*” and the significant difference among the methods M1-M8 for each type of biomass are represented as ‘a’ obtained from one way analysis of variance (corresponding p-values for * = 0; ** = 0.022; a = 0)

Wet biomass showed reduced FAME yield than any other type of biomass due to high water content of about 80% (v/w) (Komers et al. 2001). Presence of water in the wet algal biomass interferes with the acid/alkali catalyst reducing the overall catalyst availability and transesterification efficiency. Fatty acids are saponified by the alkali catalyst in presence of water which in turn results in the formation of viscous froth and hinders effective transesterification (Griffiths et al., 2010; Kusdiana and Saka, 2004). In case of transesterification with acid catalysts, the fatty acids are protonated by the acid followed by the formation of tetrahedral intermediate with alcohol and finally the proton migrates to form FAME (Lotero et al. 2005). In the presence of water, acid catalyst binds to water leading to a reversible acid catalyst deactivation and the water molecules masks the acid by forming proton clusters around them (Lotero et al. 2005) and characteristic decrease of FAME yield in presence of water was also reported (Liu et al., 2006). Depending upon the type of biomass, the degree of transesterification varied significantly among the eight different methods. Maximum FAME yield was obtained in the two stage DT method M7 for lyophilized biomass in comparison to all other methods. M5 showed maximum FAME yield in cases of both wet and oven dried biomass when compared with other evaluated methods (Fig. 4.2).

Conventional Bligh and Dyer lipid extraction-transesterification method (M1) resulted in lowest FAME yield (7.87%, w/w in lyophilized biomass) in all types of biomass. The commonly used Bligh and Dyer method underestimated the FAME yield which may be attributed to inadequate extraction and unoptimized solvent ratios (Griffiths et al., 2010; Laurens et al., 2012). Three different catalysts (NaOH, HCl and H₂SO₄) were used to determine the individual effect on the single stage DT (M2-M4). Very less FAME yield was obtained in case of NaOH and HCl as catalysts (M2 and M3) in comparison to conventional extraction transesterification which may be due to incomplete extraction and

transesterification in the single stage DT methods M2 and M3. When CH_3ONa was used as catalyst in single stage transesterification, no FAME yield was detected in case of *Nannochloropsis* sp. and reported that two stages ($\text{CH}_3\text{ONa} / \text{BF}_3$) are necessary to obtain higher transesterification efficiency (Laurens et al., 2012). However, when H_2SO_4 was used as single catalyst in M4, a 2.4 fold increase in FAME yield was obtained in comparison to conventional method M1 and single stage DT methods M2 and M3 applied to lyophilized biomass. The two stage DT methods M5 and M7 with base and acid catalyzed treatments for first and second stage respectively showed higher FAME yield. Interestingly, when catalysts order was reversed in M6 and M8, the process resulted in lower FAME yield. In a recent study, it has been reported that the alkaline hydrolysis of algal biomass in the first stage of DT prior to methylation might have lead towards higher FAME yield (Griffiths et al., 2010). DT is effective transesterification method that can bypass the oil extraction step by merging it into transesterification step (Cheng et al., 2011) with subsequent reduction in the production cost of biodiesel from algal feedstock. The sequential two stages DT method M7 with lyophilized algal biomass was selected for further optimization using CCD on the basis of highest FAME yield obtained.

4.3.2 Optimization of process parameters for transesterification

A CCD was constructed to optimize the three transesterification parameters CBR (alkali or acid catalyst), MBR and RT involved in both the stages of DT method M7 (Table 4.2). All the 16 experiments were conducted in two different sets and the results were analyzed through multiple regression analysis. The coefficients were calculated using regression analysis and tested their significance based on p-value (Table 4.3). The best fitting model and the main effects of parameters were depicted using analysis of variance (ANOVA) for both the stages of DT (Table 4.3). All the three linear, quadratic and interaction terms determined by the model in the first and second stage of transesterification

were found significant (Table 4.3) except interaction of MBR and RT in first stage of transesterification and interaction of CBR and MBR in second stage of transesterification. F-values of 144.91 for first and 17.20 for second stage were greater than the critical values which show their significance and the low probability of getting errors in their value. The regression model provided the predicted FAME yield with R^2 value of 0.99 and 0.96 for the first and second stage of transesterification respectively (Table 4.2). The signal to noise ratios of 41.83 and 13.23 were found greater than their critical value 4 for first and second stage of optimization respectively showing very less noise disturbance in the models. Therefore, the model fit to the experimental system was adequate. The model equations for first and second stage are shown in the equations 4.2 and 4.3 respectively,

$$Y = -134.1 + 183.42X_1 + 2.19X_2 + 6.48X_3 - 141.54X_1^2 - 0.026X_2^2 - 0.15X_3^2 + 0.45X_1 * X_2 - 0.97X_1 * X_3 + 0.002X_2 * X_3 \quad (4.2)$$

$$Y = -41.01 + 30.6X_1 + 1.43X_2 + 2.01X_3 - 7.9X_1^2 - 0.012X_2^2 - 0.026X_3^2 + 0.089X_1 * X_2 - 0.32X_1 * X_3 - 0.014X_2 * X_3 \quad (4.3)$$

Fig. 4.3 shows the response surface and contours for the effect of different combinations of transesterification parameters in both the stages. Each plot of FAME yield is a representation of different combinations of two parameters at one time while keeping the third parameter constant at its middle value (Fig. 4.3A-4.3F). NaOH to biomass ratio 0.67, MBR 49.51 and RT 19.33 min were found as optimal points of FAME yield in first stage modeling (Fig. 4.3A-4.3C). Likewise in second stage optimization, surface plots (Fig.4.3D-4.3F) revealed that optimum resides at H_2SO_4 to biomass ratio 2.07, MBR 61.07 and RT 10 min. The variations in parameter values from their optimal region resulted in negative effect on FAME yield.

Table 4.3 ANOVA for the quadratic regression model obtained from CCD-RSM employed in optimization of parameters involved in two stage sequential direct transesterification of lipid from *Chlorella* sp. FC2 IITG

Source	ANOVA for first stage (alkali catalyst) regression model					ANOVA for second stage (acid catalyst) regression model				
	Sum of Squares	DOF	Mean Square	F value	p-value*	Sum of Squares	DOF	Mean Square	F Value	p-value
Model	518.42	9	57.6	144.91	< 0.0001	863.29	9	95.92	17.2	0.0013
X ₁	1.5	1	1.5	3.77	0.1004	57.34	1	57.34	10.28	0.0184
X ₂	2.51	1	2.51	6.31	0.0458	31.05	1	31.05	5.57	0.0563
X ₃	13.54	1	13.54	34.06	0.0011	106.79	1	106.79	19.15	0.0047
X ₁ ²	142.63	1	142.63	358.81	< 0.0001	523.22	1	523.22	93.83	< 0.0001
X ₂ ²	469.16	1	469.16	1180.25	< 0.0001	103.66	1	103.66	18.59	0.005
X ₃ ²	136.4	1	136.4	343.14	< 0.0001	63.86	1	63.86	11.45	0.0148
X ₁ *X ₂	12.63	1	12.63	31.76	0.0013	16.76	1	16.76	3.01	0.1337
X ₁ *X ₃	5.2	1	5.2	13.08	0.0111	79.63	1	79.63	14.28	0.0092
X ₂ *X ₃	0.23	1	0.23	0.59	0.4715	43.8	1	43.8	7.86	0.0311
Residual	2.39	6	0.4	--	--	33.46	6	5.58	--	--
Lack of fit	2.37	5	0.47	37.07	0.124	33.21	5	6.64	26.35	0.1468
Pure Error	0.013	1	0.013	--	--	0.25	1	0.25	--	--
Total	520.8	15	--	--	--	896.75	15	--	--	--
	R ² = 0.9954 Signal to noise ratio = 41.83					R ² = 0.9627 Signal to noise ratio = 13.23				

* - p value >0.05 is considered as insignificant

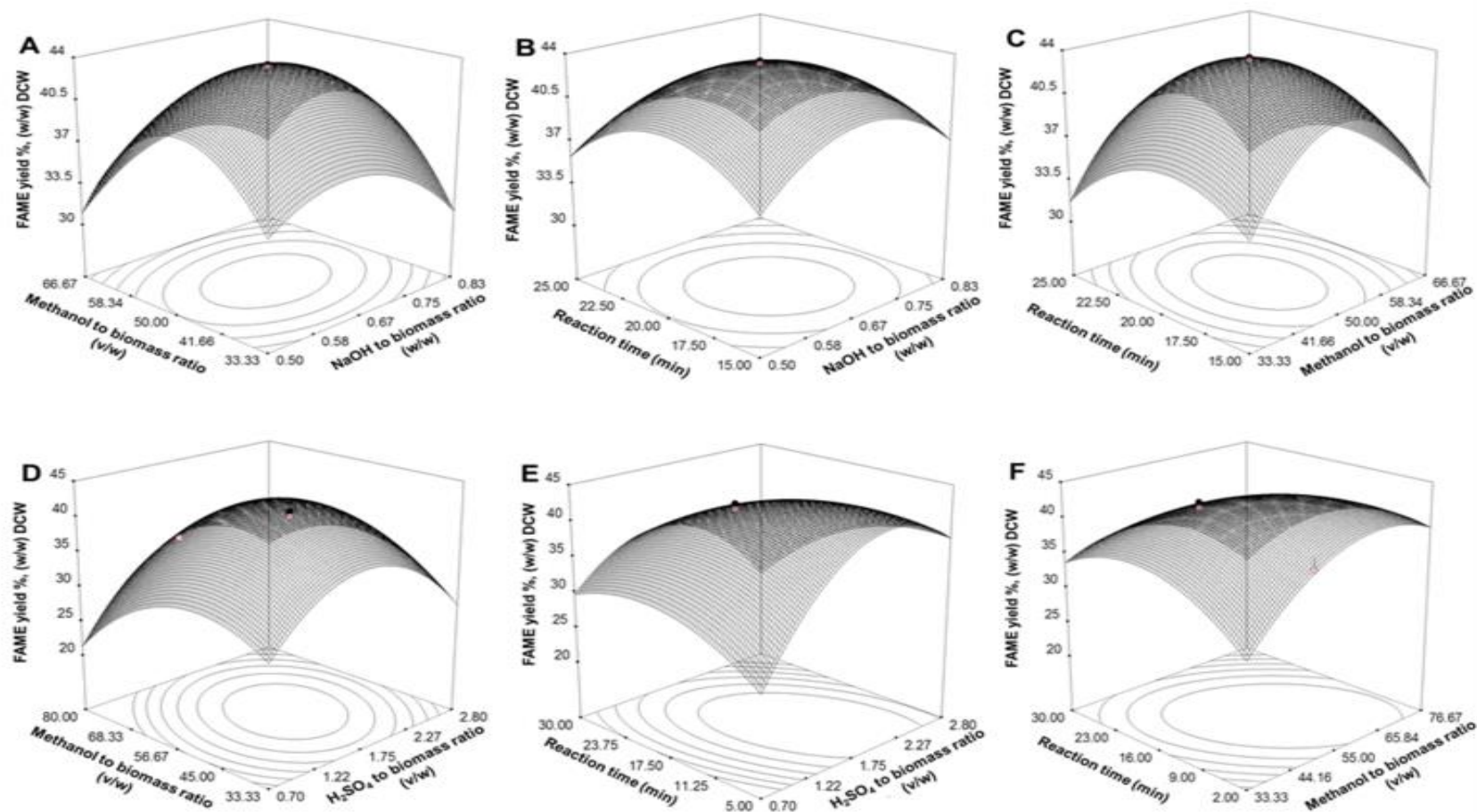


Fig. 4.3 Response surface plots representing the effect of various parameters and their interaction on FAME yield. (A) methanol to biomass ratio and NaOH to biomass ratio (B) reaction time and NaOH to biomass ratio (C) reaction time and methanol to biomass ratio (D) methanol to biomass ratio and H₂SO₄ to biomass ratio (E) reaction time and H₂SO₄ to biomass ratio (F) reaction time and methanol to biomass ratio.

In the first stage of transesterification, MBR up to 50 (v/w) was found to affect significantly the FAME yield in which the methanol acts not only as the reactant for transesterification but also as a solvent in cell lysis. Increased volumes of methanol used decreased the FAME yield which may be due to the dilution of NaOH catalyst concentration and/or lipid (Patil et al., 2011; Zhang et al., 2010) and use of such high volumes of solvent augments the cost of solvent recovery and purification. At lower volumes of methanol, the extraction and transesterification processes were hindered due to limited availability of the solvent (Zhang et al., 2010). Similar response for increasing MBR (61.07, v/w) was obtained in the second stage of transesterification. At a lower NaOH to biomass ratio, catalyst was insufficient to carry out complete reaction whereas in higher ratios, decrease in FAME yield was observed attributed to increased formation of fatty acid salts (Leung and Guo, 2006). Lower reaction time caused incomplete extraction and transesterification of intracellular lipid while higher reaction time encouraged degradation of FAME as well as soap formation (Eevera et al., 2009). The acid catalyst availability was low to carry out complete DT at lower ratio of H₂SO₄ to biomass while in higher ratio; excess acid caused loss of unsaturated esters leading to undesirable side reactions (Morrison and Smith, 1964). Validation of the predicted optimum through experiment resulted in similar FAME yields (44.3%, w/w DCW) as predicted by the model (44.15% w/w, DCW). In comparison to the un-optimized two stage DT method M7, the RSM optimized method showed 13% increase in FAME yield. The optimized method showed 462.6% increase in FAME yield when compared with conventional Bligh and Dyer method M1 (Fig. 4.4). The optimized DT method M7 was further tested with another microalgal strain *Chlorella sorokiniana* FC6 IITG and the FAME yield was compared with the corresponding value obtained from conventional method M1. An increment of 445.4% FAME yield from the optimized DT in comparison to conventional Bligh and Dyer method for *Chlorella sorokiniana* FC6 (Fig. 4.4).

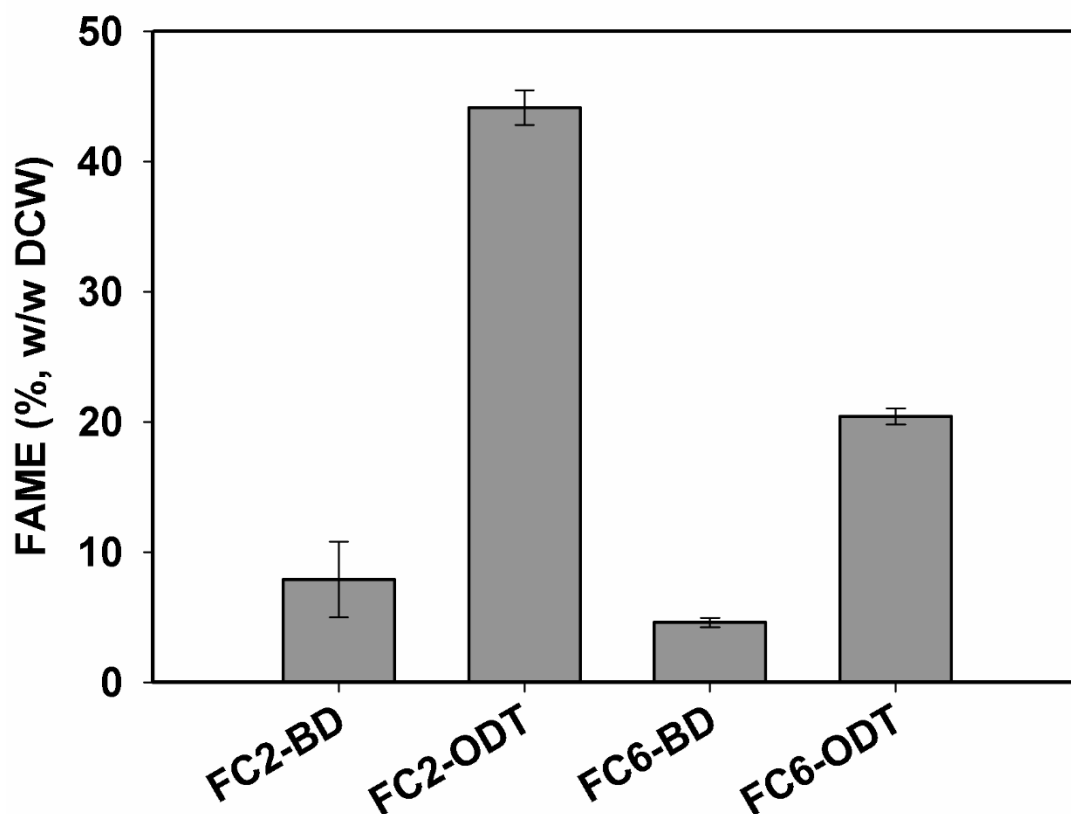


Fig. 4.4 Comparison of FAME yield (% w/w DCW) obtained by Bligh Dyer method (BD) and optimized DT method (ODT). FC2-BD and FC2-ODT represents conventional Bligh Dyer method and optimized DT method respectively for *Chlorella* sp. FC2 IITG. FC6-BD and FC6-ODT represents conventional Bligh Dyer method and optimized DT method respectively for *Chlorella sorokiniana* FC6 IITG.

4.3.3 Effect of transesterification methods on hydrolysis and transesterification efficiency

Rehydrated lyophilized cells of *Chlorella* sp. FC2 IITG and the residues after DT methods M4, M8 and optimized M7 were collected and the SEM images of the cells were obtained to understand the degree of hydrolysis (Fig. 4.5). The control cells (untreated) were analyzed to determine the native structural organization whereas the post transesterified biomass residues from the method M4 was chosen for analysis attributed to its higher FAME yield in single stage DT methods. The algal residues after transesterification from method M8 (reverse order of M7) and optimized M7 were also chosen, to understand the effect of

catalyst order on two stage DT methods. The lyophilized control algal biomass appeared rigid, regular, spherical without any demarcations and measured about 2-5 μm in diameter (Fig. 4.5A).

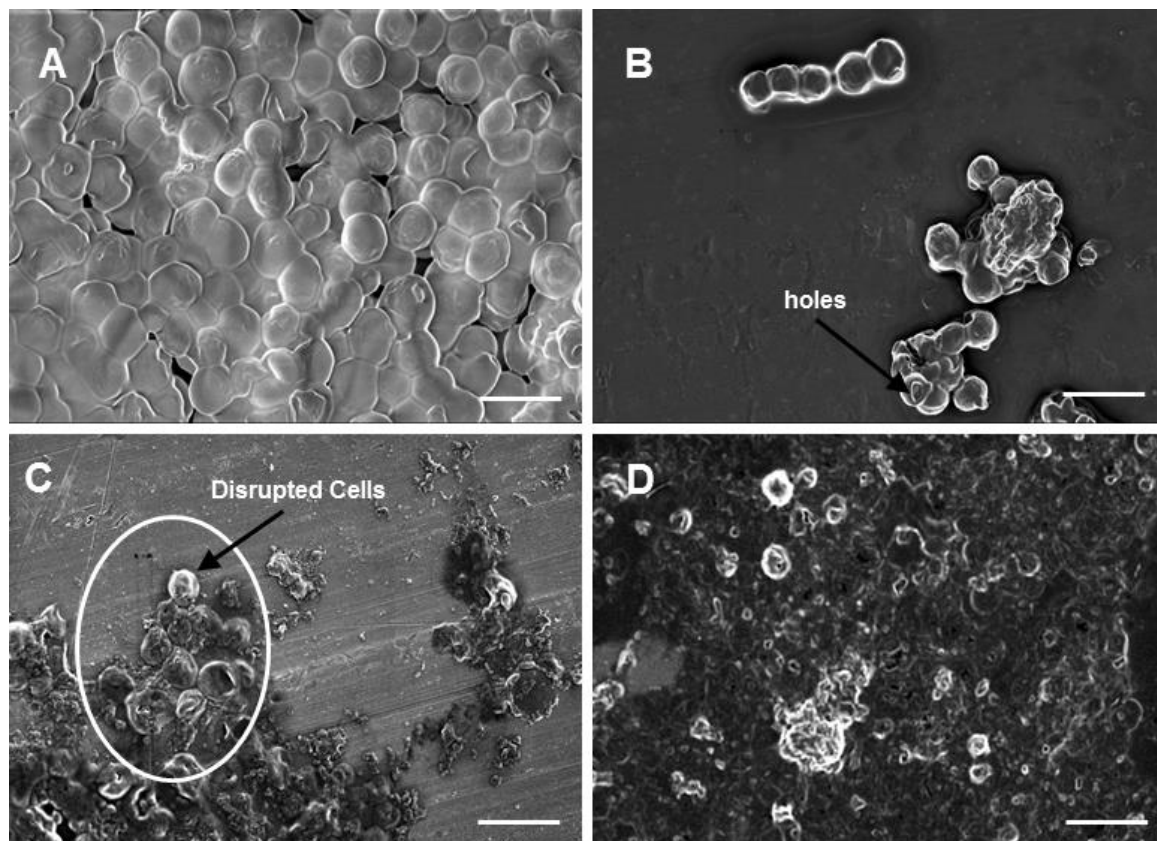


Fig. 4.5 Field emission scanning electron microscopic images for the (A) control (untreated) algal cells and the residual materials obtained after DT methods (B) M4, (C) M8 and (D) optimized M7. The images were in uniform scale of 10 μm . For details on the sample preparation method refer to the material and method section 4.2.4.

From the figures (Fig. 4.5), it is evident that the FAME yield is dependent on the degree of hydrolysis of algal biomass which in turn depends purely on the type of catalyst used in different transesterification methods. For instance, while in case of M4 only destabilized cell wall with pores on cell surface was evident from FESEM image (Fig. 4.5B), cells from M8 were found to be completely destabilized (Fig. 4.5C). Interestingly, in the optimized M7 method we could not find any intact cells in the field (Fig. 4.5D). Therefore, use of alkali catalyst either in first (M7) or second stage (M8) of transesterification resulted in

significantly improved hydrolysis of algal biomass as compared to acid catalyst used in M4. Hence, a lower FAME yield in M4 as compared to two stage methods can be attributed to inefficient hydrolysis of cell mass. Interestingly, catalyst order used in M8 and M7 are also found to critically influence the FAME yield. Higher FAME yield was obtained for the method M7 where NaOH was used in the first stage followed by H₂SO₄ in the second stage of transesterification. However, the reverse order of catalyst used in M8 resulted in less FAME yield. Use of alkali catalyst in the first stage resulted in efficient hydrolysis of cell mass releasing the intracellular lipid bodies for subsequent transesterification in the second step. However, the reverse catalyst order did not effectively hydrolyze the cell mass and hence, reduced lipid availability for transesterification in the second step. Griffith et al. (2010) also suggested that sequential use of base and acid catalyst in the first and second steps results in increased FAME yield contributed to the effective alkaline hydrolysis in first step and efficient transesterification in second step. In order to obtain transesterification efficiency, the methods M1-M8 and the optimized M7 with lyophilized biomass were spiked with C17 (Fig. 4.6). Maximum transesterification efficiency was obtained (98.96%) for optimized M7 method whereas the methods un-optimized M7 and M5 showed the next high transesterification efficiency of 94.5% and 93% respectively. Sequential combination of alkali catalyst followed by acid catalyst (M7 and M5) gave higher transesterification efficiency in comparison to sequential combination of acid catalyst followed by alkali catalyst (40.98% for M6 and 44.7% for M8). In case of single stage DT (M2-M4) using single catalyst either alkali or acid spiked with C17 showed less transesterification efficiency 24.9%, 22.7% and 48.5% (Fig. 4.6). Single catalysts (NaOH and HCl) showed more or less same transesterification efficiency and different FAME yield, so it is hypothesized that there may be a significant difference in the hydrolysis efficiency.

However H_2SO_4 have more transesterification efficiency with more FAME yield in comparison to NaOH and HCl might be due to efficient hydrolysis of cells.

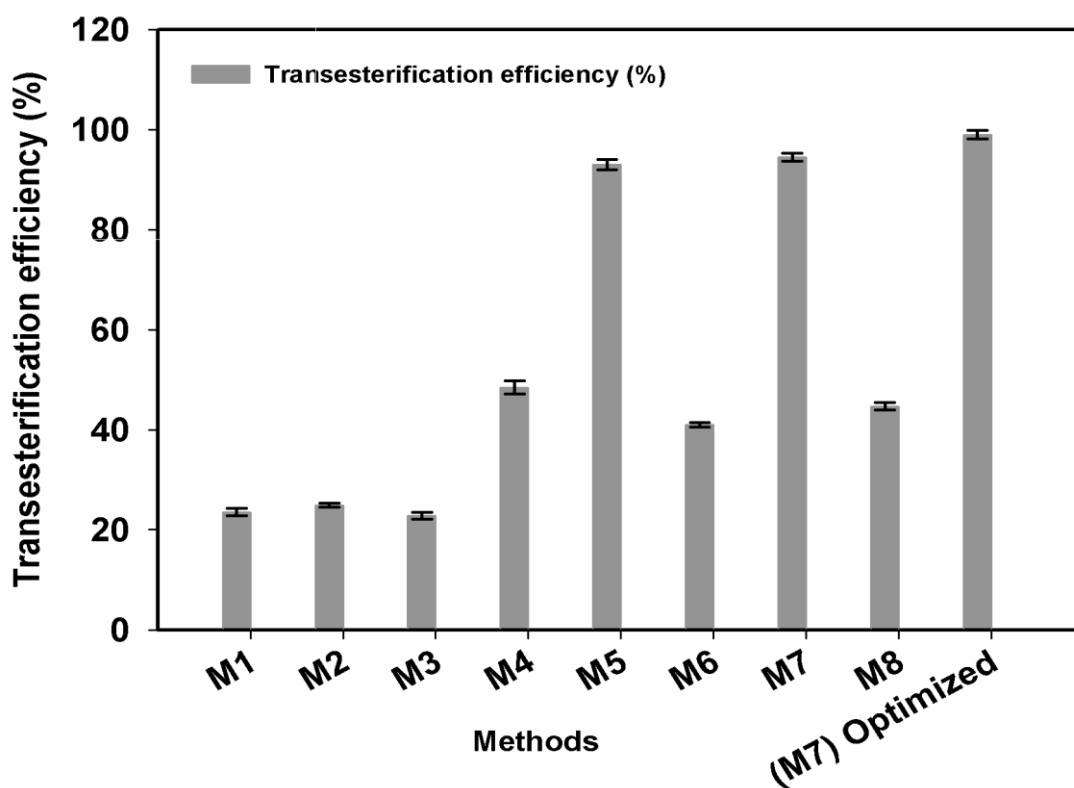


Fig. 4.6 Comparison of transesterification efficiency for eight different transesterification methods (M1-M8) and optimized M7 method with glyceryl-triheptadecanoate as internal standard. For experimental details refer Fig. 4.1

4.3.4 Fourier transform infrared (FTIR) spectroscopy

Crude biodiesel (FAME) obtained after two stage DT are shown in Fig 4.7A. FTIR spectra of petro diesel, mustard oil biodiesel and algal biodiesel are presented in Fig. 4.7B. While the FTIR spectra of all three type of diesel showed significant similarities, presence of ester peaks at 1743cm^{-1} ($-\text{C}=\text{O}$) vibration was evident only in case of algal and mustard biodiesel. Since biodiesel is mainly composed of mono alkyl esters, the intense ($-\text{C}=\text{O}$) stretching band of methyl ester appears at 1743 cm^{-1} . The main constituents of diesel are aliphatic hydrocarbons, whose chemical structures are similar to long carbon chain of the main components of biodiesel. The transmittance peaks obtained at 1200 cm^{-1} and 1183 cm^{-1} may correspond to the anti-symmetric axial stretching vibration of ($\text{CC}(=\text{O})-\text{O}$) bonds

of the ester and asymmetric axial stretching vibrations of (O – C – C) bonds respectively (Patil et al., 2011). The peaks observed at 1444 cm^{-1} may represent the vibrations of CH_3 anti-symmetric deformations (Silverstein and Webster, 1998). The results were in accordance with the findings obtained for algal biodiesel, petro-diesel, and camelina biodiesel by Patil et al. (2011).

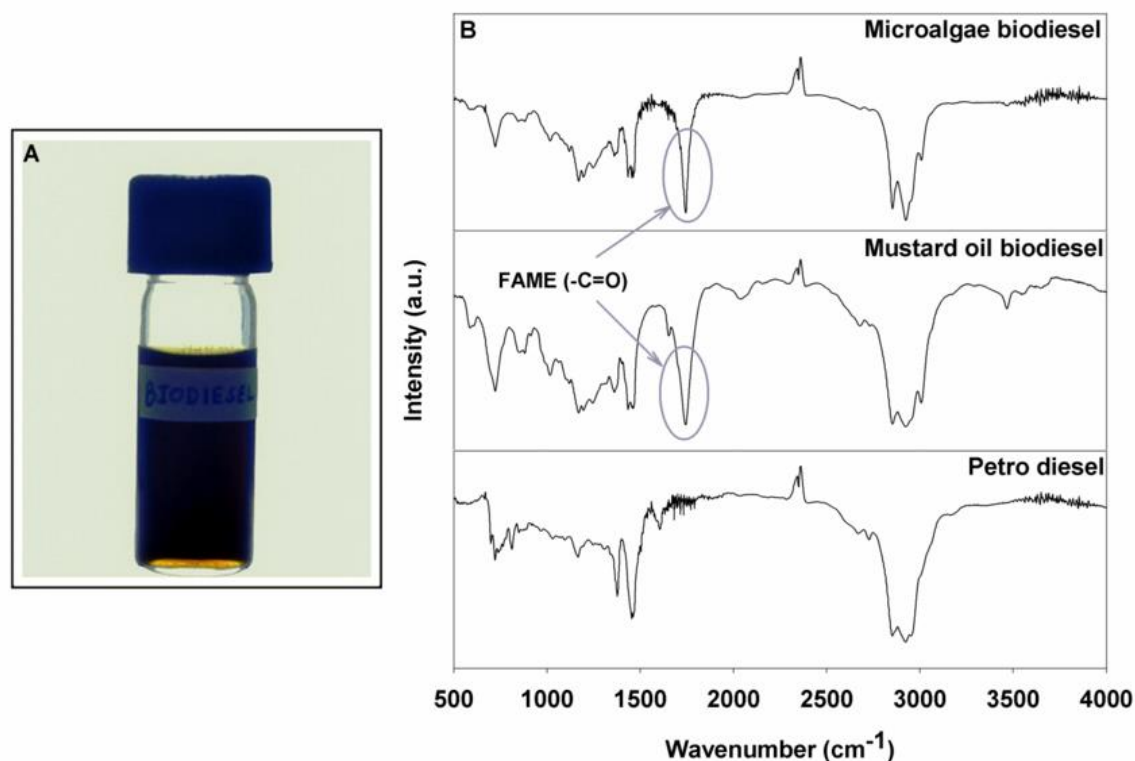
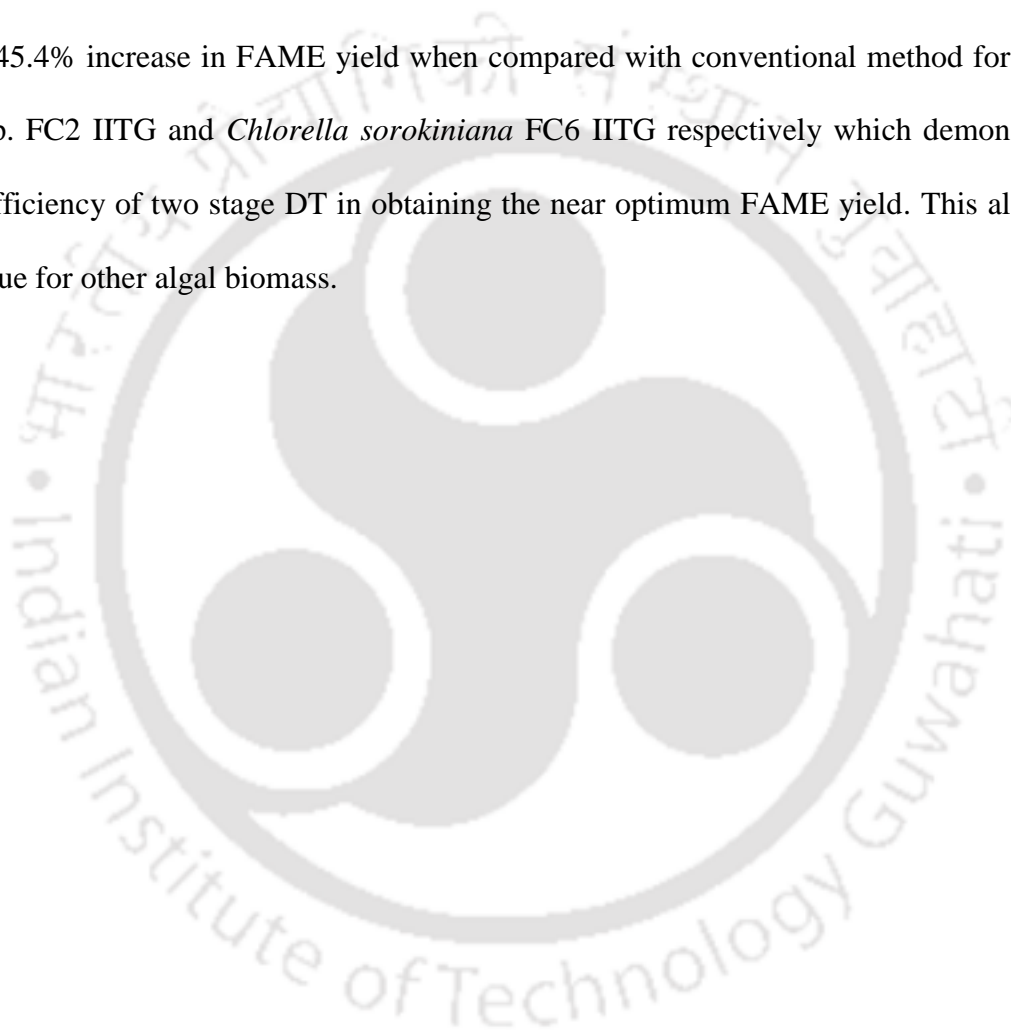


Fig. 4.7 (A) Microalgal biodiesel produced from *Chlorella* sp. FC2 IITG biomass via optimized two stage DT method (B) FTIR spectra of algal biodiesel, mustard biodiesel and petro-diesel.

4.4 Conclusions

Conventional lipid extraction (Bligh and Dyer) and transesterification method was found to underestimate the total FAME yield. The present research has identified an efficient, reliable DT method that can bypass the solvent extraction steps. Among the seven different DT methods and one conventional extraction-transesterification method experimented with three types of biomass (wet, oven dried and lyophilized biomass), M7

with lyophilized biomass (using sequential combination of NaOH catalyst in first stage and H₂SO₄ in second stage) showed maximum transesterification efficiency of 94.5% which is 4 fold higher than the conventional method M1. Further optimization of the method M7 using RSM revealed the significance of CBR, MBR and RT over the FAME yield. Optimum condition of process parameters resulted in further improvement in transesterification efficiency upto 98.96%. The optimal conditions for two stage DT has showed 462.6% and 445.4% increase in FAME yield when compared with conventional method for *Chlorella* sp. FC2 IITG and *Chlorella sorokiniana* FC6 IITG respectively which demonstrates the efficiency of two stage DT in obtaining the near optimum FAME yield. This also may be true for other algal biomass.



4.5 References

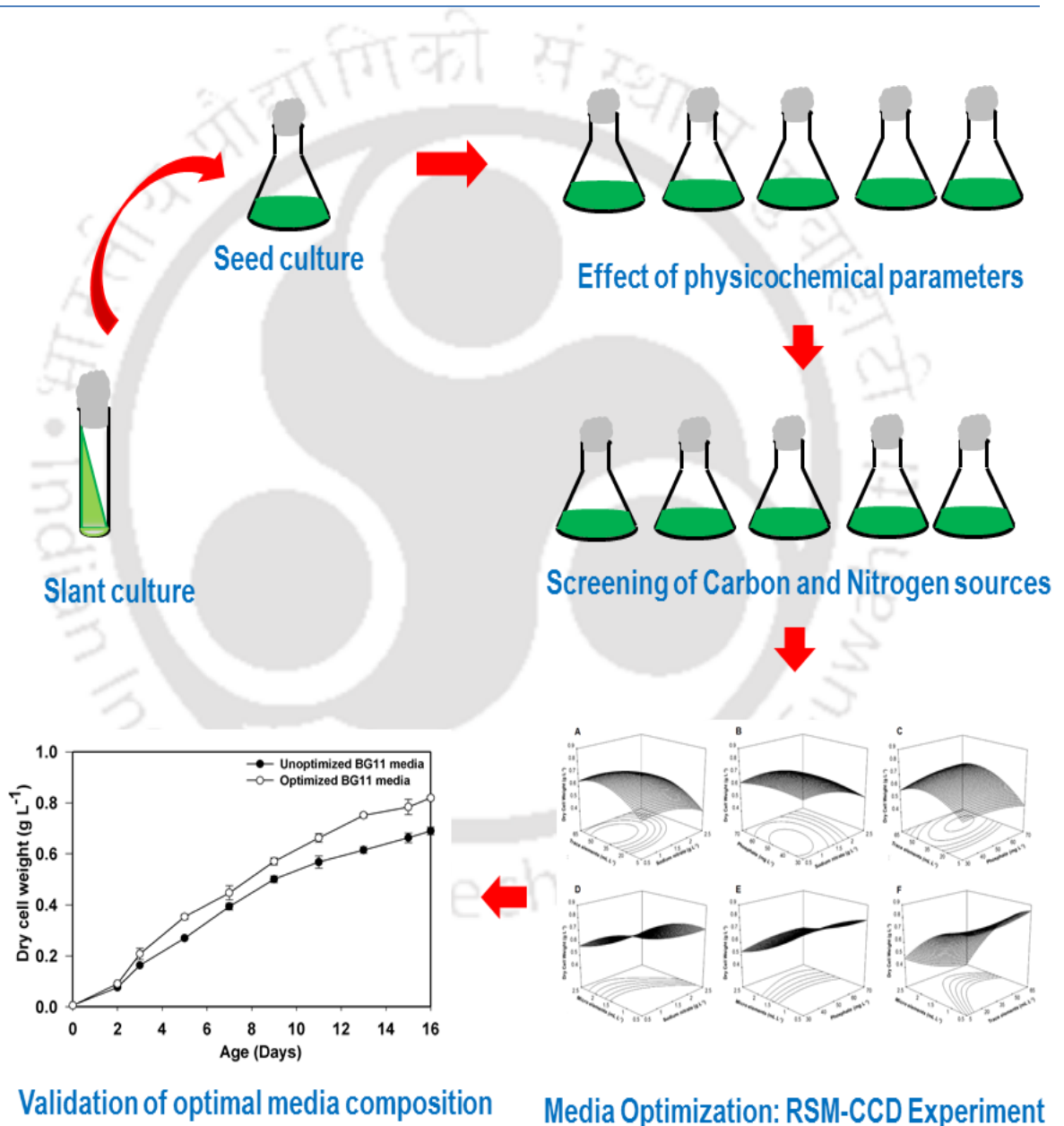
1. Bligh, E.G., Dyer, W.J., 1959. A rapid method of total lipid extraction and purification. *Can. J. Biochem.* 8, 911-917.
2. Cheng, C.H., Du, T.B., Pi, H.C., Jang, S.M., Lin, Y.H., Lee, H.T., 2011. Comparative study of lipid extraction from microalgae by organic solvent and supercritical CO₂. *Bioresour. Technol.* 102, 10151-10153.
3. Davis, R., Aden, A., Pienkos, P.T., 2011. Techno-economic analysis of autotrophic microalgae for fuel production. *Appl. Energy* 88, 3524-3531.
4. Eevera, T., Rajendran, K., Saradha, S., 2009. Biodiesel production process optimization and characterization to assess the suitability of the product for varied environmental conditions. *Renew. Energy* 34, 762-765.
5. Folch, J., Lees, M., Stanley, G.H.S., 1957. A simple method for the isolation and purification of total lipids from animal tissues. *J. Biol. Chem.* 226, 497-509.
6. Griffiths, M.J., Hille-van, R.P., Harrison, S.T.L., 2010. Selection of direct transesterification as the preferred method for assay of fatty acid content of microalgae. *Lipids* 45, 1053-1060.
7. Iverson, S.J., Lang, S.L.C., Cooper, M.H., 2001. Comparison of the Bligh and Dyer and Folch methods for total lipid determination in a broad range of marine tissue. *Lipids* 36, 1283-1287.
8. Jeong, G.T., Yang, H.S., Park, D.H., 2009. Optimization of transesterification of animal fat ester using response surface methodology. *Bioresour. Technol.* 100, 25-30.
9. Johnson, M.B., Wen, Z.Y., 2009. Production of Biodiesel Fuel from the Microalga *Schizochytrium limacinum* by Direct Transesterification of Algal Biomass. *Energy Fuels* 23, 5179-5183.
10. Komers, K., Machek, J., Stloukal, R., 2001. Biodiesel from rapeseed oil, methanol and

- KOH2. Composition of solution of KOH in methanol as reaction partner of oil. Eur. J. Lipid Sci. Technol. 103, 359-362.
11. Kusdiana, D., Saka, S., 2004. Effects of water on biodiesel fuel production by supercritical methanol treatment. Bioresour. Technol. 91, 289-295.
 12. Laurens, L. M.L., Quinn, M., Van Wychen, S., Templeton, D.W., Wolfrum, E.J., 2012. Accurate and reliable quantification of total microalgal fuel potential as fatty acid methyl esters by in situ transesterification. Anal. Bioanal. Chem. 403, 167-178.
 13. Leung, D.Y.C., Guo, Y., 2006. Transesterification of neat and used frying oil: Optimization for biodiesel production. Fuel Process. Technol. 87, 883-890.
 14. Liu, Y.J., Lotero, E., Goodwin, J.G., 2006. Effect of water on sulfuric acid catalyzed esterification. J. Mol. Catal. A Chem. 245, 132-140.
 15. Lotero, E., Liu, Y.J., Lopez, D.E., Suwannakarn, K., Bruce, D.A., Goodwin, J.G., 2005. Synthesis of biodiesel via acid catalysis. Ind. Eng. Chem. Res. 44, 5353-5363.
 16. Morrison, W.R., Smit, L.M., 1964. Preparation of fatty acid methyl esters and dimethyl acetals from lipids with boron fluoride-methanol. J. Lipid Res. 5, 600-608.
 17. Muthuraj, M., Kumar, V., Palabhanvi, B., Das, D., 2014. Evaluation of indigenous microalgal isolate *Chlorella* sp. FC2 IITG as a cell factory for biodiesel production and scale up in outdoor conditions. J. Ind. Microbiol. Biotechnol. 41, 499-511.
 18. Muthuraj, M., Palabhanvi, B., Misra, S., Kumar, V., Sivalingavasu, K., Das, D., 2013. Flux balance analysis of *Chlorella* sp. FC2 IITG under photoautotrophic and heterotrophic growth conditions. Photosynth. Res. 118, 167-179.
 19. Oehrl, L.L., Hansen, A.P., Rohrer, C.A., Fenner, G.P., Boyd, L.C., 2001. Oxidation of phytosterols in a test food system. J. Am. Oil Chem. Soc. 78, 1073-1078.
 20. Palmquist, D.L., Jenkins, T.C., 2003. Challenges with fats and fatty acid methods. J. Anim. Sci. 81, 3250-3254.

21. Patil, P.D., Gude, V.G., Mannarswamy, A., Cooke, P., Munson-McGee, S., Nirmalakhandan, N., Lammers, P., Deng, S.G., 2011. Optimization of microwave-assisted transesterification of dry algal biomass using response surface methodology. *Bioresour. Technol.* 102, 1399-1405.
22. Patil, P.D., Gude, V.G., Mannarswamy, A., et al., 2011. Optimization of direct conversion of wet algae to biodiesel under supercritical methanol conditions. *Bioresour. Technol.* 102, 118-122.
23. Pruvost, J., Vooren, G.V., Cogne, G., Legrand, J., 2009. Investigation of biomass and lipids production with *Neochloris oleoabundans* in photobioreactor. *Bioresour. Technol.* 100, 5988-5995.
24. Silverstein, R., Webster, F., 1998. *Spectrometric identification of organic compounds*, sixth ed., Wiley, New York.
25. Singh, J., Cu, S., 2013. Commercialization potential of microalgae for biofuels production. *Renew. Sust. Energ. Rev.* 14, 2596-2610.
26. Su, Y.C., Liu, Y.A., Diaz Tovar, C.A., Gani, R., 2011. Selection of Prediction Methods for Thermophysical Properties for Process Modeling and Product Design of Biodiesel Manufacturing. *Ind. Eng. Chem. Res.* 50, 6809-6836.
27. Wahlen, B.D., Willis, R.M., Seefeldt, L.C., 2011. Biodiesel production by simultaneous extraction and conversion of total lipids from microalgae, cyanobacteria, and wild mixed-cultures. *Bioresour. Technol.* 102, 2724-2730.
28. Widjaja, A., Chien, C.C., Ju, Y.H., 2009. Study of increasing lipid production from fresh water microalgae *Chlorella vulgaris*. *J. Taiwan Inst. Chem. Eng.* 40, 13-20.
29. Zhang, S., Zu, Y.G., et al., 2010. Rapid microwave-assisted transesterification of yellow horn oil to biodiesel using a heteropolyacid solid catalyst. *Bioresour. Technol.* 101, 931-936.

CHAPTER 5

Physicochemical characterization of the strain and media optimization for maximization of growth



Effect of physicochemical parameters, screening of nitrogen & carbon sources and media optimization for optimal growth.

5.1 Background and motivation

Microalgal biomass production has mainly been achieved by photoautotrophic cultivation in open raceway pond and photobioreactors in the presence of light and CO₂ (Bernnan and Owende, 2010). However, some strains have been reported to utilize organic carbon sources like acetate, glycerol and glucose under heterotrophic and mixotrophic conditions (Alagesan et al., 2013; Muthuraj et al., 2014). The green alga *Chlamydomonas reinhardtii* can grow photoautotrophically utilizing CO₂, heterotrophically utilizing acetate, and mixotrophically utilizing both carbon sources (Heifetz et al., 2000). Mixotrophic microalgae have the ability to utilize both the organic and inorganic carbon sources for cellular growth in the presence of light as the energy source (Chen et al., 2011). Heterotrophic or mixotrophic cultivation in bioreactor provides high degree of growth control and in turn, can ensure higher biomass and lipid productivity in comparison to photoautotrophic cultivation which further reduces harvesting cost (Bernnan and Owende, 2010).

There is a large number of reports on effects of micro and macro nutrients on growth and lipid productivity of microalgae (Chen et al., 2011). These macro and micro nutrients may have significance as growth supporting or lipid inducing at their different levels of concentrations (Karemore et al., 2013). Therefore, optimization of these media components turns necessary to enhance the biomass and lipid productivity. For instance, optimization of the carbon, nitrogen and phosphate sources for photoheterotrophic growth of *Ettlia texensis* resulted in highest biomass productivity of 0.97 g L⁻¹ day⁻¹ which was ~6.5 fold higher than the biomass productivity obtained from unoptimized media composition (Isleten-Hosoglu et al., 2013). An increase in lipid productivity up to 0.19 g L⁻¹ day⁻¹ was also observed when *Botryococcus braunii* was grown in the optimized lipid production media designed using response surface methodology (Tran et al., 2010). It is also important to note that microalgal

growth and lipid production are two mutually exclusive phenomena and therefore, the optimized condition required for growth may not be suitable for oil production (Muthuraj et al., 2014). Therefore, alterations in the growth conditions will have significant influence on biomass and lipid productivity which depicts the need for characterization of the potential strains under different conditions. To that end, it is requisite to evaluate the effect of physicochemical parameters on biomass and optimization of growth media to enhance biomass productivity.

In the present study, a novel indigenous microalgal isolate *Chlorella sorokiniana* FC6 IITG was characterized for the effect of various physicochemical parameters (temperature and pH) and nutritional conditions (carbon and nitrogen sources) on its growth and lipid productivity. Characterization of the strain in wide temperature and pH ranges will show its robustness while the screening of carbon and nitrogen source will provide the appropriate nutrients required for growth of microalgae. Further, BG11 media components involved in the growth of the microalga FC6 were optimized with an aim to maximize the biomass formation.

5.2 Materials and methods

5.2.1 Microalgal strain, media composition and inoculum preparation

Chlorella sorokiniana FC6 IITG, a novel indigenous freshwater microalgal strain isolated from North-East region of India and identified as oleaginous algae (as mentioned in Section 3.4, chapter 3) was used for the present investigation. The slant culture of FC6 was revived in 250 mL Erlenmeyer flask containing 100 mL BG11 media. The BG11 media comprised of (g L^{-1}) NaNO_3 1.5 as nitrogen source, K_2HPO_4 0.04 as phosphate source, trace elements ($\text{MgSO}_4 \cdot 7\text{H}_2\text{O}$ 0.075, $\text{CaCl}_2 \cdot 2\text{H}_2\text{O}$ 0.036, Na_2CO_3 0.02, citric acid 0.006, ferric ammonium citrate 0.006, and EDTA 0.001) and microelement solution (1 mL L^{-1} that

consists of H_3BO_3 2.86, $\text{MnCl}_2 \cdot \text{H}_2\text{O}$ 1.81, $\text{ZnSO}_4 \cdot 7\text{H}_2\text{O}$ 0.222, $\text{CuSO}_4 \cdot 5\text{H}_2\text{O}$ 0.079, $\text{Na}_2\text{MoO}_4 \cdot 2\text{H}_2\text{O}$ 0.390, and $\text{Co}(\text{NO}_3)_2 \cdot 6\text{H}_2\text{O}$ 0.049). The inoculum was prepared by transferring two loops full of slant culture into 250 mL Erlenmeyer flask containing 100 mL BG11 medium and incubated in an orbital shaker under condition same as mentioned in section 3.2.1 of chapter 3. After reach of absorbance (A_{690}) 1.0, 1% (v/v) of the mid log phase culture was used as inoculum for all the experiments in the present study.

5.2.2 Characterization of the strain under different physicochemical conditions

The effect of medium pH, temperature, nitrogen and carbon sources on growth of the organism was studied under shake flask conditions in the BG11 medium. The strain was subjected to grow under different initial pH of the medium (2, 4, 6, 8 and 10), different temperatures (20, 28, 36 and 44°C) and different nitrogen sources (potassium nitrate, sodium nitrite, ammonium chloride, urea, meat extract, glycine, yeast extract and peptone) with equimolar concentration of nitrogen (0.018 M). These experiments were performed under photoautotrophic condition in the orbital shaker at 150 rpm, 28°C under $30 \mu\text{E m}^{-2} \text{s}^{-1}$ light intensity with a light: dark cycle of 16:8 h. Effect of nitrogen and carbon sources on growth and lipid content of FC6 was studied in order to identify the conditions that are growth supporting and/or lipid inducing. Screening of different nitrogen sources were carried out by replacing sodium nitrate in the original BG11 medium with equimolar concentration (0.018 M nitrogen) of alternate nitrogen source as mentioned above. Further, screening of carbon sources was carried out under both heterotrophic and mixotrophic conditions with six different carbon sources: glucose, fructose, sucrose, lactose, maltose and sodium acetate at an equimolar concentration of 6 M carbon. While light intensity of $30 \mu\text{E m}^{-2} \text{s}^{-1}$ with a light: dark regime of 16:8 h was provided under mixotrophic condition, heterotrophic cultivation was performed under complete dark condition. This screening of carbon sources was conducted under heterotrophic condition in order to understand the

ability of the strain to utilize organic carbon sources in the absence of light. The biomass was monitored at regular intervals and the final lipid content was obtained by gas chromatography (GC) at the end of the each batch.

5.2.3 Media optimization for biomass maximization using statistical tools

With the aim of maximizing the biomass titer, BG11 medium with selected nitrogen source was optimized under photoautotrophic condition. Central composite design (CCD) coupled with response surface methodology (RSM) was employed for optimization. A four factor, five level design (Table 5.1) was constructed with sodium nitrate, phosphate, trace element and microelement concentrations as the four factors. The ranges of these factors were selected based upon the preliminary experiments involving one parameter at a time strategy.

Table 5.1 Actual levels of the BG11 media components used in CCD-RSM experimental design for optimization of FC6 growth under photoautotrophic condition

Variables	Symbol	Actual levels of coded factors				
	Coded	-2	-1	0	1	2
Sodium nitrate (g L ⁻¹)	X_1	0.5	1	1.5	2	2.5
Phosphate (mg L ⁻¹)	X_2	10	30	50	70	90
Trace element (mL L ⁻¹)	X_3	5	20	35	50	65
Microelement (mL L ⁻¹)	X_4	0.5	1	1.5	2	2.5

A total of 31 experiments were designed through CCD with 7 replications at the center values to evaluate the pure error. The response was measured in terms of biomass titre (Y) at the end of 16th day. The behaviour of the system was determined by assuming a second order polynomial with linear, quadratic and interaction effects as shown by Eq. (5.1).

$$Y = \beta_0 + \sum_{i=1}^k \beta_i X_i + \sum_{i<j}^k \beta_{ij} X_i X_j + \sum_{j=1}^k \beta_{jj} X_j^2 \quad (5.1)$$

Where Y is the response; X_1, X_2, X_3 and X_4 are input variables; β_0 is constant; β_i is the linear coefficient; β_{ij} is the interaction coefficient, and β_{jj} is the quadratic coefficient. Estimation of regression coefficients and statistical tests were implemented in the MINITAB Version

15 (Minitab Inc., State College, PA, USA) statistical software based on the RSM. Analysis of variance (ANOVA) was conducted on the variables to understand the effect of individual variables on biomass. Stepwise deletion approaches of individual non-significant ($p < 0.05$) terms were conducted to simplify the regression equation by recalculation of the coefficients.

5.2.3.1 Optimization of glucose and acetate concentration for the growth of FC6

The optimal concentration of the glucose and sodium acetate used for the FC6 growth under mixotrophic and heterotrophic conditions respectively were determined using one at a time strategy. Different concentrations of glucose (5, 10, 15, 20 g L⁻¹) were supplemented in the optimized growth medium obtained from RSM and incubated at 28°C, 150 rpm with a light intensity of 30 $\mu\text{E m}^{-2} \text{s}^{-1}$ for a light: dark regime of 16:8 h to obtain the optimum concentration at mixotrophic conditions. Similarly, various concentrations of sodium acetate (5, 10, 15, 20 g L⁻¹) were supplemented in the optimized growth media obtained from RSM and tested for maximum growth under complete dark heterotrophic condition. Growth was monitored at regular intervals and the substrate concentration which showed maximum biomass production was selected as the optimum.

5.2.4 Analytical methods

5.2.4.1 Analysis of growth and fatty acids methyl esters (FAME) derived from microalgae

Analysis of growth were performed as per the protocol given in section 3.2.5.1. The total lipid content was quantified in terms of fatty acid methyl esters (FAME) via two stage *in situ* transesterification method (as mentioned in chapter 4) using gas chromatograph (GC-FID, Varian 450, Netherlands). In the first step of two stage *in situ* transesterification, 1.5 mL of 2% (w/v) NaOH in methanol was added to 30 mg lyophilized algal biomass of FC6 followed by incubation at 90°C in a shaking water bath at 150 rpm for 19.37 minutes. In the

second step, 1.8 mL 5% (v/v) H₂SO₄ in methanol was added to the mixture and was further incubated at the same conditions for 10 minutes. Double distilled water and hexane of equal volume (1.0 mL) were added to the cooled transesterified mixture to obtain the FAME in the hexane layer. The hexane layer was washed twice with water to remove any aqueous impurities and used directly for GC analysis after filtration through a 0.2 µm filter. FAME was analyzed in GC equipped with flame ionization detector and SLB-IL100 column (30 m x 0.25 mm i.d., 0.20 µm film thickness). FAME mix C14-C22 (Supelco, USA) was used as the standard for GC-FID and the lipid quantified using this method represents the total lipid of the biomass in % (w/w, DCW). Nitrogen at a constant flow rate of 0.4 m s⁻¹ was used as the carrier gas. The oven temperature started at 140°C (5 min) and increased at a rate of 3°C min⁻¹ till 220°C followed by 5 minutes holding. The injector and detector temperature was kept at 250 °C and the injection volume of 1µL at a split ratio of 1:20 was used for analysis.

5.2.5 Quality of biodiesel generated from *Chlorella sorokiniana* FC6 IITG

Quality of the biodiesel is decided by the properties such as viscosity (η), cetane number (CN), flash point (T_f), cloud point (CP), pour point (PP), saponification value (SV), iodine value (IV), degree of unsaturation (DU) and highest heating value (HV) which are in turn dependent on the carbon chain length and the amount of unsaturated fatty acids formed in the microalgal systems. Therefore, these properties of the biodiesel were determined based on the following empirical equations:

$$\eta = 0.235W_C - 0.468W_{db} \quad (5.2)$$

$$CN = 3.930W_C - 15.936W_{db} \quad (5.3)$$

$$T_f = 23.362W_C + 4.854W_{db} \quad (5.4)$$

$$CP = 18.134W_C - 0.790W_{US} \quad (5.5)$$

$$PP = 18.880W_C - 1.00W_{US} \quad (5.6)$$

$$SV = \sum(560 \times P_{FA})/MW \quad (5.7)$$

$$IV = \sum(254 \times P_{FA} \times N_D)/MW \quad (5.8)$$

$$DU = (W_{MUFA}) + (2 \times W_{PUFA}) \quad (5.9)$$

$$HV = 46.19 - \left(\frac{1794}{MW_i}\right) - 0.21 \times N_D \quad (5.10)$$

Where W_C is the weighted-average number of carbon atoms in the fatty acids, W_{db} is the weighted-average number of double bonds, W_{US} represents the total unsaturated FAME content (weight %), P_{FA} is the percentage of each fatty acid, MW is the molecular mass of individual fatty acids, N_D is the number of double bonds, W_{MUFA} is the monounsaturated fatty acids in weight percentage, W_{PUFA} is polyunsaturated fatty acids in weight percentage, MW_i represents the molecular weight of the i^{th} FAME component. The equations 5.2-5.6 were described by Su et al. (2011) and equations 5.7-5.9 were obtained from Francisco et al. (2010). The empirical equation 5.10 for heating value was taken from Ramirez-Verduzco et al. (2012).

5.3 Results and discussion

5.3.1 Effect of pH and temperature on biomass titer and intracellular lipid content

The effects of temperature and pH on biomass titer and intracellular lipid content of FC6 were studied under photoautotrophic condition (Fig. 5.1). The results showed that the strain FC6 was able to grow over a wide range of temperature 20 to 36°C, with the optimum of 28°C which supported maximum growth (Fig. 5.1 A). Further increase in cultivation temperature to 44°C resulted in two fold decreased growth as compared to optimal temperature. The changes in cultivation temperature did not affect the intracellular lipid content of the cells at this selected range. Many microalgal strains such as *C. sorokiniana*, *C. vulgaris*, *Scenedesmus* sp. and *Nannochloropsis* sp. were reported to grow well over a temperature range of 20 to 25°C (Butterwick et al., 2005) and no significant influence of temperature on the lipid content of the cells was reported (Wan et al., 2012).

Strain FC6 could also grow well over a wide range of initial pH of the medium ranging from 4 to 12 as shown in Fig. 5.1 B and its optimal growth was observed in between pH 6 to 8.

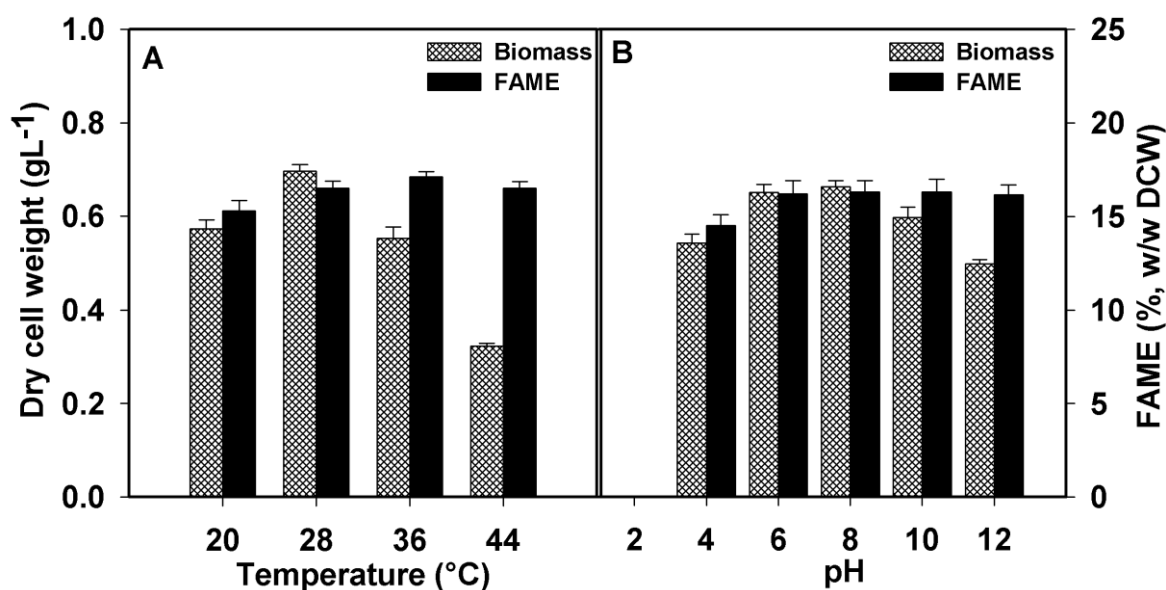


Fig. 5.1 Effect of (A) temperature and (B) initial medium pH on biomass titer in terms of dry cell weight (double crossed bars) and total lipid content in terms of fatty acid methyl esters (black shaded bars) of the strain FC6 under photoautotrophic growth condition.

Maximum growth was observed at pH 8 and no growth was observed when the strain was grown at pH 2. The effect of pH on lipid content was negligible (Fig. 5.1 B) which was similar to the observation reported by Wan et al. (2012). The survival of the organism over wide range of temperature and pH point towards metabolic flexibility of the strain in terms of its growth.

5.3.2 Effect of nitrogen sources on biomass titer and intracellular lipid content

Further screening of growth supporting and/or lipid inducing nitrogen sources were carried out under photoautotrophic condition. The strain FC6 was found to utilize both inorganic and organic nitrogen sources for growth and lipid accumulation (Fig. 5.2). Glycine was found to support maximum growth and sodium nitrate was found to be lipid inducing. Glycine forms the dissolved free amino acid source which are easily taken up by the

microalgae as nitrogen source and helps in enhancement of growth to maximum (Flynn and Butler, 1986). Even though glycine was found to be growth supporting, use of such organic compounds in large scale ponds will not be economically feasible. Sodium nitrate was found to be the next best nitrogen source among all other nitrogen sources tested while ammonium chloride was found to inhibit growth of FC6.

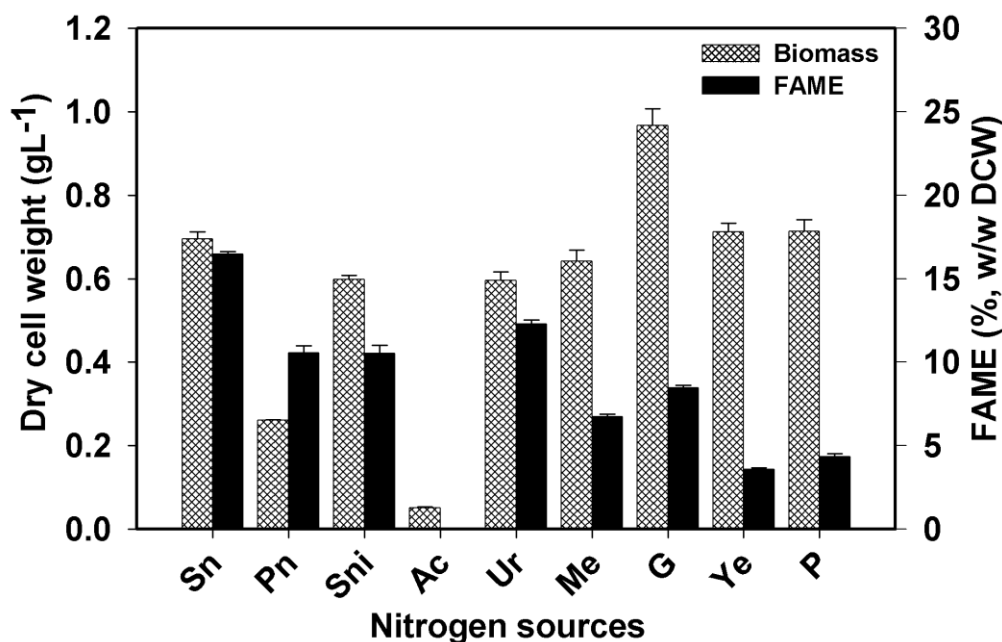


Fig. 5.2 Effect of various nitrogen sources on biomass titer in terms of dry cell weight (double crossed bars) and total lipid content in terms of fatty acid methyl esters (black shaded bars) of the strain FC6. Different nitrogen sources with equimolar concentration of nitrogen (0.018 M) was used under photoautotrophic condition: Sn sodium nitrate; Pn potassium nitrate; Sni sodium nitrite; Ac ammonium chloride; Ur urea; Me meat extract; G glycine; Ye yeast extract; P peptone

Ammonia uptake by cells release H⁺ ions in the medium which in turn makes the medium more acidic leading to the reach of early stationary phase (Isleten-Hosoglu et al., 2012; Muthuraj et al., 2014). This may be the reason that, FC6 resulted in very less growth when grown with ammonium chloride. Sodium nitrate was also reported to be the best source of nitrogen for the growth of *Chlorella* sp. FC2 IITG (Muthuraj et al., 2014), *Chlorella sorokiniana* (Wan et al., 2012), *Scenedesmus* (Basu et al., 2013) and *Neochloris oleoabundans* (Morales-Sánchez et al., 2013).

5.3.3 Effect of carbon sources on biomass titer and intracellular lipid content of FC6

The strain was further studied under heterotrophic and mixotrophic condition to evaluate its ability to utilize different carbon sources (Fig. 5.3). Effect of carbon sources on growth and intracellular lipid content was obtained by growing the culture under heterotrophic and mixotrophic conditions in: glucose, fructose, sucrose, lactose, maltose, and sodium acetate (Fig. 5.3). The shake flask results showed that the organism was unable to grow in the presence of fructose, sucrose and lactose under strict heterotrophic conditions (Fig. 5.3 A). This may be due to several reasons such as absence or less activity of certain catabolic enzymes, lack of ability to oxidize carbon compounds or the absence of appropriate permeases in the cellular membranes. (Morales-Sánchez et al. 2013). *Dunaliella tertiolecta* and *Prymnesium parvum* were unable to utilize glucose in the dark condition even though they were reported to possess the active metabolic enzymes required to utilize this particular sugar (Morales-Sanchez et al., 2013). Among rest of the carbon sources, sodium acetate supported maximum growth (0.87 g L^{-1}) with intracellular lipid content of 24.50% w/w DCW. Glucose and maltose supplemented media resulted in significant reduction in growth and lipid accumulation as compared to sodium acetate supplemented medium (Fig. 5.3 A). This observation was in contrary to the literature where *Chlorella* sp. were reported to utilize glucose as the primary carbon source for growth (Muthuraj et al, 2014; Wan et al 2012) under heterotrophic condition. Effect of carbon sources on growth and lipid accumulation was further evaluated under mixotrophic condition. Unlike heterotrophic cultivation, glucose supported the maximum growth under mixotrophic condition. Maximum biomass concentration of 2.25 g L^{-1} was achieved under mixotrophic cultivation which was ~2.14 fold higher than that obtained from mixotrophic cultivation with sodium acetate (Fig. 5.3 B). In general it has been demonstrated that glucose is the most preferred carbon source for growth of microalgae. However, glucose uptake is shown to be dependent on light and the

species type (Perez-Garcia et al., 2011). Growth of FC6 in the presence of light might have induced the proton dependent glucose (hexose) transport systems that were reported to exist in several microalgal systems (Morales-Sánchez et al, 2013). Thus, in the heterotrophic condition absence of light might have slowed down the glucose uptake system resulting in the utilization of sodium acetate over glucose as carbon source. However, irrespective of the cultivation condition sodium acetate was found to induce the intracellular lipid content in the organism FC6. Sodium acetate enters the central metabolic pathway at Acetyl CoA node, which allows the direct incorporation of incoming carbon in fatty acid biosynthesis pathway thus enhancing the lipid content of the organism (Heifetz et al, 2000).

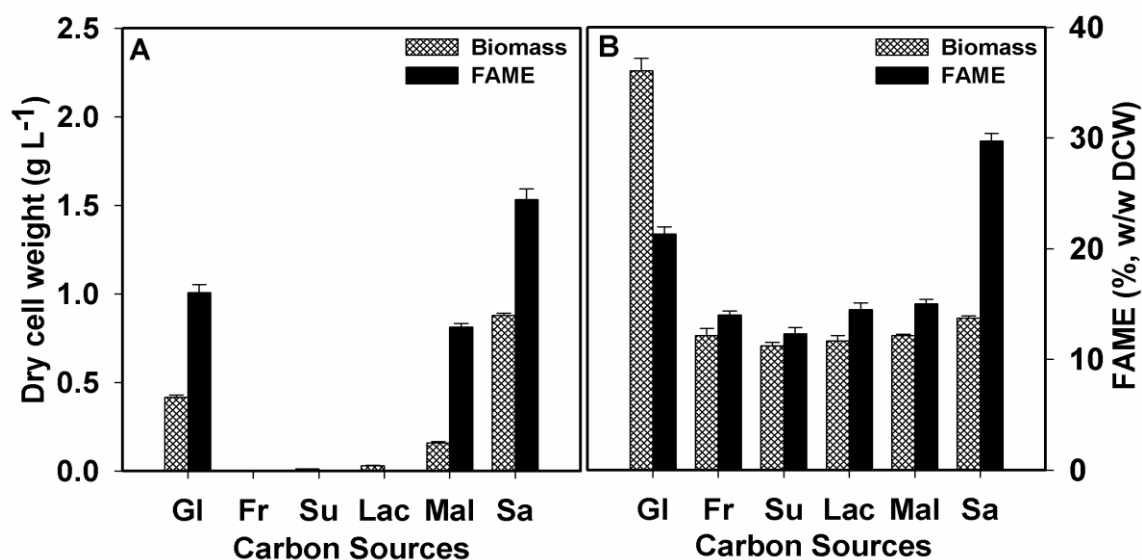


Fig. 5.3 Effect of various carbon sources under (A) heterotrophic cultivation and (B) mixotrophic cultivation, on biomass titer in terms of dry cell weight (double crossed bars) and total lipid content in terms of fatty acid methyl esters (black shaded bars) of the strain FC6. Different carbon sources with equimolar concentration (6M) of carbon was used for heterotrophic & mixotrophic conditions: GL glucose; Fr fructose; Su sucrose; Lac lactose; Mal maltose; Sa sodium acetate

Based on these observations the carbon sources have been classified as follows: (i) sodium acetate as growth supporting under heterotrophic condition; (ii) glucose as growth supporting under mixotrophic condition and (iii) sodium acetate as lipid inducing.

5.3.4 Media optimization for growth of FC6 under different cultivation conditions

5.3.4.1 Optimization of BG11 media for photoautotrophic growth

The central composite design of five levels was constructed for four parameters: (i) sodium nitrate (ii) phosphate (iii) trace elements and (iv) microelements (Table 5.2).

Table 5.2 CCD matrix of independent media components used in RSM with corresponding experimental and predicted measurements of biomass titer (g L^{-1})

S.No.	X_1 SN (g L^{-1})	X_2 P (mg L^{-1})	X_3 TE (mL L^{-1})	X_4 ME (mL L^{-1})	Biomass titer Experimental (g L^{-1})	Biomass titer Predicted (g L^{-1})
1	1	30	20	1	0.699	0.704
2	2	30	20	1	0.611	0.619
3	1	70	20	1	0.637	0.629
4	2	70	20	1	0.592	0.589
5	1	30	50	1	0.769	0.759
6	2	30	50	1	0.683	0.676
7	1	70	50	1	0.749	0.754
8	2	70	50	1	0.726	0.717
9	1	30	20	2	0.570	0.581
10	2	30	20	2	0.510	0.503
11	1	70	20	2	0.543	0.547
12	2	70	20	2	0.503	0.516
13	1	30	50	2	0.580	0.581
14	2	30	50	2	0.496	0.507
15	1	70	50	2	0.624	0.619
16	2	70	50	2	0.598	0.590
17	0.5	50	35	1.5	0.682	0.680
18	2.5	50	35	1.5	0.563	0.565
19	1.5	10	35	1.5	0.568	0.562
20	1.5	90	35	1.5	0.563	0.569
21	1.5	50	5	1.5	0.525	0.514
22	1.5	50	65	1.5	0.632	0.643
23	1.5	50	35	0.5	0.821	0.831
24	1.5	50	35	2.5	0.591	0.581
25	1.5	50	35	1.5	0.675	0.674
26	1.5	50	35	1.5	0.666	0.674
27	1.5	50	35	1.5	0.661	0.674
28	1.5	50	35	1.5	0.669	0.674
29	1.5	50	35	1.5	0.656	0.674
30	1.5	50	35	1.5	0.688	0.674
31	1.5	50	35	1.5	0.703	0.674

SN- represents sodium nitrate; P- represents the phosphate; TE- represents the trace element; ME- represents the microelement

The biomass titre of 16th day of fermentation was used as the response for optimization (Table 5.2). The 31 different combinations of the media components designed by CCD resulted in a wide range of biomass titer from 0.5 g L⁻¹ to 0.77 g L⁻¹ and biomass productivity ranging from 31.25 mg L⁻¹ day⁻¹ to 48.13 mg L⁻¹ day⁻¹. The coefficients of the model were estimated through multiple regression analysis and their significance was tested on the bases of p values (<0.05) obtained from ANOVA analysis (Table 5.3).

Table 5.3 ANOVA for the quadratic regression model obtained from CCD-RSM employed in optimization of media components for the growth of FC6

Source	DF	Seq SS	Adj MS	F	p ^a
Regression	14	5.33	0.38	70.29	0
Linear	4	3.86	0.96	178.03	0
X_1	1	0.55	0.55	101	0
X_2	1	0.00	0.00	0.41	0.529
X_3	1	0.69	0.69	127.3	0
X_4	1	2.62	2.62	483.4	0
Square	4	1.14	0.29	52.8	0
X_1^2	1	0.07	0.13	24.27	0
X_2^2	1	0.53	0.59	108.29	0
X_3^2	1	0.49	0.45	83.44	0
X_4^2	1	0.05	0.05	9.56	0.007
Interaction	6	0.33	0.05	10.14	0
$X_1 * X_2$	1	0.06	0.06	10.78	0.005
$X_1 * X_3$	1	0.00	0.00	0.05	0.828
$X_1 * X_4$	1	0.00	0.00	0.32	0.577
$X_2 * X_3$	1	0.14	0.14	25.7	0
$X_2 * X_4$	1	0.05	0.05	9.21	0.008
$X_3 * X_4$	1	0.08	0.08	14.78	0.001
Residual Error	16	0.09	0.01		
Lack-of-Fit	10	0.04	0.00	0.57	0.793
Pure Error	6	0.04	0.01		
Total	30	5.42			

a - p value >0.05 is considered as insignificant

The quadratic polynomial equation (Equation 5.11) obtained from RSM analysis was used to predict the maximum biomass titer (Y , g L⁻¹) with initial concentration of sodium nitrate (X_1 , g L⁻¹), phosphate (X_2 , g L⁻¹), trace elements (X_3 , mL L⁻¹) and microelements (X_4 , mL L⁻¹) as variable parameters.

$$Y = 0.72 + 0.024 X_1 + 0.0015 X_2 + 0.0091 X_3 - 0.224 X_4 - 0.51X_1^2 - 6.78 X_2^2 - 1.059 X_3^2 + 0.032 X_4^2 + .0011 X_1X_2 + 0.000 X_1X_3 + 0.0079 X_1X_4 + 0.000058 X_2X_3 + 0.001 X_2X_4 - 0.00178 X_3X_4 \quad (5.11)$$

High coefficient of determinant ($R^2 = 0.984$) obtained from regression analysis indicates that 98.4% of predicted results were matching with corresponding experimental values. Maximum biomass titer of 0.89 g L^{-1} was predicted by the RSM model at initial concentrations of nitrate 0.82 g L^{-1} , phosphate 44 mg L^{-1} , trace element 51.76 mL L^{-1} and microelement 0.5 mL L^{-1} . The model was validated by comparing the experimental biomass titer (0.82 g L^{-1}) with the corresponding predicted value at the optimal media compositions (Table 5.4) which was found to be with in an acceptable range.

Table 5.4 BG11 Media components, their corresponding concentrations and the biomass titer (g L^{-1}) predicted by optimization tools

Media Components	Un-optimized Medium	Optimized Medium
Sodium nitrate (g L^{-1})	1.5	0.82
Phosphate (mg L^{-1})	40	44
Trace element ^a (ml L^{-1})	20	51.76
Micro element ^b (ml L^{-1})	1	0.5
Predicted biomass titer (g L^{-1})	nd	0.89
Experimental biomass titer (g L^{-1})	0.68	0.82
% Increase^c	nd	19

a- Concentration of trace element (g L^{-1}): ($\text{MgSO}_4 \cdot 7\text{H}_2\text{O}$, 3.75; $\text{CaCl}_2 \cdot 2\text{H}_2\text{O}$, 1.35; Na_2CO_3 , 1; citric acid, 0.3; ferric ammonium citrate, 0.03 and EDTA, 0.05).

b- Concentration of micro element (g L^{-1}): (H_3BO_3 , 2.86; $\text{MnCl}_2 \cdot \text{H}_2\text{O}$, 1.81; $\text{ZnSO}_4 \cdot 7\text{H}_2\text{O}$, 0.222; $\text{CuSO}_4 \cdot 5\text{H}_2\text{O}$, 0.079; $\text{Na}_2\text{MoO}_4 \cdot 2\text{H}_2\text{O}$, 0.390 and $\text{Co}(\text{NO}_3)_2 \cdot 6\text{H}_2\text{O}$, 0.049)

c- values represents the percentage increase in the biomass titer obtained through medium optimization under shake flask conditions in comparison to the biomass titer obtained from un-optimized medium, nd – Not determined

The interference of noise in the model was negligible as signal to noise ratio (35.42) was found higher than its critical value 4. The interaction effects of four media components on the biomass formation of FC6 was depicted in Fig 5.4.

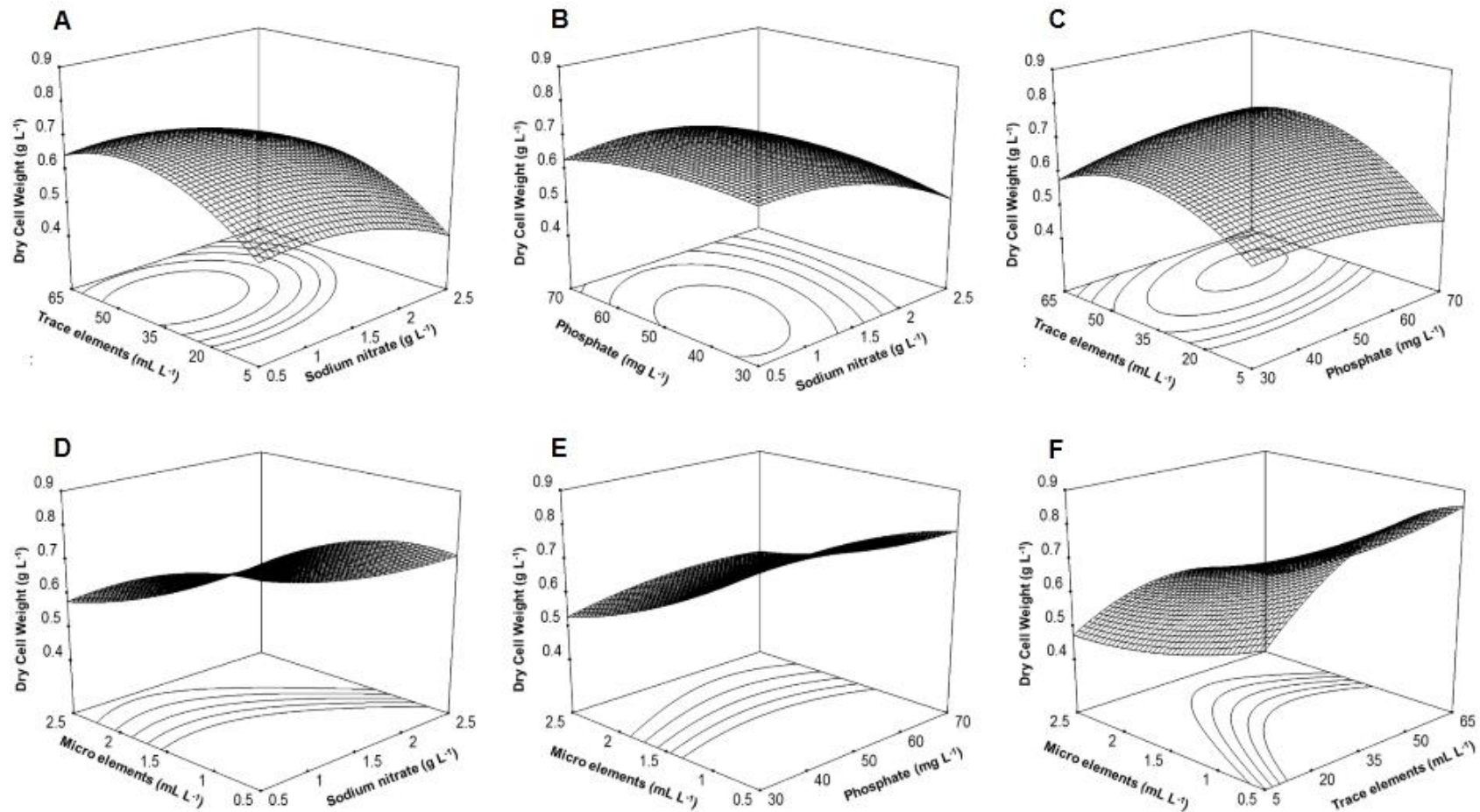


Fig. 5.4 Response surface plot representing the effect of various parameters and their interaction on biomass titer (g L^{-1}) by FC6: (A) trace element and sodium nitrate, (B) phosphate and sodium nitrate, (C) trace element and phosphate, (D) microelement and sodium nitrate, (E) microelement and phosphate, (F) microelement and trace element

The interaction between nitrate, phosphate and trace elements were highly significant while the microelements was found to have very less interaction with other components in the selected concentration ranges. Increase in the concentration of nitrate greater than 1.0 g L^{-1} decreased the biomass formation significantly and was found to be inhibitory at higher concentrations. While, increased trace elements were required for optimal growth of FC6, microelements were required in very minimal amount of 0.5 mL L^{-1} for optimal growth of FC6 which is two time lesser than the concentration available in original BG11 medium. The interaction effect between the limiting nutrients nitrate, phosphate and trace elements were highly significant (Table 5.3 and Fig. 5.4) and found to influence the production of biomass under photoautotrophic condition. The biomass titre was improved by 19 % when compared with the un-optimized BG11 medium (Fig. 5.5) under photoautotrophic cultivation in shake flask conditions.

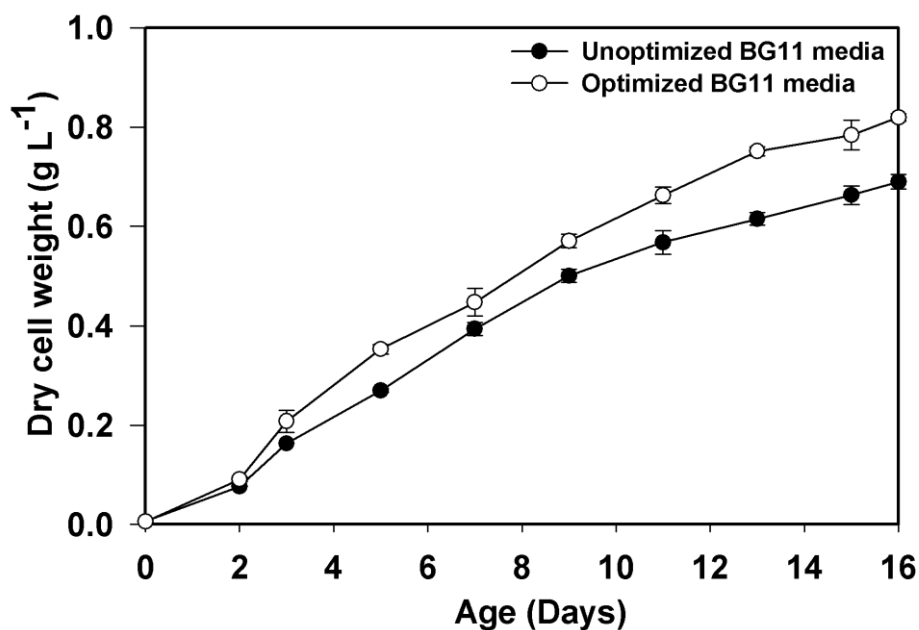


Fig. 5.5 Comparison of biomass titer (g L^{-1}) from un-optimized BG11 media and optimized BG11 media under shake flask photoautotrophic growth condition

5.3.4.2 Optimization of carbon sources under heterotrophic and mixotrophic conditions

Further, the carbon sources required for optimal growth under heterotrophic and mixotrophic conditions were optimized using one at a time strategy. Maximum biomass titer of 0.83 g L^{-1} was obtained with optimal sodium acetate concentration of 15 g L^{-1} under heterotrophic condition (Fig. 5.6 A). Optimal glucose concentration of 10 g L^{-1} resulted in maximum growth of 2.5 g L^{-1} under mixotrophic condition (Fig. 5.6 B).

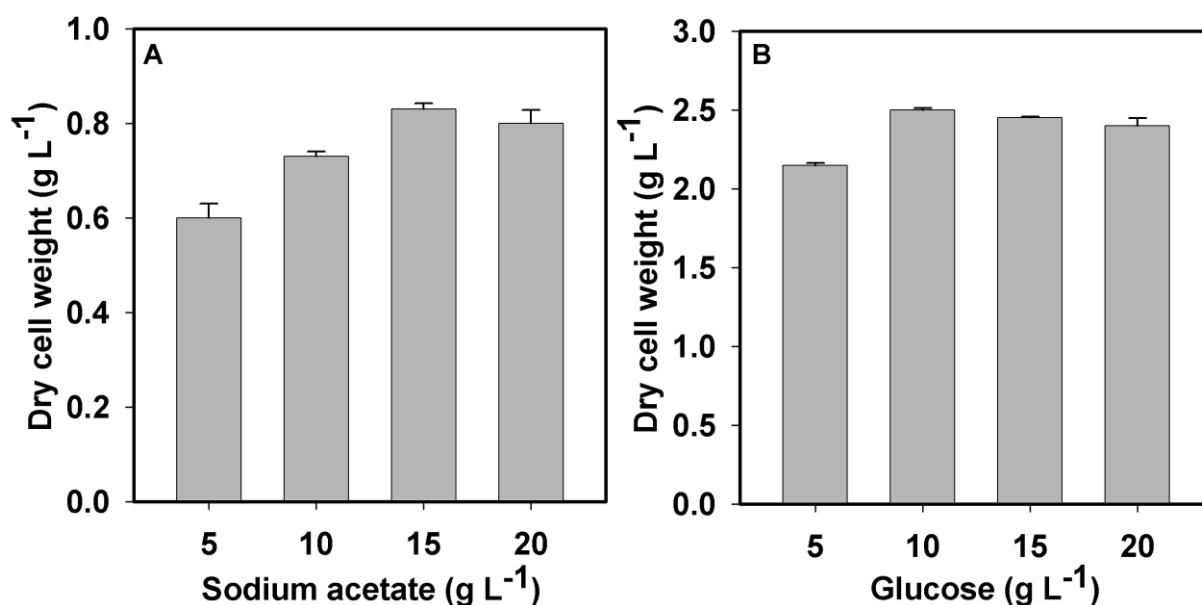


Fig. 5.6 (A) Effect of different concentrations of sodium acetate on growth of the strain under heterotrophic condition, (B) Effect of different concentrations of glucose on growth under mixotrophic cultivation

5.3.5 Effect of physicochemical parameters on FAME composition and quality of biodiesel

Fatty acid methyl ester composition of the biodiesel significantly influences the fuel properties such as cetane number, flash point, cloud point, pour point, saponification value, iodine value and degree of unsaturation. To that end, the effect of physicochemical parameters on the fatty acid composition and properties of biodiesel obtained from FC6 strain was

evaluated. The fatty acid composition under different cultivation temperatures is shown in Table 5.5. The major fatty acids components produced by microalgae *Chlorella sorokiniana* FC6 IITG were palmitic acid (C16:0), oleic acid (C18:1), and linoleic acid (C18:2). Within the temperature range of 20-44 °C, no significant change on the contents of total unsaturated fatty acids were detected. However, the ratio of monounsaturated fatty acids (MUFA) increased and the polyunsaturated fatty acids (PUFA) decreased with the change in temperature from 20–44°C. A similar trend was observed by Patterson (1970), where increase in heterotrophic growth temperature of *C. sorokiniana* from 22 to 38°C resulted in a decrease in percentage of unsaturation. The decreased degree of unsaturation with the increase of growth temperature was widely observed in many other organisms because the synthesis of unsaturated fatty acids under lower temperature could help the cell maintain the proper membrane fluidity and functions in cold environment (Gounot, 1991). The effect of initial medium pH on fatty acid composition was negligible in FC6 strain. The fatty acid composition under different initial medium pH is shown in Table 5.5. The fatty acid composition under various nitrogen sources were evaluated and shown in Table 5.6. The major fatty acid composition of C16:0, C18:1 and C18:2 was observed in case of all nitrogen sources, it was observed that nitrogen sources greatly affect the percentage of fatty acid composition and content. Similarly effect of various carbon sources on fatty acid composition were evaluated under heterotrophic and mixotrophic mode as shown in Table 5.7. The effect of physicochemical parameters on biodiesel properties are evaluated through empirical equations as a function of FAME composition obtained experimentally shown in Table 5.8.

Table 5.5 Fatty acid profile of autotrophically cultured algae *Chlorella sorokiniana* FC6 IITG at different temperature and pH

Fatty Acids	FAME (% _{w/w})	Temperature (°C)				Initial medium pH				
		20	28	36	44	4	6	8	10	12
Lauric	[C12:0]	1.20	1.28	1.42	1.48	1.20	1.23	1.28	1.24	1.23
Myristic	[C14:0]	0.45	0.47	0.53	0.55	0.43	0.46	0.47	0.43	0.47
Palmitic	[C16:0]	22.45	23.09	23.40	24.94	23.94	23.2	23.09	22.33	22.03
Palmitoleic	[C16:1]	7.64	7.28	7.94	9.23	7.32	7.83	7.28	7.38	7.63
Stearic	[C18:0]	3.04	3.14	3.39	3.45	3.16	3.93	3.14	3.93	3.93
Oleic	[C18:1]	25.54	26.46	27.89	32.44	26.38	26.27	26.46	26.87	26.73
Linoleic	[C18:2]	37.65	36.87	33.99	25.84	35.83	36.48	36.87	36.83	36.77
Arachidic	[C20:0]	0.13	0.17	0.13	0.17	0.15	0.17	0.17	0.15	0.18
Behenic	[C22:0]	0.10	0.10	0.10	0.14	0.10	0.13	0.10	0.11	0.10
	Others	1.80	1.16	1.21	1.76	1.49	0.30	1.16	0.73	0.93
	SAT FAME ^a	27.37	28.24	28.97	30.73	28.98	29.12	28.24	28.19	27.94
	MUFA ^b	33.18	33.74	35.83	41.67	33.70	34.10	33.74	34.25	34.36
	PUFA ^c	37.65	36.87	33.99	25.84	35.83	36.48	36.87	36.83	36.77
	Total FAME ^d	15.30	16.50	17.10	16.50	14.50	16.20	16.30	16.30	16.15

a-represents the total saturated fatty acid fraction in the total fatty acid methyl esters

b-represents the total monounsaturated fatty acid fraction in the total fatty acid methyl esters

c-represents the total polyunsaturated fatty acid fraction in the total fatty acid methyl esters

d-represents the total FAME expressed in %, weight fraction of dry cell weight

Table 5.6 Effect of nitrogen sources on FAME composition under photoautotrophic cultivation

Fatty Acids	FAME (% <i>, w/w</i>)	Nitrogen sources								
		Sn	Pn	Sni	Ac	Ur	Me	G	Ye	P
Lauric	[C12:0]	1.28	7.19	4.11	3.62	5.20	1.19	15.89	6.92	4.11
Myristic	[C14:0]	0.47	0.47	48.53	0.32	nd	0.66	nd	nd	48.53
Palmitic	[C16:0]	23.09	22.85	9.55	15.31	12.37	56.14	14.00	15.20	9.55
Palmitoleic	[C16:1]	7.28	12.43	6.62	19.14	22.87	5.76	15.73	19.07	6.62
Stearic	[C18:0]	3.14	1.94	1.43	0.99	1.12	5.77	2.07	2.10	1.43
Oleic	[C18:1]	26.46	17.73	7.79	27.57	27.68	9.14	30.54	26.72	7.79
Linoleic	[C18:2]	36.87	33.05	17.83	21.55	22.31	6.42	13.89	17.13	17.83
Arachidic	[C20:0]	0.17	0.11	nd	Nd	nd	0.44	nd	nd	nd
Behenic	[C22:0]	0.10	nd	nd	Nd	nd	nd	nd	nd	nd
Others		1.16	4.23	4.15	11.50	8.45	14.48	7.88	12.86	4.15
SAT FAME ^a		28.24	32.56	63.61	20.25	18.70	64.20	31.96	24.22	63.61
MUFA ^b		33.74	30.15	14.41	46.71	50.55	14.89	46.27	45.79	14.41
PUFA ^c		36.87	33.05	17.83	21.55	22.31	6.42	13.89	17.13	17.83
Total FAME ^d		16.47	10.55	10.51	12.28	6.74	8.45	3.57	4.32	10.51

Sn-sodium nitrate; Pn-potassium nitrate; Sni-sodium nitrite; Ac-ammonium chloride; Ur-urea; Me-meat extract; G-glycine; Ye-yeast extract; P-peptone

a-represents the total saturated fatty acid fraction in the total fatty acid methyl esters

b-represents the total monounsaturated fatty acid fraction in the total fatty acid methyl esters

c-represents the total polyunsaturated fatty acid fraction in the total fatty acid methyl esters

d-represents the total FAME expressed in %, weight fraction of dry cell weight

nd-not detected

Table 5.7 Effect of carbon sources on FAME composition under heterotrophic and mixotrophic cultivation

Fatty Acids	FAME (% w/w)	Heterotrophic			Mixotrophic					
		Gl	Mal	Sa	Gl	Fr	Su	Lac	Mal	Sa
Lauric	[C12:0]	2.34	8.26	1.81	2.25	2.98	0.73	13.37	8.13	0.65
Myristic	[C14:0]	0.22	0.18	0.57	0.25	0.46	0.24			0.16
Palmitic	[C16:0]	19.93	23.87	28.44	18.98	22.34	18.38	24.83	22.13	24.87
Palmitoleic	[C16:1]	12.29	7.98	7.96	13.83	10.30	5.76	6.72	6.84	6.18
Stearic	[C18:0]	1.19	5.31	1.50	1.21	3.69	5.83	3.98	4.21	8.91
Oleic	[C18:1]	27.63	10.23	15.15	25.87	17.39	26.73	10.34	9.24	22.38
Linoleic	[C18:2]	34.49	26.38	34.35	31.73	40.39	28.84	22.34	23.84	23.39
Arachidic	[C20:0]	nd	nd	nd	Nd	nd	nd	nd	nd	nd
Behenic	[C22:0]	nd	nd	nd	Nd	nd	nd	nd	nd	nd
	Others	1.91	17.78	10.21	5.88	2.45	13.49	18.42	25.61	13.46
	SAT FAME ^a	23.68	37.63	32.32	22.69	29.47	25.18	42.18	34.47	34.59
	MUFA ^b	39.92	18.21	23.12	39.70	27.69	32.49	17.06	16.08	28.56
	PUFA ^c	34.49	26.38	34.35	31.73	40.39	28.84	22.34	23.84	23.39
	Total FAME ^d	16.12	13.00	24.50	21.30	14.00	12.32	14.50	15.00	29.70

GL-glucose; Fr-fructose; Su-sucrose; Lac-lactose; Mal-maltose; Sa-sodium acetate
a-represents the total saturated fatty acid fraction in the total fatty acid methyl esters
b-represents the total monounsaturated fatty acid fraction in the total fatty acid methyl esters
c-represents the total polyunsaturated fatty acid fraction in the total fatty acid methyl esters
d-represents the total FAME expressed in %, weight fraction of dry cell weight,
nd- not detected

Table 5.8 Effect of physicochemical parameters on the quality of biodiesel obtained from the microalga *Chlorella sorokinana* FC6 IITG

Parameters	Variables	Properties								
		V ^a	CN ^a	FP ^a	CP ^a	PP ^a	SV ^a	IV ^a	DU ^a	HV ^a
Temp (°C)	20	4.35	54.51	158.15	1.62	-1.47	202.49	98.79	108.48	39.66
	28	4.36	54.76	157.89	1.66	-1.43	203.91	97.84	107.48	39.66
	36	4.37	55.20	156.90	1.65	-1.42	204.08	94.57	103.81	39.66
	44	4.42	56.51	154.85	2.26	-0.77	203.50	85.19	93.35	39.66
pH	4	4.36	54.99	157.49	2.27	-0.80	203.30	95.93	105.36	39.67
	6	4.36	54.95	157.78	1.64	-1.44	205.64	97.52	107.06	39.67
	8	4.36	54.76	157.89	1.66	-1.43	203.91	97.84	107.48	39.66
	10	4.36	54.83	158.40	1.68	-1.42	204.52	98.24	107.91	39.67
Nitrogen sources (Autotrophic)	12	4.36	54.79	158.38	1.61	-1.48	204.13	98.26	107.90	39.67
	Sn	4.34	55.13	159.20	2.71	-0.39	205.64	97.84	107.48	39.66
	Sni	4.20	55.43	148.76	0.91	-2.03	210.10	88.22	96.26	39.47
	AC	4.12	57.49	113.50	-0.19	-2.53	226.06	45.91	50.07	39.09
	Ur	4.14	58.28	162.78	7.92	4.84	203.57	82.93	89.81	39.55
	Me	4.28	53.76	146.60	-8.68	-11.75	193.52	88.13	95.17	39.59
	G	4.61	63.43	134.65	25.39	23.09	183.31	25.60	27.74	39.28
	Ye	4.23	55.07	128.85	-11.46	-14.26	201.97	68.33	74.05	39.28
Carbon sources (Heterotrophic)	P	4.31	55.03	141.75	-4.12	-7.03	185.82	74.09	80.05	39.46
	Gl	4.16	56.31	107.75	-4.71	-7.02	219.77	45.91	50.07	39.09
	Mal	4.32	53.96	155.14	-3.55	-6.68	203.64	99.59	108.90	39.61
Carbon sources (Mixotrophic)	Sa	4.29	55.53	137.96	7.67	5.04	176.63	64.95	70.97	39.42
	Gl	4.33	54.88	151.32	7.22	4.35	187.66	83.79	91.81	39.60
	Fr	4.32	54.01	154.07	-1.98	-5.06	195.82	94.54	103.16	39.60
	Su	4.29	53.72	153.40	0.11	-2.92	203.30	99.08	108.47	39.59
	Lac	4.41	55.76	159.93	10.72	7.75	177.50	82.02	90.17	39.71
	Mal	4.24	55.67	127.29	3.92	1.41	179.33	56.47	61.74	39.28
	Sa	4.28	55.44	136.58	10.32	7.76	160.32	58.32	63.76	39.40

Refer to table 5.6 and 5.7 for the abbreviations used in the table and a- section 5.2.5 for the empirical equations for calculating the biodiesel properties were depicted.

Irrespective of different growth conditions, viscosity and cetane number of the biodiesel obtained from FC6 varied in the range 4.12 to 4.61 mm² s⁻¹ and 53.72 to 63.43 respectively. Higher viscosity results in low atomization quality, large drop size with less penetration ability thereby deteriorating the flow properties of the fuel whereas cetane number influences combustion ability and engine knocking. The cloud point and pour point of the biodiesel varied significantly depending upon the nitrogen and carbon sources used in growth media. The flash point of all biodiesel obtained from different growth conditions were found to be greater than the proposed limits in ASTM and EN standards. Irrespective of various growth conditions biodiesel derived from FC6 grown at optimum temperature and pH 28 °C and 6-8 pH respectively was fulfill the ASTM and EN standards. Among the various nitrogen sources sodium nitrate was selected as best growth and lipid inducing nitrogen sources and biodiesel obtained from the FC6 strain grown on this nitrogen sources was also in accordance with ASTM and EN standards. Similarly, glucose and sodium acetate was selected as best growth supporting carbon source under mixotrophic and heterotrophic mode respectively and biodiesel obtained from FC6 strain grown on this carbon sources was found to comply with the ASTM and EN standards.

5.4 Conclusions

In this study, a novel indigenous microalga *Chlorella sorokiniana* FC6 IITG was evaluated for the effect of physicochemical parameters such as temperature, pH, nitrogen sources and carbon sources on growth and lipid content. The strain depicted its robustness in terms of growth under wide range of temperature and pH. Among the various nitrogen sources used sodium nitrate was found to be most suitable nitrogen source for growth and lipid accumulation. Sodium acetate and glucose was identified as suitable carbon sources for growth under heterotrophic and mixotrophic cultivation respectively. Media optimization of the BG11 media components resulted in the improvement of biomass titer

up to 19% through CCD-RSM under photoautotrophic cultivation mode. These results signifies the importance of physicochemical parameters on the growth and FAME composition of microalga FC6.



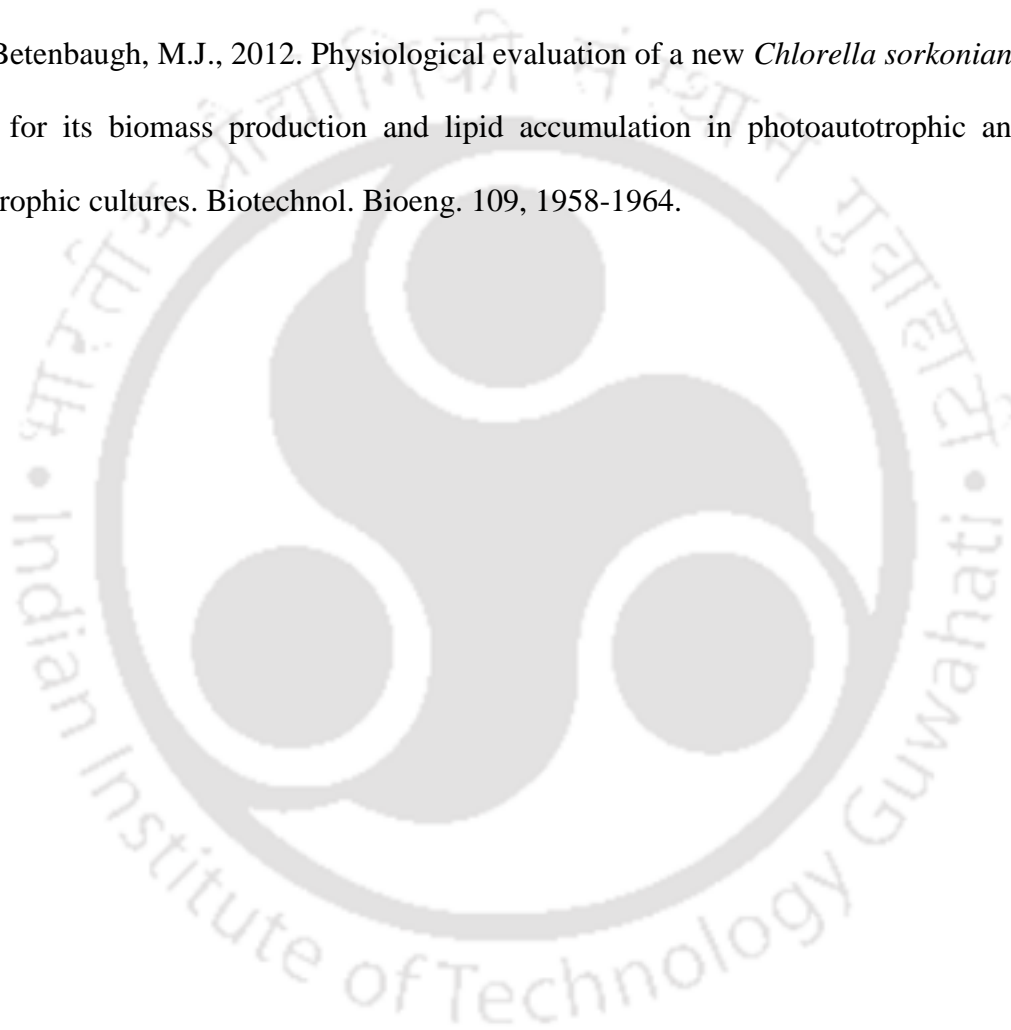
5.5 References

1. Alagesan, S., Gaudana, S.B., Sinha, A., Wangikar, P.P., 2013. Metabolic flux analysis of *Cyanothece* sp. ATCC 51142 under mixotrophic conditions. *Photosynth. Res.* 118, 191-198.
2. Basu, S., Roy, A.S., Mohanty, K., Ghoshal, A.K., 2013. Enhanced CO₂ sequestration by a novel microalga: *Scenedesmus obliquus* SA1 isolated from bio-diversity hotspot region of Assam, India. *Bioresour. Technol.* 143, 369-377.
3. Brennan, L., Owende, P., 2010. Biofuels from microalgae-A review of technologies for production, processing, and extractions of biofuels and co-products. *Renew. Sustain. Energy Rev.* 14, 557-577.
4. Butterwick, C., Heaney, S.I., Talling, J.F., 2005. Diversity in the influence of temperature on the growth rates of freshwater algae, and its ecological relevance. *Freshw. Biol.* 50, 291-300.
5. Chen, C.Y., Yeh, K.L., Aisyah, R., Lee, D.J., Chang, J.S., 2011. Cultivation, photobioreactor design and harvesting of microalgae for biodiesel production: A critical review. *Bioresour. Technol.* 102, 71-81.
6. Flynn, K.J., Butler, I., 1986. Nitrogen-Sources for the growth of marine microalgae - Role of dissolved free amino-acids. *Mar. Ecol. Prog. Ser.* 34, 281-304.
7. Francisco, É.C., Neves, D.B., Jacob-Lopes, E., Franco, T.T., 2010. Microalgae as feedstock for biodiesel production: carbon dioxide sequestration, lipid production and biofuel quality. *J. Chem. Technol. Biotechnol.* 85, 395-403.
8. Gounot, A.M., 1991. Bacterial life at low temperature: physiological aspects and biotechnological implications. *J. Appl. Microbiol.* 71, 386-397.
9. Heifetz, P.B., Forster, B., Osmond, C.B., Giles, L.J., Boynton, J.E., 2000. Effects of acetate on facultative autotrophy in *Chlamydomonas reinhardtii* assessed by

- photosynthetic measurements and stable isotope analyses. *Plant Physiol.* 122, 1439-1445.
10. Isleten-Hosoglu, M., Ayyıldız-Tamis, D., Zengin, G., Elibol, M., 2013. Enhanced growth and lipid accumulation by a new *Ettlia texensis* isolate under optimized photoheterotrophic condition. *Bioresour. Technol.* 131, 258-265.
11. Isleten-Hosoglu, M., Gultepe, I., Elibol, M., 2012. Optimization of carbon and nitrogen sources for biomass and lipid production by *Chlorella saccharophila* under heterotrophic conditions and development of Nile red fluorescence based method for quantification of its neutral lipid content. *Biochem. Eng. J.* 61, 11-19.
12. Karemore, A., Pal, R., Sen, R., 2013. Strategic enhancement of algal biomass and lipid in *Chlorococcum infusionum* as bioenergy feedstock. *Algal Res.* 2, 113-121.
13. Morales-Sanchez, D., Tinoco-Valencia, R., Kyndt, J., Martinez, A., Heterotrophic growth of *Neochloris oleoabundans* using glucose as a carbon source. *Biotechnol. Biofuels.* 6.
14. Muthuraj, M., Kumar, V., Palabhanvi, B., Das, D., 2014. Evaluation of indigenous microalgal isolate *Chlorella* sp. FC2 IITG as a cell factory for biodiesel production and scale up in outdoor conditions. *J. Ind. Microbiol. Biotechnol.* 41, 499-511.
15. Patterson, G.W., 1970. Effect of temperature of fatty acid composition of *Chlorella sorokiniana*. *Lipids.* 5, 597-600.
16. Perez-Garcia, O., Escalante, F.M.E., de-Bashan, L.E., Bashan, Y., 2011. Heterotrophic cultures of microalgae: Metabolism and potential products. *Water Res.* 45, 11-36.
17. Ramirez-Verduzco, L.F, Rodriguez-Rodriguez, J.E, Jaramillo-Jacob, A.R, 2012. Predicting cetane number, kinematic viscosity, density and higher heating value of biodiesel from its fatty acid methyl ester composition. *Fuel* 91, 102-111.
18. Su, Y.C., Liu, Y.A., Diaz Tovar, C.A., Gani, R., 2011. Selection of Prediction Methods

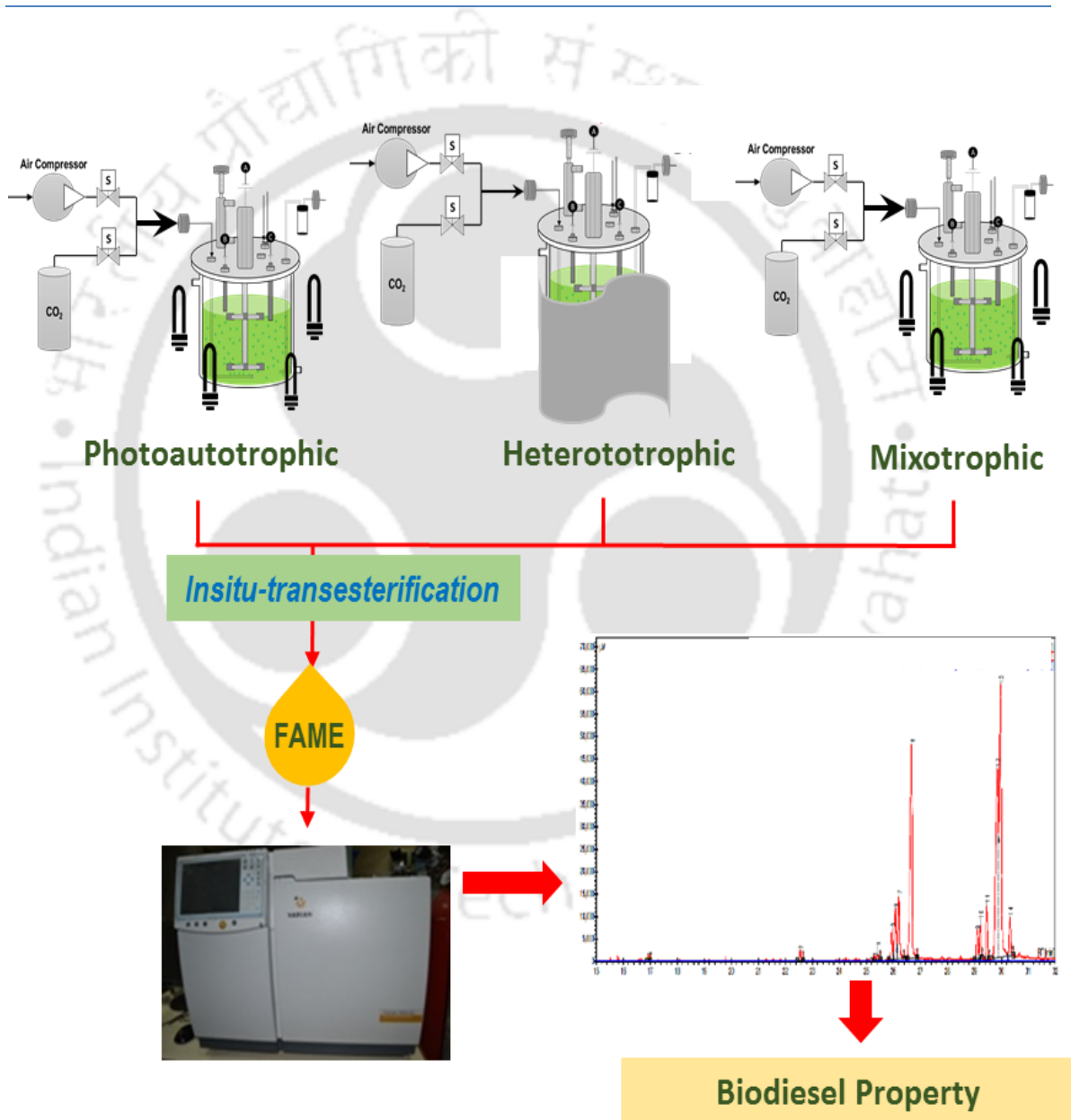
for Thermophysical Properties for Process Modeling and Product Design of Biodiesel Manufacturing. *Ind. Eng. Chem. Res.* 50, 6809-6836.

19. Tran, H-L., Kwon, J-S., Kim, Z-H., Oh, Y., Lee, C-G., 2010. Statistical optimization of culture media for growth and lipid production of *Botryococcus braunii* LB572. *Biotechnol. Bioprocess Eng.* 15, 277-284.
20. Wan, M.X., Wang, R.M., Xia, J.L., Rosenberg, J.N., Nie, Z.Y., Kobayashi, N., Oyler, G.A., Betenbaugh, M.J., 2012. Physiological evaluation of a new *Chlorella sorkoniana* isolate for its biomass production and lipid accumulation in photoautotrophic and heterotrophic cultures. *Biotechnol. Bioeng.* 109, 1958-1964.



CHAPTER 6

Biochemical characterization of the strain under different cultivation conditions



Effect of various cultivation conditions: photoautotrophic, heterotrophic & mixotrophic on growth and quality of biodiesel was evaluated for the strain *Chlorella sorokiniana* FC6 IITG

6.1 Background and motivation

Chlorella sp. has been extensively characterized under photoautotrophic, heterotrophic and mixotrophic cultivation conditions (Liu et al., 2011; Fan et al., 2012). With the change in growth conditions microalgae modulate its metabolism providing an opportunity to tune up for neutral lipids and biomass formation (Mata et al., 2010; Chen et al., 2011). For instance, lipid content of *Chlorella protothecoides* was reported to be approximately four fold higher under heterotrophic growth as compared to photoautotrophic condition (Xu et al., 2006). Mixotrophic growth of *Chlorella vulgaris* with glucose showed ~14 and ~1.5 fold higher lipid productivity as compared to photoautotrophic and heterotrophic cultivation conditions respectively (Liang et al., 2009).

Interestingly, it is not only the quantity but also the quality of lipids which varies significantly under different cultivation conditions (Liu et al., 2011). Heterotrophic growth of *Chlorella zofingiensis* resulted in accumulation of high levels of neutral lipids, whereas under photoautotrophic condition, cells accumulated high levels of glycolipid and phospholipid (Liu et al., 2011). Poly unsaturated fatty acids (PUFA) were found to be abundant when the cells were grown under photoautotrophic condition whereas mono unsaturated fatty acids (MUFA) dominate in the heterotrophic cultivation (Liu et al., 2011). It is important to note that, fractional variations of these PUFA and MUFA may have significant effect on key fuel properties such as cloud point and cetane number (Lim et al., 2012), which in turn plays a major role in meeting the specific standards of high quality biodiesel (Cha et al., 2011). Nutrient stress conditions and unfavorable growth conditions were also reported to act as the triggers for neutral lipid accumulation in many of the microalgal systems (Rodolfi et al., 2009). *Chlorella vulgaris* and *C. emersonii* were reported to accumulate 2 fold and 3 fold higher total lipid accumulation under nitrogen limited conditions respectively (Illman et al., 2000). These studies emphasize the necessity to

evaluate and characterize the novel microalgal isolate under various trophic modes to understand the physiology of biomass formation and lipid production.

The present study evaluates the indigenous novel freshwater microalgal isolate *Chlorella sorokiniana* FC6 IITG as a potential cell factory for biodiesel production. The isolate was evaluated in terms of growth and lipid productivity under photoautotrophic, heterotrophic and mixotrophic conditions. The experiments highlight the metabolic flexibility of the strain in terms of relationship between dynamic change in biomass composition, growth rate, nutrient utilizations and lipid productivity. Finally, quality of fatty acid methyl esters (FAME) in terms of fatty acid compositions of the biomass under different cultivation conditions were also evaluated by gas chromatography (GC). The outcome of the research, point towards a scope to develop this microalgal strain as a feasible feed stock for sustainable biodiesel generation under mixotrophic growth mode and process development for enhanced biomass and lipid productivity.

6.2 Materials and methods

6.2.1 Microalgal strain, media composition and inoculum preparation

The slant culture of *Chlorella sorokiniana* FC6 IITG was maintained in optimized BG11 media (as mentioned in Table 5.4 of section 5.3.4.1). Optimized BG11 media comprised of (in g L⁻¹) NaNO₃ 0.82, K₂HPO₄ 0.044, MgSO₄·7H₂O 0.194, CaCl₂·2H₂O 0.070, Na₂CO₃ 0.052, citric acid 0.016, ferric ammonium citrate 0.016, EDTA 0.003 and microelement solution (0.5 mL L⁻¹ that consists of H₃BO₃ 2.86, MnCl₂·H₂O 1.81, ZnSO₄·7H₂O 0.222, CuSO₄·5H₂O 0.079, Na₂MoO₄·2H₂O 0.390, and Co(NO₃)₂·6H₂O 0.049). The inoculum was prepared by transferring two loops full of slant culture into 250 mL Erlenmeyer flask containing 100 mL optimized BG11 medium and incubated in an orbital shaker and condition were kept same as mentioned in section 3.2.1 of chapter 3.

After reach of absorbance (A_{690}) 1.0, 1% (v/v) of the revived culture was used as inoculum for all the experiments in the present study.

6.2.2 Evaluation of the strain under different trophic modes

Detailed characterization of the strain was performed under photoautotrophic, heterotrophic and mixotrophic cultivation conditions in a 3L automated bioreactor (eZ Control, Applikon Biotechnology, Holland) with a working volume of 1.25 L containing optimized BG11 medium. The reactor was operated at 28°C, agitator speed of 400 rpm and aeration at 1vvm. The medium pH was maintained throughout the batch in between 6.0 to 8.0 by addition of 0.25 M NaOH or HCl. For photoautotrophic cultivation, cells were grown with 1% (v/v) CO₂ and light intensity of 150 $\mu\text{E m}^{-2} \text{s}^{-1}$ for a light: dark regime of 16:8 h. Cool fluorescent lamps of 23 W (Havells India Pvt. Ltd.) were used as the source of light. Lux meter (Sigma Instruments, India) was used to measure the light intensity in terms of Lux. The Lux values were converted in to corresponding $\mu\text{E m}^{-2} \text{s}^{-1}$ by multiplying with the factor of 0.0135 which is used for cool fluorescent lamps (Thimijan and Heins, 1983). The intensity over the reactor surface was measured at several points and averaged to obtain the overall light intensity. Under heterotrophic cultivation, BG11 medium was supplemented with initial sodium acetate concentration of 15 g L⁻¹ as the sole carbon and energy source in dark. Under mixotrophic condition, BG11 medium was supplemented with 10 g L⁻¹ of glucose and a light intensity of 150 $\mu\text{E m}^{-2} \text{s}^{-1}$ for a light: dark regime of 16:8 h was provided. In this cultivation condition 1% (v/v) CO₂ was supplied as carbon source in the light cycle with no supply of CO₂ in dark phase. The batch duration was varied from 10 days to 15 days depending on the cultivation conditions. The batch was terminated once the stationary phase of the biomass reached and started decreasing thereafter. A higher light intensity was provided in the bioreactor experiments in comparison to shake flask, as the optimum media composition and external source of CO₂ available in the bioreactor was expected to result

in enhanced specific growth rates and higher biomass titer leading to light attenuations. Sampling was performed at regular time intervals to obtain dynamic profiles of growth, lipid accumulation and substrate utilization.

6.2.3 Analyses of growth, substrates utilization and biomass composition

Analysis of microalgal growth, utilization of substrates and biomass composition were carried out at regular interval of time. A known volume of sample was centrifuged at 8000 x g for 10 minutes at 4°C and the supernatant was collected for extracellular substrates analyses (glucose, nitrate and phosphate). The pellet was utilized for the analysis of biomass compositions which includes carbohydrates, proteins, chlorophyll and lipid.

6.2.3.1 Analysis of growth

Algal growth was estimated by measuring the absorbance of cells at 690 nm with a UV-visible spectrophotometer (Cary 50, Varian, Australia) and the dry cell weight (DCW) was obtained using the standard curve (Fig. 6.1). The protocol for dry cell weight measurement was detailed in section 3.2.4.1 of chapter 3. The correlation equations were as follows:

$$DCW_a = 0.1896 * A_{690}, R^2 = 0.9981 \quad (6.1)$$

$$DCW_h = 0.1915 * A_{690}, R^2 = 0.9947 \quad (6.2)$$

$$DCW_m = 0.2234 * A_{690}, R^2 = 0.9965 \quad (6.3)$$

Where DCW_a , DCW_h and DCW_m are dry cell weight in g L⁻¹ for photoautotrophic, heterotrophic and mixotrophic cultivation respectively and A_{690} is the absorbance at 690 nm. The biomass productivity (P_B , g L⁻¹ day⁻¹) under different cultivation conditions were calculated based on the following equation

$$P_B = \frac{X_f - X_0}{t_f - t_0} \quad (6.4)$$

where, X_0 and X_f were the dry cell weight (g L^{-1}) obtained at initial (t_0) and final (t_f) time points (in days) respectively. Specific growth rate of the cells was calculated based on the following equation

$$\mu = \frac{\ln\left(\frac{X_2}{X_1}\right)}{(t_2 - t_1)} \quad (6.5)$$

where, X_1 and X_2 were the dry cell weight (g L^{-1}) obtained at initial (t_1) and final (t_2) time points (in days) respectively.

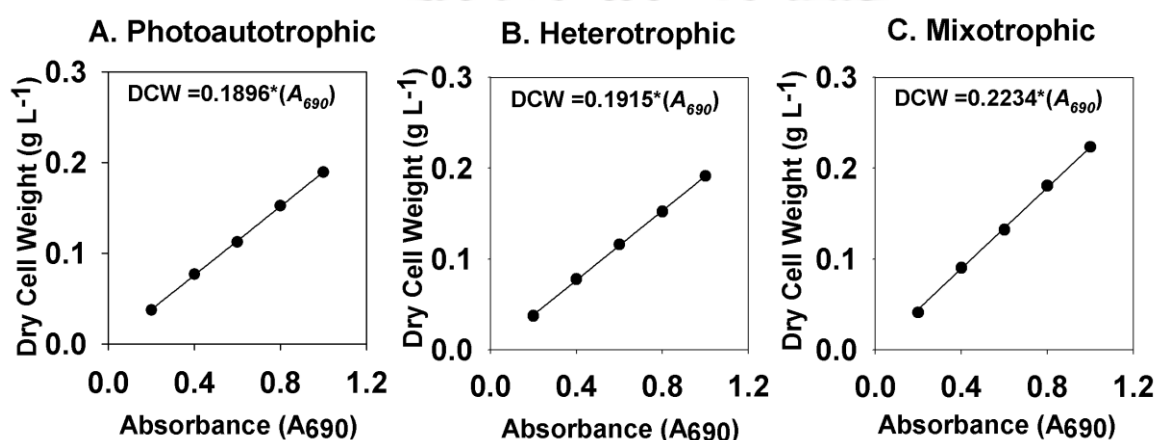


Fig. 6.1 Correlation between dry cell weight of the biomass and absorbance measured at 690 nm in a spectrophotometer under (A) photoautotrophic, (B) heterotrophic and (C) mixotrophic growth conditions

6.2.3.2 Analysis of nitrate utilization

The sodium nitrate concentrations were measured using HPLC (Agilent 1220 Infinity HPLC) equipped with a photo-diode detector. The filtered cell free supernatant of 20 μL was injected in to Zorbax Eclipse XDB-C18 HPLC column (4.6 mm \times 250 mm, 5 μm) with 0.01 M $\text{NH}_4\text{H}_2\text{PO}_4$ in 30 % (v/v) methanol as a mobile phase. A constant flow rate of 0.8 mL min^{-1} was maintained for the mobile phase and the detection was obtained at 220 nm. The corresponding standard curve is as shown in Fig. 6.2 A and calibration equation is as follows:

$$\text{Area (mAU)} = 9 \times 10^8 * \text{Nitrate concentration (g L}^{-1}\text{)}, R^2 = 0.9984 \quad (6.6)$$

6.2.3.3 Analysis of sodium acetate utilization

The sodium acetate concentrations were measured using HPLC (Agilent 1220 Infinity HPLC) equipped with a photo-diode detector. The filtered cell free supernatant of 20 μL was injected in to Zorbax Eclipse XDB-C18 HPLC column (4.6 mm \times 250 mm, 5 μm) with 0.01 M $\text{NH}_4\text{H}_2\text{PO}_4$ in 30 % (v/v) methanol as a mobile phase. A constant flow rate of 0.8 mL min^{-1} was maintained for the mobile phase and the detection was obtained at 220 nm. The corresponding standard curve is as shown in Fig. 6.2 B and calibration equation is as follows:

$$\text{Area (mAU)} = 2 \times 10^6 * \text{Sodium acetate concentration (g L}^{-1}\text{)}, R^2 = 0.9997 \quad (6.7)$$

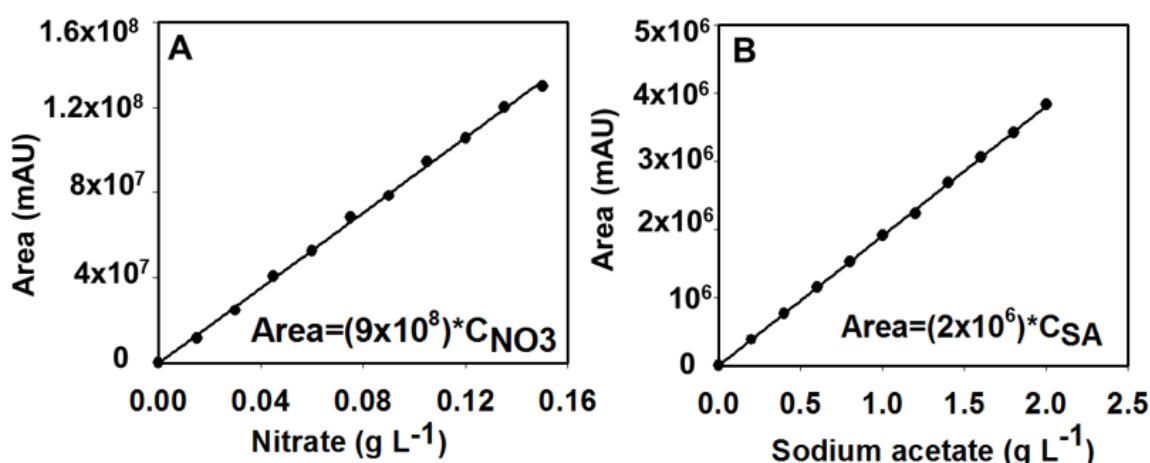


Fig. 6.2 Correlation graph between concentration of the substrates and their respective area in HPLC for the estimation of (A) sodium nitrate, C_{NO_3} represents concentration of sodium nitrate and (B) sodium acetate, C_{SA} represents concentration of sodium acetate

6.2.3.4 Analysis of phosphate utilization

Phosphate estimation was carried out using ascorbic acid method with potassium hydrogen phosphate (dibasic) as standard (Parsons et al., 1984). Combined reagent (0.32 mL) comprising (5 N) sulfuric acid, (0.018 M) antimony potassium tartrate, (0.102 M) ammonium molybdate and (0.1 M) ascorbic acid was used for estimating the phosphate content in the supernatant of 2.0 mL. The absorbance was read at 880 nm after incubation

for 10 minutes at room temperature and the standard curve is shown in Fig. 6.3A and correlation equation is as follows:

$$\begin{aligned} \text{Absorbance at } 880 \text{ nm} &= 0.1125 * \text{Phosphate concentration (mg L}^{-1}\text{)}, \\ R^2 &= 0.994, \end{aligned} \quad (6.8)$$

6.2.3.5 Analysis of glucose utilization

Glucose estimation in the medium was performed using di-nitrosalicylic acid method (Miller, 1959). Supernatant of 3 mL was added to di-nitrosalicylic acid reagent of 3 mL and incubated for 15 minutes in a boiling water bath. The absorbance was read at 575 nm after addition of 1 mL potassium sodium tartrate (40 % w/v) for stabilization. The standard curve is shown in Fig. 6.3 B and calibration equation is as follows:

$$\begin{aligned} \text{Absorbance at } 575 \text{ nm} &= 0.6471 * \text{Glucose concentration (g L}^{-1}\text{)}, \\ R^2 &= 0.9998 \end{aligned} \quad (6.9)$$

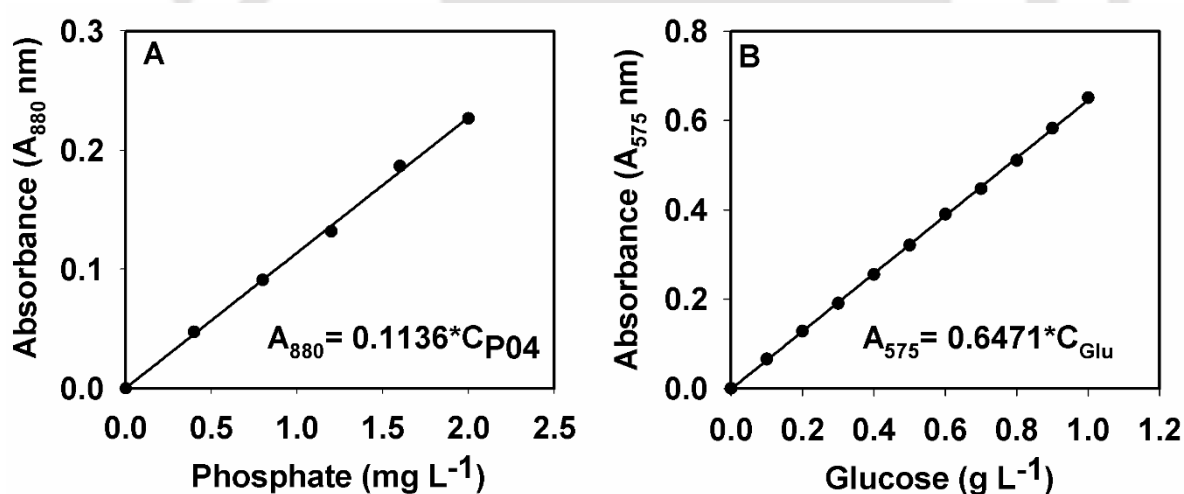


Fig. 6.3 Correlation graph between concentration of the substrates and their respective absorbance in UV-Visible spectrophotometer for estimation of (A) phosphate, C_{P04} represents concentration of phosphate and (B) glucose, C_{Glu} represents concentration of glucose

6.2.3.6 Analysis of intracellular carbohydrate formation

Estimation of carbohydrate fraction in the biomass was performed by phenol sulfuric acid method with glucose as standard (Dubois et al., 1956). The pellet obtained after

centrifugation was re-suspended in same volume of deionized water and 0.5 mL of the re-suspended pellet was used as the analytical suspension for carbohydrate estimation. Phenol (5 %, w/v) of 0.5 mL was added to 0.5 mL algal suspension, followed by 2.5 mL of concentrated sulfuric acid along the sides of the tube. After equilibration to room temperature for 10 minutes, the contents in tubes were mixed and incubated at 35°C. After 30 minutes, the absorbance was measured at 490 nm. The standard curve is shown in Fig. 6.4 A and calibration equation is as follows:

$$\text{Absorbance at 490 nm} = 4.48 * \text{Carbohydrate concentration (g L}^{-1}\text{)},$$

$$R^2 = 0.999 \quad (6.10)$$

6.2.3.7 Analysis of intracellular protein formation

Estimation of protein fraction in the biomass was performed by Lowery's method BSA standard. Standard curve is shown in Fig. 6.4 B.

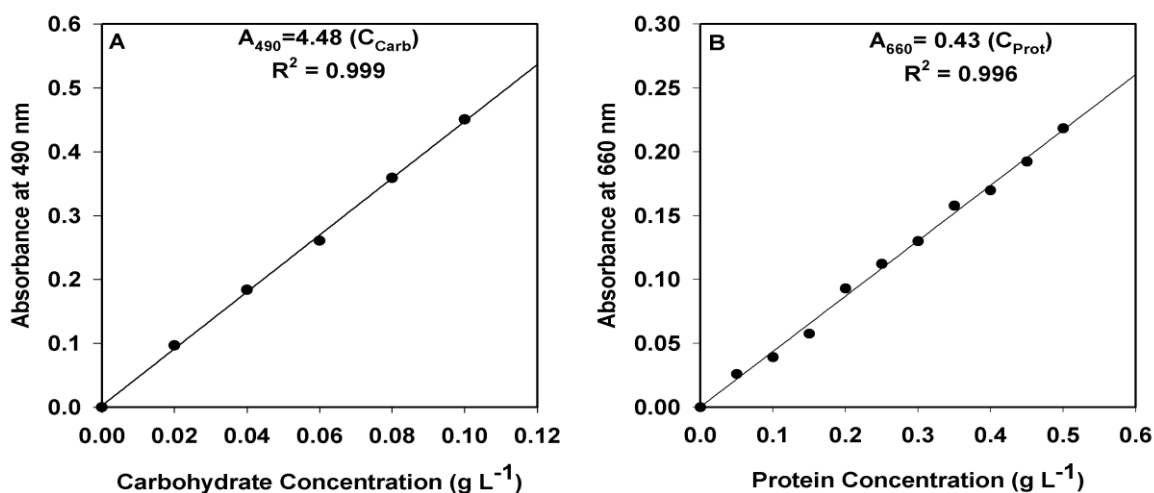


Fig. 6.4 Correlation graph between concentration of the substrates and their respective absorbance in UV-Visible spectrophotometer for the estimation of (A) carbohydrate, C_{carb} represents carbohydrate concentration; and (B) protein, C_{Prot} represents protein concentration.

For protein estimation, cell pellets were subjected to alkaline hydrolysis by boiling with 2N NaOH at 100°C for 15 minutes and then neutralized to pH 7.0 by adding 1.6N

hydrochloric acid (Pruvost et al., 2011). The neutralized solution was used for protein estimation using Lowry's method (Lowry et al., 1951). The correlation curve was obtained with bovine serum albumin as standard. Standard curve is shown in Fig. 6.4 B and correlation equation is as follows:

$$\text{Absorbance at 660 nm} = 0.43 * \text{Protein concentration (g L}^{-1}\text{)}, R^2 = 0.996 \quad (6.11)$$

6.2.3.8 Analysis of intracellular chlorophyll formation

The chlorophyll estimation was carried out using the method provided by Pruvost et al. (2011) which uses 100 % methanol for extraction at 45°C. An absorbance scan of wavelength from 400 to 800 nm was performed and the following equations given by Ritchie (2006) for organisms containing chlorophyll *a* and chlorophyll *b* were used for quantification (Eq. 6.12 and 6.13). Total chlorophyll content of the cells was expressed as the sum of chlorophyll *a* and *b*.

$$\text{Chlorophyll } a \text{ (mg L}^{-1}\text{)} = (16.52 \times [A_{665} - A_{750}]) - (8.09 \times [A_{652} - A_{750}]) \quad (6.12)$$

$$\text{Chlorophyll } b \text{ (mg L}^{-1}\text{)} = (27.44 \times [A_{652} - A_{750}]) - (12.17 \times [A_{665} - A_{750}]) \quad (6.13)$$

6.2.3.9 Analysis of fatty acids methyl esters (FAME) derived from microalgae

The total lipid content was quantified in terms of fatty acid methyl esters (FAME) via direct transesterification method using gas chromatograph (GC-FID, Varian 450, Netherlands). The FAME contents were extracted in the hexane layer and analyzed using GC equipped with flame ionization detector and SLB-IL 100 column (30 m x 0.25 mm i.d., 0.20 µm film thickness). FAME mix C14-C22 (Supelco, USA) was used as the standard for GC-FID and the lipid quantified using this method represents the total lipid of the biomass in % (w/w, DCW). The protocols are detailed in section 5.2.4.1 of chapter 5. All the experiments were conducted in triplicate and the data were expressed as mean ± standard error.

6.2.4 Quality assessment of biodiesel generated from FC6 under different cultivation conditions

Quality of the biodiesel is decided by the properties such as viscosity (η), cetane number (CN), flash point (T_f), cloud point (CP), pour point (PP), saponification value (SV), iodine value (IV), degree of unsaturation (DU) and highest heating value (HV) which are in turn dependent on the carbon chain length and the amount of unsaturated fatty acids formed in the microalgal systems. Therefore, these properties of the biodiesel were determined based on the empirical equations detailed in section 5.2.5 of chapter 5.

6.3 Results and Discussion

6.3.1 Characterization of *Chlorella sorokiniana* FC6 IITG under different trophic mode in an automated bioreactor

Biomass and lipid productivity of the organism *Chlorella sorokiniana* FC6 IITG was evaluated under photoautotrophic, heterotrophic and mixotrophic growth conditions in optimized BG11 media (Fig. 6.5). In this study sodium acetate and glucose were supplemented as the carbon source in case of heterotrophic and mixotrophic growth conditions respectively. We observed significant variations in the DCW, biomass productivity, specific growth rate, lipid content and lipid productivity for three different cultivations conditions. As shown in Table 6.1, the photoautotrophic cells grew slowly, with a specific growth rate of 1.56 day^{-1} and maximum DCW of 2.13 g L^{-1} at the end of the batch. It is also important to note that the photoautotrophic condition under reactor level showed 2.5 fold increment in biomass as compared to the shake flask conditions (section 5.3.4) attributed to the supply of 1% (v/v) CO_2 in reactor level characterization. However, heterotrophic condition exhibited a down regulated growth with a maximum DCW of 1.75 g L^{-1} and specific growth rate of 0.99 day^{-1} while, mixotrophic cultivation showed an improved biomass titer of 2.73 g L^{-1} with highest specific growth rate of 2.19 day^{-1} .

Compared to photoautotrophic and heterotrophic cultivation, mixotrophic cultivation led immediately to logarithmic growth phase with very short lag phase (Fig. 6.5 A).

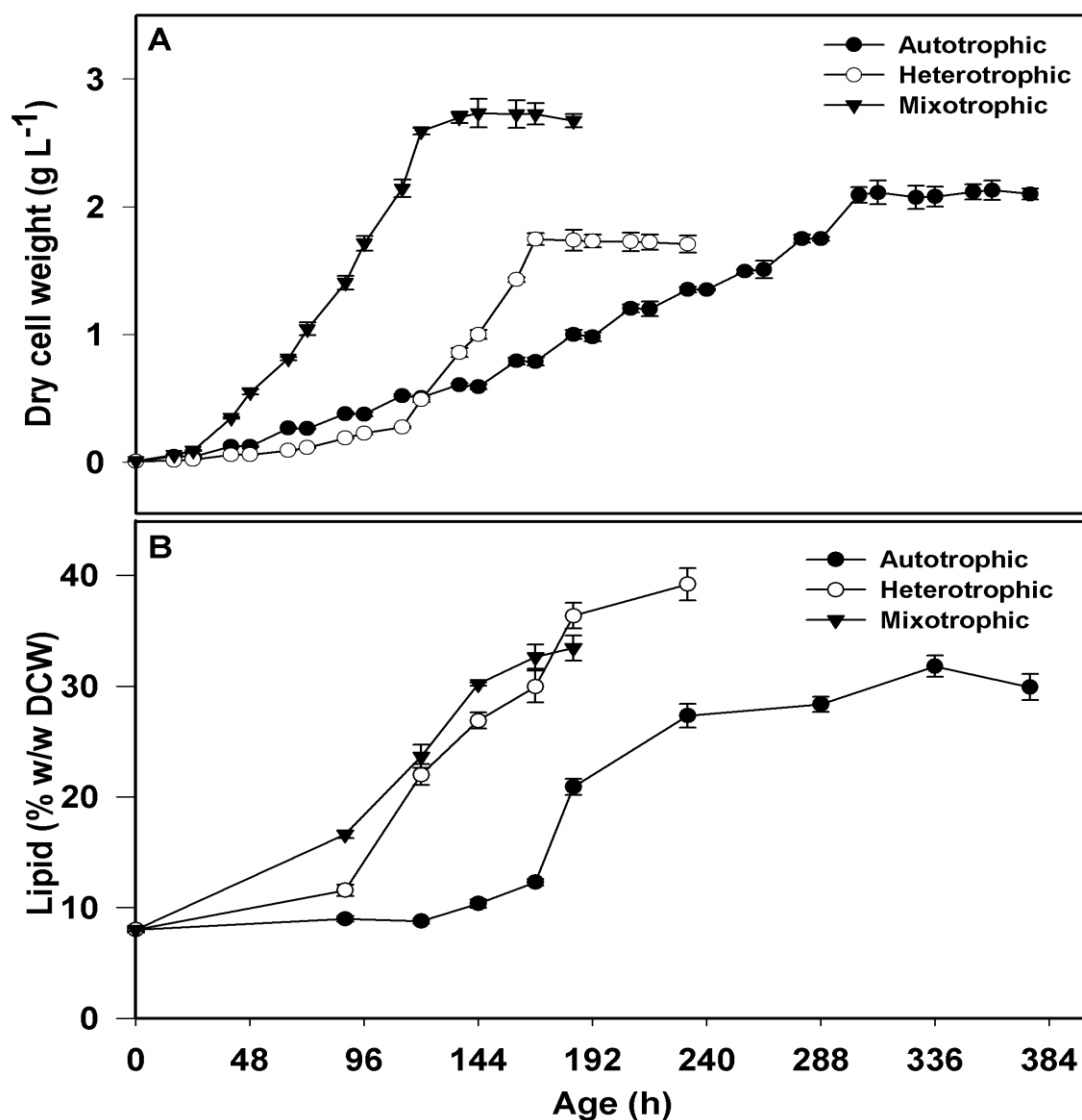


Fig. 6.5 Dynamic profiles of growth and changes in intracellular lipid accumulation of the strain FC6 under photoautotrophic (●), heterotrophic (○) and mixotrophic (▼) conditions: (A) growth, (B) lipid percentage in the biomass. The strain was grown under different growth condition at 28 °C and 400 rpm in a 3 L automated bioreactor. Light intensity of 150 $\mu\text{E m}^{-2} \text{s}^{-1}$ for 16:8 h light: dark cycle and aeration with CO_2 of 1% (v/v) was provided under photoautotrophic condition. The conditions for mixotrophic cultivation was same as photoautotrophic growth with additional supplementation of glucose in the BG11 medium. The heterotrophic growth was conducted under complete dark with supplementation of sodium acetate in the BG11 medium

Maximum biomass productivity was found to be 455.5 $\text{mg L}^{-1} \text{day}^{-1}$ under mixotrophic growth followed by heterotrophic (249.7 $\text{mg L}^{-1} \text{day}^{-1}$) and photoautotrophic (142.06 $\text{mg L}^{-1} \text{day}^{-1}$)

$^1 \text{ day}^{-1}$) cultivation conditions. Similar to the present study, increased biomass productivities were reported for many other microalgal strain grown under mixotrophic condition (Cheirsilp et al., 2012). An improved biomass concentration was reported for *C. sorokiniana* (Wan et al., 2011), *Nannochloropsis oculata* and *C. vulgaris* (Heredia-Arroyo et al., 2011) when grown under mixotrophic condition in comparison to photoautotrophic condition which supports the present study. Mixotrophic cultivation provides an opportunity to the strain to follow both heterotrophic route and light dependent route of growth in simultaneous and independent manner (Sforza et al., 2012). Therefore, growth is not strictly limited by the availability of light or availability of carbon source in the medium as is the case for photoautotrophic and heterotrophic growth respectively. The intracellular lipid induction may be attributed to the exhaustion of nutrients during transition from growth phase to the stationary phase of the cultivations. For instance, utilization profile of the substrates under all cultivation conditions (Fig. 6.6) showed that nutrient was consumed within 4-6 days of cultivation and hence, creating nutritional stress condition for the cells.

Table 6.1 Kinetic parameters for growth and lipid formation of FC6 cultivated under photoautotrophic, heterotrophic and mixotrophic cultivation conditions

Parameters ^a	Cultivation Conditions		
	Photoautotrophic	Heterotrophic	Mixotrophic
Specific growth rate μ_{\max} (day^{-1}) ^a	1.56	0.99	2.19
Dry cell mass (g L^{-1}) ^a	2.13	1.75	2.73
Biomass productivity ($\text{mg L}^{-1} \text{ day}^{-1}$) ^b	142.06	249.7	455.5
Total Lipid (% , w/w DCW) ^a	31.80	39.21	33.44
Total lipid productivity ($\text{mg L}^{-1} \text{ day}^{-1}$) ^c	47.2	67.0	111.85

a -all the parameters depicted were the maximum values obtained for FC6 growth under different cultivation conditions
b-The biomass productivity (P_X , $\text{mg L}^{-1} \text{ day}^{-1}$) under different cultivation conditions were calculated based $P_X = (X_f - X_0)/(t_f - t_0)$ where, X_0 and X_f were the dry cell weight (g L^{-1}) obtained at initial (t_0) and final (t_f) time points (in days) respectively
c-The total lipid productivity (P_{TL} , $\text{mg L}^{-1} \text{ day}^{-1}$) under different cultivation conditions were calculated based $P_{TL} = (TL_f - TL_0)/(t_f - t_0)$ where, TL_0 and TL_f were the dry cell weight (g L^{-1}) obtained at initial (t_0) and final (t_f) time points (in days) respectively

A large pool of literature has demonstrated that the phosphate and nitrate starvation (or limitation) serve as the drivers for lipid accumulation in the microalgal strains (Illman

et al., 2000; Feng et al., 2012; Sforza et al., 2012). Maximum lipid content (39.21 % w/w DCW) was obtained for heterotrophic growth followed by mixotrophic and photoautotrophic conditions (Fig. 6.5 B).

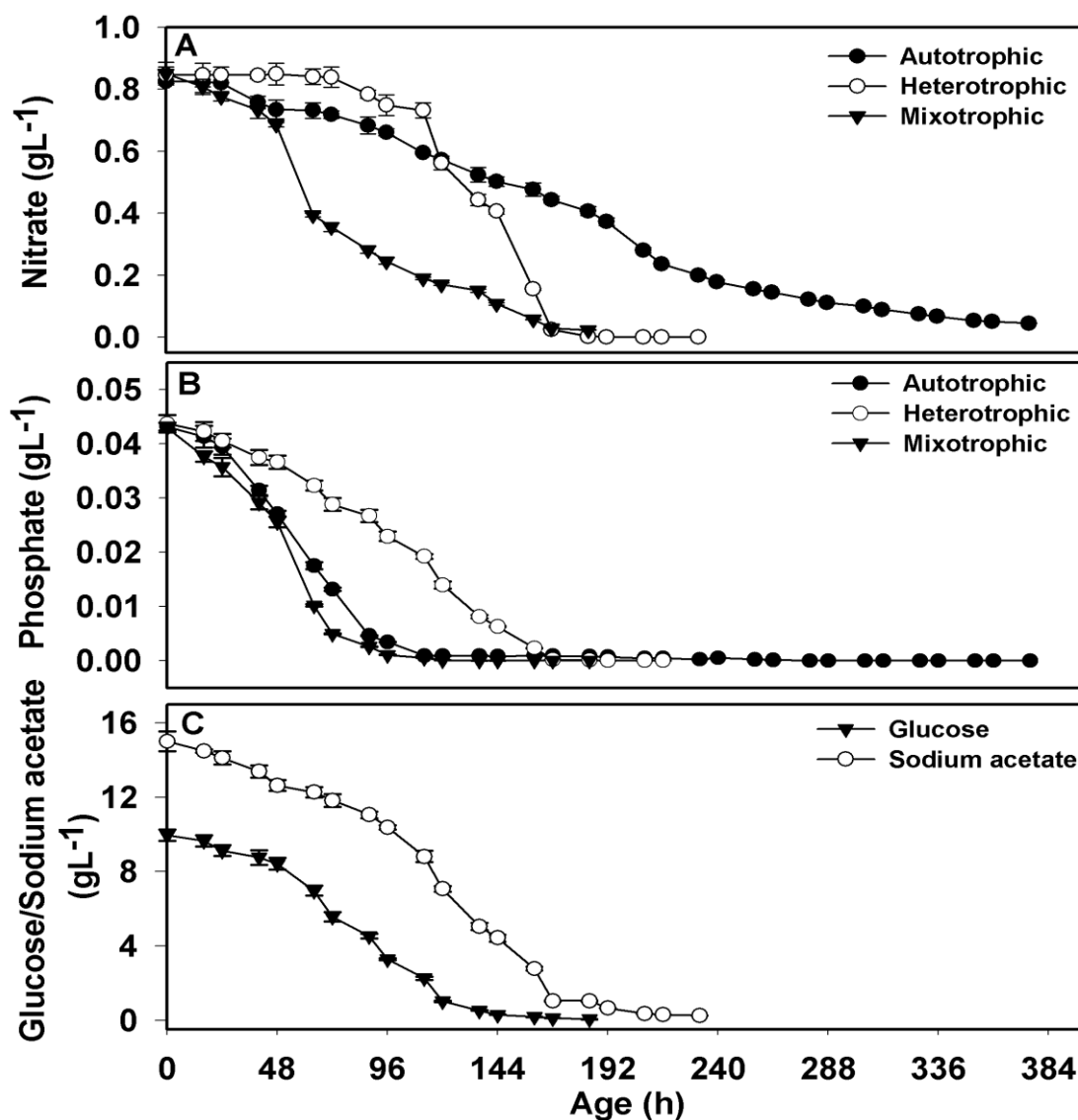


Fig. 6.6 Substrate utilization profile of the strain *Chlorella sorokiniana* FC6 IITG grown under photoautotrophic (●), heterotrophic (○) and mixotrophic (▼) conditions: (A) nitrate utilization profile, (B) phosphate utilization profile, (C) glucose utilization profile under mixotrophic growth (▼) and sodium acetate utilization profile under heterotrophic cultivation condition (○). The strain was grown under different growth condition at 28 °C and 400 rpm in a 3 L automated bioreactor. Light intensity of 150 $\mu\text{E m}^{-2} \text{s}^{-1}$ for 16:8 h light: dark cycle and aeration with CO₂ of 1% (v/v) was provided under photoautotrophic condition. The conditions for mixotrophic cultivation was same as photoautotrophic growth with additional supplementation of glucose in the BG11 medium. The heterotrophic growth was conducted under complete dark with supplementation of sodium acetate in the BG11 medium

In heterotrophic cultivation sodium acetate was used as carbon source which also acts as a precursor for lipid synthesis and hence, results in comparatively higher lipid accumulation in comparison to mixotrophic and photoautotrophic culture. This variation in the lipid accumulation may also be attributed to different exhaustion time of extracellular nutrients from broth, which in turn is responsible for lipid induction (Fig. 6.6). For instance, extracellular nitrate was exhausted earlier under the heterotrophic and mixotrophic cultivation conditions, while significant amount of nitrate was still remaining under phototrophic mode of cultivation at the same time as observed (Fig. 6.6 A). Phosphate was found to be limiting in all the nutritional conditions which gets depleted at very early stage of growth phase around four days of cultivation period in all cultivation conditions (Fig. 6.6 B).

The effect of phosphate and nitrate starvation (or limitation) on induction of lipid accumulation in the microalgal strains was well reviewed in large pool of literature (Muthuraj et al., 2013; Muthuraj et al., 2014). Redirection of carbon flux from carbohydrate and protein fractions of the biomass towards accumulation of lipid was also evident from changes in macromolecular composition of the cells during the transition from exponential phase to the stationary phase of growth under all cultivation conditions (Fig. 6.7). Decrease in carbohydrate and protein fractions of the biomass is concomitant with the increase in neutral lipid content (Illman et al., 2000; Feng et al., 2012; Rodolfi et al., 2009). Similarly, a major metabolic shift in the biomass composition of two freshwater microalgae *Neochloris oleoabundans* and *Chlorella vulgaris* grown under photoautotrophic condition with nitrogen starvation was reported by Pruvost et al. (2011) which signify the reduction in intracellular protein content from 60% to 20% in both the species with an increase in neutral lipid accumulation.

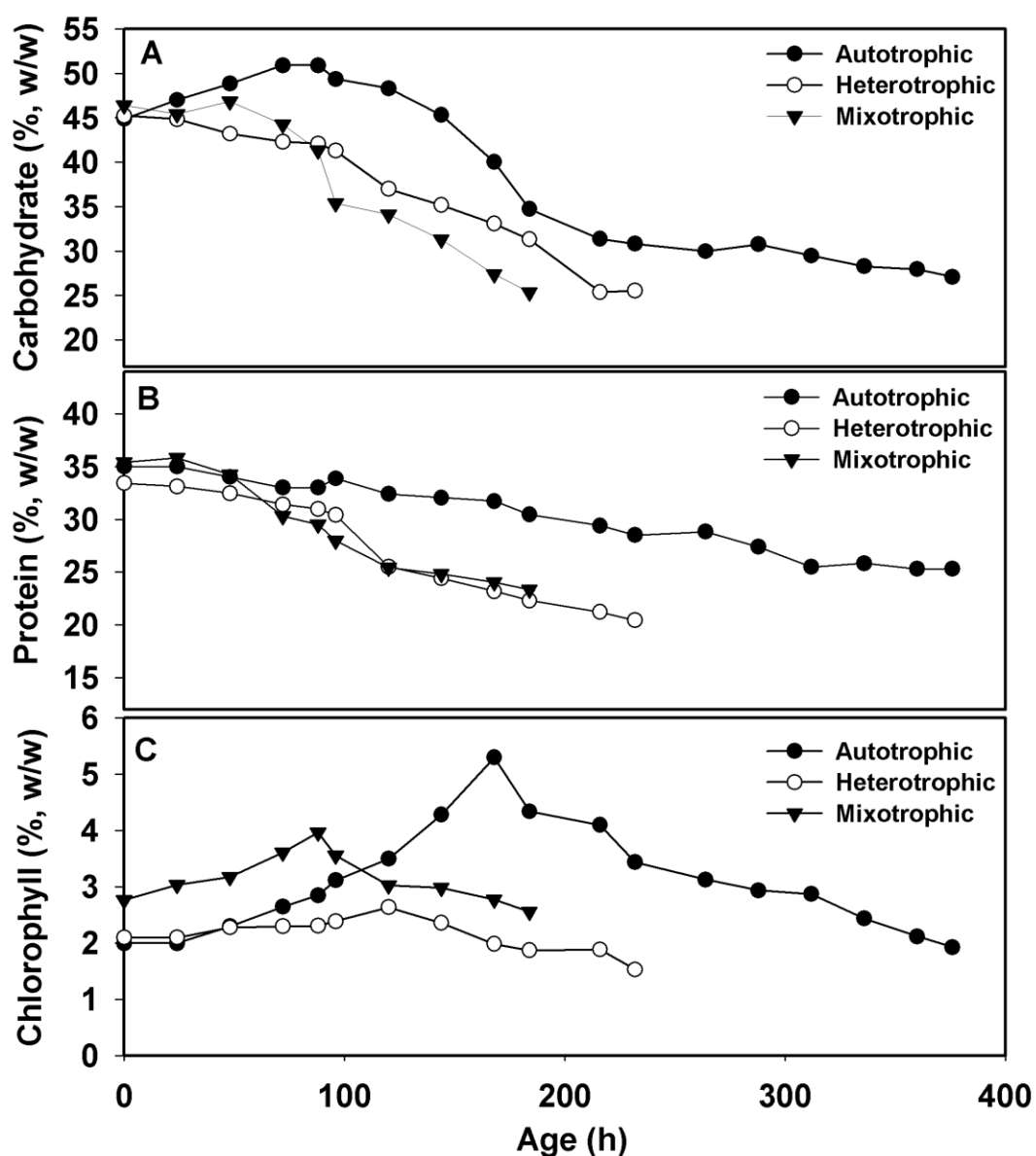


Fig. 6.7 Intracellular composition of macromolecules in the strain *Chlorella sorokiniana* FC6 IITG grown under different trophic modes: (A) Carbohydrate content; (B) protein content; and (C) total chlorophyll content. The strain was grown under photoautotrophic (●), heterotrophic (○) and mixotrophic (▼) conditions on modified BG11 medium at 28°C and 400 rpm in a 3 L automated bioreactor

The intracellular compositions of carbohydrate and neutral lipid of *Pseudochlorococcum* cells grown under high light and nitrate concentration varied from 12.2%, 3% on day 2 to 6.3% and 52.1% of dry cell weight on day 10 as reported by Li et al. (2011). Further, *Pseudochlorococcum* sp. was found to accumulate starch as the major energy storage

compound during nitrogen sufficient condition whereas under nitrogen depleted condition, the strain accumulated neutral lipids with significant reduction in the carbohydrate content (Li et al., 2011).

With changes in cultivation mode, a significant variation in the lipid productivity in the range of 47.42 mg L⁻¹ day⁻¹ to 111.85 mg L⁻¹ day⁻¹ was observed. Among all the cultivation mode mixotrophic culture showed maximum lipid productivity. Even though higher specific growth rate (Table 6.1) of the strain was observed under mixotrophic condition, the growth of organism was stopped nearly after 4 days due to exhaustion of the glucose (Fig. 6.6 C). This may provide the opportunity to develop a fed-batch fermentation under mixotrophic condition to enhance biomass titer in shorter batch operation time which may aid in lowering operational cost. These characterization experiments has showed mixotrophic conditions as the best nutritional mode for the growth and lipid productivity from *Chlorella sorokiniana* FC6 IITG.

6.3.2 Composition of FAME obtained from *Chlorella sorokiniana* FC6 IITG grown under different cultivation conditions

Fatty acid methyl ester composition of the biodiesel significantly influences the fuel properties such as cetane number, cold flow properties, viscosity and lubricity (Cha et al., 2011). To that end, the FAME composition of the *Chlorella sorokiniana* FC6 IITG was analyzed for photoautotrophic, heterotrophic and mixotrophic cultivation conditions using gas chromatography (Table 6.2). Significant variations in the fatty acid profile were observed with changes in the cultivation conditions. Fractions of palmitic acid (C16:0), palmitoleic acid (C16:1), stearic acid (C18:0), oleic acid (C18:1) and linoleic acid (C18:2) were found dominant, measuring about 90 % of total FAME content in all cultivation conditions. These fatty acids were also found to be abundant in other *Chlorella* sp. reported in the literature (Liu et al., 2011). Interestingly, linolenic acid (C18:3) and other higher

unsaturated fatty acids (greater than 4 double bonds) were absent in the strain under all cultivation conditions which should not exceed 12 mol% and 1 mol% respectively as per European standards (Gouveia and Oliveira, 2009). The ratio of unsaturated (monounsaturated plus polyunsaturated) to saturated fatty acid fractions were distinct for heterotrophic cultivation condition with a value of 1.63 while all other conditions showed about 2.5-3.0 implying high content of unsaturated fatty acids. The distribution of fatty acid composition corresponded with several other microalgae reported in the literature (Gouveia and Oliveira 2009).

Table 6.2 Fatty acid methyl esters (FAME) profile of strain FC6 grown under different cultivation conditions

Fatty Acids	FAME (% w/w)	Photoautotrophic	Heterotrophic	Mixotrophic
Lauric	[C12:0]	1.27	1.85	2.33
Miristic	[C14:0]	0.47	0.43	0.21
Palmitic	[C16:0]	23.09	29.76	19.93
Palmitoleic	[C16:1]	7.28	8.25	12.28
Stearic	[C18:0]	3.13	1.63	1.19
Oleic	[C18:1]	26.45	11.42	27.62
Linoleic	[C18:2]	36.86	35.23	34.48
Arachidic	[C20:0]	0.165	0	0
Behenic	[C22:0]	0.101	0	0
	SAT FAME ^a	28.23	33.67	23.68
	MUFA ^b	33.73	19.67	39.91
	PUFA ^c	36.86	35.23	34.48
	Others	1.159	11.43	1.914
	Total FAME ^d	29.91	39.21	33.44

a-represents the total saturated fatty acid fraction in the total fatty acid methyl esters

b-represents the total monounsaturated fatty acid fraction in the total fatty acid methyl esters

c-represents the total polyunsaturated fatty acid fraction in the total fatty acid methyl esters

d-represents the total FAME expressed in %, weight fraction of dry cell weight

In the present study, the strain *Chlorella sorokiniana* FC6 IITG was able to produce fatty acids with 82 to 86% contributions from saturated (C16:0) and unsaturated (C18:2, C18:2) fatty acids, which are considered to be the key elements for suitable quality biodiesel (Liu et al., 2011). Hence, *Chlorella sorokiniana* FC6 IITG can be a potential candidate for good quality biodiesel production.

6.3.3 Evaluation of biodiesel quality obtained from *Chlorella sorokiniana* FC6 IITG grown under different cultivation conditions

Quality assessment of the biodiesel obtained from FC6 grown under different cultivation conditions was carried out through empirical equations as a function of FAME composition obtained experimentally (Su et al. 2011; Francisco et al. 2010; Ramirez-Verduzco et al. 2012). The properties showed better agreement with the ASTM 6751 and EN 14214 standards (Table 6.3). Viscosity and cetane number of the FC6 derived biodiesel were $\sim 4.32 \text{ mm}^2 \text{ s}^{-1}$ and ~ 53.96 respectively which did not show any significant changes with variation in cultivation conditions or FAME compositions. In general, higher viscosity results in poor flow properties with less atomization quality, drop size and low penetration ability of the fuel, whereas cetane number influences combustion ability and engine knocking. The cloud point and pour point of the biodiesel varied significantly depending upon the cultivation conditions. Biodiesel obtained from heterotrophic condition showed very high cloud point and pour point which depicts that this biodiesel cannot be used in regions with temperatures less than 8°C . All other biodiesel derived from FC6 showed better cloud and pour points which ranged in between -3.51 to 1.68°C and -1.4 to -6.64°C respectively (Table 6.3). Therefore, biodiesel derived from FC6 grown under mixotrophic will be able to maintain its fluidity up to temperature -6.64°C which makes the fuel suitable for Indian perspectives where the ambient temperature does not go below -5°C even during winter season. Because of the large seasonal and geographic temperature variability, neither the U.S. nor European biodiesel standards have sharp specifications for these low temperature properties. However, very less cloud point and pour point maintain the fluidity of the fuel at very low ambient temperatures and therefore such fuels are preferred for efficient functioning.

Table 6.3 Quality analysis of the biodiesel obtained under different cultivation conditions from the microalga *Chlorella sorokiniana* FC6 IITG and comparison with European/ASTM standards

Biodiesel Properties	Units	Growth Conditions			Standards	
		Auto ^b	Hetero ^b	Mixo ^b	ASTM	EN
Viscosity ^a	(mm ² s ⁻¹)	4.36	4.32	4.32	1.9-6	3.5-5.0
Cetane Number ^a		54.76	54.80	53.96	47(min)	51(min)
Flash Point ^a	(°C)	157.90	150.22	155.17	93	101
Cloud Point ^a	(°C)	1.68	8.41	-3.51	nd	nd
Pour Point ^a	(°C)	-1.40	5.59	-6.64	nd	nd
SV ^a	mg KOH g ⁻¹	203.81	185.57	203.53	nd	nd
Iodine value ^a	gI ₂ (100 g oil) ⁻¹	97.82	82.32	99.55	nd	120
DU ^a		107.45	90.13	108.86	nd	nd
Heating value ^a	MJ kg ⁻¹	39.66	39.58	39.61	nd	nd

a – the empirical equations for calculating the biodiesel properties were depicted in equations 5.2-5.10 of chapter 5.

b- auto, hetero and mixo represents the photoautotrophic, heterotrophic and mixotrophic mode of growth DU-represents degree of unsaturation; SV-represents saponification value; nd –not defined;

The flash point of all biodiesel obtained from different cultivation conditions were found to be greater than the proposed limits in ASTM and EN standards. Saponification value (SV) is the measure of milligrams of potassium hydroxide (KOH) requires to completely saponify one gram of oil. The European and Indian biodiesel standards have not included the SV as a restricted property of biodiesel oil (Predojevic´ et al., 2012). In the present study the SV was found in the range of 185.57 – 203.81 mg KOH g⁻¹ (Table 6.3) which is comparable to the SV of *Chlorella luteoviridis* (207.91) calculated by Osundeko et al. (2013). Irrespective of different cultivation conditions biodiesel derived from FC6 was found to comply with the ASTM and EN standards. Thus, FC6 could be a potential cell factory for the synthesis of high quality biodiesel.

6.4 Conclusions

Evaluation of the novel indigenous microalgal strain *Chlorella sorokiniana* FC6 IITG under different trophic modes has proven the immense potentials of the strain in terms of biomass and lipid productivity. The difference in cultivation conditions resulted in significant variation in the biomass productivity (142.06 to 455.5 mg L⁻¹ day⁻¹) and total

lipid productivity (47.20 to 111.85 mg L⁻¹ day⁻¹) of the strain. Mixotrophic cultivation mode resulted maximum biomass and lipid productivity and fatty acid profiling revealed abundance of palmitic acid (C16:0), oleic acid (C18:1) and linoleic acid (C18:2) which are considered to be the key elements for suitable quality biodiesel. The analysis of biodiesel quality showed compliance with the ASTM and EN standards. Thus, *Chlorella sorokiniana* FC6 IITG could be a potential cell factory for the synthesis of high quality biodiesel under mixotrophic cultivation mode.



6.5 References

1. Cha, T.S., Chen, J.W., Goh, E.G, Aziz, A., Loh, S.H., 2011. Differential regulation of fatty acid biosynthesis in two *Chlorella* species in response to nitrate treatments and the potential of binary blending microalgal oils for biodiesel application. *Bioresour. Technol.* 102, 10633-10640.
2. Cheirsilp, B., Torpee, S., 2012. Enhanced growth and lipid production of microalgae under mixotrophic culture condition: effect of light intensity, glucose concentration and fed-batch cultivation. *Bioresour. Technol.* 110, 510-516.
3. Chen, C.Y., Yeh, K.L., Aisyah, R., Lee, D.J., Chang, J.S., 2011. Cultivation, photobioreactor design and harvesting of microalgae for biodiesel production: A critical review. *Bioresour. Technol.* 102, 71-81.
4. Chojnacka, K., Noworyta, A., 2004. Evaluation of *Spirulina* sp. growth in photoautotrophic, heterotrophic and mixotrophic cultures. *Enzym. Microb. Technol.* 34, 461-465.
5. Dubois, M., Gilles, K.A., Hamilton, J.K., Rebers, P.A., Smith, F., 1956. Colorimetric method for determination of sugars and related substances. *Anal. Chem.* 28, 350-356.
6. Fan, J., Huang, J., Li, Y., Han, F., Wang, J., Li, X., 2012 Sequential heterotrophy dilution photoinduction cultivation for efficient microalgal biomass and lipid production. *Bioresour. Technol.* 112, 206-211.
7. Feng, P., Deng, Z., Fan, L., Hu, Z., 2012. Lipid accumulation and growth characteristics of *Chlorella zofingiensis* under different nitrate and phosphate concentrations. *J. Biosci. Bioeng.* 114, 405-410.
8. Francisco, É.C., Neves, D.B., Jacob-Lopes, E., Franco, T.T., 2010. Microalgae as feedstock for biodiesel production: carbon dioxide sequestration, lipid production and biofuel quality. *J. Chem. Technol. Biotechnol.* 85, 395-403.

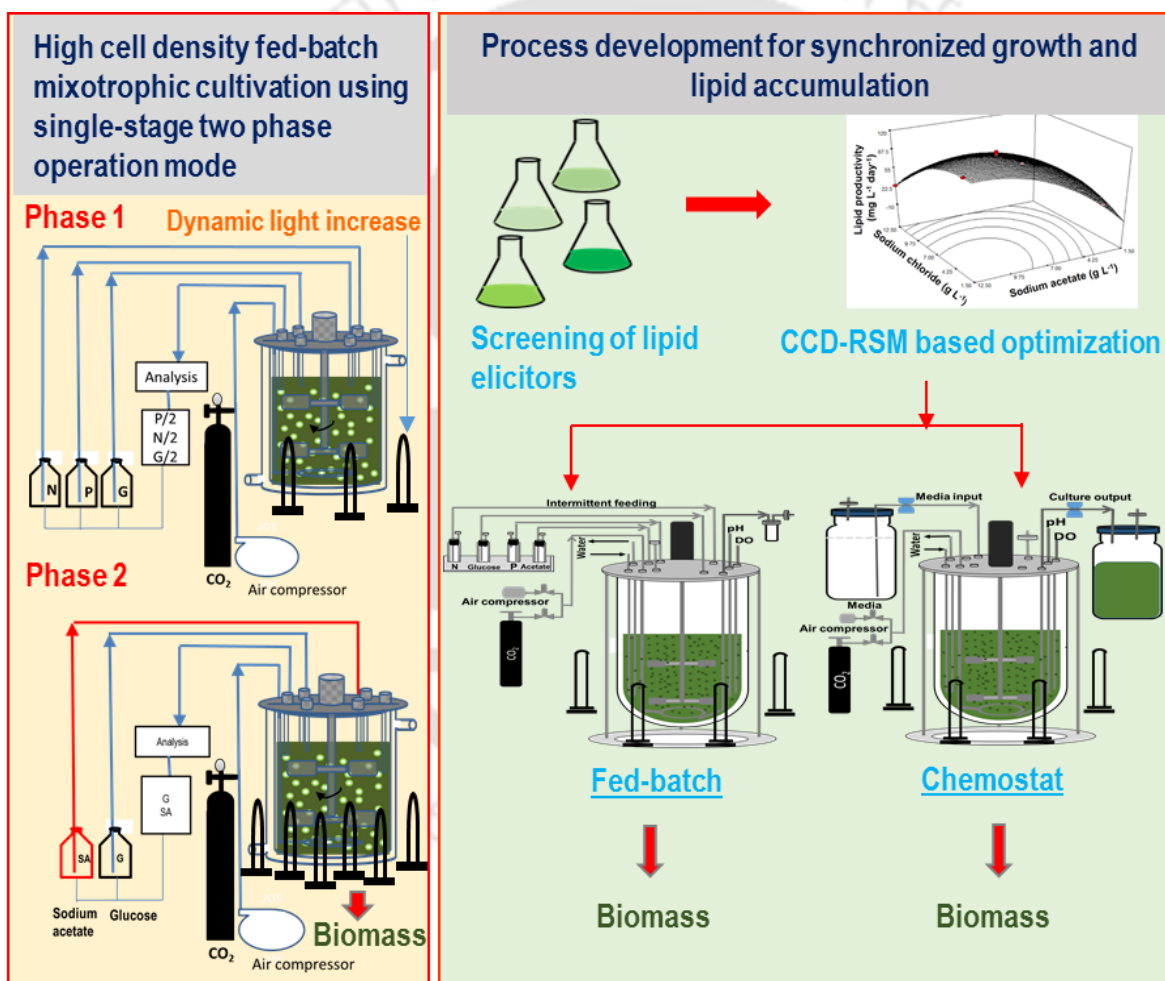
9. Gouveia, L., Oliveira, A.C., 2009. Microalgae as a raw material for biofuels production. *J. Ind. Microbiol. Biotechnol.* 36, 269-274.
10. Heredia-Arroyo, T., Wei, W., Ruan, R., Hu, B., 2011. Mixotrophic cultivation of *Chlorella vulgaris* and its potential application for the oil accumulation from non-sugar materials. *Biomass Bioenergy* 35, 2245-2253.
11. Illman, A.M., Scragg, A.H., Shales, S.W., 2000. Increase in *Chlorella* strains calorific values when grown in low nitrogen medium. *Enzym. Microb. Technol.* 27, 631-635.
12. Li, Y., Han, D., Sommerfeld, M., Hu, Q., 2011. Photosynthetic carbon partitioning and lipid production in the oleaginous microalga *Pseudochlorococcum* sp. (Chlorophyceae) under nitrogen limited conditions. *Bioresour. Technol.* 102, 123-129.
13. Liang, Y.N., Sarkany, N., Cui, Y., 2009. Biomass and lipid productivities of *Chlorella vulgaris* under autotrophic, heterotrophic and mixotrophic growth conditions. *Biotechnol. Lett.* 31, 1043-1049.
14. Lim, D.K.Y., Garg, S., Timmins, M., Zhang, E.S.B., Thomas-Hall, S.R., Schuhmann, H. L. Y., Schenk, P.M., 2012. Isolation and Evaluation of Oil-Producing Microalgae from Subtropical Coastal and Brackish Waters. *PLoS ONE* 7(7). doi:10.1371/journal.pone.0040751.
15. Liu, J., Huang, J., Sun, Z., Zhong, Y., Jiang, Y., Chen, F., 2011. Differential lipid and fatty acid profiles of photoautotrophic and heterotrophic *Chlorella zofingiensis*: Assessment of algal oils for biodiesel production. *Bioresour. Technol.* 102, 106-110.
16. Lowry, O.H., Rosebrough, N.J., Farr, A.L., Randall, R.J., 1951, Protein measurement with the Folin phenol reagent. *J. Biol. Chem.* 193, 265-275.
17. Mata, T.M., Martins, A.A., Caetano, N.S., 2010. Microalgae for biodiesel production and other applications: a review. *Renew. Sustainable Energy Rev.* 14, 217-232.

18. Miller, G.L., 1959. Use of dinitrosalicylic acid reagent for determination of reducing sugar. *Anal. Chem.* 31, 426-428.
19. Muthuraj, M., Kumar, V., Palabhanvi, B., Das, D., 2014. Evaluation of indigenous microalgal isolate *Chlorella* sp. FC2 IITG as a cell factory for biodiesel production and scale up in outdoor conditions. *J. Ind. Microbiol. Biotechnol.* 41, 499-511.
20. Muthuraj, M., Palabhanvi, B., Misra, S., Kumar, V., Sivalingavasu, K., Das, D., 2013. Flux balance analysis of *Chlorella* sp. FC2 IITG under photoautotrophic and heterotrophic growth conditions. *Photosynth. Res.* 118, 167-179.
21. Osundeko, O., Davis, H., Pittman, J.K., 2013. Oxidative stress-tolerant microalgae strains are highly efficient for biofuel feedstock production on wastewater. *Biomass Bioenergy* 56, 284-294.
22. Parsons, T. R., Maita Y., Lalli, C. M., 1984. A manual of chemical and biological methods for seawater analysis. first ed. Pergamon Press Ltd., Great Britain.
23. Predojevic', Z., Škrbic ', B., Durišić '-Mladenovic', N., 2012. Transesterification of linoleic and oleic sunflower oils to biodiesel using CaO as a solid base catalyst. *J. Serb. Chem. Soc.* 77, 815-832.
24. Pruvost, J., Vooren, G.V., Gouic, B.L., Couzinet-Mossion, A., Legrand, J., 2011. Systematic investigation of biomass and lipid productivity by microalgae in photobioreactors for biodiesel application. *Bioresour. Technol.* 102, 150-158.
25. Ramirez-Verduzco, L.F, Rodriguez-Rodriguez, J.E, Jaramillo-Jacob, A.R, 2012. Predicting cetane number, kinematic viscosity, density and higher heating value of biodiesel from its fatty acid methyl ester composition. *Fuel* 91, 102-111.
26. Ritchie, R.J., 2006. Consistent sets of spectrophotometric chlorophyll equations for acetone, methanol and ethanol solvents. *Photosynth. Res.* 89, 27-41.

27. Rodolfi, L., Zittelli, G.C., Bassi, N., Padovani, G., Biondi, N., Bonini, G., Tredici, M.R., 2009. Microalgae for oil: strain selection, induction of lipid synthesis and outdoor mass cultivation in a low-cost photobioreactor. *Biotechnol. Bioeng.* 102, 100-112.
28. Sforza, E., Cipriani, R., Morosinotto, T., Bertucco, A., Giacometti, G.M., 2012. Excess of CO₂ supply inhibits mixotrophic growth of *Chlorella protothecoides* and *Nannochloropsis salina*. *Bioresour. Technol.* 104, 523-529.
29. Su, Y.C., Liu, Y.A., Diaz Tovar, C.A., Gani, R., 2011. Selection of Prediction Methods for Thermophysical Properties for Process Modeling and Product Design of Biodiesel Manufacturing. *Ind. Eng. Chem. Res.* 50, 6809-6836.
30. Thimijan, R.W., Heins, R.D., 1983. Photometric, Radiometric, and Quantum Light Units of Measure: A Review of Procedures for Interconversion. *HortScience* 18, 818-822.
31. Wan, M., Liu, P., Xia, J., Rosenberg, J.N., Oyler, G.A., Betenbaugh, M.J., Nie, Z., Qiu, G., 2011. The effect of mixotrophy on microalgal growth, lipid content, and expression levels of three pathway genes in *Chlorella sorokiniana*. *Appl. Microbiol. Biotechnol.* 91, 835-844.
32. Xu, H., Miao, X., Wu, Q., 2006. High quality biodiesel production from a microalga *Chlorella protothecoides* by heterotrophic growth in fermenters. *J. Biotechnol.* 126, 499-507.

CHAPTER 7

Process development for high cell density lipid rich microalgae cultivation and enhanced lipid productivity via synchronized growth and lipid accumulation under fed-batch & chemostat mode



Lipid rich microalgal biomass with enhanced biomass and lipid productivity

High cell density lipid rich microalgae cultivation was achieved by intermittent feeding of rate limiting nutrient followed by addition of sodium acetate and enhanced lipid productivity via synchronized growth and lipid accumulation under fed-batch & chemostat mode.

7.1 Background and motivation

Characterization of FC6 under different growth conditions in batch mode using optimized BG11 media, showed maximum biomass and lipid productivity under mixotrophic cultivation condition. Mixotrophic batch mode resulted 455.5 mg L⁻¹ day⁻¹ and 111.85 mg L⁻¹ day⁻¹ biomass and lipid productivity respectively (section 6.4, chapter 6). Further enhancement of the biomass productivity can be achieved by fed-batch or continuous mode of operations. In general, microbial fermentation in fed-batch mode has been an effective technique for improved biomass and product titer and productivity (Xie et al., 2013). The fed-batch mode involves intermittent feeding of the limiting substrates thereby minimizing the substrate restriction to the organism and in turn, enable them to remain in exponential-phase of growth during the fermentation period. Fed-batch operation with intermittent feeding of the stoichiometrically limiting and rate limiting nutrients along with dynamic increase in light intensity was reported to result enhanced biomass titer (Muthuraj et al., 2015). However, to achieve sustainability in algae based biodiesel production the net lipid productivity remains an important parameter to be maximized which in turn is a function of biomass titer and the lipid content of the biomass. Lipid content and biomass productivity are two mutually exclusive properties and simultaneous enhancement of both these parameters remains a challenge in algae based biodiesel production (Hu et al., 2008). Further, in order to solve this problem of trade-off between growth and lipid accumulation, these two processes needs to be decoupled. Different strategies were proposed to enhance the lipid content without affecting the biomass productivity (Hu et al., 2008; Rodolfi et al., 2009). Two-stage cultivation strategies have been reported to achieve high cell density lipid rich algal biomass (Karemore et al., 2013). In the first stage of cultivation, cells were grown under optimal conditions for maximum biomass formation followed by their harvesting. The harvested cells were re-suspended in the nutrient starved

medium for maximization of lipid accumulation during the second stage of the process. However, this two-stage process involves higher capital cost, additional harvesting and medium requirement (Xia et al., 2014). Therefore, a single-stage cultivation will be appropriate where biomass growth and lipid enrichment can take place in a single bioreactor. Some of the researcher suggested simultaneous growth and neutral lipid accumulation as an effective strategy to obtain maximum lipid productivity (Tevetia et al., 2014; Klok et al., 2013). Limited literature are available on the aspect of simultaneous growth and lipid production. The strategies employed are regulation of concentration of limiting nutrients in the broth or manipulating the substrate feed rates in continuous cultivation of microalgae. Klok et al. (2013) reported simultaneous growth and lipid accumulation in *Neochloris oleoabundans* by combining growth limiting nitrogen supply rates and excess photointensities under continuous mode of operation. The study highlighted the importance of light energy utilization under nutrient stress to control lipid productivities. Adams et al. (2013) designed a fed-batch experiment with precise control of nitrate supply rates on six different microalgal strains to obtain tailored growth and lipid accumulation. Regulation of the specific nitrate feed rate in the range of 0.78 to 4.66 mmol g⁻¹ day⁻¹ has maximized the lipid productivity up to 0.15 g L⁻¹ day⁻¹ from 0.09 g L⁻¹ day⁻¹ in continuous cultivation of *Chlorella pyrenoidosa* XQ-20044 (Wen et al., 2014). However, all these strategies employed nutrient limitation to obtain simultaneous growth and neutral lipid accumulation in microalgae compromising with their optimal growth potential. To that end, it is essential to develop a process which will enable concomitant biomass generation and lipid enrichment without compromising the growth rate of microalgae. Also, the neutral lipid productivities attained with the current state of art have been negligible, thus making the sustainable commercial scale biodiesel production technology far from reality which mandates further research in these aspects (Klok et al., 2013; Tevatia et al., 2014).

Georgianna and Mayfield (2012) suggested strain development and process engineering are necessary to make algal biofuels practical and economically viable.

Therefore, the present study concentrates on the process development using *Chlorella sorokiniana* FC6 IITG as a model organism for enhanced lipid productivity via two different strategy: (i) fed-batch cultivation for generation of lipid rich biomass with intermittent feeding of limiting nutrients followed by supplementation of lipid inducer in stationary phase; and (ii) process engineering for synchronized growth and lipid accumulation in fed-batch & chemostat operation mode. Fatty acid methyl ester composition and biodiesel properties were also evaluated for the biomass obtained through this strategy.

7.2 Materials and Methods

Two different strategy were employed for enhanced lipid productivity: (i) High cell density lipid rich microalgae cultivation in a single stage fed-batch mixotrophic mode with intermittent feeding of limiting nutrients followed by supplementation of lipid inducer in stationary phase; and (ii) process engineering for synchronized growth and lipid accumulation in fed-batch & chemostat operation mode.

7.2.1 Generation of high cell density lipid rich biomass using single-stage two phase fed-batch mode

A single-stage fed-batch strategy was employed for high cell density lipid-rich cultivation of FC6 under mixotrophic condition. The batch comprised of two phases: while the first phase was targeted to enhance the biomass productivity, the second phase was aimed at enhancing the lipid content of the cells. The experiment was conducted in a 3.0 L automated bioreactor (eZ Control, Applikon Biotechnology, Holland) with working volume of 1.5 L and the conditions were kept same as that of the mixotrophic batch experiment mentioned in previous section (6.2.2 of chapter 6). In order to achieve high cell density in

the first phase of cultivation, the concentrations of key nutrients glucose, nitrate and phosphate were maintained above half of their initial concentration in the optimized BG11 medium via intermittent feeding. The light intensity was dynamically increased at a rate of $25 \mu\text{E m}^{-2} \text{s}^{-1}$ per day from $150 - 350 \mu\text{E m}^{-2} \text{s}^{-1}$ for initial 8 days of cultivation period and then maintained constant at $350 \mu\text{E m}^{-2} \text{s}^{-1}$ throughout the batch. Further increase in the light intensity above $350 \mu\text{E m}^{-2} \text{s}^{-1}$ was found to be detrimental for the photosynthetic apparatus leading to reduction in growth of FC6. From the previous experiment sodium acetate was found as lipid inducer (section 5.3.3, chapter 5). After the reach of stationary phase of cell growth, optimum concentration of sodium acetate of 15 g L^{-1} was added to the media as elicitor for lipid enhancement. The intermittent feeding of other nutrients glucose, nitrate and phosphate were stopped during this second phase of fed-batch for lipid enhancement.

7.2.2 Screening and optimization of elicitor molecules for lipid induction

Though from our previous experiment sodium acetate was found as lipid inducer, further screening of lipid inducer was performed to identify effective combination of lipid inducers which supports maximum lipid induction without hampering growth. To that end the organism was grown on modified BG11 medium supplemented with individual elicitor molecule and 15 g L^{-1} glucose as the primary carbon source for growth under mixotrophic condition. Nine different elicitor molecules sodium acetate, sodium chloride, glycerol, bovine serum albumin, magnesium chloride, hydrogen peroxide, trisodium citrate, ferric chloride and calcium chloride at four different concentrations of each (Table 7.1) were used for the characterization of the strain. It is important to note that in order to eliminate any possible effect of nutritional starvation on lipid induction the experiments were carried out under nutrient sufficient condition through intermittent feeding of nitrate, phosphate and glucose (Palabhanvi et al., 2014).

Table 7.1 Screening of elicitor molecules for lipid induction and also supports synchronized growth and lipid accumulation in *Chlorella sorokiniana* FC6 IITG

Inducers	Concentrations (g L ⁻¹)			
Sodium acetate	5	10	15	20
Glycerol	5	10	15	20
Sodium chloride	5	10	15	20
Ferric chloride	0.05	0.10	0.15	0.20
Trisodium citrate	0.05	0.10	0.15	0.20
Magnesium chloride	0.05	0.10	0.15	0.20
Hydrogen peroxide	0.05	0.10	0.15	0.20
Bovine serum albumin	0.05	0.10	0.15	0.20
Calcium chloride	0.05	0.10	0.15	0.20

Feeding of these nutrients was done to maintain broth concentration above 50% of their initial value. All the screening experiments were conducted at shake flask under mixotrophic condition at 28°C, 150 rpm, and continuous light intensity of 30 $\mu\text{E m}^{-2} \text{s}^{-1}$. Sampling was performed at regular time intervals for monitoring the growth and lipid accumulation in the strain.

Once, the effective elicitor molecules were screened, their combined effect on lipid productivity was assessed by growing the organism in presence of these elicitors at different concentration. Further, concentrations of these elicitor molecules were optimized via central composite design (CCD) of experiment and response surface methodology (RSM) with maximization of net lipid productivity as the objective function. A total of thirteen experiments were designed through CCD with five replications at the center values to evaluate the pure error. The response was measured in terms of maximum net lipid productivity (Y) on 16th day batch. The behaviour of the system was determined by assuming a second order polynomial with linear, quadratic and interaction effects as shown by Eq. (7.1).

$$Y = \beta_0 + \sum_{i=1}^k \beta_i X_i + \sum_{i<j}^k \beta_{ij} X_i X_j + \sum_{j=1}^k \beta_{jj} X_j^2 \quad (7.1)$$

Where Y is the response; X_1 and X_2 , and are input variables; β_0 is constant; β_i is the linear coefficient; β_{ij} is the interaction coefficient, and β_{jj} is the quadratic coefficient. Estimation

of regression coefficients and statistical tests were carried out in the MINITAB (Version 16, Minitab Inc., State College, PA, USA) statistical software based on RSM. Analysis of variance (ANOVA) was conducted on the variables to understand the effect of individual factors on lipid productivity. The optimized elicitor concentrations were further validated in shake flask. The conditions in the shake flask were kept similar to all the conditions as discussed in above section 7.2.2. The best combination of lipid inducers with their optimal concentration was used for lipid enrichment in process development for synchronized growth and lipid accumulation.

7.2.3 *Process development for synchronized growth and neutral lipid accumulation in automated photobioreactor under fed-batch & chemostat operation mode*

The inoculum was prepared by transferring two loops full of slant culture into 250 mL Erlenmeyer flask containing 100 mL modified BG11 medium supplemented with 15 g L⁻¹ glucose and incubated in an orbital shaker under mixotrophic condition at 28°C, 150 rpm, and continuous light intensity of 30 μE m⁻² s⁻¹. This concentration of glucose was found to be optimal for growth when FC6 was characterized under different concentration of glucose (5, 10, 15 and 20 g L⁻¹) under mixotrophic condition. Actively growing mid log phase seed culture of 1% (v/v) was used as inoculum in all the experiments. Two different experiments were conducted with the dual aim of: (i) simultaneous growth and lipid enrichment and (ii) maximization of neutral lipid productivity. These objectives will be achieved via supplementation of specific lipid inducers in the growth media for lipid enrichment and maintaining higher specific growth rate of the organism throughout the entire cultivation period to enhance the biomass and lipid productivity. To that end, in the first experiment the organism was grown under fed-batch mode of cultivation with intermittent feeding of nitrate, phosphate, glucose and sodium acetate. The broth concentrations of all the nutrients and inducers were maintained above 50% of their initial

concentration in the medium. In the second experiment the organism was grown in a chemostat with continuous feeding of modified BG11 media supplemented with glucose and lipid elicitor molecules (sodium chloride and sodium acetate). Initially the strain FC6 was grown under fed-batch mode of operation with intermittent feeding of limiting nutrients for a period of 5-6 days till 2.23 g L^{-1} of biomass (equivalent to absorbance at 690 nm, A_{690} -10) was reached. Once the desired cell density was reached, the mode of operation was switched to chemostat. In continuous mode, the modified BG11 medium containing all the nutrients along with the optimal concentration of elicitors were fed at different dilution rates ranging from 0.9 day^{-1} to 0.18 day^{-1} resulting in sequential steady state of the culture. Two variable speed peristaltic pump with the maximum and minimum flow rate of 2.8 mL min^{-1} and 0.28 mL min^{-1} respectively was used for continuous feeding and removal of medium from the reactor. Sampling was performed at regular time intervals for monitoring the growth, lipid production and substrate utilization. These experiments were carried out in a 7.5 L automated bioreactor (Bioflo 115, New Brunswick Pvt. Ltd., USA) with working volume of 4 L at agitation speed of 250 rpm and continuous illumination of $350 \mu\text{E m}^{-2} \text{ s}^{-1}$ provided by 23 W CFL lights (Havells Pvt. Ltd., India) arranged surrounding the reactor surface. The pH of the medium was maintained at 8 ± 0.2 via purging air mixed with 1-2% (v/v) of CO_2 at the flow rate of 4 L min^{-1} . In both the experiments, modified BG11 medium containing 15.0 g L^{-1} glucose along with optimal concentration of both the lipid inducers were used as the starting media.

7.2.4 Analysis of growth, substrate utilization and FAME composition

Algal growth was estimated by measuring the absorbance of cells at 690 nm with a UV-visible spectrophotometer (Cary 50, Varian, Australia) and the dry cell weight (DCW) were obtained using correlation equation detailed in section 6.2.3.1, Chapter 6. For mixotrophic grown cell: one cell density corresponded to $0.2234 \text{ g dry cells L}^{-1}$ with R^2 of

0.99. (Fig. 6.1 C, in chapter 6). The utilization of inorganic phosphate in the culture media was measured colorimetrically by ascorbic acid method (Parsons et al., 1984) as detailed in Section 6.2.3.4 of chapter 6. The sodium nitrate and sodium acetate concentrations were measured using HPLC (Agilent 1220 Infinity HPLC, USA) equipped with a photo-diode detector at 220 nm (detailed protocol in section 6.2.3.2 & 6.2.3.3 of chapter 6). Glucose concentration in media was measured in HPLC with refractive index detector at temperature 28°C using a Rezex ROA-Organic acid H+ (8%) Column (300 mm × 7.8 mm, Phenomenex, USA) linked to a guard column (50 mm × 7.8 mm, Phenomenex, USA) with 0.005 N H₂SO₄ as eluent at a flow rate of 0.5 mL min⁻¹.

Neutral lipid content of the biomass was estimated by Nile-red based neutral lipid assay method as detailed in section 3.2.4.2 of chapter 3. The dynamic profile of neutral lipid accumulation in the biomass was obtained by Nile-red based assay method and the total lipid content along with fatty acid composition in terms of fatty acid methyl esters were obtained from gas chromatography (GC) based analysis. The two-step direct transesterification method as discussed in chapter 4 was used to quantify the total lipid in terms of FAME. The FAME was analyzed in GC equipped with FID detector using SLB-IL 100 column (30 m × 0.25 mm i.d., 0.20 µm film thickness) (detailed protocol in section 5.2.4.1 of chapter 5). FAME mix C14-C22 (Supelco, USA) was used as the standard for GC-FID and the lipid quantified using this method represents the total lipid of the biomass in % (w/w, DCW).

The properties of the biodiesel was determined as described earlier (details in Section 5.2.5 of chapter 5). All the experiments were conducted in triplicate and the data were expressed as mean ± standard error. Statistical analysis of the lipid content obtained from different lipid inducers and at different concentration was performed using Tukey's method (Minitab® 16.1.1, Lead Technologies Inc.).

Biomass productivity (B_p , g L⁻¹ day⁻¹) and neutral lipid productivity (L_p , g L⁻¹ day⁻¹) under batch and fed-batch mode of operations were obtained based on the following equations:

$$B_p = \frac{(X_f - X_0)}{(t_f - t_0)} \quad (7.2)$$

$$L_p = B_p \times X_{FA} \quad (7.3)$$

Where, X_0 and X_f were the dry cell weight (g L⁻¹) obtained at initial (t_0) and final (t_f) time points (in days) respectively under batch and fed-batch mode. X_{FA} represents the mass fraction of fatty acid in the biomass. For continuous cultivation mode the biomass productivity (B_{pC}) was obtained using equation 7.4 whereas the neutral lipid productivity was obtained using equation 7.3.

$$B_{pC} = X_m \times D \quad (7.4)$$

where X_m is the concentration of biomass and D is the dilution rate. The term lipid productivity represents the neutral lipid productivity unless otherwise mentioned in the present study.

7.3 Results and discussion

7.3.1 Generation of high cell density lipid rich biomass using single-stage two phase fed-batch mode

The effective application of algal biomass as a potential bio-energy feedstock is largely governed by the substantial improvement in biomass and lipid productivity. However, biomass and lipid productivity are two mutually exclusive parameters attributed to stress induced lipid accumulation at the cost of growth i.e., either high lipid productivity with low biomass titer or vice versa. Therefore, these two processes needs to be decoupled to achieve a process with high cell density and enhanced lipid content. In general, such high cell density lipid-rich cultivation of microalgae were performed in two-stage process with

biomass enhancement in the first step under nutrient sufficient conditions followed by harvesting and subsequent re-suspension of the cells in the nutrient depleted medium of the second stage for lipid enrichment (Zhang et al., 2014). The additional costs involved in the biomass collection, centrifugation and re-suspension in nutrient starved media makes the process infeasible for large scale applications. Therefore in the present study, we demonstrated a strategy for high cell density biomass generation and lipid enrichment under mixotrophic condition via single-stage fed-batch operation with growth supporting and lipid inducing carbon sources glucose and sodium acetate respectively.

With glucose as the growth supporting carbon source the first phase of the mixotrophic fed-batch resulted in a maximum biomass titer of 15.46 g L⁻¹ and biomass productivity of 1.93 g L⁻¹ day⁻¹ (Fig. 7.1 A). In comparison to the mixotrophic batch experiment, the fed-batch with dynamic increase in light intensity has resulted in 323.7 % increased biomass productivity. Thus, the stepwise increase in light intensity (Fig. 7.1 B) and the intermittent feeding of the limiting nutrients nitrate, phosphate and glucose (Fig. 7.2) has contributed to such high biomass productivity. A 1.2 fold increase in biomass titer was reported for *Chlorella* sp. when the rate limiting nutrient glucose was replenished in the growth medium (Cheirsilp and Torpee, 2012). Once the cell reached the stationary phase, the lipid enrichment was initiated with addition of sodium acetate at a concentration of 15 g L⁻¹. After sodium acetate supplementation no significant changes in the growth of FC6 was observed. However, there was a sharp increase in the total lipid accumulation as depicted in the Fig. 7.1 A. Maximum lipid content of 55 % (w/w, DCW) and lipid productivity of 550 mg L⁻¹ day⁻¹ was obtained from this fed-batch operational strategy which was 4.9 fold higher than the lipid productivity obtained from mixotrophic batch experiment. Utilization profile of sodium acetate depicted in Fig. 7.2 C shows that a significant amount of sodium acetate (~10 g L⁻¹) remains unutilized by the organism.

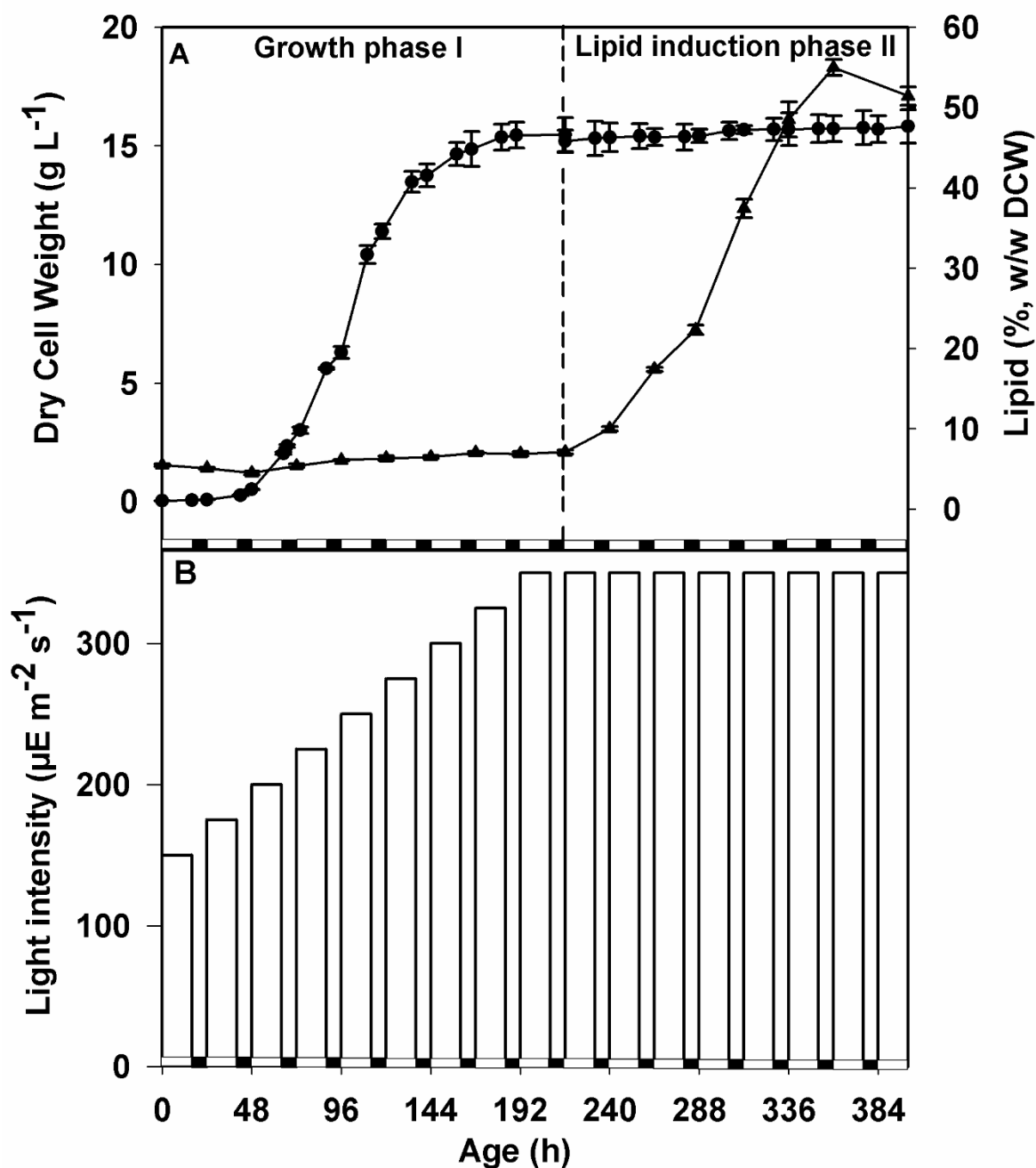


Fig 7.1 Dynamic profiles of growth, lipid and step-wise increase in light intensity under single stage fed-batch mixotrophic cultivation: (a) biomass (●) and lipid content (▲) and (b) step-wise increase in light intensity. The strain was grown in a 3 L automated bioreactor at 28°C, 400 rpm with 150 to 350 $\mu\text{E m}^{-2} \text{s}^{-1}$ light intensity for 16:8 h light: dark cycle and aerated with CO₂ of 1% (v/v). The white and black bars on X-axis shows the 16 h light and 8 h dark cycle. The process involves two phases: first phase represents the production of high cell density biomass with intermittent feeding of nitrate, phosphate and glucose along with dynamic change in light intensity and second phase represents lipid induction phase with sodium acetate as elicitor for lipid enrichment

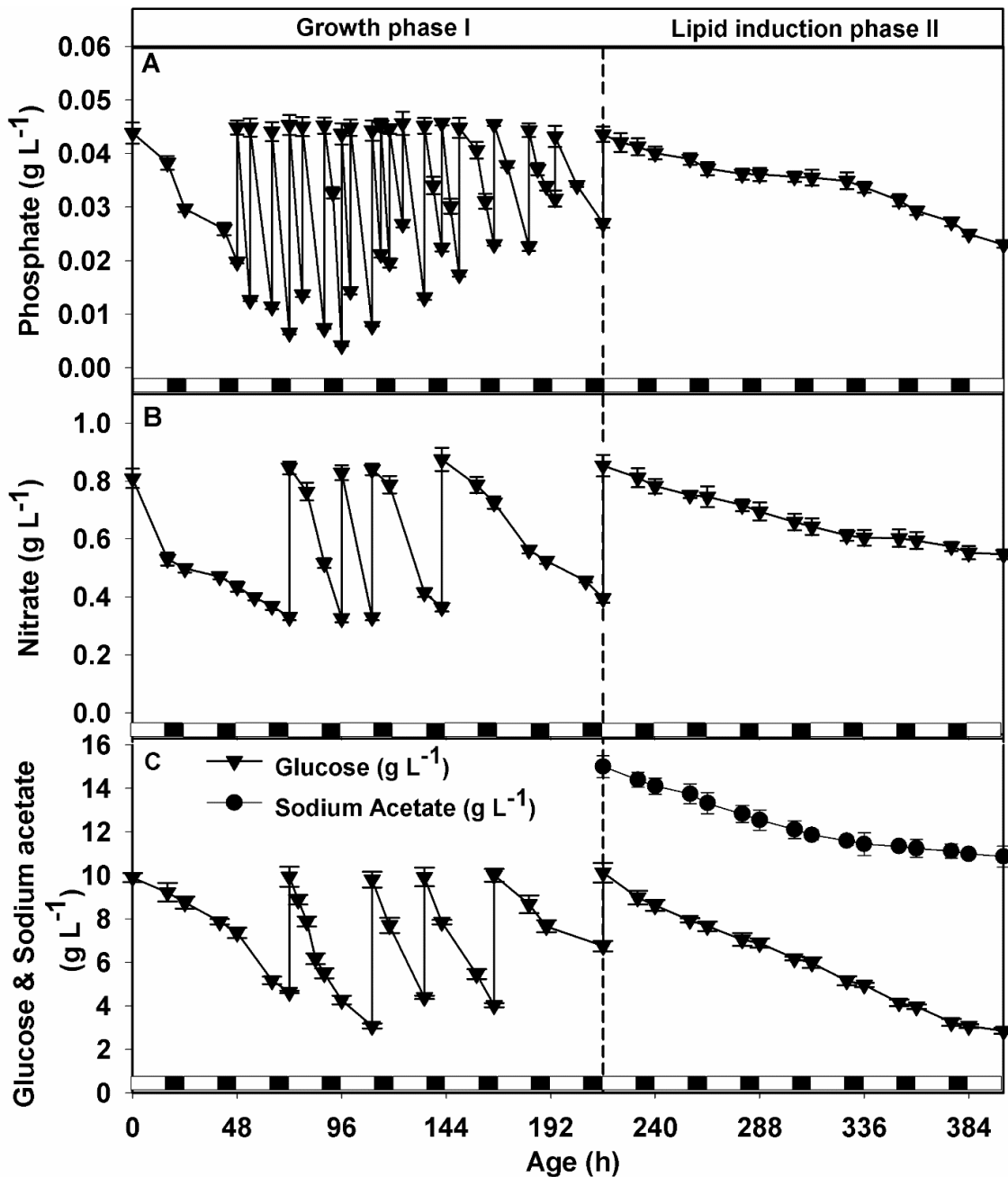


Fig. 7.2 Dynamic profiles of substrate utilization and intermittent feeding of substrates for single stage fed-batch mixotrophic cultivation of FC6 (a) phosphate profile (b) nitrate profile (c) glucose profile (\blacktriangledown) and sodium acetate profile (\bullet). For experimental details, refer to the legend of figure 7.2

It is important to mention here that the additional production cost if any, which might be incurred due to this high amount of unutilized sodium acetate can be neutralized via single stage cultivation as oppose to conventional two stage process which bypasses the need of harvesting and other nutritional requirements (Rai et al., 2013). Hence the process is

expected to be cost efficient. Also, sodium acetate present in the anaerobic digestate in significant amount may be used as a cheaper elicitor for lipid induction in order to meet the economic viability to the process (Nie et al., 2009).

It is interesting to note that this organism exhibits substantially higher biomass and lipid productivity obtained from mixotrophic fed-batch cultivation as compared to majority of the strains reported in the literature (Table 1, Appendix). Therefore, Fed-batch mixotrophic cultivation for generation of lipid rich microalgal biomass using single-stage two phase operation mode could be one strategy for feedstock generation for biodiesel production.

7.3.2 Screening of elicitor molecules for improved lipid productivity of *Chlorella sorokiniana* FC6 IITG

Screening of suitable elicitors for lipid induction was carried out by growing the organism on optimized BG11 medium supplemented with nine individual elicitor molecules with four different concentrations of each (Fig. 7.3 & 7.4). These nine different elicitor molecules were selected for the screening experiments based on their role in neutral lipid induction as reported in different literature. Elevated or reduced concentrations of metal ions such as Fe^{3+} , Mg^{2+} and Ca^{2+} and EDTA were reported to enhance lipid accumulation in *Scenedesmus* sp. under heterotrophic condition (Ren et al., 2014). Similarly, sodium acetate and hydrogen peroxide were reported to induce neutral lipid accumulation in *Chlorella sorokiniana* and *Chlorella vulgaris* strains respectively (Menon et al., 2013) and therefore included in the screening experiment. It was also reported that supplementation of tryptophan in medium induced neutral lipid accumulation in *Chlorella sorokiniana* under mixotrophic condition and therefore, bovine serum albumin a source for multiple amino acids was used in the screening for lipid elicitors (Ngangkham et al., 2012).

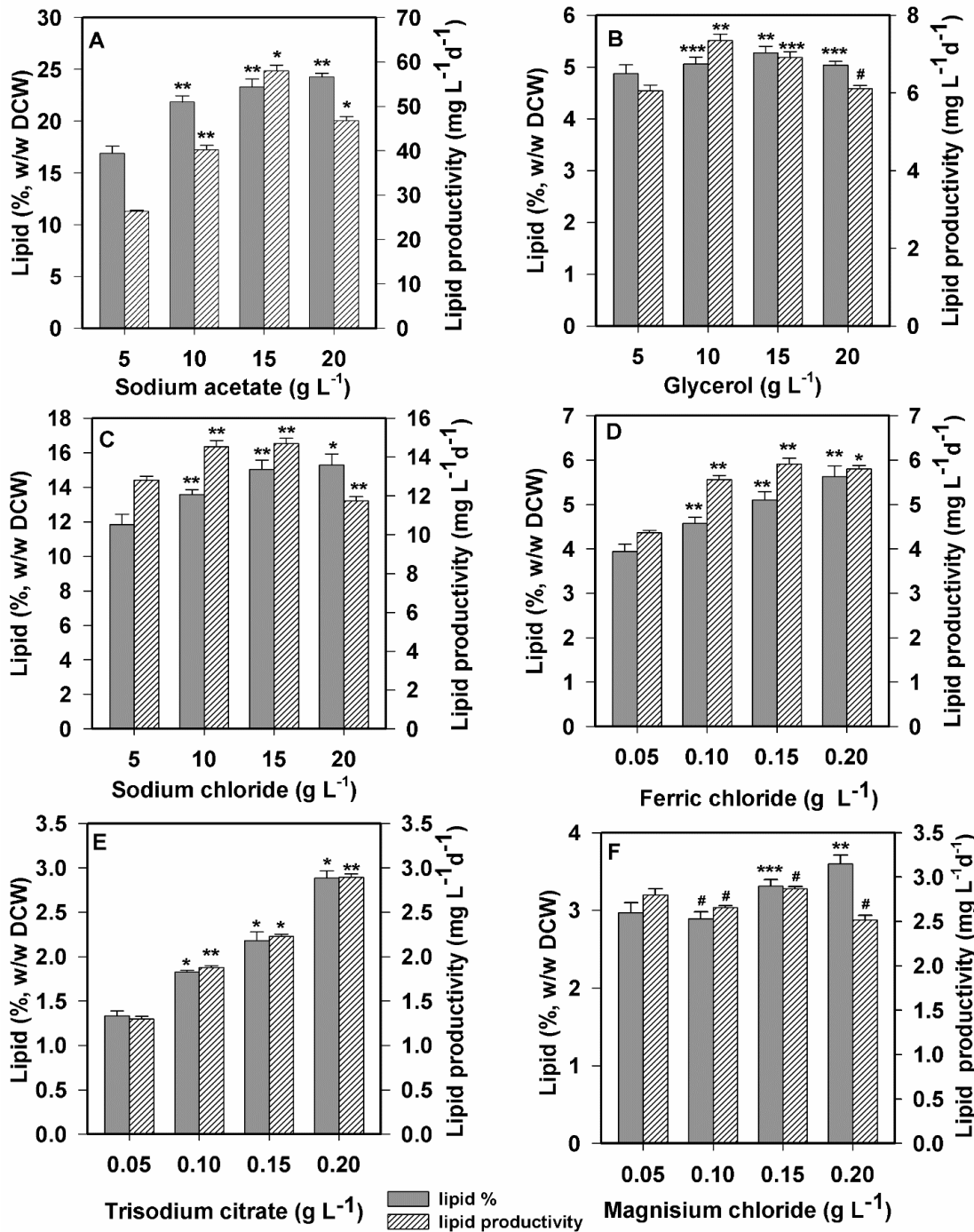


Fig 7.3 Effect of inducer molecules with their various levels of concentration on lipid content and lipid productivity of the FC6 grown under mixotrophic cultivation in shake flask. Different symbols indicate significant difference in biomass titer and lipid productivity obtained from the use of various lipid inducers analyzed using one way analysis of variance (*-represents $P = 0$; **-represents $0 < P < 0.05$; ***-represents $0.05 < P < 0.5$ and #-represents > 0.5). For statistical analysis the lowest concentration of the respective lipid inducer was kept as control group

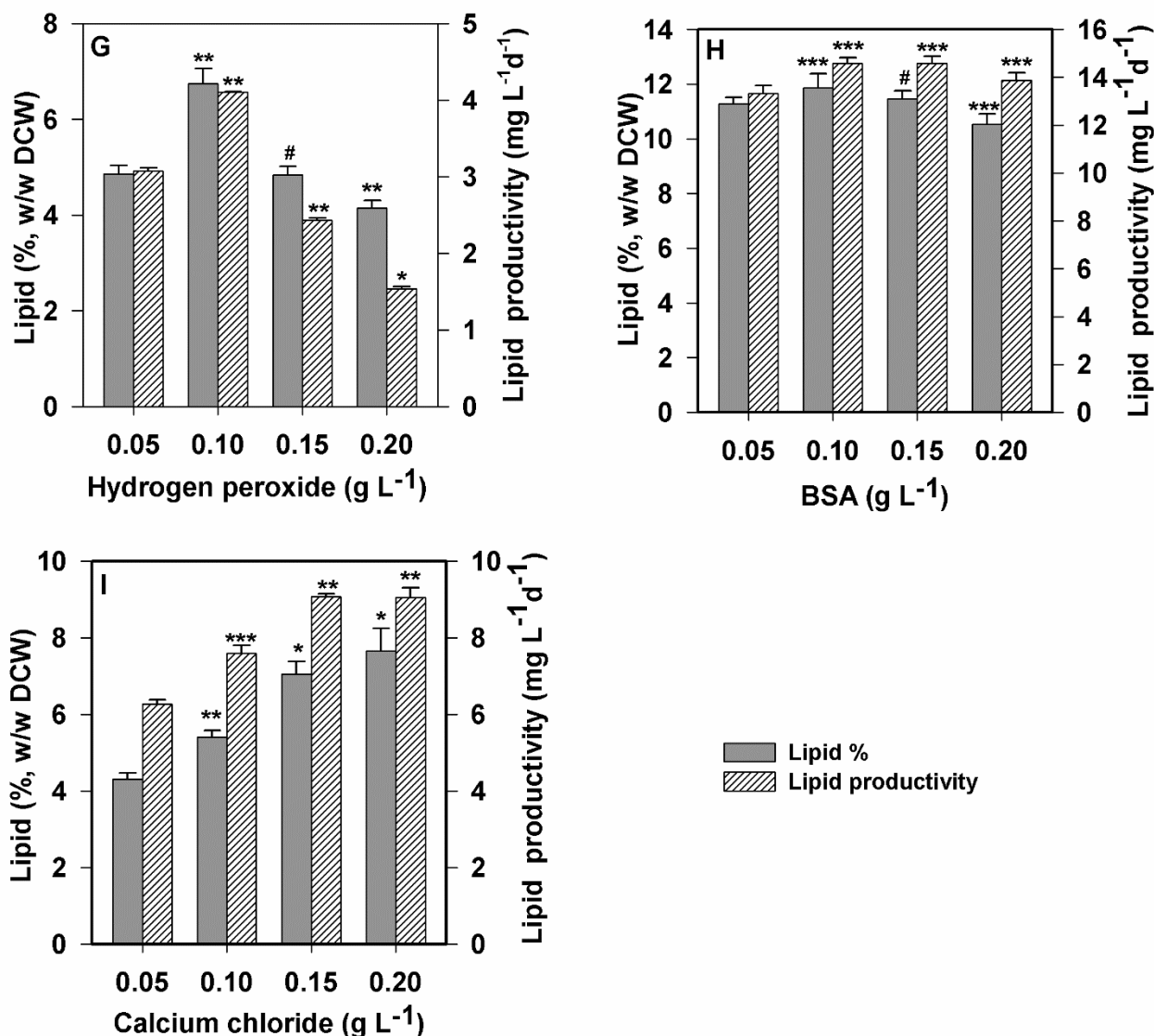


Fig 7.4 Effect of inducer molecules with their various levels of concentration on lipid content and lipid productivity of the FC6 grown under mixotrophic cultivation in shake flask. Different symbols indicate significant difference in biomass titer and lipid productivity obtained from the use of various lipid inducers analyzed using one way analysis of variance (*-represents P value = 0; **-represents $0 < P < 0.05$; ***-represents $0.05 < P < 0.5$ and #-represents > 0.5). For statistical analysis the lowest concentration of the respective lipid inducer was kept as control group

Maximum lipid productivity of $58.03 \text{ mg L}^{-1} \text{ day}^{-1}$ was achieved when the organism was grown in presence of 15 g L^{-1} sodium acetate followed by $14.5 \text{ mg L}^{-1} \text{ day}^{-1}$ in case of 15 g L^{-1} sodium chloride (Fig. 7.5). These lipid productivities on sodium acetate and sodium chloride were 6 and 1.5 fold higher in comparison to the control batch where the organism was grown without addition of any elicitor molecules. Supplementation of bovine serum

albumin (BSA) also resulted in similar lipid productivity as that for sodium chloride (Fig. 7.5). Use of sodium acetate resulted in an increase of neutral lipid productivity of the strain *Chlorella vulgaris* and *Leptolyngbya* sp. under mixotrophic condition which supports the present observation (Silaban et al., 2014). The uptake of sodium acetate results in an elevated flux towards lipid biosynthesis as it integrates into the central metabolism as acetyl Co-A which is the key precursor for lipid biosynthesis in microalgae (Heifetz et al., 2000; Muthuraj et al., 2013).

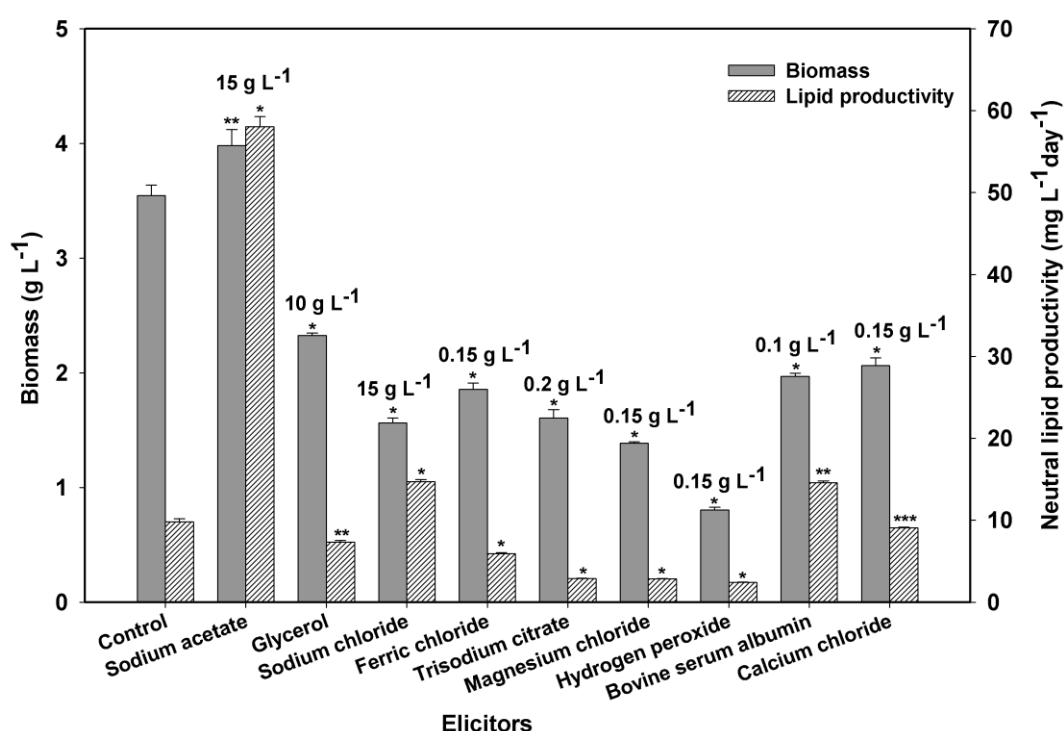


Fig. 7.5 Effect of various elicitors on growth and lipid productivity of *Chlorella sorokiniana* FC6 IITG. The organism was grown on optimized BG11 medium supplemented with individual elicitor molecule and 15 g L⁻¹ glucose as the primary carbon source for growth under mixotrophic condition in shake flask at 28°C, 150 rpm, and continuous light intensity of 30 μE m⁻² s⁻¹. The values mentioned on top of bars represents the concentration of respective elicitor at which it supports maximum lipid productivity. Different symbols indicate significant difference in biomass titer and lipid productivity obtained from the use of various lipid inducers analyzed using one way analysis of variance (*-represents P value = 0; **-represents 0<P<0.05 and ***-represents 0.05<P<0.5). The condition with glucose and no additional lipid inducer was taken as the control for statistical analysis

However, in case of sodium chloride, increase of media salinity increases the oxidative stress on organism resulting in higher induction of neutral lipid (Pancha et al., 2015). An

increase in lipid productivity from $63.3 \text{ mg L}^{-1} \text{ day}^{-1}$ to $79 \text{ mg L}^{-1} \text{ day}^{-1}$ was reported for the strain *Chlorella saccharophila* while grown on 0.15 M sodium chloride (Herrera-Valencia et al., 2011). Even though BSA resulted in improved lipid productivity, its application for energy biosynthesis will be restricted owing to its high cost. Lipid productivities for other inducers such as hydrogen peroxide, magnesium chloride, ferric chloride, calcium chloride, glycerol and trisodium citrate were found to be inferior as compared to the control condition. It is important to note that supplementation of sodium acetate in BG11 medium resulted in improvement of both biomass titer (Fig. 7.5) and intracellular neutral lipid content of the organism FC6 (Fig. 7.3 A) as compared to the control batch. This combined improvement in growth and lipid content resulted in significantly improved net lipid productivity. While supplementation of sodium chloride exhibited elevated neutral lipid content, the growth of the organism was compromised under this condition and hence, improvement in net lipid productivity was moderate. For rest of the elicitor molecules growth was significantly down regulated which in turn resulted in reduced net lipid productivity. Based on these observations, sodium acetate and sodium chloride were chosen as the suitable lipid inducer for the strain FC6 and their combined effect on growth and lipid productivity was evaluated.

7.3.2.1 Evaluation and optimization of combined effect of sodium acetate and sodium chloride on neutral lipid productivity

With the aim of maximizing neutral lipid productivity, the combined effect of sodium chloride and sodium acetate was evaluated by growing the organism in presence of both these elicitors at different concentration maintaining a ratio of 1:1 (Fig. 7.6). It was observed that combination of sodium chloride and sodium acetate at a concentration of 10 g L^{-1} each resulted in maximum neutral lipid productivity of $77 \text{ mg L}^{-1} \text{ day}^{-1}$ which was highest amongst any of the inducers analyzed individually. Zhou et al. (2013) reported that a

combination of 10 g L⁻¹ sodium chloride and sodium acetate favored maximum lipid accumulation and lipid yield for the strain *Chlorella* sp. (FACHB-1748).

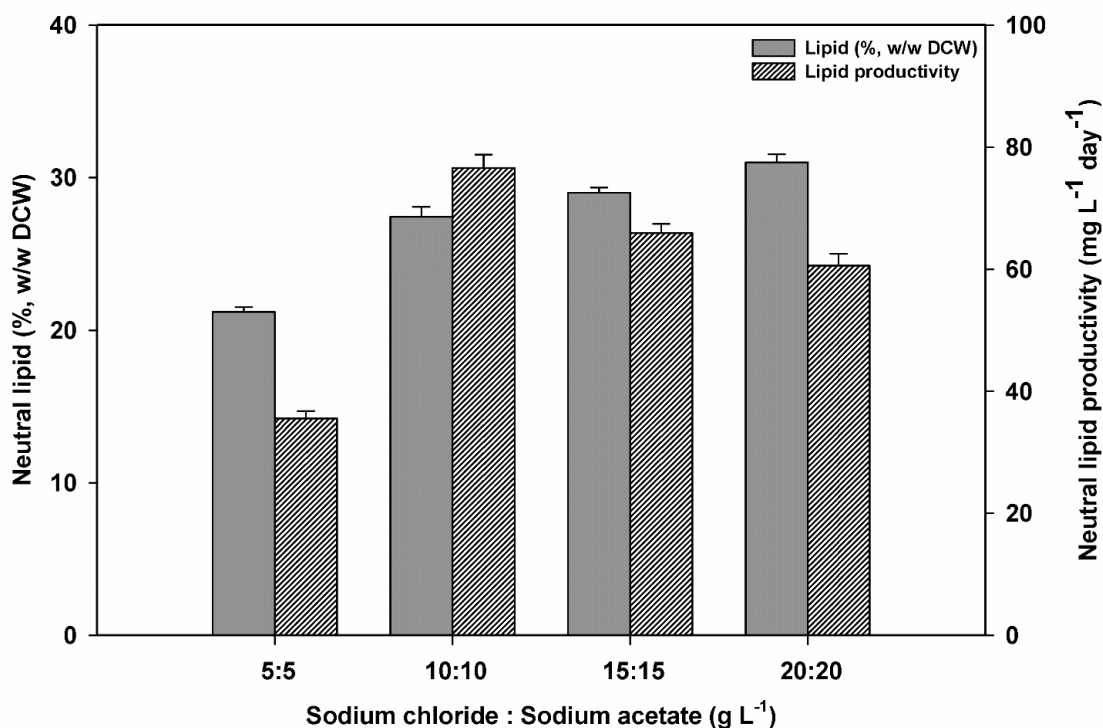


Fig 7.6 Combined effect of different concentrations of sodium chloride and sodium acetate in the ratio of 1:1 (w/w) on lipid content and lipid productivity of the strain grown under mixotrophic condition in shake flask

Further, the concentration of sodium acetate and sodium chloride was optimized using CCD coupled with RSM. A two factor, five level design (Table 7.2) was constructed with sodium chloride, and sodium acetate concentrations as the two factors.

Table 7.2 Actual levels of the inducer concentration used in CCD-RSM experimental design for optimization of inducer concentration for maximum lipid productivity under mixotrophic condition

Variables	Symbol	Actual levels of coded factors				
	Coded	-2	-1	0	1	2
Sodium chloride (g L ⁻¹)	X_1	0.43	2.5	7.5	12.5	14.57
Sodium acetate (g L ⁻¹)	X_2	0.43	2.5	7.5	12.5	14.57

In all the experiment, maximum lipid productivity was used as response in multiple regression analysis and compared with corresponding predicted values (Table 7.3).

Maximum lipid productivity at end of 16th day batch was used as the response for

optimization. Thirteen different combinations of the inducer concentration was designed by CCD resulted in wide range of lipid productivity from 16.59 mg L⁻¹ day⁻¹ to 109.81 mg L⁻¹ day⁻¹ (Table 7.3).

Table 7.3 CCD matrix of independent inducer components used in RSM with corresponding experimental and predicted measurements of lipid productivity (mg L⁻¹ day⁻¹)

S.No.	X_1 Sodium chloride (g L ⁻¹)	X_2 Sodium acetate (g L ⁻¹)	Lipid productivity Experimental (mg L ⁻¹ day ⁻¹)	Lipid productivity Predicted (mg L ⁻¹ day ⁻¹)
1	2.50	2.50	22.60	25.89
2	12.50	2.50	24.36	27.56
3	2.50	12.50	109.81	109.67
4	12.50	12.50	24.52	24.28
5	0.43	7.50	83.80	82.20
6	14.57	7.50	24.46	23.00
7	7.50	0.43	16.59	12.64
8	7.50	14.57	68.67	69.56
9	7.50	7.50	94.24	94.64
10	7.50	7.50	92.51	94.64
11	7.50	7.50	93.91	94.64
12	7.50	7.50	97.44	94.64
13	7.50	7.50	95.11	94.64

The significance of model parameters and coefficient were analyzed on the basis of p-values (<0.05) of ANOVA obtained from regression analysis (Table 7.4). The quadratic polynomial equation obtained from regression analysis was used to predict the maximum lipid productivity (Y , mg L⁻¹ day⁻¹) with concentration of sodium chloride (X_1 , g L⁻¹) and sodium acetate (X_2 , g L⁻¹) as variable parameters.

$$Y = 94.64 - 20.93X_1 + 20.13X_2 - 21.02X_1^2 - 26.77X_2^2 - 21.76X_1X_2 \quad (7.5)$$

Regression analysis showed R^2 value of 0.996 which indicates that 99.6% of the predicted results were identical with experimental value. Maximum lipid productivity of 111.19 mg L⁻¹ day⁻¹ was predicted by RSM based model at predicted optimal concentration of sodium

chloride 3.14 g L⁻¹ and sodium acetate 11.14 g L⁻¹. The model was validated by comparing the predicted lipid productivity with experimentally obtained value (110.59 mg L⁻¹ day⁻¹).

Table 7.4 ANOVA for the quadratic regression model obtained from CCD-RSM employed in optimization of inducer concentration for the maximization of lipid productivity

Source	DF	Seq SS	Adj MS	F	p ^a
Regression	5	15798.3	3159.66	398.54	0.0
Linear	2	6744.9	3372.46	425.38	0.0
X ₁	1	3504.6	3504.58	442.04	0.0
X ₂	1	3240.3	3240.33	408.71	0.0
Square	2	7158.7	3579.35	451.47	0.0
X ₁ ²	1	2173.9	3073.18	387.63	0.0
X ₂ ²	1	4984.8	4984.77	628.74	0.0
Interaction	1	1894.7	1894.69	238.98	0.0
X ₁ *X ₂	1	1894.7	1894.69	238.98	0.0
Residual Error	7	55.5	7.93	NA	--
Lack-of-Fit	3	42.2	14.07	4.24	0.098
Pure Error	4	13.3	3.32	--	--
Total	12	15853.8	--	--	--

^a - p value >0.05 is considered as insignificant

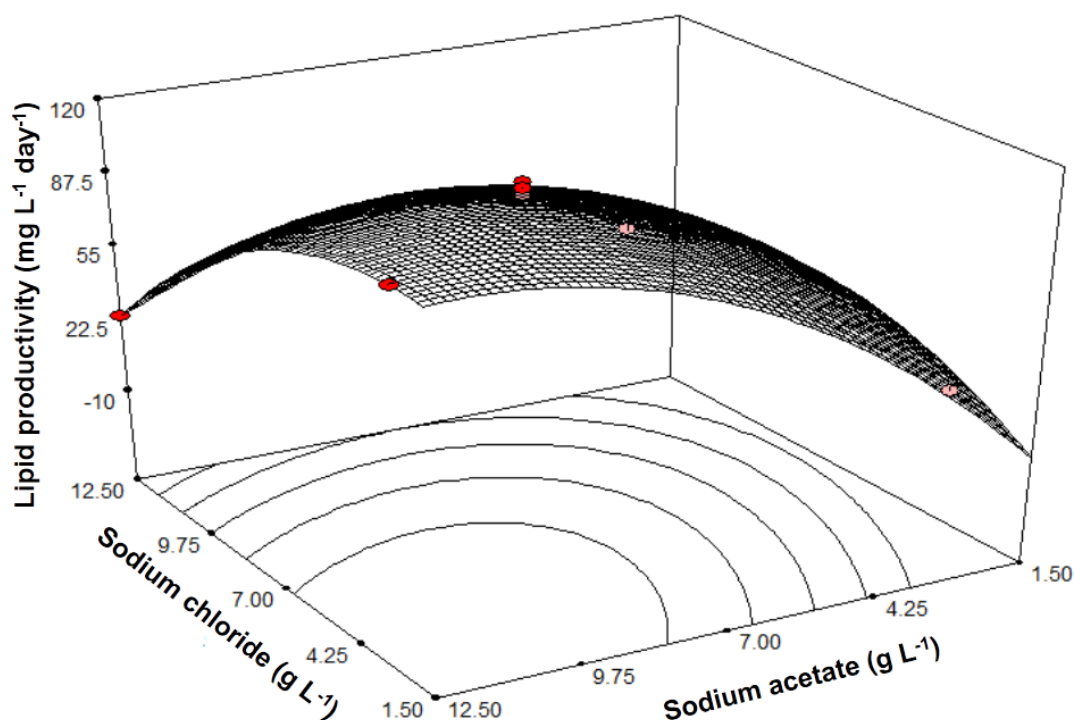


Fig. 7.7 Response surface plot representing the interaction effect of sodium chloride and sodium acetate on lipid productivity (mg L⁻¹day⁻¹) of FC6 grown under mixotrophic condition in shake flask

The interaction effect of these two inducers on lipid productivity of FC6 is presented in Fig. 7.7. Increase in the concentration of sodium chloride greater than 3.14 g L^{-1} decreased the lipid productivity significantly and was found to be inhibitory on biomass growth at higher concentration. While increased sodium acetate concentration of 11.14 g L^{-1} was required for maximizing both the lipid content and biomass productivity, further increase in the concentration did not result in significant improvement in lipid productivity. Use of cheaper lipid inducer molecules such as sodium acetate and sodium chloride bypasses the intermittent harvesting and re-suspension involved in two stage nutrient starvation strategy for lipid induction and yields synchronized growth and lipid accumulation leading to high lipid productivities. Thus the process involving these inducer molecules are expected to be energetically favorable. Moreover, acetate is generated in larger quantities during the treatment and hydrolysis of hemicellulosic biomass (Yang et al., 2014) and as a product from anaerobic digestate (Nie et al., 2009). Sodium acetate generated from such renewable process can be utilized further as the lipid inducer in the current process which is expected to minimize the cost of substrates. In comparison to sodium acetate, sodium chloride is a relatively cheaper lipid inducer and can be availed easily in bulk quantities (Mohan and Devi, 2014). In addition, an efficient harvesting method such as electroflotation can be utilized in the process without affecting the media properties that can open up scope for reutilization of the residual media components.

7.3.3 Process development for synchronized growth and neutral lipid accumulation in an automated photobioreactor

The maximization of lipid productivity can be achieved via high concentration of lipid rich biomass in fed-batch or high biomass productivity with lipid rich cells in continuous mode of cultivation.

7.3.3.1 Fed-batch cultivation with intermittent feeding of limiting nutrients and elicitors

To achieve simultaneous growth and lipid accumulation towards high lipid productivity, fed-batch cultivation was performed through intermittent feeding of growth limiting nutrients nitrate, phosphate, glucose and lipid inducer sodium acetate. Maximum biomass titer of 18.24 g L^{-1} with neutral lipid content of 55% w/w, DCW was achieved over a period of 12 days (Fig. 7.8 A).

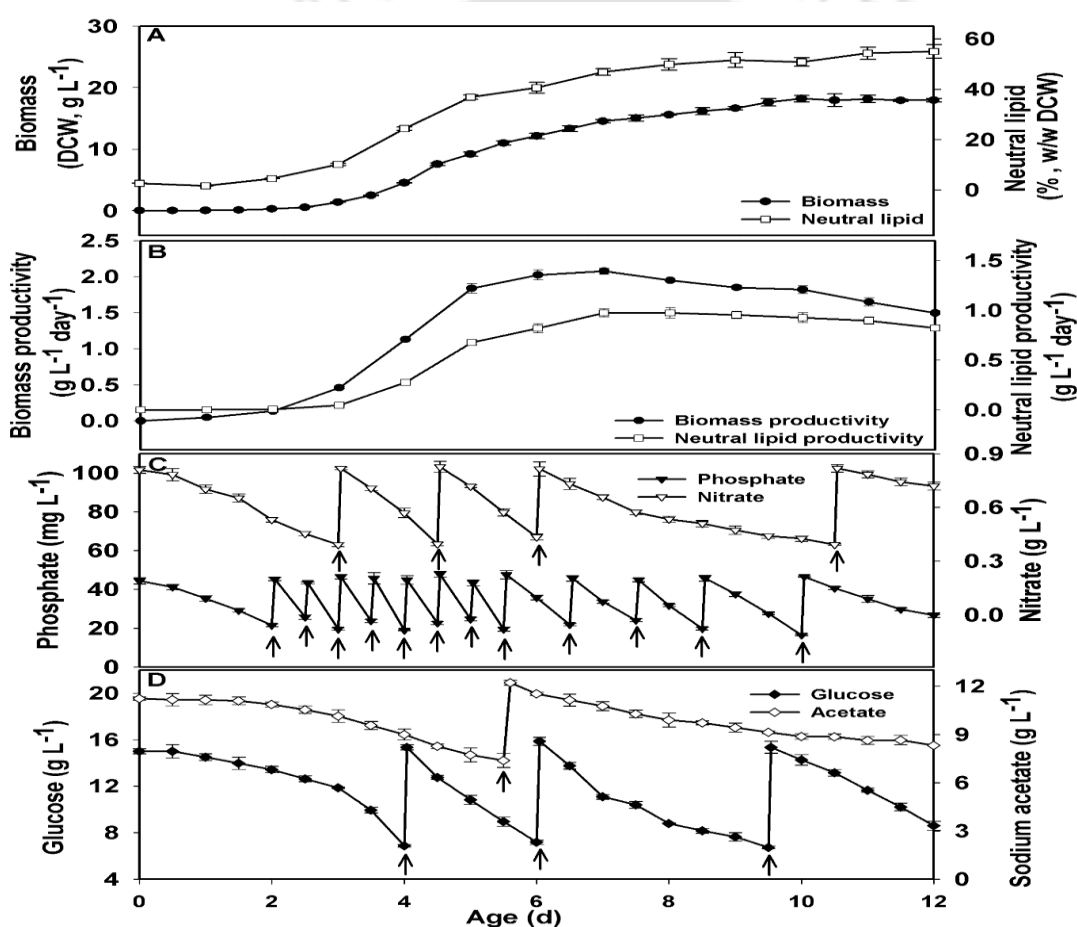


Fig. 7.8 Dynamic profiles for growth, intracellular lipid content, biomass & lipid productivity and substrate utilization pattern for the strain FC6 grown under mixotrophic fed-batch mode of operation in automated bioreactor of 7.5 L at 28°C , 250 rpm with $350 \mu\text{E m}^{-2} \text{ s}^{-1}$ continuous light intensity. The profiles represents: (A) biomass formation ($\text{---}\bullet\text{---}$) & neutral lipid content ($\text{---}\square\text{---}$); (B) biomass productivity ($\text{---}\bullet\text{---}$) & neutral lipid productivity ($\text{---}\square\text{---}$); (C) Nitrate ($\text{---}\blacktriangledown\text{---}$) & phosphate ($\text{---}\nabla\text{---}$) concentration, and (D) Glucose ($\text{---}\blacklozenge\text{---}$) & sodium acetate ($\text{---}\diamond\text{---}$) concentrations. Solid arrow mark (\uparrow) shows the feeding of respective substrate

Dynamic profile of biomass formation and neutral lipid accumulation showed synchronized growth and neutral lipid accumulation in microalgae FC6 (Fig. 7.8 A). Maximum biomass and lipid productivity was found to be $2.08 \text{ g L}^{-1} \text{ day}^{-1}$ and $0.97 \text{ g L}^{-1} \text{ day}^{-1}$ respectively (Fig. 7.8 B). It is important to note that feeding of nutrients and sodium acetate was done based on their observed utilization profile in order to maintain their concentration above 50% of their initial value in the BG11 medium (Fig. 7.8 C and D). It is important to note that sodium chloride is used as trace element (25 mg L^{-1}) for growth of fresh water microalgae which is consumed by the organisms in very small amount and hence, will not have any significant effect on the concentration of sodium chloride (3.14 g L^{-1}) used in the present study as lipid inducer. Therefore, sodium chloride was not fed intermittently in the fed batch.

7.3.3.2 *Continuous mode of cultivation of FC6*

Continuous cultivation of the organism was carried out for various dilution rates by supplying the modified BG11 media along with optimized concentrations of the inducers sodium acetate and sodium chloride. Chemostat was operated for five different dilution rates over the time period of 25 days in a sequential manner. The steady state conditions of the reactor were confirmed after achieving constant values in growth, lipid content and substrate utilization profiles. Biomass titer and lipid content were found to increase with decrease in dilution rate and attained their maximum value of 6.61 g L^{-1} and 58.89% (w/w DCW) respectively at dilution rate of 0.18 day^{-1} (Fig. 7.9). This was apparently due to availability of higher residence time for growth, lipid accumulation and substrate utilization at lower dilution rate.

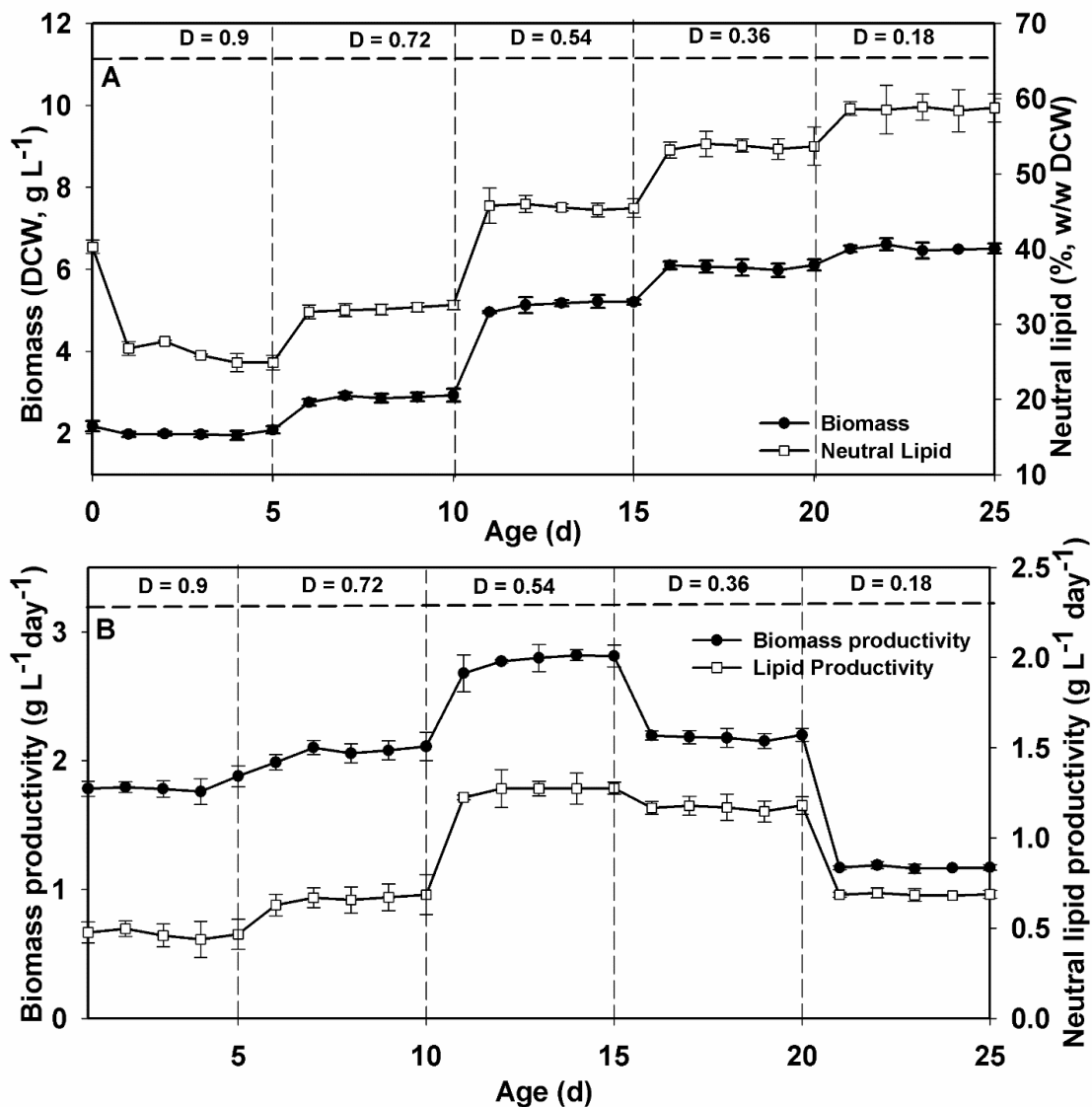


Fig. 7.9 Dynamic profiles for growth, intracellular lipid content, biomass and lipid productivity for the strain FC6 grown under mixotrophic continuous mode of operation in an automated bioreactor of 7.5 L at 28°C, 250 rpm with 350 $\mu\text{E m}^{-2} \text{s}^{-1}$ continuous light intensity. The profiles represents: (A) biomass formation (—●—) & neutral lipid content (—□—) and (B) biomass productivity (—●—) and neutral lipid productivity (—□—). The values of D depicts the dilution rate maintained in continuous cultivation

Substrate utilization profile also showed that maximum amount of nutrients were consumed at lower dilution rates rather than higher ones (Fig. 7.10). However, organism showed their maximum biomass and lipid productivity of 2.81 $\text{g L}^{-1} \text{day}^{-1}$ and 1.27 $\text{g L}^{-1} \text{day}^{-1}$ respectively at the dilution rate of 0.54 day^{-1} . This biomass and lipid productivity in chemostat showed an improvement of 35% and 31% respectively in comparison with fed-batch cultivation.

This might be due to ability to maintain higher specific growth rate of the organism throughout the entire batch cycle.

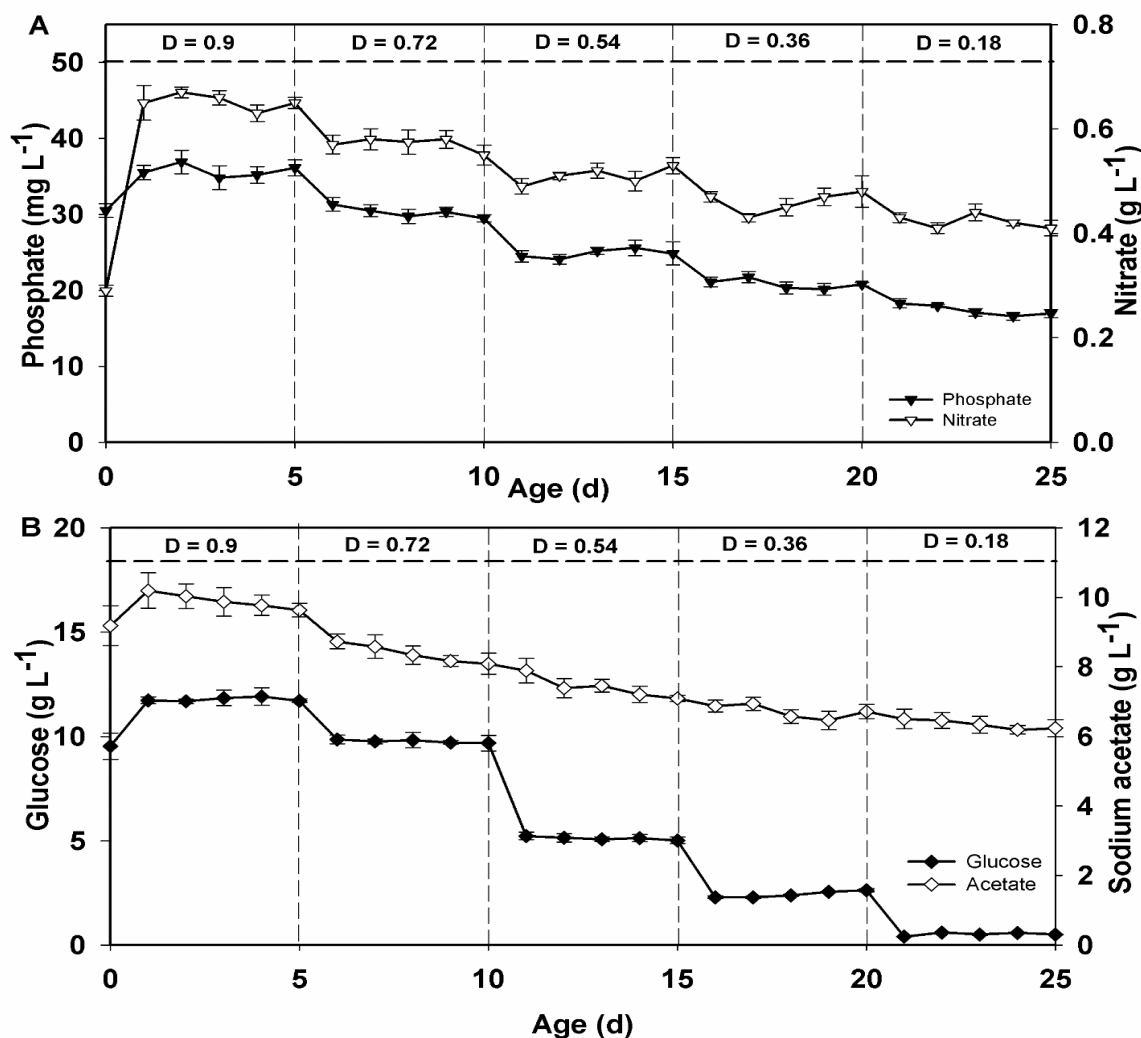


Fig. 7.10 Dynamic profiles for substrate utilization and concentration of lipid inducer for the strain FC6 grown under mixotrophic continuous mode of operation in an automated bioreactor of 7.5 L at 28°C, 250 rpm with 350 $\mu\text{E m}^{-2} \text{s}^{-1}$ continuous light intensity. The profiles represents: (A) phosphate (\blacktriangledown) & nitrate (∇) concentration and (B) glucose (\blacklozenge) & sodium acetate (\diamond) concentration. The values of D depicts the dilution rate maintained in continuous cultivation

In accordance with present findings, simultaneous growth and lipid production was achieved by growing *Chlorella pyrenoidosa* in continuous mode of operation at dilution rate of 0.48 day⁻¹ (Wen et al., 2014). Sobczuk and Chisti (2010) also reported the maximal biomass productivity of 351 mg L⁻¹ day⁻¹ along with lipid productivity of 82 mg L⁻¹ day⁻¹ in

continuous cultivation of *Choricystis minor* at dilution rate of 0.336 day^{-1} . Present findings of biomass productivity and lipid productivity were compared in detail with literature (Table 2, Appendix) and found to be significantly higher than many characterized strains so far. Biomass yield with respect to glucose ($Y_{X/Glu}$) was found to increase with increase in dilution rate and achieved maximum value of 0.63 g g^{-1} glucose at dilution rate of 0.9 day^{-1} . Availability of light source might be excess due to lesser value of steady state biomass concentration in the higher dilution rates, hence organism might have consumed glucose as a carbon source rather than energy source leading to increased value of biomass yield.

7.3.4 FAME composition and biodiesel property

In order to assess the suitability of biodiesel produced from FC6 under fed-batch and continuous mode of cultivation, *in situ* transesterification was carried out to generate FAME for further analysis. The quality of biodiesel was evaluated by using empirical formulas based on experimentally determined FAME composition (Francisco et al., 2010; Su et al., 2011; Ramirez-Verduzcoas et al., 2012). FAME profile reveals the majority of fatty acid was C16:0, C16:1, C18:0, C18:1 and C18:2 (Table 7.5) which depicts its suitability as biodiesel (Cheirsilp and Torpee, 2012). Viscosity and cetane number of the FC6 derived biodiesel were varied from 4.33 to $4.39 \text{ mm}^2 \text{ s}^{-1}$ and 54.41 - 56.20 respectively, which did not show any significant changes with variation in cultivation mode (Table 7.6). In general, higher viscosity results in poor flow properties with less atomization quality, drop size and low penetration ability of the fuel, whereas cetane number influences combustion ability and engine knocking. Flash point value was found to be much higher than the minimum threshold specific by the ASTM standard (Table 7.6). Biodiesel derived from FC6 showed better cloud and pour points which were -2.76 to 1.57 and -5.78 to -1.43°C respectively (Table 7.6).

Table 7.5 Fatty acid methyl esters (FAME) profile of strain FC6 grown under different cultivation mode

Fatty Acids	FAME (%, w/w)	Cultivation mode						
		Fed batch (SSTP)	Fed batch (SGLA)	Chemostat				
				D = 0.18	D = 0.36	D = 0.54	D = 0.72	D = 0.90
Lauric	[C12:0]	2.01	2.37	1.98	2.23	2.46	2.65	2.78
Myristic	[C14:0]	0.98	0.27	0.94	0.97	1.23	1.34	1.39
Palmitic	[C16:0]	23.54	19.72	25.4	26.81	27.38	25.09	25.94
Palmitoleic	[C16:1]	7.97	11.76	7.29	7.36	7.65	7.98	8.32
Stearic	[C18:0]	1.98	1.35	1.56	1.88	2.12	2.45	2.56
Oleic	[C18:1]	29.13	29.85	28.19	29.19	29.53	29.87	30.12
Linoleic	[C18:2]	32.56	31.8	33.25	30.92	28.72	28.39	28.12
Arachidic	[C20:0]	0.11	0.08	0.22	0.18	0.38	0.43	0.52
Behenic	[C22:0]	0.06	0.03	0.07	0.09	0.12	0.16	0.19
	SAT FAME ^a	28.68	23.82	30.17	32.16	33.69	32.12	33.38
	MUFA ^b	37.10	41.61	35.48	36.55	37.18	37.85	38.44
	PUFA ^c	32.56	31.8	33.25	30.92	28.72	28.39	28.12
	Others	1.66	2.77	1.1	0.37	0.41	1.64	0.06
	Total FAME ^d	54.95	63.13	60.73	63.76	44.83	38.98	32.34

^a - represents the total saturated fatty acid fraction in the total fatty acid methyl esters

^b - represents the total monounsaturated fatty acid fraction in the total fatty acid methyl esters

^c - represents the total polyunsaturated fatty acid fraction in the total fatty acid methyl esters

^d - represents the total FAME expressed in %, weight fraction of dry cell weight

SSTP- represents single stage two phase cultivation mode

SGLA- represents synchronized growth and lipid accumulation

Table 7.6 Estimated properties of algal biodiesel obtained from strain FC6 grown under different operational modes

Biodiesel Properties	FAME (%, w/w)	Cultivation mode						
		Fed batch (SSTP)	Fed batch (SGLA)	Chemostat (SGLA)				
				D = 0.18	D = 0.36	D = 0.54	D = 0.72	D = 0.90
Viscosity ^a	(mm ² s ⁻¹)	4.35	4.33	4.36	4.38	4.39	4.39	4.39
Cetane Number ^a		54.95	54.41	55.24	55.76	56.19	56.04	56.20
Flash Point ^a	(°C)	155.65	155.14	154.72	153.47	152.29	152.60	152.08
Cloud Point ^a	(°C)	-2.36	-2.67	0.91	1.10	1.57	1.49	0.89
Pour Point ^a	(°C)	-5.47	-5.78	-2.14	-1.92	-1.43	-1.51	-2.11
Saponification Value ^a	mg KOH g ⁻¹	214.09	201.76	205.21	207.14	207.47	204.81	208.29
Iodine value ^a	gI ₂ (100 g oil) ⁻¹	99.46	96.18	92.85	89.60	86.21	86.25	86.32
Degree of Unsaturation ^a		109.22	105.21	101.98	98.39	94.62	94.63	94.68
Heating value ^a	MJ kg ⁻¹	39.64	39.62	39.64	39.63	39.63	39.62	39.62

^a - the empirical equations for calculating the biodiesel properties were depicted in equations 5.2-5.10 (details in section 5.2.5 of chapter 5)

SSTP- represents single stage two phase mixotrophic fed-batch cultivation mode

SGLA- represents synchronized growth and lipid accumulation

Therefore, biodiesel obtained from microalga FC6 grown under mixotrophic fed-batch or chemostat condition under the influence of inducer molecule can be used for commercial applications as it satisfies overall ASTM D6751–15a and EN 14,214 standards.

7.4 Conclusions

In the present study we demonstrated two strategy for enhanced biomass and lipid productivity. (i) Coupling intermittent feeding of limiting nutrients (fed-batch mode) and addition of lipid inducer in stationary phase results high cell density cultivation for generation of lipid rich microalgal biomass using single-stage two phase mixotrophic fed-batch operation mode. (ii) a process engineering strategy to achieve synchronized growth and lipid accumulation in FC6 under fed-batch and continuous mode of operation with sodium acetate and sodium chloride as triggers for lipid accumulation. The chemostat resulted in maximum biomass and lipid productivity of 2.81 and 1.27 g L⁻¹ day⁻¹ respectively, which was significantly higher among many other strains characterized so far. Thus, using combination of sodium chloride and sodium acetate as lipid inducers in chemostat could be an effective alternate of the conventional nutrient limitation strategies used to achieve synchronized growth and lipid accumulation without compromising growth.

7.5 References

1. Adams, C., Godfrey, V., Wahlen, B., Seefeldt, L., Bugbee, B., 2013. Understanding precision nitrogen stress to optimize the growth and lipid content tradeoff in oleaginous green microalgae. *Bioresour. Technol.* 131, 188-194.
2. Cheirsilp, B., Torpee, S., 2012. Enhanced growth and lipid production of microalgae under mixotrophic culture condition: effect of light intensity, glucose concentration and fed-batch cultivation. *Bioresour. Technol.* 110, 510-516.
3. Francisco, É.C., Neves, D.B., Jacob-Lopes, E., Franco, T.T., 2010. Microalgae as feedstock for biodiesel production: carbon dioxide sequestration, lipid production and biofuel quality. *J. Chem. Technol. Biotechnol.* 85, 395-403.
4. Georgianna, D.R., Mayfield, S.P., 2012. Exploiting diversity and synthetic biology for the production of algal biofuels. *Nature.* 488, 329-335.
5. Heifetz, P.B., Forster, B., Osmond, C.B., Giles, L.J., Boynton, J.E., 2000. Effects of acetate on facultative autotrophy in *Chlamydomonas reinhardtii* assessed by photosynthetic measurements and stable isotope analyses. *Plant Physiol.* 122, 1439-1445.
6. Herrera-Valencia, V.A., Contreras-Pool, P.Y., Lopez-Adrian, S.J., Peraza-Echeverria, S., Barahona-Perez, L.F., 2011. The green microalga *Chlorella saccharophila* as a suitable source of oil for biodiesel production. *Curr. Microbiol.* 63, 151-157.
7. Hu, Q., Sommerfeld, M., Jarvis, E., Ghirardi, M., Posewitz, M., Seibert, M., Darzins, A., 2008. Microalgal triacylglycerols as feedstocks for biofuel production: perspectives and advances. *Plant J.* 54, 621-639.
8. Karemore, A., Pal, R., Sen, R., 2013. Strategic enhancement of algal biomass and lipid in *Chlorococcum infusionum* as bioenergy feedstock. *Algal Res.* 2, 113-121.

9. Klok, A.J., Martens, D.E., Wijffels, R.H., Lamers, P.P., 2013. Simultaneous growth and neutral lipid accumulation in microalgae. *Bioresour. Technol.* 134, 233-243.
10. Lee, C.G., 1999. Calculation of light penetration depth in photobioreactors. *Biotechnol. Bioprocess Eng.* 4, 78-81.
11. Menon, K.R., Balan, R., Suraishkumar, G.K., 2013. Stress induced lipid production in *Chlorella vulgaris*: relationship with specific intracellular reactive species levels. *Biotechnol. Bioeng.* 110, 1627-1636.
12. Mohan, S.V., Devi, M.P., 2014. Salinity stress induced lipid synthesis to harness biodiesel during dual mode cultivation of mixotrophic microalgae. *Bioresour. Technol.* 165, 288-294.
13. Muthuraj, M., Chandra, N., Palabhanvi, B., Kumar, V., Das, D., 2015. Process Engineering for High-Cell-Density Cultivation of Lipid Rich Microalgal Biomass of *Chlorella* sp. FC2 IITG. *BioEnergy Res.* 8, 726-739.
14. Muthuraj, M., Palabhanvi, B., Misra, S., Kumar, V., Sivalingavasu, K., Das, D., 2013. Flux balance analysis of *Chlorella* sp. FC2 IITG under photoautotrophic and heterotrophic growth conditions. *Photosynth. Res.* 118, 167-179.
15. Ngangkham, M., Ratha, S.K., Prasanna, R., Saxena, A.K., Dhar, D.W., Sarika, C., Prasad, R.B.N., 2012. Biochemical modulation of growth, lipid quality and productivity in mixotrophic cultures of *Chlorella sorokiniana*. *Springerplus* 1, 1-13.
16. Palabhanvi, B., Kumar, V., Muthuraj, M., Das, D., 2014. Preferential utilization of intracellular nutrients supports microalgal growth under nutrient starvation: Multi-nutrient mechanistic model and experimental validation. *Bioresour. Technol.* 173, 245-255.

17. Pancha, I., Chokshi, K., Maurya, R., Trivedi, K., Patidar, S.K., Ghosh, A., Mishra, S., 2015. Salinity induced oxidative stress enhanced biofuel production potential of microalgae *Scenedesmus* sp. CCNM 1077. *Bioresour. Technol.* 189, 341-348.
18. Parsons, T.R., Maita, Y., Lalli, C.M., 1984. A manual of chemical and biological methods for seawater analysis. Pergamon Press Ltd, Great Britain.
19. Rai, M.P., Nigam, S., Sharma, R., 2013. Response of growth and fatty acid compositions of *Chlorella pyrenoidosa* under mixotrophic cultivation with acetate and glycerol for bioenergy application. *Biomass Bioenergy* 58, 251-257.
20. Ramirez-Verduzco, L.F., Rodriguez-Rodriguez, J.E., Jaramillo-Jacob, A.R., 2012. Predicting cetane number, kinematic viscosity, density and higher heating value of biodiesel from its fatty acid methyl ester composition. *Fuel*. 91, 102-111.
21. Ren, H.Y., Liu, B.F., Kong, F., Zhao, L., Xie, G.J., Ren, N.Q., 2014. Enhanced lipid accumulation of green microalga *Scenedesmus* sp. by metal ions and EDTA addition. *Bioresour. Technol.* 169, 63-767.
22. Rodolfi, L., Zittelli, G.C., Bassi, N., Padovani, G., Biondi, N., Bonini, G., Tredici, M.R., 2009. Microalgae for oil: strain selection, induction of lipid synthesis and outdoor mass cultivation in a low-cost photobioreactor. *Biotechnol. Bioeng.* 102, 100-112.
23. Silaban, A., Bai, R., Gutierrez-Wing, M.T., Negulescu, I.I., Rusch, K.A., 2014. Effect of organic carbon, C:N ratio and light on the growth and lipid productivity of microalgae/cyanobacteria coculture. *Eng. Life Sci.* 14, 47-56.
24. Sobczuk, T., Chisti, Y., 2010. Potential fuel oils from the microalga *Choricystis minor*. *J. Chem. Technol. Biotechnol.* 85, 100-108.
25. Su, Y.C., Liu, Y.A., Diaz Tovar, C.A., Gani, R., 2011. Selection of prediction methods for thermophysical properties for process modeling and product design of biodiesel manufacturing. *Ind. Eng. Chem. Res.* 50, 6809-6836.

26. Tevatia, R., Allen, J., Blum, P., Demirel, Y., Black, P., 2014. Modeling of rhythmic behavior in neutral lipid production due to continuous supply of limited nitrogen: Mutual growth and lipid accumulation in microalgae. *Bioresour. Technol.* 170, 152-159.
27. Wen, X., Geng, Y., Li, Y., 2014. Enhanced lipid production in *Chlorella pyrenoidosa* by continuous culture. *Bioresour. Technol.* 161, 297-303.
28. Xia, L., Rong, J., Yang, H., He, Q., Zhang, D., Hu, C., 2014. NaCl as an effective inducer for lipid accumulation in freshwater microalgae *Desmodesmus abundans*. *Bioresour. Technol.* 161, 402-409.
29. Xie, Y., Ho, S.H., Chen, C.N., Chen, C.Y., Ng I.S., Jing, K.J., Chang, J.S., Lu, Y., 2013. Phototrophic cultivation of a thermo-tolerant *Desmodesmus* sp. for lutein production: Effects of nitrate concentration, light intensity and fed-batch operation. *Bioresour. Technol.* 144, 435-444.
30. Zhang, D., Xue, S., Sun, Z., Liang, K., Wang, L., Zhang, Q., Cong, W., 2014. Investigation of continuous-batch mode of two-stage culture of *Nannochloropsis* sp. for lipid production. *Bioprocess Biosyst. Eng.* 37, 2073-2082.

8.1 Background and motivation

Production of biodiesel involve multiple steps starting from strain selection, process development for lipid enrichment in cells followed by harvesting of biomass and its subsequent drying and final processing for conversion of intracellular lipids in to biodiesel via transesterification (Lundquist et al., 2010; Mata et al., 2010; Neveux et al., 2014; Xu et al., 2014; Zhang et al., 2014). Thus with such multiple unit operations, the commercial scale production of biodiesel remains economically infeasible. In the previous chapters, a feasible upstream process was developed for the optimal production of lipid rich biomass with enhanced lipid productivity while further economic feasibility will be achieved by optimizing the downstream operations involved in the microalgal biodiesel production process. To that end, an improved and efficient downstream process targeted towards biodiesel production from oleaginous microalgae will be developed. Harvesting of algal biomass or dewatering remains one of the major rate limiting steps in the biodiesel production process that hinders commercial feasibility (Rawat et al., 2013; Coons et al., 2014). This is due to the dilute nature of the broth and small size of the cells which further elevates the operational cost making the process un-economical (Vandamme et al., 2011). Harvesting and dewatering the algal biomass, in particular, is estimated to be 15-30% of the overall cost per gallon of biodiesel (Uduman et al., 2011; Davis et al., 2012) and the U.S. Department of Energy has targeted a 50% cost reduction in algal harvesting step in order to achieve a cost competitive biofuel (U.S. DOE, 2010). However, there are several methods used for harvesting of microalgae which are categorized as chemical, mechanical, electrical and biological methods based on their mode of separation which can be applied as individual or in combination (Danquah et al., 2009). Chemical dewatering methods are mostly flocculation induced by inorganic or organic polyelectrolyte (polymer) flocculants. Chemical flocculants can be expensive especially at high dose and may cause contamination

issue to the harvested biomass and medium. Mechanical techniques include natural sedimentation, centrifugation, filtration, flotation, and foam separation. The gravity sedimentation is the most common and conventional techniques used to harvest microalgal. This method is suitable for microalgae with high density and large size such as *Spirulina*. Major limitation of this method is low density microalgae do not settle well and are poorly removed by sedimentation, this is slow and time consuming process. Centrifugation method involves centripetal force to separate the microalgae culture into two different density areas greater and less density areas. The process is rapid and energy intensive which need high energy cost and high maintenance cost. The filtration process involved the microalgae culture runs via filters by trapping microalgae and only allow water to pass through the filter. The main drawback of filtration is the cost required to replace the membrane is very high and it needs to be replaced very frequently when used on a larger scale of production. Harvesting by above mentioned conventional methods of centrifugation and filtration are expensive for production of low value product like biodiesel due to relatively dilute cultures that require processing large volumes of water (Amaro et al., 2011). A potential solution to this problem is to use electrolytic methods. Electrolytic dewatering techniques are based on electro-coagulation and electroflocculation processes. The advantages of using electrochemical processes include environmental compatibility, energy efficient, selective and cost effective (Christenson and Sims, 2011). Though not fully developed for commercial application, it is imperative to find an efficient, cost effective and ecofriendly harvesting and dewatering technique to attain sustainability and economic feasibility (Greenwell et al., 2010; Christenson and Sims, 2011; Soomro et al., 2016). The major lookout while developing an efficient harvesting technique is that the quality of the stored lipid should not be degraded or compromised with a minimal investment, energy and maintenance (Poelman et al., 1997). Presence of acidic polysaccharides viz pectin imparts

a net negative charge to the microalgal cell wall (Safi et al., 2014). This negative charge, if neutralized can form microalgal cell aggregates, which can be easily separated from medium. This coagulation concept can be used for harvesting of microalgal biomass (Safi et al., 2014). There exists a huge number of coagulants and flocculants of both natural and chemical origin, but, their over dosage should not adversely affect the biomass quality. Electrochemical harvesting is currently being examined for its potent and effective recovery of biomass by researchers globally (Vandamme et al., 2011; Kim et al., 2012a; Lee et al., 2013). The major roadblock to electrochemical harvesting so far has been the depletion of metallic electrodes (Kim et al., 2012a; Kim et al., 2012b) which in due course can contaminate microalgal biomass. Depletion of electrodes further increases the cost of harvesting as well as hampers the quality of lipids due to metallic contamination (Uduman et al., 2011; Kim et al., 2012a; Kim et al., 2012b). To overcome this limitation the application of non-depleting electrodes are required for the electrochemical harvesting of microalgae. Non-depleting electrodes totally avoid formation of metal hydroxide unlike metallic electrodes, and thus can be used as replacements in conventional electrochemical harvesting process. Harvesting by electrochemical methods is a novel approach and the use of non-depleting electrodes has not yet been investigated thoroughly.

This work aims to demonstrate the electrochemical harvesting of microalgae *Chlorella sorokiniana* FC6 IITG by using non-depleting carbon electrodes which is a combination of electro-flocculation and electro-floatation processes. The effect of several important variables on the electrochemical harvesting process were investigated, such as applied voltage, broth pH and electrolyte concentration (by adding additional electrolyte). Earlier investigations of electrochemical processes for harvesting of microalgal biomass have not thoroughly evaluated the effect of the electrochemical harvesting process on the further

downstream processes i.e. their effect on FAME composition and biodiesel quality which has been included in the present study.

8.2 Materials and methods

8.2.1 Microalgal strain, media composition and microalgae cultivation

Chlorella sorokiniana FC6 IITG was evaluated as a cell factory for biodiesel production in our present study (section 6.4 of chapter 6). Optimized BG11 media (composition as mentioned in Table 5.4 of chapter 5) supplemented with glucose 15 g L^{-1} , sodium acetate 11.14 g L^{-1} and sodium chloride 3.14 g L^{-1} was used as a growth media (detailed in chapter 7). The inoculum was prepared as mentioned in previous section (7.2.2 of chapter 7). Synchronized growth and lipid accumulation was achieved under chemostat cultivation of *Chlorella sorokiniana* FC6 IITG carried out at a dilution rate of 0.54 day^{-1} by using modified BG11 media under mixotrophic cultivation to generate lipid rich biomass with improved biomass and lipid productivity as discussed before (detailed in chapter 7). These experiments were carried out in a 7.5 L automated bioreactor (Bioflo 115, New Brunswick Pvt. Ltd., USA) with working volume of 4 L and condition were kept same as mentioned in section 7.2.2.2 of chapter 7. The broth obtained from the mixotrophic growth of FC6 was used further in all experiments for evaluating the harvesting strategy.

8.2.2 Pre-concentration of algal biomass via electrochemical harvesting using carbon electrode

Pre-concentration of algal biomass via electrochemical harvesting was carried out in a batch reactor (dimension: 15 cm (length) \times 10 cm (width) \times 14 cm (height)) using 0.5 L of microalgal culture at a concentration of 5.2 g L^{-1} biomass. Two carbon cathodes were kept apart in the reactor and one anode was placed in the middle of the reactor (Fig. 8.1).

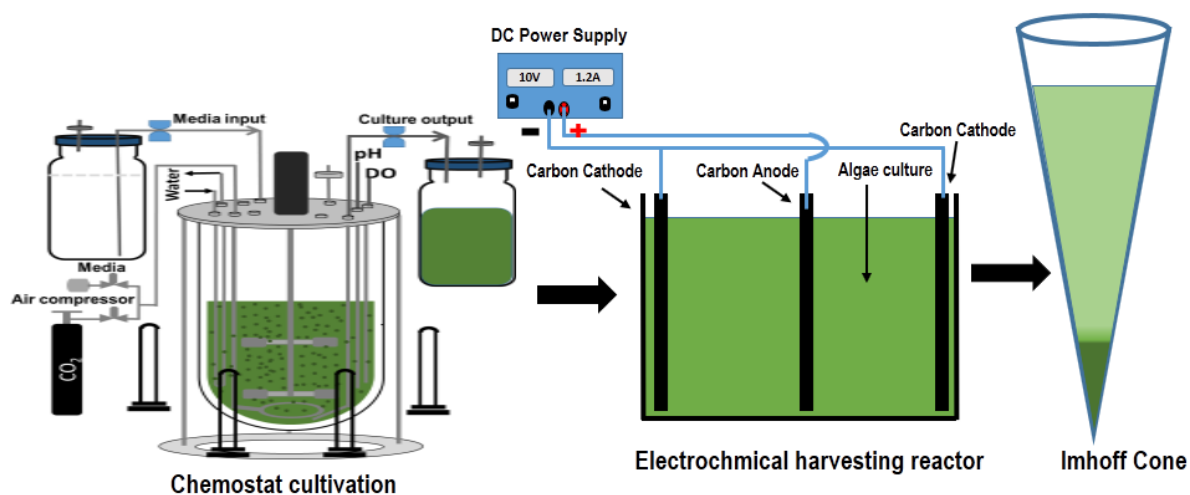


Fig. 8.1 Schematic diagram of electrochemical harvesting unit

Both carbon cathodes and carbon anode were connected to negative and positive poles of the DC power supply unit respectively (PS 3005, Sigma, India). All the experiment was performed at room temperature. The applied voltage was regulated from the DC power supply which was operated in the constant voltage mode. Sodium chloride acts as electrolyte which was added in the media initially. To determine the effect of initial pH, this was varied within the range of 4-10 by using HNO₃ and NaOH respectively prior to start the experiment. After electrochemical treatment microalgae culture was transferred to Imhoff cone for settling. Samples were collected from middle of Imhoff cone after 30 min of settling. Microalgae algae recovery efficiency was determined by using the following equation:

$$\text{Microalgae recovery efficiency } (\mu_a) = [(OD_i - OD_f)/OD_i] \times 100$$

Where OD_i is the optical density of the sample prior to the start of the electrochemical process, and OD_f is the optical density of the sample at time t . The pre-concentrated biomass obtained from electrochemical harvesting was further concentrated via centrifugation.

8.2.3 Analytical methods

Algal growth and harvesting efficiency was estimated by measuring the absorbance of cells at 690 nm with a UV-visible spectrophotometer (Cary 50, Varian, Australia) and the dry cell weight (DCW) were obtained using correlation equation detailed in section 6.2.3.1, Chapter 6. Total lipid content along with fatty acid composition in terms of fatty acid methyl esters were obtained from gas chromatography (GC) based analysis. The two-step direct transesterification method were used to quantify the total lipid in terms of FAME. FAME composition was analyzed in GC equipped with FID detector using SLB-IL 100 column (30 m × 0.25 mm i.d., 0.20 μm film thickness) (detailed protocol in section 5.2.4.1 of chapter 5). FAME mix C14-C22 (Supelco, USA) was used as the standard for GC-FID and the lipid quantified using this method represents the total lipid of the biomass in % (w/w, DCW). Properties of the biodiesel was evaluated as discussed earlier (details in Section 5.2.5).

8.3 Results and Discussion

8.3.1 Pre-concentration of algal biomass via electrochemical harvesting using carbon electrode

Upstream process development strategies employed in the previous chapters resulted in maximum biomass and lipid productivity of 2.81 g L⁻¹ day⁻¹ and 1.27 g L⁻¹ day⁻¹ respectively under chemostat cultivation of *Chlorella sorokinana* FC6 IITG at the dilution rate of 0.54 day⁻¹ (section 7.4 of chapter 7). The same culture broth containing biomass titer of 5.2 g L⁻¹ and lipid content of 44.83% (w/w DCW) obtained from chemostat was used to evaluate the electrochemical harvesting strategy. The broth collected was placed in the electrochemical chamber as shown in Fig. 8.1 and electricity was applied to the electrodes which enables the movement of negatively charged microalgae toward the anode. After reaching the anode, the negatively charged microalgal particles lose their charge and form

aggregate among themselves. The electrochemical harvesting process is affected by several operating parameters, such as applied voltage or current, medium pH, electrolyte concentration and treatment time. To that end, the present study aimed to optimize these parameters to achieve maximum harvesting efficiency.

8.3.1.1 Effect of applied voltage on microalgal recovery efficiency

Effect of applied voltage on the microalgal recovery efficiency at different time points were obtained and summarized in Fig. 8.2. The maximum microalgal recovery efficiency obtained after 90 minutes of electrochemical treatment at 10, 15, 20, 25 and 30 V applied voltage were found to be 22.11%, 32.83%, 41.48%, 53.46% and 55.32% respectively at pH 8 (Fig. 8.2).

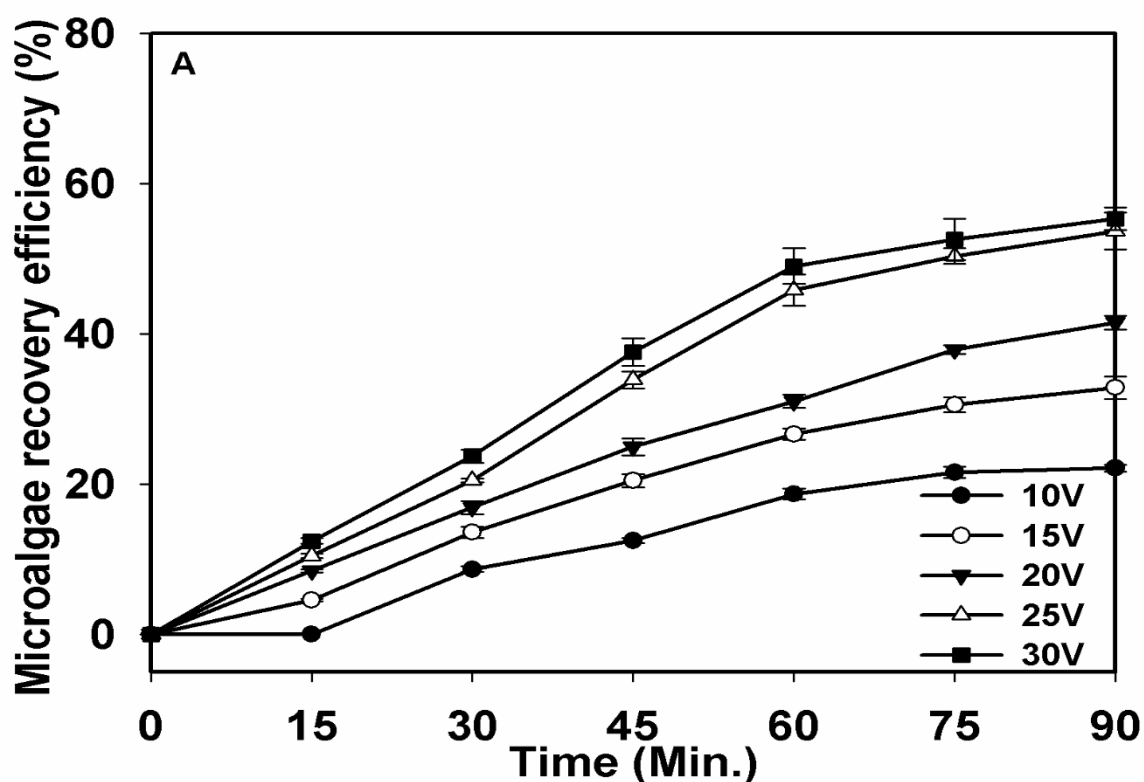


Fig 8.2 Effect of applied voltage on microalgal recovery efficiency during electrochemical harvesting treatment. Data expressed as mean \pm standard error (n= 3)

It was observed that an increase in applied voltage resulted in increased efficiency up to a maximum of 55.32% at 30V. The amount of voltage applied for electrochemical harvesting

determines the amount of charge that release from respective electrodes. When a large amount of current or high voltage is applied it results in elevated energy input which increases the process cost (Vandamme et al., 2011). Apart from that it results in generation of bubbles which improves the efficiency of recovery process but carries a risk of heating the microalgal broth or harvesting system (Gao et al., 2010a). Treatment time, medium pH and conductivity of microalgal broth also affected the recovery efficiency.

8.3.1.2 Effect of broth pH on microalgal recovery efficiency

Initial pH of the microalgal culture broth is another important parameter that influence the electrochemical harvesting efficiency (Kim et al., 2012a). Therefore, to study the effect of initial pH on efficiency of microalgal recovery through electrochemical harvesting process different culture pH in the range of 4-12 were tested at a constant optimal applied voltage of 30 V. The pH was varied in the range 4 to 12 using 1 M HCl and 1 M HNO₃ and obtained their effect on microalgae recovery efficiency (Fig. 8.3). Initial culture pH of 4 showing harvesting efficiency of 72% after a treatment time of 75 minute was found to be the best in terms of microalgal recovery (Fig. 8.3). pH determines the speciation of charged particles in the solution and the formation of positively charged ions therefore it is considered as an important factor in electrochemical harvesting (Vandamme et al., 2011). During electrochemical harvesting process using initial pH of 4, a slight increase in pH was observed with the progression of electrolysis. Evolution of H₂ during electrolysis results in continuous formation of OH⁻ ions at the cathode which in turn causes the gradual pH increase as observed in our study. In another scenario when an alkaline pH of 10 or 12 was used, an initial dip in pH was observed followed by a phase of almost constant pH which continued till the end of the process. This initial decrease in pH may be attributed to the consumption of OH⁻ ions. As microalgal culture pH is normally alkaline, addition of HNO₃ for decreasing pH adds an extra step in the harvesting process thus increasing the process

cost (Gao et al., 2010a). To that end, using carbon dioxide for lowering of pH could provide a viable solution for industrial scale harvesting process.

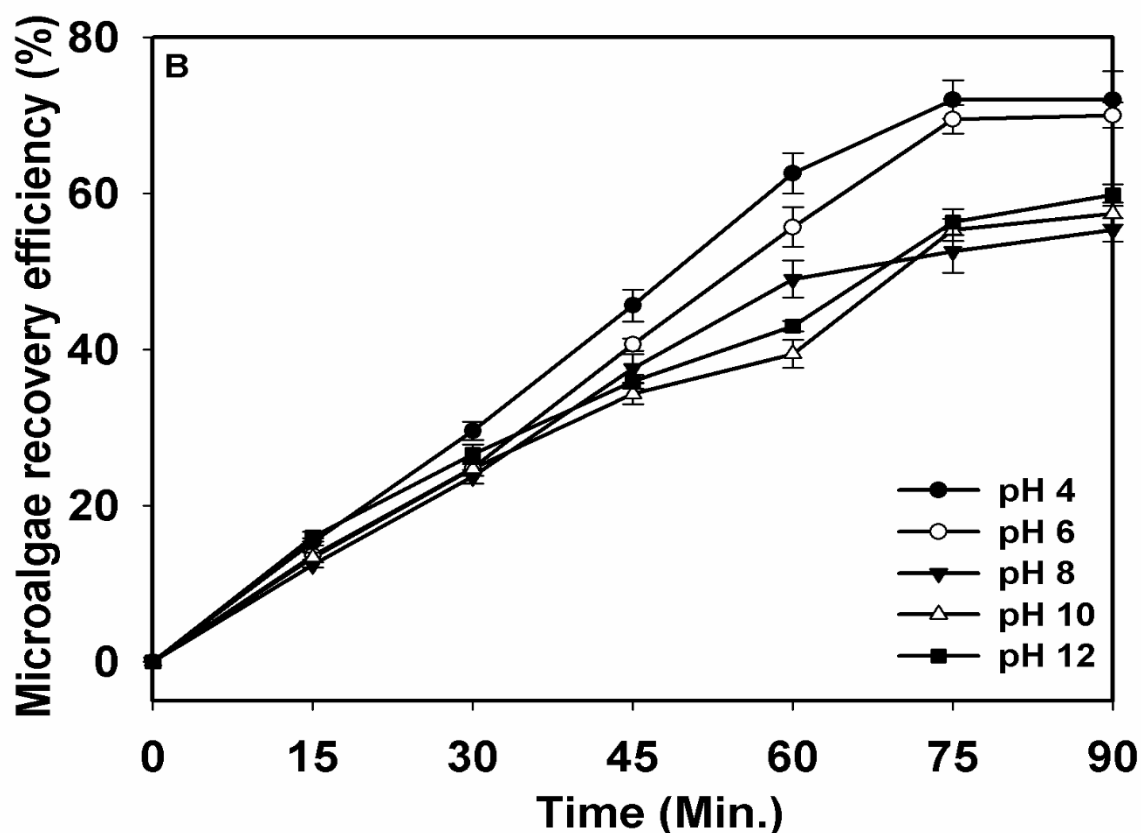


Fig 8.3 Effect of initial culture pH on microalgal recovery efficiency in electrochemical harvesting treatment. Data expressed as mean \pm standard error ($n=3$)

8.3.1.3 Effect of electrolyte on microalgal recovery efficiency

Initially NaCl was supplemented in the media as a lipid inducer which may also act as electrolyte in electrochemical harvesting. However, an additional amount of electrolyte with three different concentration of 3.14 g L^{-1} , 4 g L^{-1} and 5 g L^{-1} was supplemented in the broth to test its effect on recovery efficiency (Fig. 8.4). Together with carrying electric charge, chloride ions were found to significantly reduce the adverse effect of other anions present in the microalgal broth (Gao et al., 2010b). The addition of NaCl in to the microalgal culture as additional electrolyte slightly enhances the microalgal recovery efficiency. This could be attributed to the formation of active chlorine species and increased conductivity

due to presence of chloride ions. Microalgal recovery efficiency peaked up at 81% with the addition of 5 g L⁻¹ of electrolyte (NaCl), while it was 78.5% and 72% with 4 g L⁻¹ and 3.14 g L⁻¹ concentration of NaCl respectively. However, keeping in mind requirement of media recycling this additional addition of electrolyte may not be preferred.

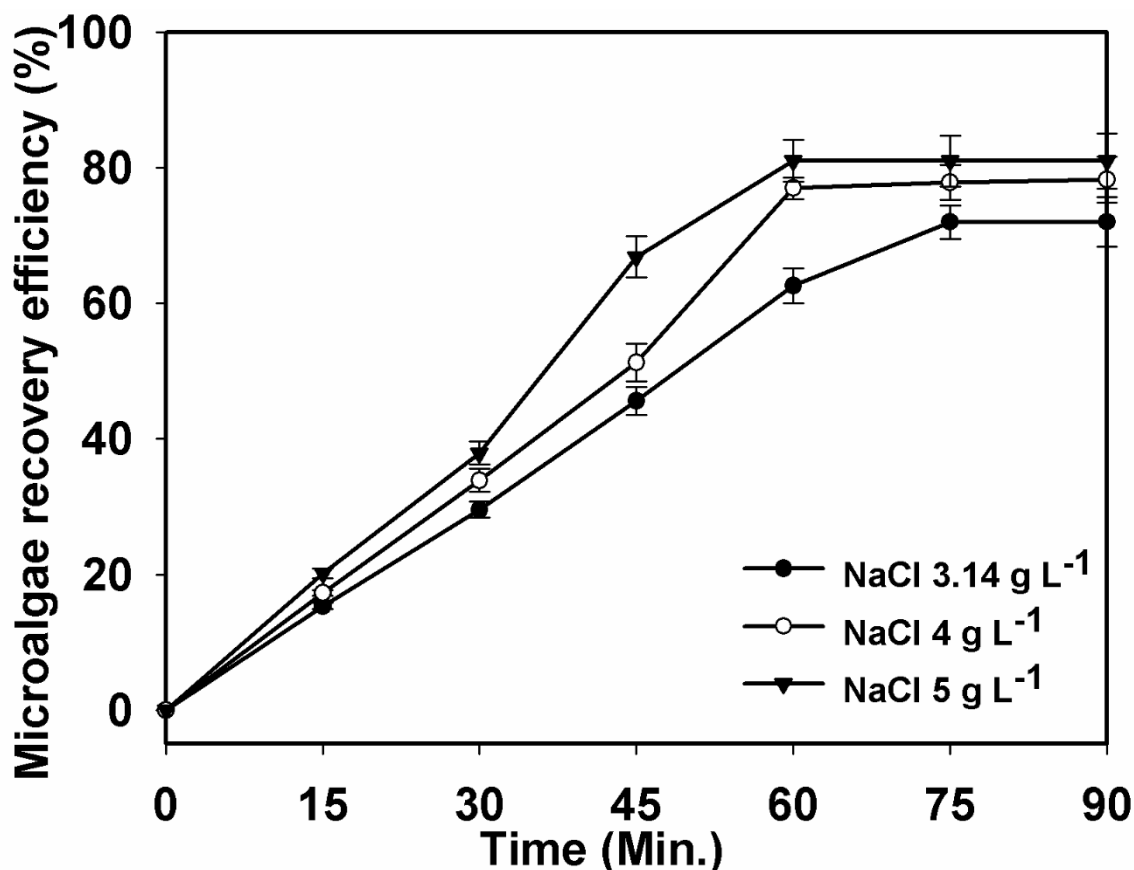


Fig 8.4 Effect of electrolyte (NaCl) concentration on microalgal recovery efficiency of *Chlorella sorokiniana* FC6 IITG in electrochemical harvesting treatment. Data expressed as mean \pm standard error (n= 3)

8.3.1.4. Effect of electrochemical harvesting process on lipid yield and fatty acid composition

Wet algal biomass obtained after electrochemical harvesting followed by centrifugation further required evaluation of their effect on lipid content and FAME composition. Kim et al. (2012b) speculated that due to formation of oxidative chemicals there is a visual change in the color of microalgal flocs and thus emphasized on the need of further studies on effect

of the electrochemical harvesting process on lipid extraction and conversion. In this study, wet microalgal biomass was subjected to freeze drying followed by direct-transesterification (detailed in 5.2.4.1, chapter 5) to assess its effect on lipid content and FAME composition. Biomass harvested with conventional centrifugation process was used as a control. Lipid yields were in the range of 44-45% by dry cell weight (DCW) which is shown in Fig. 8.5 A and 8.5 B. Lipid yield of control biomass was 44.83% DCW. Fig 8.5 shows that there is no significant difference in lipid yield of biomass recovered from electrochemical harvesting processes conducted with different voltage and pH. Thus it can be concluded that the electrochemical harvesting process has no adverse effect on lipid extraction. Fatty acid composition determines the properties of biodiesel produced, especially oxidative stability, ignition quality, kinematic viscosity, hydrocarbon emission and cold flow properties (Singh et al., 2014). Fatty acids particularly polyunsaturated fatty acids are vulnerable to various factors like temperature, pH, light, nutrient stress etc. (Borges et al., 2011). Thus it becomes necessary to assess the effect of electrochemical harvesting process on lipid composition of the microalgae. Fatty acid composition of extracted lipids was determined by gas chromatography analysis and identification was done by FAME mix C14-C22 (Supelco, USA). Table 8.1 depicts the fatty acid composition of biodiesel produced via direct transesterification of *Chlorella sorokiniana* FC6 IITG biomass harvested by electrochemical harvesting process and control. Major contributing fatty acids in all the cases were C16:0, C16:1, C18:1, C18:2, and C18:0. Fatty acid composition of biomass harvested by electrochemical harvesting process of FC6 strains, has not shown much deviation when compared to fatty acids composition of control biomass. Biodiesel properties of the produced FAME were evaluated by using correlation equation and shown in table 8.2. No significant change was observed in the properties of biodiesel.

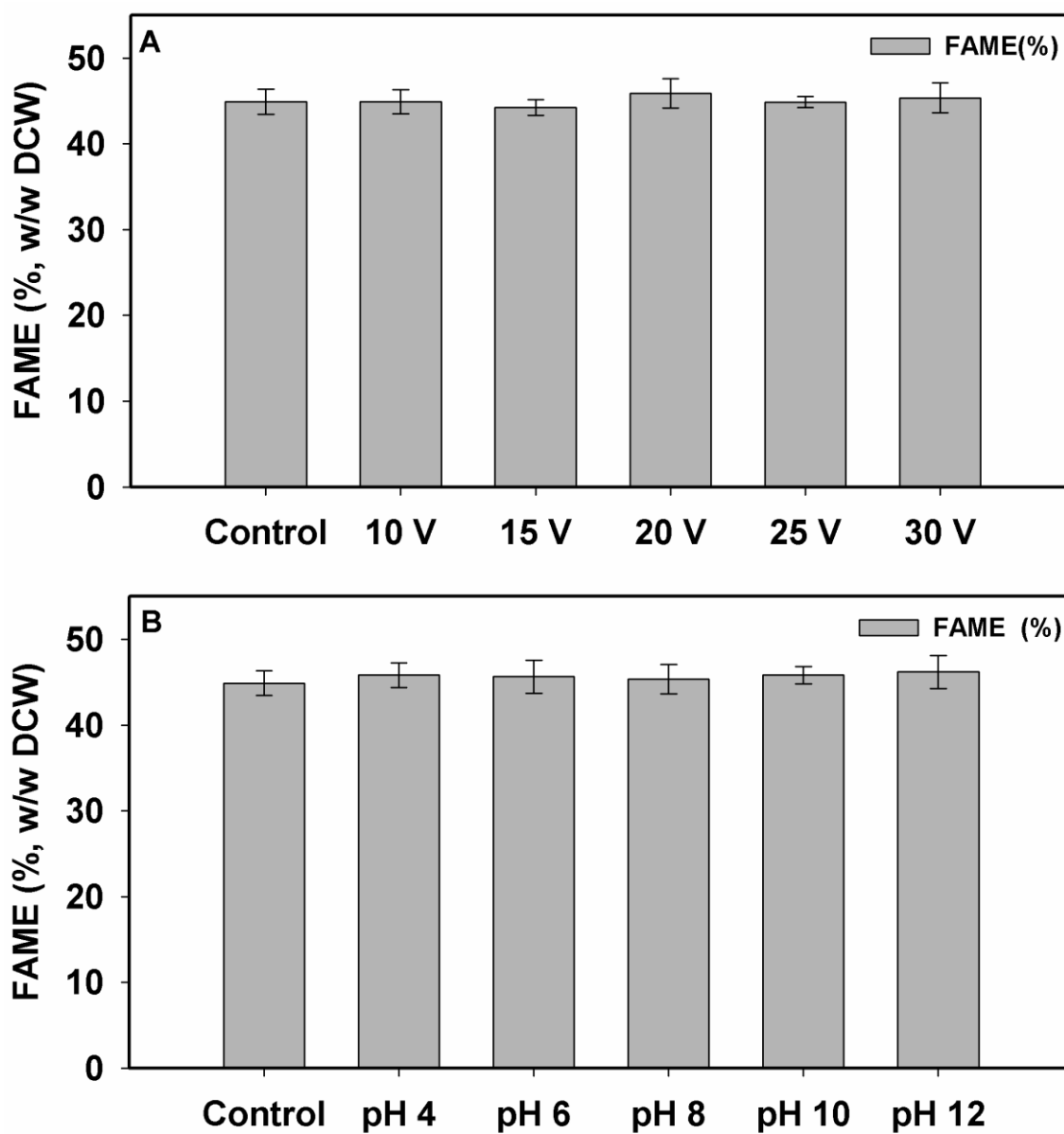


Fig. 8.5 Effect of applied current and initial culture pH on lipid yields of biomass harvested by electrochemical harvesting process. Data expressed as mean \pm standard error (n= 3)

Table 8.1 Fatty acid composition (%) of microalgae *Chlorella sorokiniana* FC6 IITG harvested by electrochemical harvesting coupled with centrifugation and compared with control

Parameters	Fatty acids										SFA ^a	MUFA ^b	PUFA ^c	FAME ^d
	C12:0	C14:0	C16:0	C16:1	C18:0	C18:1	C18:2	C20:0	C22:0	Others				
Control	2.46	1.23	27.38	7.65	2.12	29.53	28.72	0.38	0.12	0.41	33.69	37.18	28.72	44.88
Voltage														
10 V	2.15	1.35	27.12	7.83	2.75	28.16	28.13	0.31	0.14	97.94	33.82	35.99	28.13	44.88
15 V	2.19	1.3	27.37	7.12	2.83	28.65	28.12	0.24	0.1	97.92	34.03	35.77	28.12	44.24
20 V	2.33	1.42	28.19	7.29	2.93	28.83	28.19	0.24	0.14	99.56	35.25	36.12	28.19	45.87
25 V	2.01	1.53	28.34	7.68	2.87	28.65	28.45	0.28	0.16	99.97	35.19	36.33	28.45	44.86
30 V	2.15	1.35	27.12	7.83	2.75	28.16	28.13	0.31	0.14	97.94	33.82	35.99	28.13	45.34
pH														
4	2.25	1.25	27.93	7.83	2.93	28.39	27.98	0.29	0.13	1.02	34.78	36.22	27.98	45.81
6	2.19	1.34	27.98	7.72	2.82	28.28	27.69	0.27	0.13	98.42	34.73	36	27.69	45.62
8	2.23	1.3	27.87	7.85	2.92	28.18	27.57	0.29	0.12	98.33	34.73	36.03	27.57	45.34
10	2.38	1.38	27.73	7.8	2.93	28.09	27.42	0.28	0.13	98.14	34.83	35.89	27.42	45.82
12	2.3	1.49	27.91	7.87	2.87	27.93	27.1	0.25	0.13	97.85	34.95	35.8	27.1	46.18

^a - represents the total saturated fatty acid fraction in the total fatty acid methyl esters

^b - represents the total monounsaturated fatty acid fraction in the total fatty acid methyl esters

^c - represents the total polyunsaturated fatty acid fraction in the total fatty acid methyl esters

^d - represents the total FAME expressed in %, weight fraction of dry cell weight

Table 8.2 Estimated properties of the algal biodiesel obtained from *Chlorella sorokinana* FC6 IITG biomass harvested by electrochemical harvesting followed by centrifugation

Biodiesel Properties	Unit	Process parameters										
		Control	Voltage					pH				
			10V	15V	20V	25V	30V	4	6	8	10	12
Viscosity ^a	(mm ² s ⁻¹)	4.38	4.39	4.39	4.39	4.40	4.39	4.39	4.39	4.39	4.39	4.39
CN ^a		55.99	56.16	56.26	56.36	56.32	56.16	56.30	56.34	56.34	56.34	56.41
Flash Point ^a	(°C)	152.20	152.26	152.41	151.90	152.23	152.26	151.98	151.87	151.80	151.49	151.30
Cloud Point ^a	(°C)	1.15	2.70	3.07	2.38	2.22	2.70	2.47	2.82	2.83	2.83	3.06
Pour Point ^a	(°C)	-1.85	-0.27	0.10	-0.59	-0.77	-0.27	-0.50	-0.14	-0.14	-0.13	0.10
SV ^a	mg KOH g ⁻¹	207.55	204.04	203.92	207.53	208.25	204.04	206.30	205.17	205.01	204.75	204.21
Iodine value ^a	gI ₂ (100 g oil) ⁻¹	87.25	84.94	84.46	84.92	85.73	84.94	84.82	84.03	83.91	83.48	82.74
DU ^a		95.38	92.87	92.49	92.98	93.79	92.87	92.76	91.92	91.75	91.29	90.50
Heating value ^a	MJ kg ⁻¹	39.62	39.63	39.63	39.63	39.63	39.63	39.63	39.63	39.62	39.62	39.62

^a- the empirical equations for calculating the biodiesel properties were depicted in equations 5.2-5.10 (details in section 5.2.5 of chapter 5)

CN- represents cetane number

DU- represents degree of unsaturation

SV- represents saponification value

Results have shown that electrochemical harvesting process has no deteriorating effect on microalgal fatty acid composition and biodiesel properties. This could be because electrochemical process operates at normal room temperature and there is no addition of any chemical flocculants thus electrochemical harvesting process is not causing any oxidative cleavage of unsaturated bonds in fatty acids.

8.4 Conclusions

In this investigation the electrochemical harvesting process showed encouraging results with *Chlorella sorokiniana* FC6 IITG which proved that electrochemical process can be advantageous process for harvesting of microalgae. By using non depleting carbon electrode metallic contamination in the harvested microalgae and electrode depletion is completely avoided. Electro chemical harvesting process has no deteriorating effect on the lipid extraction process as well as composition of lipids from microalgae. These results denote that electrochemical process could be used as promising harvesting step in commercial scale microalgal biodiesel production.

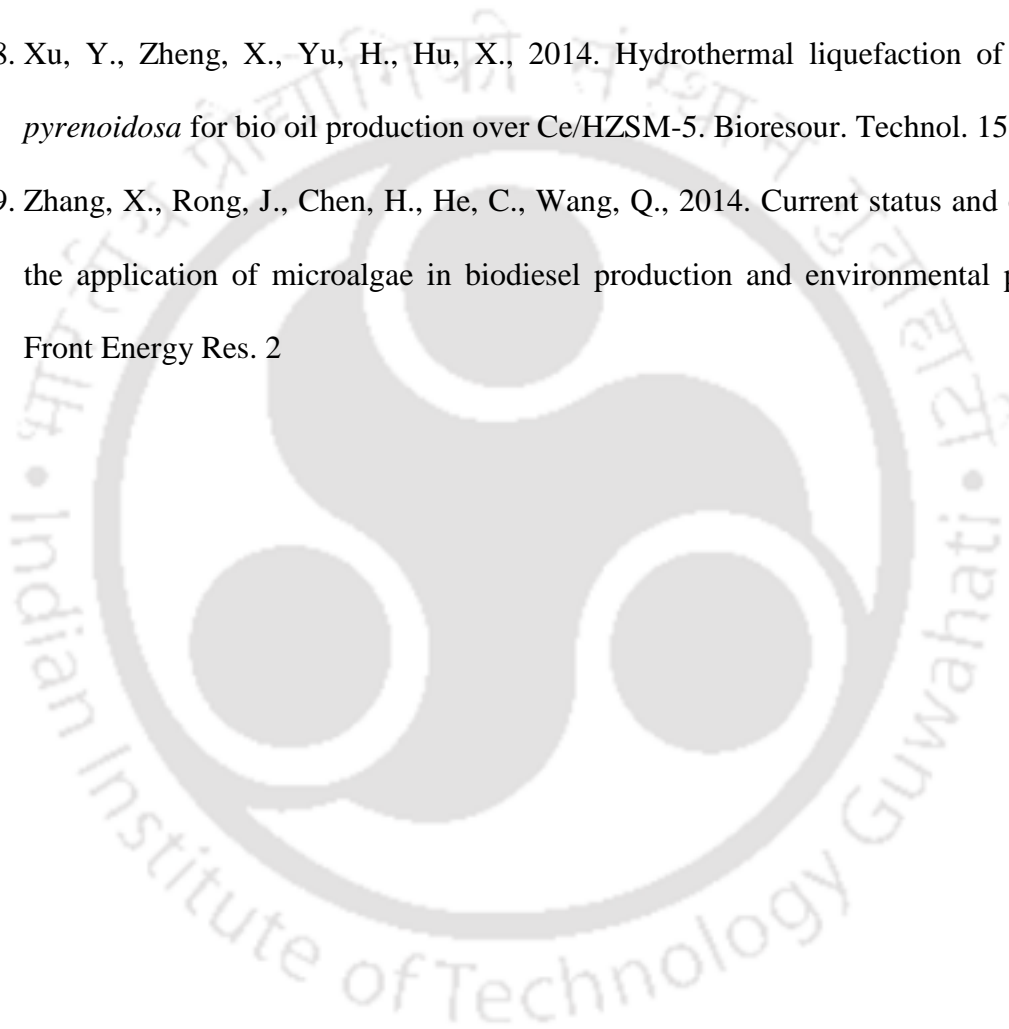
8.5 References

1. Amaro, H.M., Guedes, A.C., Malcata, F.X., 2011. Advances and perspectives in using microalgae to produce biodiesel. *Appl. Energy* 88, 3402-3410.
2. Borges, L., Morón-Villarreyes, J.A., D'Oca, M.G.M., Abreu, P.C., 2011. Effects of flocculants on lipid extraction and fatty acid composition of the microalgae *Nannochloropsis oculata* and *Thalassiosira weissflogii*, *Biomass Bioenergy*. 35, 4449-4454.
3. Christenson, L., and Sims, R., 2011. Production and harvesting of microalgae for wastewater treatment, biofuels, and bioproducts. *Biotechnol. Adv.* 29, 686-702.
4. Coons, J.E., Kalb, D.M., Dale, T., Marrone, B.L., 2014. Getting to low-cost algal biofuels: a monograph on conventional and cutting-edge harvesting and extraction technologies. *Algal Res.* 6. 250-270.
5. Danquah, M. K., Gladman, B., Moheimani, N., and Forde, G. M., 2009. Microalgal growth characteristics and subsequent influence on dewatering efficiency. *Chem. Eng. J.* 151, 73-78.
6. Davis, R., Fishman, D., Frank, E.D., Wigmosta, M.S, Aden, A., Coleman, A.M., Pienkos, P.T., Skaggs, R.J., Venteris, E.R., Wang, M.Q., 2012. Renewable diesel algal lipids: an integrated baseline for cost, emissions, and resource potential from a harmonized model. Technical report. U.S. Department of Energy Biomass Program: Oak Ridge, USA, <http://www.nrel.gov/docs/fy12osti/55431.pdf> .
7. DOE, 2010. National algal biofuels technology roadmap, Rep. DOE/EE-0332, Biomass Program, Off. of Energy Efficiency and Renewable Energy, Washington, D. C.
8. Gao, S., Du, M., Tian, J., Yang, J., Yang, J., Ma, F., Nan, J., 2010b. Effects of chloride ions on electro-coagulation–flotation process with aluminum electrodes for algae removal, *J. Hazard. Mater.* 182, 827-834.

9. Gao, S., Yang, J., Tian, J., Ma, F., Tu, G., Du, M., 2010a. Electro-coagulation–flotation process for algae removal. *J. Hazard. Mater.* 177, 336-343.
10. Greenwell, H., Laurens, L., Shields, R., Lovitt, R., and Flynn, K., 2010. Placing microalgae on the biofuels priority list: a review of the technological challenges. *J. R. Soc. Interface.* 7, 703-726.
11. Gui, M., Lee, K., Bhatia, S., 2009. Supercritical ethanol technology for the production of biodiesel: process optimization studies. *J. Superc. Fluids.* 49, 286–292
12. Kim, J., Ryu, B.G., Kim, B.K., Han, J.I., Yang, J.W., 2012a. Continuous microalgae recovery using electrolysis with polarity exchange. *Bioresour. Technol.* 111, 268-275.
13. Kim, J., Ryu, B.G., Kim, K., Kim, B.K., Han, J.I., Yang, J.W., 2012b. Continuous microalgae recovery using electrolysis: effect of different electrode pairs and timing of polarity exchange. *Bioresour. Technol.* 123, 164-170.
14. Kusdiana, D., Saka, S., 2004. Effects of water on biodiesel fuel production by supercritical methanol treatment. *Bioresour. Technol.* 91, 289-95.
15. Lee, A.K., Lewis, D.M., Ashman, P.J., 2013. Harvesting of marine microalgae by electroflocculation: the energetics, plant design, and economics. *Appl. Energy* 108, 45-53.
16. Lundquist, T.J., Woertz, I.C., Quinn, N.W.T., Benemann, J.R., 2010. A Realistic Technology and Engineering Assessment of Algae Biofuel Production. Energy Biosciences Institute, U.C. Berkeley, CA
17. Mata, T.M., Martins, A.A., Caetano, N.S., 2010. Microalgae for biodiesel production and other applications: a review. *Renew. Sust. Energ. Rev.* 14, 217–232
18. Neveux, N., Yuen, A.K.L., Jazrawi, C., Magnusson, M., Haynes, B.S., Masters, A.F., Montoya, A., Paul, N.A., Maschmeyer, T., de Nys, R., 2014. Biocrude yield and

- productivity from the hydrothermal liquefaction of marine and freshwater green macroalgae. *Bioresour. Technol.* 155, 334-341.
19. Patil, P.D., Gude, V.G., Mannarswamy, A., Cooke, P., Nirmalakhandan, N., Lammers, P., Deng, S.G., 2012. Comparison of direct transesterification of algal biomass under supercritical methanol and microwave irradiation conditions. *Fuel* 97, 822-831.
20. Patil, P.D., Gude, V.G., Mannarswamy, A., Deng, S.G., Cooke, P., Munson-McGee, S., Rhodes, I., Lammers, P., Nirmalakhandan, N., 2011. Optimization of direct conversion of wet algae to biodiesel under supercritical methanol conditions. *Bioresour. Technol.* 102, 118-122.
21. Poelman, E., De Pauw, N., Jeurissen, B., 1997. Potential of electrolytic flocculation for recovery of microalgae. *Resour. Conserv. Recycl.* 19, 1-10.
22. Rawat, I., Kumar, R. R., Mutanda, T., and Bux, F., 2013. Biodiesel from microalgae: a critical evaluation from laboratory to large scale production. *Applied Energy.* 103, 444-467.
23. Safi, C., Zebib, B., Merah, O., Pontalier, P.Y., Vaca-Garcia, C., 2014. Morphology, composition, production, processing and applications of *Chlorella vulgaris*. *Renew. Sust. Energy Rev.* 35, 265-278.
24. Singh, B., Guldhe, A., Rawat, I., Bux, F., 2014. Towards a sustainable approach for development of biodiesel from plant and microalgae. *Renew. Sustain. Energy Rev.* 29, 216-245.
25. Soomro, R.R., Ndikubwimana, T., Zeng, X., Lu, Y., Lin, L., Danquah, M.K., 2016. Development of a Two-Stage Microalgae Dewatering Process – A Life Cycle Assessment Approach. *Frontiers in Plant Science*, 7, 113. <http://doi.org/10.3389/fpls.2016.00113>

26. Uduman, N., Bourniquel, V., Danquah, M.K., Hoadley, A.F.A., 2011. A parametric study of electrocoagulation as a recovery process of marine microalgae for biodiesel production. *Chem. Eng. J.* 174, 249–257.
27. Vandamme, D., Pontes, S.C.V., Goiris, K., Foubert, I., Pinoy, L.J.J., Muylaert, K. (2011). Evaluation of electro-coagulation-flocculation for harvesting marine and freshwater microalgae. *Biotechnol. Bioeng.* 108, 2320-2329.
28. Xu, Y., Zheng, X., Yu, H., Hu, X., 2014. Hydrothermal liquefaction of *Chlorella pyrenoidosa* for bio oil production over Ce/HZSM-5. *Bioresour. Technol.* 15, 1-5.
29. Zhang, X., Rong, J., Chen, H., He, C., Wang, Q., 2014. Current status and outlook in the application of microalgae in biodiesel production and environmental protection. *Front Energy Res.* 2



CHAPTER 9

Conclusions

A novel indigenous microalgal strain *Chlorella sorokiniana* FC6 IITG was isolated & analyzed for neutral lipid accumulation and selected as model organism for this study. A direct transesterification method was developed for reliable and accurate quantification for total lipid in terms of FAME that can bypass the solvent extraction steps. The optimal conditions for direct transesterification has showed 462.6% and 445.4% increase in FAME yield when compared with conventional method for *Chlorella* sp. FC2 IITG and *C. Sorokiniana* FC6 IITG respectively. Characterization of the strain under different pH and temperature revealed the robustness of the strain to grow in wide range of pH from 4 to 10 and temperatures of range 20-44°C. The strain was also found to be capable of utilizing both organic and inorganic nitrogen sources under photoautotrophic growth condition, among various nitrogen sources sodium nitrate was found best suitable nitrogen source in terms of growth and lipid productivity. It was also observed that the strain had the capability to utilize various carbon sources in both heterotrophic and mixotrophic growth conditions. Among the various carbon sources sodium acetate and glucose was found to be the most suitable carbon source under heterotrophic and mixotrophic growth mode, respectively. Screening of carbon sources also depicted glucose and sodium acetate was identified as growth supporting and lipid inducing nutrients, respectively. Media optimization resulted in a 19% improvement in biomass titer of the strain when compared with the unoptimized BG11 media under photoautotrophic conditions.

The strain was further evaluated in terms of biomass and lipid productivity under different trophic (photoautotrophic, heterotrophic and mixotrophic) batch modes in automated photo bioreactor. Significant variation in the biomass productivity (142.06 to 455.5 mg L⁻¹ day⁻¹) and total lipid productivity (47.2 to 111.8 mg L⁻¹ day⁻¹) was observed for the *Chlorella sorokiniana* FC6 IITG under different trophic modes. Mixotrophic cultivation mode was found to be superior to photoautotrophic and heterotrophic mode in terms of biomass and lipid productivity with biomass titer of 2.73 g L⁻¹ day⁻¹. To that end, mixotrophic mode was preferred for developing a process strategy for generation of lipid rich microalgal biomass. For enhanced biomass and lipid productivity two strategy was demonstrated (i) single stage two phase fed-batch mixotrophic cultivation, involves coupling intermittent feeding of limiting nutrients and addition of lipid inducer in stationary phase results high cell density cultivation for generation of lipid rich microalgal biomass (ii) a process engineering strategy to achieve synchronized growth and lipid accumulation in *Chlorella sorokiniana* FC6 IITG under fed-batch and continuous mode of operation with sodium acetate and sodium chloride as triggers for lipid accumulation.

The single-stage two phase fed-batch mixotrophic cultivation resulted high cell density lipid-rich biomass titer (15.81 g L⁻¹ day⁻¹) with a lipid content (54.95%, w/w DCW) and lipid productivity (550 mg L⁻¹ day⁻¹). Though from our previous experiment sodium acetate was found as lipid inducer, further screening of lipid inducer was performed to identify effective combination of lipid inducers which supports maximum lipid induction without hampering growth. To that end various lipid inducers was evaluated to identify the suitable lipid inducer. Amongst various lipid inducers combination of sodium acetate and sodium chloride was found to be the most suitable elicitor. A process engineering strategy to achieve for simultaneous growth and lipid accumulation in *Chlorella sorokiniana* FC6 IITG under continuous mode of operation with sodium acetate and sodium chloride as triggers for lipid

accumulation. The fed-batch cultivation of the strain in bioreactor with intermittent feeding of limiting nutrients and lipid resulted in maximum biomass and lipid productivity of 2.08 and 0.97 g L⁻¹ day⁻¹ respectively. Chemostat operation mode resulted in improvement in biomass and lipid productivity of 2.81 and 1.27 g L⁻¹ day⁻¹ respectively, at a dilution rate of 0.54 day⁻¹; the result being significantly higher when compared to other characterized strains. Thus, using lipid inducers in chemostat could be an effective alternate to the conventional nutrient limitation strategies used to achieve synchronized growth and lipid accumulation without compromising growth. Further, electrochemical harvesting was evaluated and found suitable for efficient harvesting of *Chlorella sorokiniana* FC6 IITG strain with a harvesting efficiency of 72% at optimum condition. No change was observed in FAME composition when biomass was harvested by electrochemical harvesting followed by centrifugation. Hence electrochemical harvesting was suggested as suitable method for harvesting of *Chlorella sorokiniana* FC6 IITG. Fatty acid methyl ester (FAME) composition analysis reveals the majority of fatty acids to be C16:0, C16:1, C18:0, C18:1 and C18:2 and quality analysis of their biodiesel properties showed better agreement with the ASTM and European standards. Thus, proving the immense potential of the strain to be cell factory for biodiesel production.

Future Prospects

- ✓ Evaluation and demonstration of the synchronized growth and lipid accumulation process strategy at pilot scale plant.
- ✓ Development of energy efficient and scalable process for direct conversion of wet algal biomass to biodiesel.
- ✓ Detailed characterization of biodiesel and process development for deoxygenation via catalytic upgradation of the produced biodiesel.
- ✓ Economic and feasibility analysis of the technology.

Appendix

Table T1 Comparison of biomass and lipid productivity ($\text{mg L}^{-1} \text{day}^{-1}$) for different microalgae grown under various cultivation conditions in batch mode with *Chlorella sorokiniana* FC6IITG

Organism	BT (g L^{-1})	BP ($\text{mg L}^{-1} \text{day}^{-1}$)	LC (%, g g^{-1} DCW)	LP ($\text{mg L}^{-1} \text{day}^{-1}$)	Condition	Carbon Source (g L^{-1}) ⁺	Light intensity ($\mu\text{E m}^{-2} \text{s}^{-1}$) ⁺⁺	Reference
<i>Nannochloropsis</i> sp.	2.94	210.00	29.60	61.00	Photoautotrophic#	CO ₂ 5%	100 Continuous	Rodolfi et al., 2009
<i>Nannochloropsis</i> sp.	2.38	170.00	35.70	60.90	Photoautotrophic#	CO ₂ 5%	100 Continuous	Rodolfi et al., 2009
<i>Scenedesmus</i> sp.	3.64	260.00	21.10	53.90	Photoautotrophic#	CO ₂ 5%	100 Continuous	Rodolfi et al., 2009
<i>Chlorococcum</i> sp.	3.92	280.00	19.30	53.70	Photoautotrophic#	CO ₂ 5%	100 Continuous	Rodolfi et al., 2009
<i>Pavlova lutheri</i>	1.96	140.00	35.50	50.20	Photoautotrophic#	CO ₂ 5%	100 Continuous	Rodolfi et al., 2009
<i>Pavlova salina</i>	2.24	160.00	30.90	49.40	Photoautotrophic#	CO ₂ 5%	100 Continuous	Rodolfi et al., 2009
<i>Nannochloropsis</i> sp.	2.80	200.00	24.40	48.20	Photoautotrophic#	CO ₂ 5%	100 Continuous	Rodolfi et al., 2009
<i>Chlorella sorokiniana</i> FC6 IITG	2.13	142.06	31.80	47.20	Photoautotrophic	CO₂ 1%	150 (16h L: 8h D)	present Study

Table T1 Contd...								
Organism	BT (g L ⁻¹)	BP (mg L ⁻¹ day ⁻¹)	LC (%, g g ⁻¹ DCW)	LP (mg L ⁻¹ day ⁻¹)	Condition	Carbon Source (g L ⁻¹) ⁺	Light intensity ($\mu\text{E m}^{-2} \text{s}^{-1}$) ⁺⁺	Reference
<i>Phaeodactylum tricornutum</i>	3.36	240.00	18.70	44.80	Photoautotrophic#	CO ₂ 5%	100 Continuous	Rodolfi et al., 2009
<i>Chlorella sorokiniana</i>	3.22	230.00	19.30	44.70	Photoautotrophic#	CO ₂ 5%	100 Continuous	Rodolfi et al., 2009
<i>Scenedesmus</i> sp.	2.94	210.00	19.60	40.80	Photoautotrophic#	CO ₂ 5%	100 Continuous	Rodolfi et al., 2009
<i>Isochrysis</i> sp.	1.96	140.00	27.40	37.80	Photoautotrophic#	CO ₂ 5%	100 Continuous	Rodolfi et al., 2009
<i>Isochrysis</i> sp.	2.38	170.00	22.40	37.70	Photoautotrophic#	CO ₂ 5%	100 Continuous	Rodolfi et al., 2009
<i>Nannochloropsis</i> sp.	2.38	170.00	21.60	37.60	Photoautotrophic#	CO ₂ 5%	100 Continuous	Rodolfi et al., 2009
<i>Chlorella vulgaris</i>	2.80	200.00	18.40	36.90	Photoautotrophic#	CO ₂ 5%	100 Continuous	Rodolfi et al., 2009
<i>Tetraselmis suecica</i>	3.92	280.00	12.90	36.40	Photoautotrophic#	CO ₂ 5%	100 Continuous	Rodolfi et al., 2009
<i>Scenedesmus quadricauda</i>	2.66	190.00	18.40	35.10	Photoautotrophic#	CO ₂ 5%	100 Continuous	Rodolfi et al., 2009
<i>Chlorella</i> sp. FC2 IITG	0.70	114.00	45.18	35.02	Photoautotrophic	CO ₂ 1%	20 (16h L: 8h D)	Muthuraj et al., 2014
<i>Porphyridium cruentum</i>	5.18	370.00	9.50	34.80	Photoautotrophic#	CO ₂ 5%	100 Continuous	Rodolfi et al., 2009
<i>Chlorella vulgaris</i>	2.38	170.00	19.20	32.60	Photoautotrophic#	CO ₂ 5%	100 Continuous	Rodolfi et al., 2009
<i>Chlorella zofingiensis</i>	1.90	118.75	25.80	30.64	Photoautotrophic	Air	30 Continuous	Liu et al., 2011
<i>Monodus subterraneus</i>	2.66	190.00	16.10	30.40	Photoautotrophic#	CO ₂ 5%	100 Continuous	Rodolfi et al., 2009
<i>Skeletonema</i> sp.	1.26	90.00	31.80	27.30	Photoautotrophic#	CO ₂ 5%	100 Continuous	Rodolfi et al., 2009
Table T1 Contd...								

Organism	BT (g L ⁻¹)	BP (mg L ⁻¹ day ⁻¹)	LC (%, g g ⁻¹ DCW)	LP (mg L ⁻¹ day ⁻¹)	Condition	Carbon Source (g L ⁻¹) ⁺	Light intensity ($\mu\text{E m}^{-2} \text{s}^{-1}$) ⁺⁺	Reference
<i>Tetraselmis suecica</i>	4.48	320.00	8.50	27.00	Photoautotrophic#	CO ₂ 5%	100 Continuous	Rodolfi et al., 2009
<i>Scenedesmus quadricauda</i>	1.12	140.00	15.90	22.30	Photoautotrophic	CO ₂ 2%	73 Continuous	Zhao et al., 2012
<i>Chaetoceros muelleri</i>	0.98	70.00	33.60	21.80	Photoautotrophic#	CO ₂ 5%	100 Continuous	Rodolfi et al., 2009
<i>Scenedesmus</i> sp.	3.04	217.00	9.51	20.65	Photoautotrophic	CO ₂ 10%	150 Continuous	Yoo et al., 2010
<i>Chaetoceros calcitrans</i>	0.56	40.00	39.80	17.60	Photoautotrophic#	CO ₂ 5%	100 Continuous	Rodolfi et al., 2009
<i>Thalassioria psedonana</i>	1.12	80.00	20.60	17.40	Photoautotrophic#	CO ₂ 5%	100 Continuous	Rodolfi et al., 2009
<i>Skeletonema costatum</i>	1.12	80.00	21.10	17.40	Photoautotrophic#	CO ₂ 5%	100 Continuous	Rodolfi et al., 2009
<i>Chlorella vulgaris</i>	1.46	104.00	6.64	6.91	Photoautotrophic	CO ₂ 10%	150 Continuous	Yoo et al., 2010
<i>Nannochloropsis</i> sp. BR2	0.53	76.00	56.10	6.20	Photoautotrophic *	Air	100 (12h L: 12h D)	Lim et al., 2012
<i>Botryococcus braunii</i>	0.37	26.50	20.75	5.51	Photoautotrophic	CO ₂ 10%	150 Continuous	Yoo et al., 2010
<i>Dunaliella salina</i>	0.37	53.00	43.00	4.80	Photoautotrophic *	Air	100 (12h L: 12h D)	Lim et al., 2012
<i>Chlorella vulgaris</i>	0.25	10.00	38.00	4.00	Photoautotrophic	Air	Continuous Light	Liang et al., 2009
<i>Chlorella</i> sp. BR2	0.59	84.00	31.40	3.90	Photoautotrophic *	Air	100 (12h L: 12h D)	Lim et al., 2012
<i>Chaetoceros muelleri</i>	0.50	71.00	29.50	3.30	Photoautotrophic *	Air	100 (12h L: 12h D)	Lim et al., 2012
<i>Chaetoceros calcitrans</i>	ND	ND	29.00	3.20	Photoautotrophic *	Air	100 (12h L: 12h D)	Lim et al., 2012

Table T1 Contd...

Organism	BT (g L ⁻¹)	BP (mg L ⁻¹ day ⁻¹)	LC (%, g g ⁻¹ DCW)	LP (mg L ⁻¹ day ⁻¹)	Condition	Carbon Source (g L ⁻¹) ⁺	Light intensity ($\mu\text{E m}^{-2} \text{s}^{-1}$) ⁺⁺	Reference
<i>Pavlova salina</i>	1.68	24.00	19.00	2.10	Photoautotrophic *	Air	100 (12h L: 12h D)	Lim et al., 2012
<i>Tetraselmis</i> sp. M8	0.75	107.00	18.70	2.10	Photoautotrophic *	Air	100 (12h L: 12h D)	Lim et al., 2012
<i>Isochrysis galbana</i>	0.45	64.00	17.60	2.00	Photoautotrophic *	Air	100 (12h L: 12h D)	Lim et al., 2012
<i>Pavlova lutheri</i>	0.45	64.00	17.90	2.00	Photoautotrophic *	Air	100 (12h L: 12h D)	Lim et al., 2012
<i>Tetraselmis chui</i>	0.42	60.00	13.50	1.50	Photoautotrophic *	Air	100 (12h L: 12h D)	Lim et al., 2012
<i>Tetraselmis suecica</i>	0.73	104.00	13.40	1.50	Photoautotrophic *	Air	100 (12h L: 12h D)	Lim et al., 2012
<i>Phaeodactylum tricornutum</i>	0.46	ND	ND	ND	Photoautotrophic	CO ₂	50 (12h L: 12h D)	Liu et al., 2009
<i>Chlorella protothecoides</i>	3.97	930.00	20.33	190.00	Heterotrophic	Glycerol	Dark	Heredia-Arroyo and Hu, 2010
<i>Chlorella protothecoides</i>	3.62	840.00	19.74	170.00	Heterotrophic	Acetate	Dark	Heredia-Arroyo and Hu, 2010
<i>Chlorella protothecoides</i>	4.00	930.00	15.73	150.00	Heterotrophic	Glucose	Dark	Heredia-Arroyo and Hu, 2010
<i>Scenedesmus quadricauda</i>	3.39	484.00	22.12	107.00	Heterotrophic	Glucose	Dark	Zhao et al., 2012
<i>Chlorella sorokiniana</i> FC6 IITG	1.75	249.70	39.21	67.00	Heterotrophic	Sodium acetate	Dark	Present Study
<i>Chlorella</i> sp. FC2 IITG	0.68	112.00	64.52	48.95	Heterotrophic	Glucose	Dark	Muthuraj et al 2014
<i>Chlorella vulgaris</i>	1.20	151.00	23.00	35.00	Heterotrophic	Glucose	Dark	Liang et al., 2009
Table T1 Contd...								

Organism	BT (g L ⁻¹)	BP (mg L ⁻¹ day ⁻¹)	LC (%, g g ⁻¹ DCW)	LP (mg L ⁻¹ day ⁻¹)	Condition	Carbon Source (g L ⁻¹) ⁺	Light intensity ($\mu\text{E m}^{-2} \text{s}^{-1}$) ⁺⁺	Reference
<i>Chlorella zofingiensis</i>	9.70	606.25	51.10	30.97	Heterotrophic	Glucose	Dark	Liu et al., 2011
<i>Chlorella vulgaris</i>	0.99	87.00	31.00	27.00	Heterotrophic	Acetate	Dark	Liang et al., 2009
<i>Chlorella protothecoides</i>	4.07	1360.00	14.06	190.00	Mixotrophic	Glucose	16h L:8 h D	Heredia-Arroyo and Hu, 2010
<i>Chlorella protothecoides</i>	1.62	540.00	29.45	160.00	Mixotrophic	Acetate	16h L:8 h D	Heredia-Arroyo and Hu, 2010
<i>Scenedesmus quadricauda</i>	2.80	350.00	33.10	115.80	Mixotrophic	CO ₂ 2%; Glucose	73 Continuous	Zhao et al., 2012
<i>Chlorella sorokiniana</i> FC6 IITG	2.19	455.50	33.44	111.85	Mixotrophic	CO₂ (1%, v/v) & glucose	150 (16h L: 8h D)	Present Study
<i>Nannochloropsis sp.</i>	3.83	383.00	19.30	74.00	Mixotrophic	Glucose	40 (16h L:8h D)	Cherisilp and Totpee, 2012
<i>Chlorella sp.</i>	3.76	376.00	15.60	58.80	Mixotrophic	Glucose	40 (16h L:8h D)	Cherisilp and Torpee, 2012
<i>Chlorella vulgaris</i>	1.69	254.00	21.00	54.00	Mixotrophic	Glucose+ Air	Continuous Light	Liang et al., 2009
<i>Chlorella sp.</i> FC2 IITG	1.03	73.00	68.75	50.42	Mixotrophic	CO ₂ 1% & glucose	20 (16h L: 8h D)	Muthuraj et al., 2014
<i>Phaeodactylum tricornutum</i>	0.71	ND	ND	ND	Mixotrophic	Glycerol	50 (12h L: 12h D)	Liu et al., 2009
<i>Phaeodactylum tricornutum</i>	0.59	ND	ND	ND	Mixotrophic	Acetate	50 (12h L: 12h D)	Liu et al., 2009
<i>Phaeodactylum tricornutum</i>	0.56	ND	ND	ND	Mixotrophic	Glucose	50 (12h L: 12h D)	Liu et al., 2009

- The biomass titre was calculated approximately based on the assumption that all the cultures were grown for a period of two week as mentioned by Rodolphi et al., 2009.

* - Represents that the cells were grown under photoautotrophic condition for 7 days & then transferred to nitrate starvation for next 2 days as mentioned by Lim et al., 2012

+ - represents the % CO₂ supplied for the growth of organism in volume fractions; ++ - shows that L represents the light cycle and D represents the dark cycle provided for growth
BT - represents Biomass Titer; BP - represents Biomass Productivity; LC - represents Lipid Content; LP - represents Lipid Productivity; ND - not defined

Table T2 Comparison of biomass and lipid productivity ($\text{mg L}^{-1} \text{day}^{-1}$) for different microalgae grown under different operation mode (fed-batch & continuous mode) with the strain *Chlorella sorokiniana* FC6 IITG grown

Organism	BT (g L^{-1})	BP ($\text{g L}^{-1} \text{day}^{-1}$)	LC (% g g^{-1} DCW)	LP ($\text{mg L}^{-1} \text{day}^{-1}$)	Condition	Energy Source	Cultivation mode	Reference
<i>Chlorella sorokiniana</i>	103.8	10.38	38.70	4000.2	Heterotrophic	Glucose	Fed-batch	Zang et al., 2013
<i>Chlorella sorokiniana</i> FC6 IITG	6.61	2.81	58.89	1270	Mixotrophic	CO ₂ (1% v/v), glucose & acetate	Continuous (SGLA)	Present study
<i>Chlorella sorokiniana</i> FC6 IITG	18.24	2.08	55	970	Mixotrophic	CO ₂ (1% v/v), glucose & acetate	Fed-Batch (SGLA)	Present study
<i>Chlorella sorokiniana</i> FC6 IITG	15.81	1.93	54.95	550	Mixotrophic	CO ₂ 1% (v/v), glucose & sodium acetate	Fed-batch (SSTP)	Present study
<i>N. oleoabundans</i>	14.2	1.42	33.6	478	Heterotrophic	Glucose	Fed-batch	Morales-Sánchez et al., 2013
<i>Nannochloropsis</i> sp.	ND	ND	ND	148.3	Mixotrophic	CO ₂ , Glucose & high light	Fed-batch	Cheirsilp and Torpee, 2012
<i>C. pyrenoidosa</i> XQ-20044	ND	0.42	ND	144.93	Photoautotrophic	CO ₂	Continuous	Wen et al., 2014
<i>Chlorella</i> sp.	ND	ND	ND	112.4	Mixotrophic	CO ₂ , Glucose & high light	Fed-batch	Cheirsilp and Torpee, 2012
<i>Choricystis minor</i> B. Fott	ND	0.35	ND	82	ND	ND	Chemostat	Sobczuk & Chisti, 2010
<i>Muriellopsis</i> sp	2.42	0.73	11	80.7	Photoautotrophic	CO ₂	Continuous	Río et. al., 2015
<i>Pseudokirchneriella subcapitata</i>	2.09	0.63	12.7	79.8	Photoautotrophic	CO ₂	Continuous	Río et. al., 2015
<i>Chlorococcum oleofaciens</i>	2.53	0.76	10.5	79.2	Photoautotrophic	CO ₂	Continuous	Río et. al., 2015
<i>Scenedesmus almeriensis</i>	2.61	0.80	9.9	79	Photoautotrophic	CO ₂	Continuous	Río et. al., 2015
<i>Neochloris oleoabundans</i>	1.91	0.57	13.6	77.9	Photoautotrophic	CO ₂	Continuous	Río et. al., 2015

Organism	BT (g L⁻¹)	BP (g L⁻¹ day⁻¹)	LC (% g g⁻¹ DCW)	LP (mg L⁻¹ day⁻¹)	Condition	Energy Source	Cultivation mode	Reference
<i>Muriella decolor</i>	2.30	0.69	9.6	66	Photoautotrophic	CO ₂	Continuous	Río et. al., 2015
<i>Chlorella fusca</i>	2.20	0.66	8.3	54.7	Photoautotrophic	CO ₂	Continuous	Río et. al., 2015
<i>C. minutissima</i>	0.4	0.14	38	52	Photoautotrophic	CO ₂	Continuous	Tang et al., 2012
<i>Tetraselmis suecica</i>	1.19	0.36	9.6	34.6	Photoautotrophic	CO ₂	Continuous	Río et. al., 2015
<i>Monoraphidium braunii</i>	1.19	0.36	7.5	27	Photoautotrophic	CO ₂	Continuous	Río et. al., 2015
<i>Muriella aurantiaca</i>	1.18	0.35	5.7	19.8	Photoautotrophic	CO ₂	Continuous	Río et. al., 2015

ND - not defined

BT - represents Biomass Titer

BP - represents Biomass Productivity

LC - represents Lipid Content

LP - represents Lipid Productivity

SGLA- represents synchronized growth and lipid accumulation

SSTP- single stage two phase cultivation

References

1. Cheirsilp, B., Torpee, S., 2012. Enhanced growth and lipid production of microalgae under mixotrophic culture condition: Effect of light intensity, glucose concentration and fed-batch cultivation. *Bioresour. Technol.* 110, 510-516.
2. Heredia-Arroyo, T., Hu, W.W.B., 2010. Oil accumulation via heterotrophic/mixotrophic *Chlorella protothecoides*. *Appl. Biochem. Biotechnol.* 162, 1978-1995.
3. Liang, Y., Sarkany, N., Cui, Y., 2009. Biomass and lipid productivities of *Chlorella vulgaris* under autotrophic, heterotrophic and mixotrophic growth conditions. *Biotechnol. Lett.* 31, 1043-1049.
4. Lim, D.K.Y., Garg, S., Timmins, M., Zhang, E.S.B., Thomas-Hall, R., Schuhmann, H., Li, Y., Schenk, P.M., 2012. Isolation and Evaluation of Oil-Producing Microalgae from Subtropical Coastal and Brackish Waters. *PLoS ONE*. 7, doi:10.1371/journal.pone.0040751.
5. Liu, J., Huang, J., Sun, Z., Zhong, Y., Jiang, Y., Chen, F., 2011. Differential lipid and fatty acid profiles of photoautotrophic and heterotrophic *Chlorella zofingiensis*: Assessment of algal oils for biodiesel production. *Bioresour. Technol.* 102, 106-110.
6. Liu, X., Duan, S., Li, A., Xu, N., Cai, Z., Hu, Z., 2009. Effects of organic carbon sources on growth, photosynthesis, and respiration of *Phaeodactylum tricornutum*. *J. Appl. Phycol.* 21, 239-246.
7. Morales-Sánchez, D., Tinoco-Valencia, R., Kyndt, J., Martinez, A., 2013. Heterotrophic growth of *Neochloris oleoabundans* using glucose as a carbon source. *Biotechnol. Biofuels.* 6 (100), 1-12.

8. Muthuraj, M., Kumar, V., Palabhanvi, B., Das, D., 2014. Evaluation of indigenous microalgal isolate *Chlorella* sp. FC2 IITG as a cell factory for biodiesel production and scale up in outdoor conditions. *J. Ind. Microbiol. Biotechnol.* 41, 499-511.
9. Río, E.D., Armendáriz, A., García-Gómez, E., García-González, M., Guerrero, M.G., 2015. Continuous culture methodology for the screening of microalgae for oil. *J. Biotechnol.* 195, 103-107.
10. Rodolfi, L., Zittelli, G.C., Bassi, N., Padovani, G., Biondi, N., Bonini, G., Tredici, M.R., 2009. Microalgae for oil: strain selection, induction of lipid synthesis and outdoor mass cultivation in a low-cost photobioreactor. *Biotechnol. Bioeng.* 102, 100-112.
11. Sobczuk, T., Chisti, Y., 2010. Potential fuel oils from the microalga *Choricystis minor*. *J. Chem. Technol. Biotechnol.* 85, 100-108.
12. Tang, H., Chen, M., Ng, K.Y.S., Salley, S.O., 2012. Continuous microalgae cultivation in a photobioreactor. *Biotechnol. Bioeng.* 109, 2468-2474.
13. Wen, X., Geng, Y., Li, Y., 2014. Enhanced lipid production in *Chlorella pyrenoidosa* by continuous culture. *Bioresour. Technol.* 161, 297-30.
14. Yoo, C., Jun, S., Lee, J., Ahn, C., Oh, H., 2010. Selection of microalgae for lipid production under high levels carbon dioxide. *Bioresour. Technol.* 101, S71-S74.
15. Zhao, G., Yu, J., Jiang, F., Zhang, X., Tan, T., 2012. The effect of different trophic modes on lipid accumulation of *Scenedesmus quadricauda*. *Bioresour. Technol.* 114, 466-471.
16. Zheng, Y., Li, T., Yu, X., Bates, P.D., Dong, T., Chen, S., 2013. High-density fed-batch culture of a thermotolerant microalga *Chlorella sorokiniana* for biofuel production. *Appl. Energy* 108, 281-287.

List of Publications

Published Manuscripts

1. **Vikram Kumar**, Muthusivaramapandian Muthuraj, Basavaraj Palabhanvi, Debasish Das* (2016) Synchronized growth and neutral lipid accumulation in *Chlorella sorokiniana* FC6 IITG under continuous mode of operation. *Bioresource Technology* 200:770-779. (IF: 4.49)
2. **Vikram Kumar**, Muthusivaramapandian Muthuraj, Basavaraj Palabhanvi, Alope K Ghoshal, Debasish Das* (2014) High cell density lipid rich cultivation of a novel microalgal isolate *Chlorella sorokiniana* FC6 IITG in a single-stage fed-batch mode under mixotrophic condition. *Bioresource Technology* 170:115-124. (**Cover page article**, IF: 4.49)
3. **Vikram Kumar**, Muthusivaramapandian Muthuraj, Basavaraj Palabhanvi, Alope K Ghoshal, Debasish Das* (2014) Evaluation and optimization of two stage sequential *in situ* transesterification process for fatty acid methyl ester quantification from microalgae. *Renewable Energy* 68:560-569. (IF: 3.47)

Manuscripts under preparation

4. **Vikram Kumar**, Muthusivaramapandian Muthuraj, Basavaraj Palabhanvi, Debasish Das* (2016) A strategy for biodiesel production involving upstream and downstream process: *Chlorella sorokiniana* FC6 IITG as a model system.

Manuscripts from collaborative work

1. Basavaraj Palabhanvi, Muthusivaramapandian Muthuraj, **Vikram Kumar**, Mayurketan Mukherjee, Saumya Ahlawat, Debasish Das *. (2017) Continuous cultivation of lipid rich microalga *Chlorella* sp. FC2 IITG for improved biodiesel productivity via control variable

- optimization and substrate driven pH control. *Bioresource Technology*, 224:481-489. (IF: 4.49)
2. Basavaraj Palabhanvi, Muthusivaramapandian Muthuraj, Mayurketan Mukherjee, **Vikram Kumar**, Debasish Das* (2016) Process engineering strategy for high cell density-lipid rich cultivation of *Chlorella* sp. FC2 IITG via model guided feeding recipe and substrate driven pH control. *Algal Research* 16: 317-329. (IF: 5.01)
 3. Muthusivaramapandian Muthuraj, **Vikram Kumar**, Basavaraj Palabhanvi, Debasish Das* (2015) Process engineering for photoautotrophic cultivation of high cell density lipid rich biomass of *Chlorella* sp. FC2 IITG. *Bioenergy Research* 8:726-739. (IF: 3.54).
 4. Basavaraj Palabhanvi, **Vikram Kumar**, Muthusivaramapandian Muthuraj, Debasish Das* (2014) Preferential utilization of intracellular nutrients supports microalgal growth under nutrient starvation: Multi-nutrient mechanistic model and experimental validation. *Bioresource Technology* 173:245-255. (IF: 4.49)
 5. Muthusivaramapandian Muthuraj, **Vikram Kumar**, Basavaraj Palabhanvi, Debasish Das* (2014) Evaluation of indigenous microalgal isolate *Chlorella* sp. FC2 IITG as a cell factory for biodiesel production and scale up in outdoor conditions. *Journal of Industrial Microbiology and Biotechnology* 41:499-511 (IF: 2.44)
 6. Muthusivaramapandian Muthuraj, Basavaraj Palabhanvi, Shamik Misra, **Vikram Kumar**, Kumaran Sivalingavas, Debasish Das* (2013) Flux balance analysis of *Chlorella* sp. FC2 IITG under photoautotrophic and heterotrophic growth conditions. *Photosynthesis Research* 118: 167-179. (IF: 3.50)

Conferences/Symposia/Meetings

1. **Vikram Kumar**, Muthusivaramapandian Muthuraj, Basavaraj Palabhanvi, Mayurketan Mukherjee, Debasish Das (2015). Mutual growth and neutral lipid accumulation in *Chlorella sorokiniana* FC6 IITG under chemostat cultivation. Workshop on “Advances in Algal Biotechnology” Organised by IIT Bombay, Mumbai
2. Muthusivaramapandian Muthuraj, Baskar Selvaraj, Basavaraj Palabhanvi, **Vikram Kumar**, Debasish Das (2015). Improvement of lipid content in *Chlorella* sp. FC2 IITG via conventional mutagenesis using Ultra-violet radiations. Workshop proceedings, Frontier Energy Research with Industry Academia Partnership (FERIAP 2015) Organised by IIT Guwahati.
3. Basavaraj Palabhanvi, Muthusivaramapandian Muthuraj, **Vikram Kumar**, Debasish Das (2015). Screening and optimization of lipid inducers towards biodiesel production. Workshop proceedings, Frontier Energy Research with Industry Academia Partnership (FERIAP 2015) Organised by IIT Guwahati.
4. **Vikram Kumar**, Muthusivaramapandian Muthuraj, Basavaraj Palabhanvi, Basker Selvaraj, Alope Kumar Ghoshal, Debasish Das (2014). Evaluation of new isolate *Chlorella sorokiniana* FC6 IITG: feed stock for biodiesel production. International Conference on New Dimension in Chemistry & Chemical Technologies-Applications in Pharma Industry (NDCT-2014) Organized by Jawaharlal Nehru Technological University Hyderabad.
5. Basavaraj Palabhanvi, Muthusivaramapandian Muthuraj, **Vikram Kumar**, Baskar Selvaraj and Debasish Das (2014). Process optimization for high cell density cultivation of novel microalga *Chlorella* sp. FC2 IITG towards biodiesel production. International Conference on New Dimension in Chemistry & Chemical Technologies-Applications in Pharma Industry (NDCT-2014) Organized by Jawaharlal Nehru Technological University Hyderabad.
6. Sumanth Govathati, Basavaraj Palabhanvi, **Vikram Kumar**, Muthusivaramapandian Muthuraj, Debasish Das (2014). Screening and optimization of lipid inducer for single stage lipid rich cultivation of *Chlorella* sp. FC2 IITG targeted towards biodiesel production. Institute of Chemical Technology, Mumbai.

7. **Vikram Kumar**, Basavaraj Palabhanvi, Muthusivaramapandian Muthuraj, Ghoshal A.K., Debasish Das (2012). Optimization of two step sequential direct transesterification for biodiesel production from *Chlorella* sp. FC2 IITG. Indo-US workshop on "Cyanobacteria: Molecular Networks to Biofuels" organized by IIT Bombay and Purdue university, India.
8. Basavaraj Palabhanvi, Muthusivaramapandian Muthuraj, **Vikram Kumar**, Debasish Das (2012). Characterization of a novel freshwater isolate *Navicula* sp. FD1 IITG under nutritional stress conditions: strategy for enhanced lipid productivity. Indo-US workshop on "Cyanobacteria: Molecular Networks to Biofuels" organized by IIT Bombay and Purdue university, Pune, India (**Awarded second best poster**).
9. **Vikram Kumar**, Muthusivaramapandian Muthuraj, Alope Kumar Ghoshal, Debasish Das (2012). Characterization of potential algal isolate as a cell factory for biodiesel production. Secone society, Guwahati, Assam, India.

Vitae

The author was born on January 26th 1983 in Katihar, Bihar, India. He passed the Secondary and Senior Secondary School Examination conducted by the Bihar School Examination Board, Patna, Bihar in 1998 and 2000 respectively. He completed B. Tech Biotechnology (Genetic Engineering) from Allahabad Agricultural Institute, deemed University, Allahabad, Uttar Pradesh in 2008. He did his M. Tech in Chemical Technology (Specialization in Biochemical Engineering) from Harcourt Butler Technological Institute, Kanpur, Uttar Pradesh in 2011.

Vikram Kumar joined his PhD. Programme in July 2011 at Centre for Energy, Indian Institute of Technology Guwahati, Assam, India. He received Junior and Senior research fellowships under the scheme run by the Ministry of Human Resource and Development (MHRD), India. He successfully completed the course work with 8.00/10 Cumulative Point Index (CPI). He gave the open (PhD Synopsis) Seminar on January 1st 2016 and presented his thesis work before the Doctoral Committee and his performance was satisfactory. He submitted the PhD thesis in April 2016.